PhD IN DRUG DEVELOPMENT, INNOVATION AND TECHNOLOGY

PhD IN BIOMEDICINE

NOPAL CACTUS AS A NEW BIOACTIVE INGREDIENT:

Phytochemical study and effects of *Nopalea cochenillifera* (L.) Salm-Dick extract on experimental models of intestinal inflammation and metabolic syndrome.

Doctoral Thesis

Emanuella de Aragão Tavares

2023

UNIVERSIDADE FEDERAL DO RIO GRANDE DO NORTE
CENTRO DE CIÊNCIAS DA SAÚDE
PROGRAMA DE PÓS-GRADUAÇÃO EM DESENVOLVIMENTO E INOVAÇÃO TECNOLÓGICA EM MEDICAMENTOS

UNIVERSIDAD DE GRANADA

FACULTAD DE FARMACIA
DEPARTAMENTO DE FARMACOLOGÍA
PROGRAMA DE DOCTORADO EM BIOMEDICINA

NOPAL CACTUS AS A NEW BIOACTIVE INGREDIENT:

Effects of *Nopalea cochenillifera* (L.) Salm-Dick extract on experimental models of intestinal inflammation and metabolic syndrome.

Emanuella de Aragão Tavares

Bajo la dirección,

Silvana Maria Zucolotto Langassner

María Elena Rodríguez Cabezas

2023

Editor: Universidad de Granada. Tesis Doctorales
Autor: Emanuella de Aragao Tavares
ISBN: 978-84-1195-004-6
URI: https://hdl.handle.net/10481/84469

EMANUELLA DE ARAGÃO TAVARES

NOPAL CACTUS AS A NEW BIOACTIVE INGREDIENT:

Phytochemical study and effects of *Nopalea cochenillifera* Salm-Dick extract on experimental models of intestinal inflammation and metabolic syndrome

Tese em cotutela submetida ao Programa de Pós-Graduação em Desenvolvimento e Inovação Tecnológica em Medicamentos da Universidade Federal do Rio Grande do Norte (PPgDITM/UFRN) como requisito à obtenção do grau de Doutor em Desenvolvimento e Inovação Tecnológica em Medicamentos.

Área: Inovação Tecnológica em Medicamentos.

Orientadora:
Profa. Dra. Silvana Maria Zucolotto Langassner

Orientadora em Cotutela:
Profa. Dra. María Elena Rodríguez Cabezas

2023

El doctorando / The *doctoral candidate* **Emanuella de Aragão Tavares** y los directores de la tesis / and *the Thesis supervisor/s*: **Silvana Maria Zucolotto Langassner** y **María Elena Rodríguez Cabezas**

Garantizamos, al firmar esta Tesis Doctoral, que el trabajo ha sido realizado por el doctorando bajo la dirección de los directores de la tesis y hasta donde nuestro conocimiento alcanza, en la realización del trabajo, se han respetado los derechos de otros autores a ser citados, cuando se han utilizado sus resultados o publicaciones.

/

Guarantee, by signing this Doctoral Thesis, that the work has been done by the doctoral candidate under the direction of the thesis supervisor/s and, as far as our knowledge reaches, in the performance of the work, the rights of other authors to be cited (when their results or publications have been used) have been respected.

Lugar y fecha / *Place and date*:

Granada, 20 de mayo de 2023

Director/es de la Tesis / *Thesis supervisor/s*;

Fdo.: Silvana Maria Zucolotto Langassner Fdo.: **María Elena Rodríguez Cabezas**

Doctorando / *Doctoral candidate*:

Fdo.: Emanuella de Aragão Tavares

Aos meus avós: Inês e Manoel,

e ao meu filho: Lucas Manuel,

Dedico.

AGRADECIMENTOS

Neste momento, eu olho para trás e vejo muitas pessoas queridas de mãos dadas comigo. E mais uma vez, assim como ao longo desses anos, tenho a certeza que a caminhada sempre foi compartilhada. "*Quem caminha sozinho pode até chegar mais rápido, mas aquele que vai acompanhado, com certeza vai mais longe*". Sem vocês eu não teria conseguido. GRATIDÃO!

De modo especial, agradeço as minhas orientadoras, Profa. Silvana Zucolotto e Profa. Gerlane Guerra, pelo apoio permanente durante todo este trabalho. A minha eterna gratidão pela formação científica e humana que recebi de vocês, levarei para sempre o exemplo de ética, compromisso e dedicação que dispensam em tudo que fazem. Muito grata pela oportunidade de trabalhar com vocês. Profa. Silvana, obrigada por tantas vezes ter acreditado mais em mim do que eu mesma.

Al grupo de la Universidad de Granada, a la profesora María Elena por haber aceptado ser mi supervisora en cotutela. Gracias por todas las grandes ayudas, especialmente por la amabilidad y buena voluntad con la que lo hicisteis. Al profesor Julio Gálvez por recibirme en su laboratorio durante 1 año, así como todos del "Team Gálvez", en especial, a los que me acompañaron en ese periodo (Jose Alberto "Chufy", María Jesús "Marí", Antonio, Alba, Laura Hidalgo, Laura López, Lucrezia, Irene, Patricia "Patri", Amanda, Maycon, Zainab, Luz y Marta) ustedes hicieron de mi estancia en Granada una experiencia inolvidable personal y profesionalmente. ¡Muchas gracias!

A todos do grupo PNBio, em especial aos colegas com quem pude desfrutar da companhia de forma mais constante, e assim, estreitar laços de amizade. Vocês tornaram essa jornada ainda mais especial e significativa: Larissa, Nadja, Valéria, Elaine, Anderson, Edilane, Renata, Gabriela, Natasha e Renato (El "Baby"), meu amigo de desabafos, risos e lutas, desde a seleção do doutorado até o final dele.

Agradeço ao Prof. Arnóbio da Silva Júnior, a doutoranda Thayse Medeiros e ao laboratório de Tecnologia e Biotecnologia Farmacêutica (TecBioFar — UFRN), cuja colaboração permitiu o desenvolvimento das nanopartículas.

Aos técnicos em laboratório, Luiz Ricardo, Dona Neida, Flávio Maurílio e César Augusto, pelo apoio durante alguns experimentos desta pesquisa.

Aos meus avós, aos que amo e amarei para sempre, meu ponto de apoio no mundo. Obrigada por sempre acreditarem nos meus estudos e neste sonho, mesmo sem entendê-lo bem.

A minha mãe Goreth, meu grande exemplo de mulher forte. Obrigada por sempre acreditar, apoiar e incentivar cada passo que escolho dar, seja aqui, do outro lado do atlântico ou em qualquer lugar do mundo. Ao meu Pai, Zacarias, que sempre demonstrou um orgulho genuíno em relação a mim. Aos meus irmãos, Talita, Gabriela, Vicente e Mariana, e aos meus sobrinhos, Rafael, Esther e Martina, por todo carinho e torcida.

Ao meu querido filho, Lucas Manuel, luz da minha vida, minha maior inspiração e motivação. Obrigada por acompanhar a mamãe nesses 4 anos de doutorado, durante os seus primeiros 4 anos de vida. *Não sei se o mundo é bom, mas ele ficou melhor quando você chegou*. Te amo infinitamente!

Ao meu companheiro, Samir, pelo amor e paciência, por me apoiar e me motivar em todas as fases deste projeto, por segurar a barra para que eu pudesse continuar. Obrigada por compartilhar os vinhos e a vida comigo. Te amo!

A Pró-Reitoria de Pós-Graduação e a todos que fazem parte do PPgDITM, obrigada pelo apoio concedido sempre que precisei.

A UFRN, pelos 12 anos de formação que recebi. Aqui realizei meu grande sonho de criança (passar no vestibular) e realizarei também um sonho da vida adulta (concluir o doutorado).

À Coordenação de Aperfeiçoamento de Pessoal de Nível Superior (CAPES), pelo auxílio financeiro a essa pesquisa, e ao Programa de Internacionalização CAPES — PrInt, pela bolsa de doutorado sanduíche que possibilitou 1 ano de estágio doutoral na *Universidad de Granada*, Espanha.

A força interior, a qual chamo de Deus, que se faz presente renovando minhas energias, guiando minha intuição e fortalecendo a minha esperança.

Para hacer las cosas bien es necesario: Primero el amor;

Segundo, la técnica.

(Antoni Gaudí)

“Estou entre aqueles que acham que a ciência tem uma grande beleza.”

(Marie Curie)

APRESENTAÇÃO

Este documento consiste na tese doutoral de Emanuella de Aragão Tavares, realizada em regime de cotutela pelo Programa de Pós-Graduação em Desenvolvimento e Inovação Tecnológica em Medicamentos (PPgDITM) na UNIVERSIDADE FEDERAL DO RIO GRANDE DO NORTE — UFRN (BRASIL) e pelo *Programa de Doctorado en Biomedicina* pela UNIVERSIDAD DE GRANADA — UGR (ESPANHA). A tese foi elaborada conforme com as normas que regem os estudos de doutorado em ambas as instituições, e intitula-se: **"Nopal cactus as a new bioactive ingredient: Effects of *Nopalea cochenillifera* (L.) Salm-Dick extract on experimental models of intestinal inflammation and metabolic syndrome".** Esta apresentação descreve brevemente como o manuscrito está organizado.

Inicialmente o conteúdo desta pesquisa foi apresentado de maneira sistematizada por meio de um resumo expandido em português e em espanhol. A tese está estruturada em 5 seções principais. A seção I compreende a Introdução, na qual integra uma revisão de literatura sobre os temas que envolvem esta pesquisa. Na seção II, é apresentado a hipótese e os objetivos deste estudo. Na sequência, a seção III inclui o material e métodos empregados. Os resultados são apresentados na seção IV, estão organizados em ordem cronológica da execução dos experimentos. Os resultados apresentados são referentes aos experimentos realizados na UFRN e aos obtidos durante o estágio doutoral realizado na UGR, pelo programa institucional de internacionalização (CAPES-PrInt), em colaboração com Prof. Dr. Julio Juan Gálvez Peralta e a Profa. Dra. María Elena Rodríguez Cabezas. A seção V é subdividida em duas partes, sendo a primeira referente a discussão dos resultados relacionados à inflamação intestinal e a segunda focada nos resultados relacionados à síndrome metabólica. As conclusões gerais do estudo são apresentadas em seguida.

Ao final, são incluídos as referências bibliográficas, apêndice (no qual inclui resultados complementares) e três anexos na seguinte ordem: ANEXO I: Artigo publicado na revista "*Plants*" — (Fator de impacto 4.658), referente a estudos parciais do projeto de tese, intitulado: **"Toxicity and anti-inflammatory activity of phenolic-rich extract from *Nopalea cochenillifera* (Cactaceae): A preclinical study on the prevention of inflammatory bowel diseases"**; ANEXO II — Comprovante CEUA e ANEXO III — Atividades desenvolvidas durante o período doutoral.

ABBREVIATIONS

Akt	Protein kinase B
AMPK	AMP-activated protein kinase
AOAC	Association of Official Analytical Chemists
APC	Antigen presenting cell
AUC	Area under curve
CD	Crohn's disease
DAI	Disease activity index
DC	Dendritic cell
DNBS	Dinitrobenzene sulfonic acid
DSS	Dextran sulfate sodium
EUD S100	Eudragit S100
FITC	Fluorescein isothiocyanate
GADPH	glyceraldehyde-3-phosphate dehydrogenase
GLUT	Glucose transporter
GTT	Glucose tolerance test
HDL	High-density lipoprotein
HFD	High-fat diet
HOMA-IR	Homeostatic model assessment of insulin resistance
HPLC	High-performance liquid chromatography
EE	Encapsulation efficiency
ESI-MS	Electrospray ionization Mass spectrometric
FTIR	Fourier Transform Infrared
IBD	Inflammatory bowel disease
ICAM-1	Inter-Cellular Adhesion Molecule – 1
IL	Interleukin
iNOS	Inducible Nitric Oxide Synthase
IRS-1	Insulin receptor substrate-1
JNK	c-Jun N-terminal kinase
LDL	Low-density lipoprotein
LPS	Lipopolysaccharide
MAPK	Mitogen-activated protein kinase
MCP-1	Monocyte chemoattractant protein-1

MDA	Malondialdehyde
MIP-1	Macrophage inflammatory protein-1
MPO	Myeloperoxidase
MUC	Mucin
NC	*Nopalea cochenillifera*
NCE	*Nopalea cochenillifera* extract
NF-κB	Nuclear factor kappa B
NO	Nitric oxide
NP	Nanoparticles
NPB	Blank nanoparticles
NPE	Extract-loaded nanoparticles
NPE-ROD	Extract-loaded nanoparticles with rodamin
OECD	Organisation for Economic Cooperation and Development
PAMP	Patogen-associated molecular pattern
PdI	Polydispersity Index
PI3K	Phosphoinositide-3-kinase
PPAR	Peroxisome proliferator activated receptors
PRR	Pattern recognition receptor
ROS	Reactive oxygen species
TBARS	Thiobarbituric acid reactive substances
TFF	Trefoil factor
TFC	Total flavonoid content
TLR	Toll-like receptor
TLR4	Toll-like receptor 4
TNF-α	Tumor necrosis factor alpha
TPC	Total phenolic content
UC	Ulcerative colitis
ZO	Zonula occludens protein
ZP	Zeta potential

RESUMO

INTRODUÇÃO

As doenças inflamatórias intestinais (DII's) e a síndrome metabólica são duas condições de saúde em ascensão em todo o mundo, principalmente nos países desenvolvidos (1–3). As DII's, incluindo a doença de Crohn e a colite ulcerativa, são doenças crônicas que afetam o trato gastrointestinal e podem causar sintomas como rectorragia, diarreia com muco ou sangue, dor abdominal, fadiga e perda de peso (4). A síndrome metabólica, por sua vez, é um conjunto de condições médicas, incluindo obesidade abdominal, hipertensão arterial, aumento dos níveis de açúcar no sangue e dislipidemia (5).

Ambas são enfermidades multifatoriais e complexas, cuja etiopatologia envolve uma combinação de fatores genéticos, ambientais e comportamentais. No caso das DII's, acredita-se que a interação entre a microbiota intestinal, o sistema imunológico e os fatores ambientais possam desempenhar um papel importante no seu desenvolvimento. Além disso, fatores como o tabagismo, o estresse e o uso prolongado de anti-inflamatórios não esteroides também podem contribuir para o desenvolvimento das DII's (6,7).

Assim como as DII's, a síndrome metabólica também está associada a uma inflamação crônica implicada na sua patogênese. O conjunto de fatores de risco, como obesidade abdominal, resistência à insulina, hipertensão arterial e dislipidemia aumentam o risco de desenvolver doenças cardiovasculares, como ataque cardíaco e acidente vascular cerebral (8). A inflamação crônica ocorre quando o sistema imunológico do corpo é ativado persistentemente, o que leva à produção contínua de citocinas pró-inflamatórias e a um estado inflamatório crônico. O tratamento da síndrome metabólica muitas vezes envolve a redução da inflamação crônica por meio de mudanças no estilo de vida, como dieta saudável, exercícios físicos regulares e controle do estresse, além de medicamentos para controlar a pressão arterial, reduzir os níveis de açúcar no sangue e reduzir os níveis de colesterol e triglicerídeos. Embora as DII's e a síndrome metabólica sejam condições diferentes, elas podem estar relacionadas em certos indivíduos, e um melhor entendimento da inflamação crônica pode ajudar no desenvolvimento de tratamentos complementares para ambas as condições (9).

Evidências clínicas mostram que o uso de fenólicos isolados ou de extratos ricos em fenólicos administrados em combinação com medicamentos já utilizados na terapia das DII's e da síndrome metabólica contribuem com a melhoria da qualidade de vida dos pacientes e para manter a doença no estado remissivo (10,11). Os polifenóis são metabólitos secundários produzidos por vegetais que possuem propriedade antioxidante e anti-inflamatória, o que os

torna eficazes na prevenção e tratamento dessas doenças. Sua notável capacidade anti-inflamatória e antioxidante se deve a múltiplos alvos de ação, como a inibição da produção ou da ação de mediadores pró-inflamatórios ou até mesmo sob a forte influência que pode exercer sobre a microbiota intestinal (12–14).

Neste cenário, a cactácea *Nopalea cochenillifera* (L.) Salm-Dyck, conhecida popularmente como palma, palma-forrageira e palma "doce" ou "miúda", é uma boa fonte de compostos bioativos anti-inflamatórios. Os seus cladódios são ricos em polissacarídeos e polifenois (15), e têm sido amplamente utilizados para fins agrícolas, alimentares e medicinais (16). É tradicionalmente utilizada como anti-inflamatório e curativo no tratamento de doenças como colesterol elevado, tensão arterial, problemas renais e urinários, e no tratamento da diabetes (17,18). Estudos anteriores relataram o potencial antibiótico e antifúngico da *N. cochenillifera* em ensaios *in vitro* (19,20). Além disso, foi observada a redução dos níveis de glicose em estudos *in vivo* (21) e em um ensaio clínico piloto (22). Em relação ao efeito anti-inflamatório, a administração oral do extrato hidroetanólico dos cladódios de *N. cochenillifera* demonstrou uma significativa atividade anti-inflamatória em modelos de indução de granuloma e úlcera gástrica em roedores (23,24).

Os polifenois presentes no extrato de *N. cochenillifera* já são considerados uma fonte promissora de agentes bioativos. No entanto, quando se trata de doenças inflamatórias intestinais, direcionar esses ativos para a região do cólon e reduzir as concentrações de extratos vegetais necessárias para alcançar atividade farmacológica ainda são desafios a serem superados. O desenvolvimento de sistemas de administração de medicamentos capazes de transportar as substâncias ativas do extrato até o tecido do cólon é uma alternativa promissora para melhorar a biodisponibilidade oral e prolongar sua retenção no cólon. Os sistemas nanoestruturados têm demonstrado propriedades interessantes e promissoras nesse sentido, como a melhoria da estabilidade, solubilidade e biodisponibilidade de compostos naturais, além de possibilitar o controle da liberação dos compostos bioativos e redução das doses e frequências de administração (25–27). Estratégias que envolvam a encapsulação do extrato de *N. cochenillifera* e o direcionamento da sua liberação para a região do cólon podem potencializar sua eficácia e reduzir a dose terapêutica necessária.

Considerando o potencial bioativo da *N. cochenillifera*, é relevante destacar que esta espécie é uma excelente escolha para o desenvolvimento de um insumo nacional, devido à sua adaptação à região nordeste do Brasil e à presença de cultivos estabelecidos. Isso possibilita o desenvolvimento de toda cadeia produtiva no país, desde o cultivo até o insumo e/ou o produto

acabado, o que pode ter impactos positivos na economia local, como a geração de empregos e o fomento ao desenvolvimento sustentável da região. Nesse contexto, essa proposta visa realizar um estudo fitoquímico do extrato de *Nopalea cochenillifera* e avaliar o efeito anti-inflamatório em modelos *in vivo* de inflamação intestinal e de síndrome metabólica.

OBJETIVO

Este trabalho teve como objetivo realizar um estudo fitoquímico do extrato hidroetanólico dos cladódios de *Nopalea cochenillifera*, bem como avaliar a toxicidade e eficácia nos modelos *in vivo* de inflamação intestinal e de síndrome metabólica. Além disso, este trabalho teve como objetivo desenvolver e caracterizar um sistema nanoparticulado carregado com o extrato de *N. cochenillifera* e avaliar o efeito farmacológico do extrato livre (NCE) e associado a nanopartículas (NPE)

Assim, foram propostos cinco objetivos específicos:

1. Caracterizar físico-quimicamente o extrato de *N. cochenillifera*, determinar o teor dos compostos fenólicos totais e flavonoides totais e o perfil cromatográfico por cromatografia liquida de alta eficiência acoplada a espectrometria de massas (CLAE-EM).
2. Avaliar a toxicidade oral aguda do extrato hidroetanólico de *N. cochenillifera* em ratos.
3. Avaliar o efeito anti-inflamatório intestinal de diferentes doses do extrato hidroetanólico de *N. cochenillifera* em modelo de inflamação intestinal experimental induzida por ácido 2,4-dinitrobenzeno sulfônico (DNBS) em ratos.
4. Desenvolver, caracterizar e avaliar os efeitos de um sistema nanoparticulado carregado com o extrato hidroetanólico de *N. cochenillifera* em um modelo de inflamação intestinal experimental induzida por dextrano sulfato de sódio (DSS) em camundongos.
5. Avaliar o efeito do extrato hidroetanólico de *N. cochenillifera* em um modelo experimental de síndrome metabólica induzida por dieta rica em gordura em camundongos.

METODOLOGIA

1. *Preparação e caracterização físico-química do extrato hidroetanólico de N. cochenillifera (NCE)*

Os cladódios de *N. cochenillifera* foram coletados, em seguida fragmentados em pedaços menores, secos em estufa de ar circulante, triturados e submetidos a extração pelo método de

maceração com solvente hidroetanólico na proporção 1:10 (*p/v*). Na análise físico-química do NCE, determinou-se o pH, a acidez titulável, teores de umidade, cinzas, extrato etéreo, fibra bruta, proteínas e carboidratos totais. Estas análises foram realizadas conforme recomendado pelos métodos da AOAC (2020). O teor de fenólicos total do extrato de NCE foi determinado com base no método do reagente Folin-Ciocalteu (28) e o teor de flavonoides totais foi determinado pelo método colorimétrico do cloreto de alumínio (29). O perfil cromatográfico foi determinado por cromatografia líquida de alta eficiência acoplada a espectrômetro de massas com fonte de ionização por electrospray (CLAE-IES-EM).

2. Avaliação da toxicidade oral aguda de NCE em ratos

A toxicidade aguda por via oral do extrato de *N. cochenillifera* foi realizada seguindo os critérios recomendados pela OECD, 2001 (Guidelines for Testing of Chemicals) (30). Foram utilizados Ratos da linhagem Wistar (*Rattus norvegicus*). O grupo teste recebeu uma dose única de 2000 mg/kg de NCE. Nos dias 1, 7 e 14 após administração de NCE, os animais do grupo teste e controle, foram submetidos ao teste comportamental e motor (Teste de campo aberto e rota-rod). No 15º dia, os animais foram anestesiados e feito uma coleta de sangue por punção cardíaca para a realização de exames hematológicos e bioquímicos. Os órgãos (fígado, rim e baço) dos animais foram examinados macroscópica e microscopicamente.

3. Estudo da atividade anti-inflamatória intestinal "in vivo"

A indução da inflamação intestinal foi realizada por ácido DNBS em ratas Wistar (31) e por DSS em camundongos C57BL/6J (32). No estudo com DNBS, os animais receberam três diferentes doses de NCE (100, 200 e 300 mg/kg/dia). No estudo com DSS, foi investigado o efeito anti-inflamatório do extrato livre (200 mg/kg/dia) e incorporado a nanopartículas poliméricas. Em ambos, o índice de atividade da doença (IAD) foi avaliado pela variação do peso corporal, presença de hemorragia retal e consistência das fezes (32). Após eutanásia, a expressão de marcadores inflamatórios e oxidativos, bem como análises macro e microscópica foram avaliadas nas amostras de cólon. Uma avaliação da permeabilidade intestinal pelo método de administração oral de FITC-dextrano foi realizada apenas com os animas submetidos a indução inflamatória intestinal por DSS (33).

4. Obtenção e caracterização das nanopartículas poliméricas

As nanopartículas carregadas com extrato de *N. cochenillifera* (NPE) foram preparadas pelo método de nanoprecipitação (34,35). As nanopartículas foram caracterizadas quanto ao

tamanho, índice de polidispersão (PdI), potencial zeta, eficiência de encapsulação (EE) e morfologia. A estabilidade física das nanopartículas foi avaliada durante um período de 30 dias.

5. *Estudo do efeito do extrato de N. cochenillifera (NCE) em um modelo de síndrome metabólica*

Camundongos machos C57BL/6J foram divididos aleatoriamente em quatro grupos experimentais: controle (dieta padrão); controle + NCE (dieta padrão, tratados com NCE (200 mg/kg)), controle (dieta rica em gordura) e controle + NCE (dieta rica em gordura, tratados com NCE (200 mg)). Ao longo do período experimental de 10 semanas, foram avaliados o peso corporal e a ingestão de água e comida (36). Uma semana antes da eutanásia, os camundongos foram privados de alimentos por 6 horas e um teste de tolerância à glicose foi realizado. Ao final do experimento, os animais foram anestesiados e feito uma coleta de sangue por punção cardíaca para a realização da medição os níveis plasmáticos de glicose. Fígado, baço, rins, cólon, gordura abdominal, epididimal e marrom, foram coletados, pesados e analisados macroscopicamente. Amostras de fígado, cólon e/ou tecido adiposo foram analisados microscopicamente e processados para determinações bioquímicas a fim de avaliar a expressão gênica de diferentes marcadores por PCR quantitativo em tempo real (Rt-qPCR).

RESULTADOS

O teor de fenólicos totais e flavonoides totais por grama de extrato seco foi de 67,85 mg e 46,16 mg/g, respectivamente. Através da análise por CLAE-IES-EM, foi caracterizado um total de 25 compostos tais como sacarídeos, ácidos orgânicos, ácidos fenólicos e flavonoides. No estudo de toxicidade, a dose de 2000 mg/kg de extrato administrada por via oral não mostrou sinais de toxicidade, mortalidade ou alterações significativas nos parâmetros comportamentais, bioquímicos e hematológicos.

Quanto aos efeitos anti-inflamatórios intestinais na indução com DNBS, a análise macroscópica do cólon indicou que o NCE diminuiu o índice de atividade da doença (IAD). As concentrações de interleucina 1 beta (IL-1β) e do fator de necrose tumoral alfa (TNF-α) diminuíram, a de interleucina 10 (IL-10) aumentou e os níveis de malondialdeido (MDA) e mieloperoxidase (MPO) diminuíram quando comparados com o grupo controle. Além disso, foi observada uma diminuição da expressão gênica de marcadores inflamatórios como proteína quinase ativada por mitógeno 1 (MAPK-1) e fator nuclear kappa B (NF-κB p65) nas amostras de cólon. A integridade epitelial foi melhorada segundo as análises histopatológica e imunohistoquímica. Os grupos que receberam doses de 200 e 300 mg/kg apresentaram melhores resultados.

Análises físico-químicas mostraram que as nanopartículas carregadas com extrato (NPE) são esféricas com carga superficial positiva, tamanho de 76,45 nm, potencial zeta positivo, alta eficiência de encapsulamento (EE = 100%) e estáveis por 30 dias. Quanto aos efeitos anti-inflamatórios intestinais na indução com DSS, foi observado que o tratamento com o extrato livre NCE (200 mg/kg) e com NPE (4 mg/kg) também reduziram o índice de atividade da doença (IAD), preveniram o encurtamento do cólon e promoveram redução na expressão de marcadores inflamatórios como IL-1β, TNF-α, interleucina 6 (IL-6), receptor *toll-like* tipo 4 (TLR-4), proteína quimiotática de monócitos 1 (MCP-1), proteína inflamatória de macrófagos 2 (MIP-2), molécula de adesão intercelular 1 (ICAM-1) e óxido nítrico sintase induzível (iNOS). Uma melhora da integridade da mucosa intestinal dos animais tratados com NCE e NPE também foi observada mediante um aumento na expressão de marcadores de barreira como Zona de oclusão 1 (ZO-1), Ocludina (OCLN) e Mucina 3 (MUC-3), os achados histopatológicos corroboraram com estes resultados.

Os efeitos do NCE também foram positivos no modelo de síndrome metabólica induzida em camundongos utilizando dieta rica em gordura. A administração de NCE em camundongos obesos reduziu significativamente o ganho de peso corporal, quando comparado ao grupo não tratado, embora não tenham sido observadas diferenças significativas no consumo de energia entre estes grupos. A administração de NCE também reduziu a glicemia basal e a resistência à insulina, mostrou uma melhora no perfil lipídico plasmático em comparação com os camundongos obesos não tratados e resultou significativamente em um aumento da expressão do transportador de glicose GLUT-4 no fígado, confirmando assim o aumento da sinalização da insulina, evidenciado pela melhora dos níveis de glicose no sangue dos camundongos obesos tratados. A expressão do receptor de leptina (Leptin-R) no tecido hepático dos camundongos obesos tratados foi reduzida, mas houve uma recuperação significativa com o tratamento com NCE. Além disso, foi observado um aumento na expressão do receptor alfa ativado por proliferador de peroxissomo (PPAR-α) no grupo tratado. A expressão proteica da proteína quinase ativada por monofosfato de adenosina (AMPK) e da fosfoinositídeo 3-quinase (PI3K) no fígado dos camundongos alimentados por HFD foi diminuída, porém, houve uma recuperação significativa nos animais tratados. Análises da expressão dos marcadores de barreira intestinal (ZO-1 e MUC-3) em amostras de cólon de camundongos obesos tratados indicaram que o extrato conseguiu melhorar a integridade da barreira intestinal, a qual é normalmente comprometida em camundongos obesos.

CONCLUSÃO

Em relação aos efeitos de NCE do modelo de inflamação intestinal por DNBS e de NCE e NPE no modelo por DSS, foi observado que ambos apresentaram efeito preventivo e anti-inflamatório por meio da redução no escore do índice de atividade da doença e nos danos macroscópicos e microscópicos do cólon. Através das análises moleculares realizadas, foi possível observar que NCE e NPE diminuíram os níveis de mediadores inflamatórios e oxidativos, e promoveram a regulação negativa da expressão de genes de importantes vias inflamatórias e oxidativas. Além disso, NCE e NPE contribuíram para a melhora da integridade epitelial de acordo com as análises de marcadores de barreira e através das técnicas histológicas. O extrato livre e o associado a nanopartículas apresentaram resultados semelhantes, no entanto, a dose de NCE incorporado no NPE foi 50x menor que a dose de extrato livre avaliado no ensaio de indução inflamatória intestinal por DSS.

Nos ensaios de síndrome metabólica induzida por dieta, o NCE apresentou uma melhora no perfil metabólico dos camundongos obesos, assim também como uma significativa redução do ganho de peso corporal. Estes efeitos foram associados a uma melhora no estado inflamatório sistêmico e diferentes mecanismos parecem estar envolvidos, destacamos os possíveis efeitos imunomoduladores dos fenólicos, já que esses compostos podem ter efeitos benéficos na regulação de genes envolvidos em processos metabólicos, inflamatórios e de estresse oxidativo. No entanto, é necessário realizar mais estudos para entender completamente os mecanismos subjacentes.

Os resultados pré-clínicos *in vivo* indicam que NCE livre ou incorporado a nanopartículas é benéfico na prevenção da colite induzida e na síndrome metabólica, portanto, os resultados deste estudo dão suporte a futuras investigações sobre o potencial terapêutico do extrato de *N. cochenillifera* no tratamento das doenças inflamatórias intestinais e da síndrome metabólica e indica seu potencial promissor como um ingrediente bioativo para o desenvolvimento de um fitoterápico ou um suplemento funcional inovador no tratamento complementar destas doenças.

RESUMEN

INTRODUCCIÓN

Las enfermedades inflamatorias intestinales (EII) y el síndrome metabólico son dos trastornos de salud en aumento en todo el mundo, especialmente en los países desarrollados (1–3). Las EII, incluidas la enfermedad de Crohn y la colitis ulcerosa, son enfermedades crónicas que afectan al tracto gastrointestinal y pueden causar síntomas como rectorragia, diarrea con moco o sangre, dolor abdominal, fatiga y pérdida de peso (4). El síndrome metabólico, por su parte, es un conjunto de afecciones médicas que incluyen obesidad abdominal, hipertensión, aumento de los niveles de azúcar en sangre y dislipidemia (5).

Ambas son enfermedades multifactoriales y complejas, en cuya etiopatogenia interviene una combinación de factores genéticos, ambientales y conductuales. En el caso de la EII, se cree que la interacción entre la microbiota intestinal, el sistema inmunitario y los factores ambientales puede desempeñar un papel importante en su desarrollo. Además, factores como el tabaquismo, el estrés y el uso prolongado de antiinflamatorios no esteroideos también pueden contribuir al desarrollo de la EII (6,7).

Así como las EII, el síndrome metabólico también está asociado con una inflamación crónica implicada en su patogénesis. El conjunto de factores de riesgo, como la obesidad abdominal, resistencia a la insulina, hipertensión arterial y dislipidemia, aumentan el riesgo de desarrollar enfermedades cardiovasculares, como un ataque cardíaco o un accidente cerebrovascular (8). La inflamación crónica ocurre cuando el sistema inmunológico del cuerpo se activa de forma persistente, lo que lleva a una producción continua de citocinas proinflamatorias y a un estado inflamatorio crónico. El tratamiento del síndrome metabólico a menudo implica la reducción de la inflamación crónica a través de cambios en el estilo de vida, como una dieta saludable, ejercicio regular y control del estrés, además de medicamentos para controlar la presión arterial, reducir los niveles de azúcar en sangre y disminuir los niveles de colesterol y triglicéridos. Aunque las EII y el síndrome metabólico son condiciones diferentes, pueden estar relacionadas en ciertos individuos, y una mejor comprensión de la inflamación crónica puede ayudar en el desarrollo de tratamientos más efectivos para ambas condiciones (9).

Las evidencias clínicas han mostrado que el uso de fenoles aislados o de extractos ricos en fenoles administrados en combinación con medicamentos ya utilizados en la terapia de las EII y del síndrome metabólico ha contribuido a mejorar la calidad de vida de los pacientes y para mantener la enfermedad en remisión (10,11). Los polifenoles son metabolitos secundarios producidos por plantas que poseen propiedades antioxidante y antiinflamatoria, lo que los hace

efectivos en la prevención y tratamiento de estas enfermedades. Su notable capacidad antiinflamatoria y antioxidante se debe a múltiples mecanismos de acción, como la inhibición de la producción o acción de mediadores proinflamatorios o incluso su fuerte influencia sobre la microbiota intestinal (12–14).

En este escenario, la cactácea *Nopalea cochenillifera* (L.) Salm-Dyck, conocida popularmente como nopal, nopal cactus o "*palma forrageira doce ou miúda*" en portugués, es una buena fuente de compuestos bioactivos antiinflamatorios. Sus cladodios son ricos en polisacáridos y polifenoles (15), y se han utilizado ampliamente con fines agrícolas, alimentarios y medicinales (16). Tradicionalmente, se ha usado como antiinflamatorio y cicatrizante en el tratamiento de enfermedades como la hipercolesterolemia, la presión arterial, problemas renales y urinarios, y en el tratamiento de la diabetes (17,18). Estudios anteriores han informado sobre el potencial antibiótico y antifúngico del *N. cochenillifera* en ensayos *in vitro* (19,20). Además, se ha observado la reducción de los niveles de glucosa en estudios *in vivo* (21) y en un ensayo clínico piloto (22). En cuanto a su efecto antiinflamatorio, la administración oral del extracto hidroalcohólico de los cladodios de *N. cochenillifera* ha demostrado una significativa actividad antiinflamatoria en modelos de inducción de granuloma y úlcera gástrica en roedores (23,24).

Los polifenoles presentes en el extracto de *N. cochenillifera* ya se consideran una fuente prometedora de agentes bioactivos. Sin embargo, cuando se trata de enfermedades inflamatorias intestinales, dirigir estos compuestos activos a la región del colon y reducir las concentraciones de extractos vegetales necesarias para lograr actividad farmacológica todavía son desafíos por superar. El desarrollo de sistemas de administración de medicamentos capaces de transportar las sustancias activas del extracto hasta el tejido del colon es una alternativa prometedora para mejorar la biodisponibilidad oral y prolongar su retención en el colon. Los sistemas nanoestructurados han mostrado propiedades interesantes y prometedoras en este sentido, como la mejora de la estabilidad, solubilidad y biodisponibilidad de compuestos naturales, así como la posibilidad de controlar la liberación de los compuestos bioactivos y reducir las dosis y frecuencias de administración (25–27). Estrategias que involucren la encapsulación del extracto de *N. cochenillifera* y la dirección de su liberación hacia la región del colon pueden potenciar su eficacia y reducir la dosis terapéutica necesaria.

Teniendo en cuenta el potencial bioactivo de *N. cochenillifera*, es relevante destacar que esta especie es una excelente opción para el desarrollo de un insumo nacional, debido a su adaptación a la región nordeste de Brasil y a la presencia de cultivos establecidos. Esto permite el desarrollo de toda la cadena productiva en el país, desde el cultivo hasta el insumo y/o

producto terminado, lo que puede tener impactos positivos en la economía local, como la generación de empleos y la promoción del desarrollo sostenible de la región. En este contexto, la presente propuesta tiene como objetivo realizar un estudio fitoquímico del extracto de *N. cochenillifera* y evaluar el efecto antiinflamatorio en modelos *in vivo* de inflamación intestinal y síndrome metabólico.

OBJETIVO

El presente trabajo tuvo como objetivo realizar un estudio fitoquímico del extracto hidroalcohólico de cladodios de *Nopalea cochenillifera*, así como evaluar la toxicidad y eficacia en modelos in vivo de inflamación intestinal y síndrome metabólico. Además, este trabajo tuvo como objetivo desarrollar y caracterizar un sistema nanoparticulado cargado con el extracto de *N. cochenillifera* y evaluar el efecto farmacológico del extracto libre (NCE) y asociado a nanopartículas (NPE).

De esta manera, se propusieron cinco objetivos específicos:

1. Caracterizar fisicoquímicamente el extracto hidroalcohólico de *N. cochenillifera*, determinar el contenido de compuestos fenólicos totales y flavonoides totales y el perfil cromatográfico mediante cromatografía líquida de alta resolución acoplada a espectrometría de masas (CLAE-EM).
2. Evaluar la toxicidad oral aguda del extracto hidroalcohólico de *N. cochenillifera* en ratas.
3. Evaluar el efecto antiinflamatorio intestinal de diferentes dosis del extracto hidroalcohólico de *N. cochenillifera* en un modelo de inflamación intestinal experimental inducido por ácido 2,4-dinitrobenceno sulfónico (DNBS) en ratas.
4. Desarrollar, caracterizar y evaluar los efectos de un sistema nanoparticulado cargado extracto hidroalcohólico de *N. cochenillifera* en un modelo de inflamación intestinal experimental inducido por sulfato de sodio de dextrano (DSS) en ratones.
5. Evaluar el efecto del extracto hidroalcohólico de *N. cochenillifera* en un modelo experimental de síndrome metabólico inducido por una dieta alta en grasas en ratones.

METODOLOGÍA

1. *Preparación y caracterización fisicoquímica del extracto hidroalcohólico de N. cochenillifera (NCE)*

Los cladodios de *N. cochenillifera* fueron recolectados, luego fragmentados en pedazos más pequeños, secados en estufa de aire circulante, triturados y sometidos a extracción por el método de maceración con solvente hidroalcohólico en la proporción 1:10 (*p/v*). En el análisis fisicoquímico del NCE, se determinaron el pH, la acidez titulable, los contenidos de humedad, cenizas, extracto etéreo, fibra bruta, proteínas y carbohidratos totales. Estos análisis se realizaron de acuerdo con los métodos recomendados por AOAC (2020). El contenido total de fenoles del extracto de NCE se determinó mediante el método del reactivo Folin-Ciocalteu (28) y el contenido total de flavonoides se determinó mediante el método colorimétrico del cloruro de aluminio (29). El perfil cromatográfico se determinó mediante cromatografía líquida de alta eficiencia acoplada a espectrómetro de masas con fuente de ionización por electrospray (CLAE-IES-EM).

2. Evaluación de la toxicidad oral aguda del NCE en ratas

La toxicidad aguda por vía oral del extracto de *N. cochenillifera* se llevó a cabo siguiendo los criterios recomendados por la OECD, 2001 (*Guidelines for Testing of Chemicals*) (30). Se utilizaron ratas de la cepa Wistar (*Rattus norvegicus*). El grupo de prueba recibió una dosis única de 2000 mg/kg de NCE. En los días 1, 7 y 14 después de la administración de NCE, se sometió a los animales del grupo de prueba y de control a pruebas de comportamiento y motor (prueba de campo abierto y rota-rod). En el día 15, los animales fueron anestesiados y se realizó una extracción de sangre por punción cardíaca para realizar análisis hematológicos y bioquímicos. Los órganos (hígado, riñón y bazo) de los animales fueron examinados macroscópica y microscópicamente.

3. Estudio de la actividad antiinflamatoria intestinal "in vivo"

La inducción de la inflamación intestinal se efectuó mediante el uso de DNBS en ratas (31) y DSS en ratones C57BL/6J (32). En el estudio con DNBS, se administraron 3 diferentes dosis de NCE (100, 200 y 300 mg/kg/día) a los animales. En el estudio con DSS, se investigó el efecto antiinflamatorio del extracto libre (200 mg/kg/día) y del extracto incorporado en nanopartículas poliméricas. En ambos casos, se evaluó el índice de actividad de la enfermedad (IAD) mediante la variación del peso corporal, la presencia de hemorragia rectal y la consistencia de las heces (32). Después de la eutanasia, se evaluó la expresión de marcadores inflamatorios y oxidativos, así como un análisis microscópico en muestras de colon. Además, se realizó una evaluación de la permeabilidad intestinal mediante el método de administración

oral de FITC-dextrano en los animales sometidos a la inducción inflamatoria intestinal por DSS (33).

4. Obtención y caracterización de las nanopartículas poliméricas

Las nanopartículas cargadas con extracto de *N. cochenillifera* (NPE) se prepararon mediante el método de nanoprecipitación (34,35). Las nanopartículas se caracterizaron según su tamaño, índice de polidispersión (PdI), potencial zeta, eficiencia de encapsulación (EE) y morfología. La estabilidad física de las nanopartículas se evaluó durante un período de 30 días.

5. Estudio del efecto del extracto de N. cochenillifera en un modelo de síndrome metabólico

Se dividieron aleatoriamente ratones machos C57BL/6J en cuatro grupos experimentales: control (dieta estándar); control + NCE (dieta estándar, tratados con NCE (200 mg/kg)), control (dieta rica en grasas) y control + NCE (dieta rica en grasas, tratados con NCE (200 mg)) (36). Durante el período experimental de 10 semanas, se evaluó el peso corporal y la ingesta de agua y comida. Una semana antes de la eutanasia, los ratones fueron privados de alimentos durante 6 horas y se realizó una prueba de tolerancia a la glucosa. Al final del experimento, los animales fueron anestesiados y se realizó una extracción de sangre por punción cardíaca para medir los niveles plasmáticos de glucosa. Se recolectaron y pesaron el hígado, bazo, riñones, colon, grasa abdominal, epididimal y marrón, y se analizaron macroscópicamente. Se procesaron muestras de hígado, colon y/o tejido adiposo para determinaciones bioquímicas y evaluar la expresión génica de diferentes marcadores mediante PCR cuantitativa en tiempo real (RT-qPCR).

RESULTADOS

El contenido de fenoles y flavonoides totales por gramo de extracto seco fue de 67,85 y 46,16 mg/g, respectivamente. A través del análisis por CLAE-IES-EM, se caracterizaron un total de 25 compuestos como sacáridos, ácidos orgánicos, ácidos fenólicos y flavonoides. En el estudio de toxicidad, la dosis de 2000 mg/kg de extracto administrada por vía oral no mostró signos de toxicidad, mortalidad o alteraciones significativas en los parámetros conductuales, bioquímicos y hematológicos.

En cuanto a los efectos antiinflamatorios intestinales en la inducción con DNBS, el análisis macroscópico del colon indicó que el NCE disminuyó el índice de actividad de la enfermedad (IAE). La concentración de interleucina (IL) 1 beta y factor de necrosis tumoral alfa (TNF-α) disminuyeron, de la IL-10 aumentó y los niveles de malondialdehído (MDA) y mieloperoxidasa (MPO) disminuyeron en comparación con el grupo control. Además, se observó una

disminución en la expresión génica de marcadores inflamatorios como proteína quinasa activada por mitógenos 1 (MAPK-1) y factor nuclear kappa B (NF-κB p65) en las muestras de colon. La integridad epitelial mejoró según los análisis histopatológicos e inmunohistoquímicos. Los grupos que recibieron dosis de 200 y 300 mg/kg presentaron mejores resultados.

Los análisis fisicoquímicos mostraron que las nanopartículas cargadas con extracto (NPE) son esféricas, con carga superficial positiva, tamaño de 76,45 nm, potencial zeta positivo, alta eficiencia de encapsulación (EE = 100%) y estables por 30 días. En cuanto a los efectos antiinflamatorios intestinales en la inducción con DSS, se observó que el tratamiento con el NCE (200 mg/kg) y con NPE (4 mg/kg) también redujo el índice de actividad de la enfermedad (IAD), previno el acortamiento del colon y promovió la reducción en la expresión de marcadores inflamatorios como IL-1β, TNF-α, IL-6, receptor *toll-like* tipo 4 (TLR-4), proteína quimioatrayente de monocitos 1 (MCP-1), proteína inflamatoria de macrófagos 2 (MIP-2), molécula de adhesión intercelular 1 (ICAM-1) y óxido nítrico sintasa inducible (iNOS). Además, se observó una mejora en la integridad de la mucosa intestinal de los animales tratados con NCE y NPE a través de un aumento en la expresión de marcadores de barrera como Zona de oclusión 1 (ZO-1), Ocludina (OCLN) y Mucina 3 (MUC-3), los hallazgos histopatológicos corroboraron estos resultados.

Los efectos del NCE también fueron positivos en un modelo de síndrome metabólico inducido en ratones mediante una dieta alta en grasas. La administración de NCE en ratones obesos redujo significativamente el peso corporal en comparación con el grupo no tratado, aunque no se observaron diferencias significativas en el consumo de energía entre estos grupos. La administración de NCE también redujo la glucemia basal y la resistencia a la insulina, mostró una mejora en el perfil lipídico plasmático en comparación con los ratones obesos no tratados y resultó en un aumento significativo en la expresión del transportador de glucosa (GLUT-4) en el hígado, confirmando así el aumento de la señalización de insulina, evidenciado por la reducción de los niveles de glucosa en sangre en los ratones obesos tratados. La expresión del receptor de leptina (Leptina-R) en el tejido hepático de los ratones obesos tratados se redujo, pero hubo una recuperación significativa con el tratamiento con NCE. Además, se observó un aumento en la expresión del receptor activado por proliferadores peroxisómicos tipo alfa (PPAR-α) en el grupo tratado. La expresión proteica de la proteína quinasa activada por monofosfato de adenosina (AMPK) y de la fosfatidilinositol 3-quinasa (PI3K) en el hígado de los ratones alimentados con HFD se redujo, pero hubo una recuperación significativa en los

animales tratados. Los análisis de la expresión de los marcadores de barrera intestinal (ZO-1 y MUC-3) en muestras de colon de ratones obesos tratados indicaron que el extracto fue capaz de mejorar la integridad de la barrera intestinal, la cual se ve normalmente comprometida en ratones obesos.

CONCLUSIÓN

La administración de NCE en el modelo DNBS de inflamación intestinal y de NCE y NPE en el modelo DSS, mostró un efecto preventivo y antiinflamatorio al reducir la puntuación del índice de actividad de la enfermedad y el daño macroscópico y microscópico del colon. A través de los análisis moleculares realizados, se pudo observar que NCE y NPE disminuyeron los niveles de mediadores inflamatorios y oxidativos, y promovieron la regulación negativa de la expresión de genes de importantes vías inflamatorias y oxidativas. Además, NCE y NPE contribuyeron a la mejora de la integridad epitelial según el análisis de marcadores de barrera y mediante técnicas histológicas. El extracto libre y el asociado a nanopartículas mostraron resultados similares, sin embargo, la dosis de NCE incorporada en NPE fue 50 veces inferior a la dosis de extracto libre evaluada en el ensayo de inducción inflamatoria intestinal por DSS.

En los ensayos de síndrome metabólico inducido por dieta, el NCE mostró una mejora del perfil metabólico de los ratones obesos, así como una reducción significativa del aumento de peso corporal. Estos efectos se asociaron a una mejora del estado inflamatorio sistémico y parecen estar implicados diferentes mecanismos, destacamos los posibles efectos inmunomoduladores de los compuestos fenólicos, ya que éstos pueden tener efectos beneficiosos sobre la regulación de genes implicados en procesos metabólicos, inflamatorios y de estrés oxidativo. Sin embargo, se necesitan más estudios para comprender plenamente los mecanismos subyacentes.

Los resultados preclínicos *in vivo* indican que el NCE libre o incorporado en nanopartículas es beneficioso para prevenir la colitis inducida y el síndrome metabólico, por lo tanto, los resultados de este estudio apoyan futuras investigaciones sobre el potencial terapéutico del extracto de *N. cochenillifera* en el tratamiento de las enfermedades inflamatorias intestinales y del síndrome metabólico e indica su prometedor potencial como un ingrediente bioactivo prometedor para el desarrollo de fitoterapéuticos o suplementos funcionales innovadores en el tratamiento complementario de estas enfermedades.

INDEX

I. INTRODUCTION

1.1 INFLAMMATORY BOWEL DISEASE (IBD)

Inflammatory bowel disease (IBD) is a group of disorders that cause chronic inflammatory conditions in the gastrointestinal tract. The incidence of IBD has been increasing in many countries over the past few decades, particularly in developing countries undergoing rapid urbanization and westernization (37). The reasons for this increase are not fully understood, but it is believed to be related to changes in diet, lifestyle, and environmental factors.

IBD is considered a public health problem in many countries due to its significant impact on healthcare utilization and costs. Recurrent hospitalizations, frequent surgeries, and the high expense of drug treatments can place a substantial burden on healthcare systems and for individuals affected by the disease. In addition, IBD can significantly impact a person's quality of life, as it can cause chronic pain, discomfort, and even disability in severe cases (38).

Crohn's disease (CD) and ulcerative colitis (UC) are the two main types of inflammatory bowel disease (IBD). In both conditions, the diagnosis of IBD usually involves a combination of medical history, physical examination, blood tests, and imaging tests such as colonoscopy. However, while they share some similarities, the CD and UC differ in symptoms, location in the gastrointestinal tract, and complications (39). Table 1 describes the main differences between Crohn's disease and ulcerative colitis.

Table 1. Differences between Crohn disease and ulcerative colitis.

Feature	Crohn's Disease	Ulcerative Colitis
Location	It can occur anywhere in the digestive tract, from mouth to anus	Limited to the colon and rectum
Inflammation	Inflammation occurs in patches, with healthy tissue in between	Inflammation is continuous along the colon
Symptoms	Abdominal pain, diarrhea, weight loss, fatigue, anemia	Abdominal pain, diarrhea, rectal bleeding, urgency, tenesmus
Complications	Fistulas (abnormal connections between different parts of the digestive tract), abscesses, strictures (narrowing of the digestive tract), bowel obstruction	Toxic megacolon (severe dilation of the colon), colon cancer, perforation, severe bleeding

Etiopathogenesis

The exact cause of IBD is still unknown, but it is believed to result from a complex interaction between genetic, environmental, and immune factors.

Genetic factors

Research suggests that specific genes may make some people more susceptible to developing IBD. Several genes have been associated with increased risk of IBD; for example, the Nucleotide Binding Oligomerization Domain Containing 2 (NOD2) gene (previously known as CARD15) participates in the regulation of the immune system and is one of the most well-studied genetic risk factors for Crohn's disease. Variations in the NOD2/CARD15 gene have been linked to a higher risk of developing the disease (40). The Interleukin 23 Receptor (IL23R) is involved in the regulation of the immune system and has been associated with both Crohn's disease and ulcerative colitis (40).

The protein-coding gene, autophagy Related 16 Like 1 (ATG16L1), plays a role in the process of autophagy and is involved in removing damaged cells from the body. Scientists have related variations in the ATG16L1 gene to an increased susceptibility to Crohn's disease (41). In addition, the immunity-related GTPase family M (IRGM) gene is also involved in the process of autophagy and has been associated with an increased risk of developing Crohn's disease (42). Finally, the tumor necrosis factor superfamily 15 (TNFSF15) is the gene most consistently associated with irritable bowel syndrome, is involved in regulating the immune system, and has been linked to Crohn's disease and ulcerative colitis (43). It is important to note that possessing these genes does not guarantee the development of the disease, and the absence of a family history of the disease does not exclude the possibility of someone developing IBD (41).

Environmental factors

Environmental factors may also play a role in the development of IBD. For example, studies have shown that diet, smoking, some medications, and exposure to certain types of bacteria or viruses may increase the likelihood of developing the condition (44–46). In addition, studies have suggested that a diet high in fat, sugar, and processed foods, may increase the risk of developing IBD. On the other hand, a diet that is high in fiber, fruits, and vegetables may be protective to avoid the disease development (47,48).

Studies have consistently shown that smoking increases the risk of developing CD and a more severe clinical course. Smoking has been shown to affect the immune system, the microbiota, and the permeability of the intestinal mucosa, leading to an influx of harmful substances and bacteria into the intestine (44,49). The link between smoking and IBD is complex, and the effects of smoking may vary depending on the type of IBD. While smoking is a risk factor for CD, it appears to have a protective effect against UC (50,51).

The use of antibiotics has been correlated with an increased risk of developing IBD, possibly by altering the gut microbiota. A recent meta-analysis of observational studies found that antibiotic use was associated with a 1.5-fold increased risk of developing IBD (52). Additionally, studies have suggested that exposure to certain types of bacteria or infections during childhood may be protective against the development of IBD. This theory has become known as the "hygiene hypothesis" (53). The intestinal microbiota is a complex and dynamic ecosystem that can influence a wide range of environmental factors, including diet, pollution, antibiotics, and infectious agents. Understanding these influences is crucial for implementing strategies to prevent and treat IBD.

Intestinal microbiota in IBD

The intestinal microbiota participates in many processes, including digestion, nutrient absorption, immune system function, and the production of vitamins and other essential compounds. It also helps prevent harmful microorganisms from colonizing the digestive tract and can impact overall health and disease. The intestinal microbial communities in patients with IBD are significantly different from those in healthy individuals, a condition called dysbiosis. Studies have shown that the bacteria concentration is higher in IBD patients than in healthy controls (54–56).

However, despite the increase in bacterial concentration, the gut microbiota in IBD patients is characterized by fewer bacterial species and is unstable over time, even in patients in remission (56). In a healthy gut, the microbiota is dominated by the phyla *Bacillota* (synonym *Firmicutes*) and *Bacteroidota*, followed by *Actinobacteria* and *Proteobacteria* in lesser amounts. In contrast, in IBD, there is a decrease in *Firmicutes* and *Bacteroidetes*, while *Actinobacteria* and *Proteobacteria* are considerably increased (57). Furthermore, IBD patients show reduced diversity of the gut microbiota, which is correlated with a decline in the diversity of *Firmicutes* and in genera such as *Faecalibacterium*, *Bifidobacterium*, and *Lactobacillus*, which are associated with mucosal protection in the intestine (58,59). On the other hand, species belonging to the family *Enterobacteriaceae* are relatively expanded in fecal samples from IBD patients, including facultative aerobes and different translocating and gram-negative pathogens like adherent invasive *Escherichia coli* (60,61).

Gram-negative bacterial overgrowth in the intestine has been linked to increased lipopolysaccharides (LPS) levels, which can trigger an immune response and lead to chronic inflammation. In addition, dysbiosis can also lead to an oxidative stress environment in the

intestine, which in turn can contribute to tissue damage and a further increase in pro-inflammatory cytokines. This cycle of chronic inflammation and tissue damage can lead to the development and exacerbation of IBD (62). In summary, Figure 1 shows various factors that can interfere with the composition of the gut microbial community and some effects of dysbiosis in IBD.

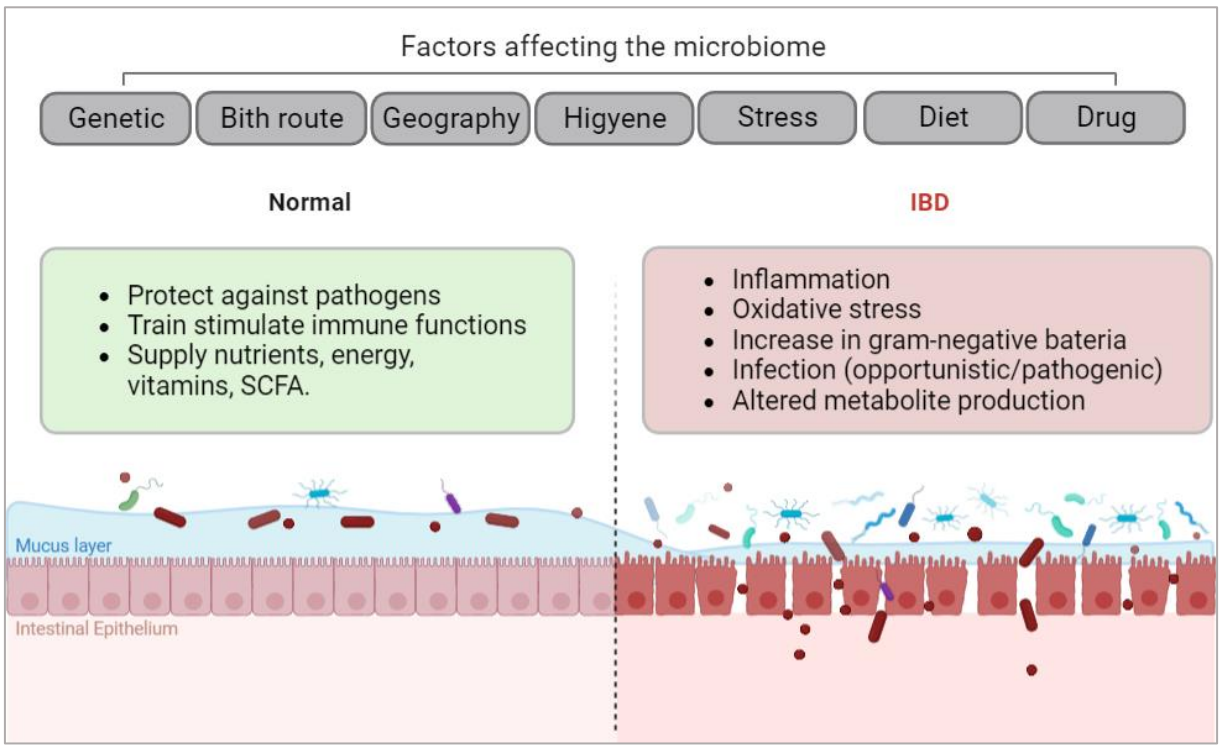

Figure 1. Factors affecting the stability and complexity of the intestine microbiome in health and inflammatory bowel disease (IBD). In the healthy intestine, important physiological processes are preserved, such as protection against pathogens, immune system training, and food digestion to supply energy and nutrients, including vitamins and short-chain fatty acids (SCFAs). Many factors are indicated to impact the microbiome throughout life, including genetics, diet, and medication, among others (marked in the grey boxes at the top of the figure). The characteristics of an imbalanced microbiome in the case of IBD include, for example, an increase in Gram-negative bacteria linked to an environment of oxidative stress and inflammation.

In some cases, specific interventions such as probiotics or fecal microbiota transplantation (FMT) may be used to restore the gut microbiota and alleviate symptoms of IBD (63–65). In addition to these interventions, studies have suggested that dietary phenolic compounds found in many plant-based foods may have anti-inflammatory effects and help alleviate symptoms of IBD. In animal studies, these compounds have been shown to modulate the gut microbiota and reduce inflammation. In addition, some human studies have suggested that phenolic compounds may benefit people with IBD (66,67).

Intestinal Barrier Dysfunction in IBD

The intestinal barrier is a complex structure composed of several components that work together to maintain its integrity. These components include the intestinal epithelial cells, the mucus layer, and the intestinal microbiota. The intestinal epithelial cells are the primary physical barrier between the luminal contents and the underlying tissues. These cells are tightly packed together, forming a layer preventing harmful substances from passage. In addition, the tight junctions between the epithelial cells are critical for maintaining the integrity of the barrier, as they contain the movement of large molecules and pathogens (68).

Intestinal barrier dysfunction in IBD can be attributed to multiple factors, including changes to the mucus layer and alterations to the intestinal microbiome. In IBD, the mucus layer that lines the intestine is thinner and less effective, which enables harmful bacteria to interact with epithelial cells and trigger an inflammatory response. Mucins are large, highly glycosylated proteins that protect the gastrointestinal tract by forming a protective barrier against luminal contents, including bacteria and toxins (69). In addition, goblet cells are responsible for producing and secreting various bioactive molecules such as mucins and trefoil factor peptides (TFFs). The secreted mucins include the secretory mucin glycoproteins (MUC-2) and epithelial membrane-bound mucins (MUC-1 and MUC-3). MUC-2 is the major secreted mucin in the small intestine and colon and is critical for forming the mucus layer in the gastrointestinal tract (70).

The intestinal epithelial barrier can also be compromised due to changes in the tight junctions (TJ) and desmosomes, the primary intercellular junctions that provide the structural integrity of the intestinal epithelium (68). Tight junctions, also known as zonula occludens (ZO), are the most apical component of the epithelial junctional complex and form a seal between adjacent cells, preventing the paracellular movement of solutes, ions, and immune cells. TJ consist of transmembrane proteins, including claudins, occludin, and junctional adhesion molecules (JAMs), which interact with cytoplasmic scaffolding proteins, such as ZO (ZO-1, ZO-2, and ZO-3) (71). For example, ZO-1 is a positive regulator of the mucosal barrier, and the negative regulation of this protein increases its permeability (72) (Figure 2).

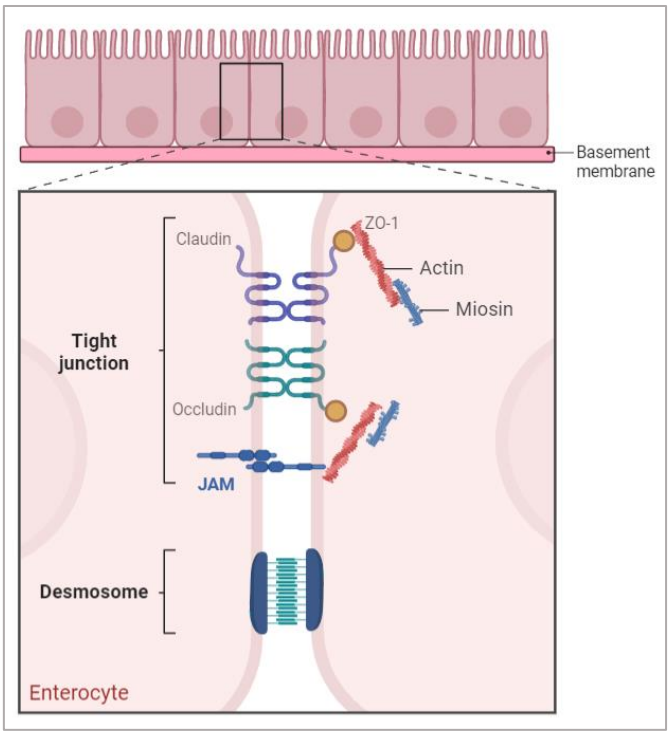

Figure 1. Structural integrity of the intestinal epithelial barrier and interactions between adjacent cells via the tight junctions. The proteins forming these junctions are claudin, occludin, and zonula occludens-1 (*Zo-1*), interacting with the cytoskeletal filaments (actin and myosin). The proteins of the junctional adhesion molecules (JAMs) that interact with actin. Further down is the desmosome.

In IBD, the expression and distribution of tight junction proteins, including occludin and claudin, can be altered, leading to increased permeability of the intestinal epithelium. Studies have shown that reduced expression of occludin and claudin-1 is associated with increased intestinal permeability in patients with IBD. Overall, alterations in the TJ in IBD can lead to increased intestinal permeability, allowing for the translocation of luminal antigens, such as bacteria and endotoxins, into the lamina propria, triggering an immune response and inflammation (71).

Immune Response

IBD involves a dysregulated immune response in the gut, including innate and adaptive immune responses. The innate immune system is composed of physical and chemical barriers and various defense cells. The principal cells of the immune system are macrophages, neutrophils, mast cells, eosinophils, basophils, T and B lymphocytes, natural killer (NK) cells, and dendritic cells. These cells work together to recognize and eliminate foreign particles, such as viruses, bacteria, and parasites, to protect the body from infection and disease. The innate immune system acts as the first line of defense, while the adaptive immune system, which includes T and B lymphocytes, provides a more specific and targeted response to invading pathogens (73–75).

During an intestinal inflammatory response, leukocytes (including macrophages, neutrophils, lymphocytes, and dendritic cells) interact with inflammatory mediators such as nuclear factor kappa b (NF-κB p65), TNF-α, interleukins (IL-1β and IL-6), and cyclooxygenases (COXs), through the activation of signaling molecules. These interactions lead to the recruitment of other immune cells to the area of inflammation and the release of cytokines and chemokines that promote inflammation. The intestinal inflammatory response typically occurs in four phases: the initiation phase, amplification phase, effector phase, and resolution phase. In the first phase, the vascular phase, vasodilation occurs, leading to an elevation of blood flow to the injury site. This causes the affected area to become reddened and warm. The inflammatory mediators also cause the vascular endothelial cells to contract, increasing capillary permeability (74).

In the second phase, circulating immune cells, including neutrophils, macrophages, and other cells, migrate from the blood vessels to the site of injury and use a variety of mechanisms to neutralize and remove the inflammatory trigger. These cells can phagocytize the invading pathogens and release cytotoxic proteins or chemicals to eliminate the pathogens. The communication between immune cells occurs through various mechanisms, including contact-mediated signaling and chemical signals from cytokines and chemokines. Chemokines such as monocyte chemoattractant protein-1 (MCP-1) and macrophage inflammatory protein-2(MIP-2) act as chemoattractants, recruiting immune cells to the site of injury or infection. This allows for a coordinated response to the inflammatory trigger, helping to clear the infection or neutralize the trigger (76,77).

After pathogen recognition, antigen-presenting cells (APCs) such as macrophages and dendritic cells process and present the antigenic fragments to T-cells and B-cells through major histocompatibility complex (MHC) proteins on their surface. This process is called antigen presentation and is essential for activating adaptive immune responses. Once activated, T and B cells differentiate into effector cells, producing specific cytokines and antibodies that help to eliminate the offending agent and promote tissue repair (78). T cells and B cells play essential roles in the adaptive immune response. T cells recognize processed antigens presented by APCs. They can activate other immune cells, such as B lymphocytes and macrophages, and coordinate the inflammatory response by releasing cytokines and chemokines. CD8+ T cells, also known as cytotoxic T cells, recognize antigen/MHC class I complexes on infected cells and promote their destruction. On the other hand, CD4+ T cells, also known as helper T cells, recognize antigen/MHC class II complexes on APCs and activate B lymphocytes to produce antibodies and macrophages to eliminate invading microorganisms. The antibodies produced

by B lymphocytes can neutralize or mark invading microorganisms for destruction by other immune cells (79).

The innate immune system also responds efficiently to a wide range of pathogens through pattern recognition receptors (PRRs) that identify pathogen-associated molecular patterns (PAMPs), which are conserved molecular structures present in pathogens but not host cells. Recognition of PAMPs by PRRs initiates the innate immune response, leading to the activation of various immune cells and the production of cytokines and chemokines. Toll-like receptors (TLRs) are PPRs that play a role in recognizing PAMPs and initiating the innate immune response (80). In IBD, TLRs can be stimulated by aggressive agents or activated dendritic cells within the intestinal epithelium, leading to chronic inflammation due to the failure of acute inflammatory mechanisms to eliminate tissue damage. The activated dendritic cells in the intestinal epithelium can stimulate TLRs and activate T cells, including CD4+ T cells. These T helper (Th) cells can then differentiate into various subsets, such as Th1, Th2, Th17, and regulatory T (Treg) cells, turning on the specific cytokine environment and the nature of the antigenic stimulation (81). Th1 cells are known to produce and secrete the cytokines interferon-gamma (IFN-γ) and TNF-β, which engage in protecting against infections by viruses and bacteria, as well as in the elimination of cancerous cells. Th2 cells, on the other hand, produce and secrete the cytokines IL-4, IL-5, IL-10, and IL-13, which are involved in activating B lymphocytes and promoting antibody production. Th17 cells have and secrete the cytokines IL-17, IL-6, IL-12, and TNF-α, which are involved in tissue inflammation and the activation of neutrophils to fight extracellular bacteria (Figure 3) (82–84).

Signaling through TLRs also activates an intracellular signaling cascade, leading to the nuclear translocation of transcription factors, such as NF-κB. Upon binding to their ligands, the TLRs receptors initiate a signaling cascade that activates IκB kinase. Activated IKK complex then phosphorylates inhibitor of kappa B (IκB), leading to its ubiquitination and subsequent degradation by the proteasome. This releases NF-κB dimers, such as p65/RelA and p50, from their cytoplasmic sequestration by IκB, allowing them to translocate to the nucleus. Once in the nucleus, NF-κB dimers bind to specific DNA sequences in the promoter regions of target genes and initiate transcription of pro-inflammatory cytokines, chemokines, adhesion molecules, and other mediators of inflammation (Figure 3) (85,86).

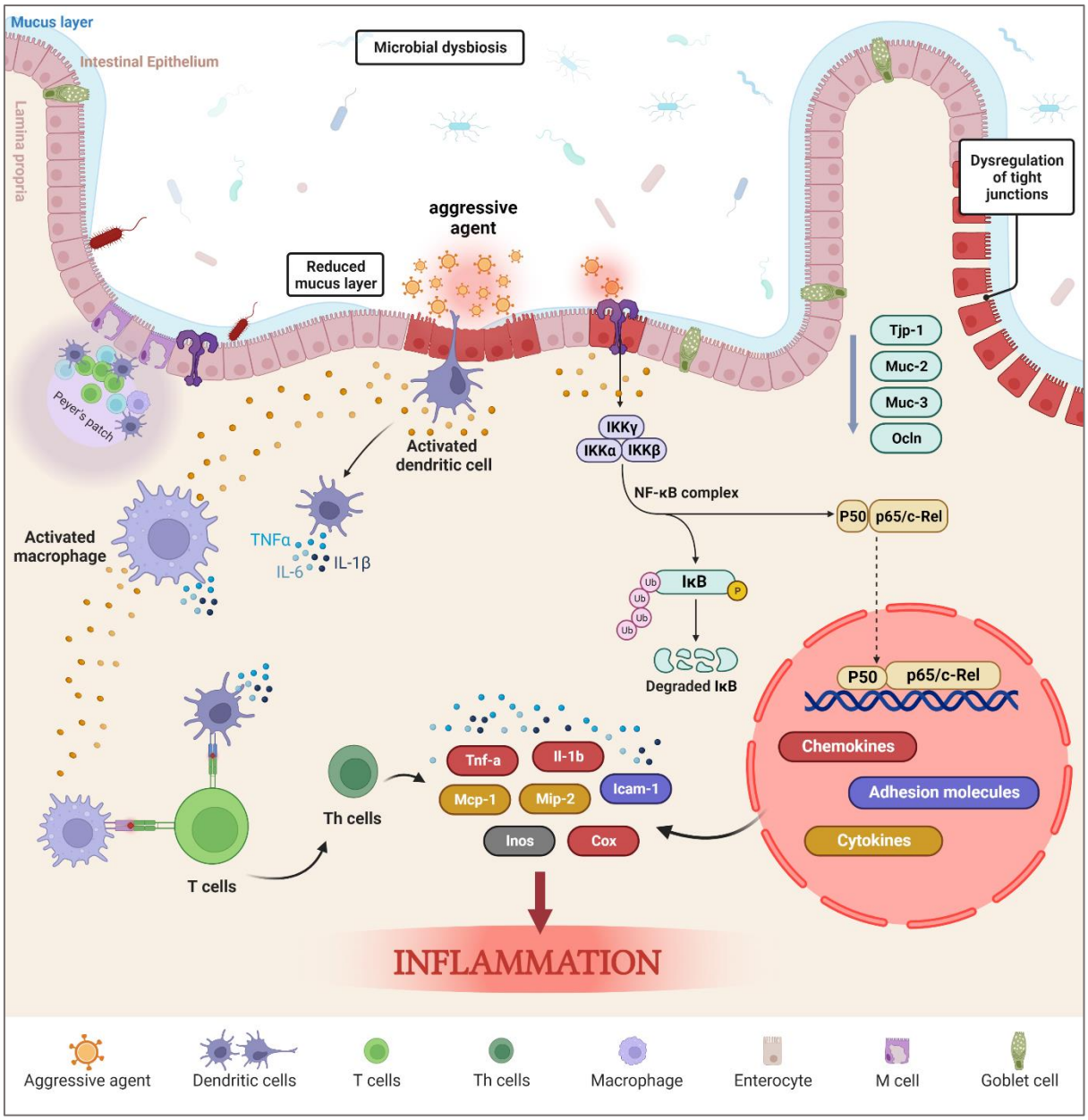

Figure 2. An aggressor agent's breakdown of intestinal homeostasis can trigger the chronic inflammatory process that characterizes IBD. During the initial inflammation, luminal antigens (substances that stimulate an immune response) activate different innate immune cells in the gut, including dendritic cells, macrophages, and T lymphocytes. The abnormally activated T helper (Th) cells, in coordination with antigen-presenting cells (APCs) such as macrophages and dendritic cells, synthesize and release distinct inflammatory mediators that generate an amplified inflammation, which leads to intestinal inflammation. The luminal antigens and activated dendritic cells can also stimulate toll-like receptors (TLRs) located on immune cells, which signal the NF-κB p65 release pathway by phosphorylation of the IKK complex. NF-κB p65 is then translocated to the cell nucleus promoting the gene transcription of different inflammatory and oxidative mediators (cytokines, chemokines, adhesion molecules, and nitric oxide inducible synthase enzyme - iNOS) that amplify the intestinal inflammatory process. In addition, NF-κB also promotes the intestinal barrier deregulation by down-regulating genes related to intestinal protection production, epithelial restitution, and intestinal permeability of the intestine.

Chronic inflammation is a prolonged and sustained immune response that can lead to tissue damage and destruction if left unchecked. In the case of IBD, chronic inflammation can cause damage to the intestinal wall, leading to complications such as strictures, abscesses, and fistulas. The goals of IBD treatment are to achieve remission of acute phase symptoms and maintain

remission by controlling chronic inflammation. This is typically done using anti-inflammatory drugs, immunosuppressants, and biological agents. In addition to managing inflammation, the treatment aims to prevent disease flares and associated complications. Improving the quality of life of patients with IBD is also an important goal of therapy, as the symptoms of the disease can significantly impact daily life (87,88).

Treatment of IBD

The treatment of IBD typically involves a combination of pharmacological and/or surgical approaches, depending on the type and severity of the disease. The primary goal of treatment is to control inflammation and reduce symptoms while promoting the healing of the damaged tissue in the digestive tract. Therefore, accurately diagnosing a patient's specific inflammatory bowel disease (IBD) type is crucial in determining the most appropriate treatment (89).

Some of the most common treatment practices include corticosteroids, such as prednisone, often used to reduce inflammation and relieve symptoms in the short term. However, they are generally not recommended for long-term use due to potential side effects. Anti-inflammatory medications like mesalazine (5-aminosalicylic acid or 5-ASA) are commonly used to treat mild to moderate cases of IBD (90,91). They work by reducing inflammation in the lining of the intestine. Immunosuppressive medications like azathioprine and cyclosporine are used to suppress the immune system, which can help to reduce inflammation in the digestive tract. These medications may be used in moderate to severe IBD cases or when other treatments are ineffective. Anti-inflammatory monoclonal antibodies, such as infliximab and adalimumab, are a newer class of medications targeting specific immune system proteins to reduce inflammation. These medications may be used for moderate to severe cases of IBD. Anti-diarrheal medications and antibiotics may also manage symptoms and prevent complications. Analgesics, or pain medications, may relieve abdominal pain associated with IBD. Iron supplements may be necessary in cases of anemia due to blood loss from the digestive tract (92,93).

In some cases, surgery may be required to remove damaged tissue or repair complications such as fistulas or strictures. Surgical options for IBD include colectomy, ileostomy, and other procedures that may be performed laparoscopically or with traditional open surgery. Other complementary therapies studied for IBD include dietary supplements, herbal medicine, functional foods, probiotics, acupuncture, and mind-body therapies. In this sense, polyphenols may have anti-inflammatory and antioxidant effects, which could benefit people with IBD. (93,94).

Alternative and complementary therapies: Polyphenolics and IBD

Polyphenols, also known as phenolic compounds, are secondary metabolites found in plants and can be found in fruits, vegetables, grains, teas, wines, and many other foods. Their chemical structure is characterized by at least one phenyl ring and one or more hydroxyl groups (-OH) directly attached to the aromatic ring (Figure 4). Phenolic compounds can be broadly classified into two main groups: flavonoids and non-flavonoids (95).

Flavonoids are characterized by their unique chemical structure composed fifteen-carbon skeleton consisting of two benzene rings (A and B) linked via a heterocyclic pyran ring (C). They can be divided into various subclasses, such as chalcones, flavonols, flavones, flavan-3-ols, isoflavones, flavanones, and anthocyanins, among others (Figure 4). Non-flavonoid phenolic compounds include phenolic acids, stilbenes, coumarins, and lignans (96,97). Phenolic acids are the most common non-flavonoid phenolics, which can be further categorized into two subgroups: hydroxybenzoic acids (e.g., gallic acid) and hydroxycinnamic acids (e.g., caffeic acid) (95).

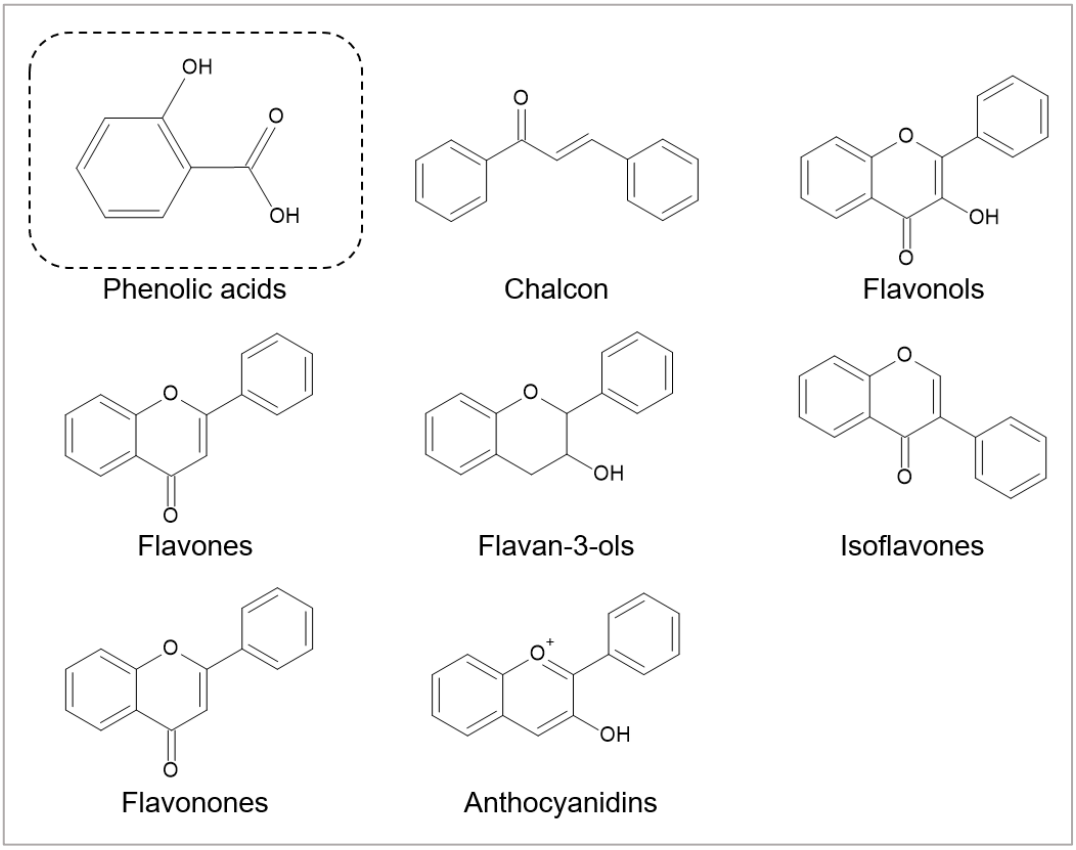

Figure 3. Basic chemical structure of phenolic acids and the major flavonoid classes.

Flavonoids can be found as aglycone or as several sorts of glycosylated. Most flavonoids are present in nature as glycosides that are associated with sugar in conjugated form as

monoglycosidic, diglycosidic derivatives. The glycosidic linkage can be located at various positions on the flavonoid molecule, but the most common positions are 3 and 7. The carbohydrate unit that is conjugated with the flavonoid can also vary, with glucose, rhamnose, galactose, and arabinose being the most common. In addition to glycosylation, flavonoids can also be acetylated, methylated, and sulfated. These modifications can affect the biological activity and bioavailability of the flavonoid, as well as its solubility and stability in different environments (95).

Studies have investigated the potential benefits of polyphenols found in various plants for managing symptoms and improving the quality of life in individuals with IBD. Quercetin, quercitrin, rutin, curcumin, naringenin, chlorogenic acid, resveratrol, and kaempferol are all polyphenols studied for their potential benefits in IBD. These compounds have been exhibited to possess anti-inflammatory and antioxidant properties, which may help decrease inflammation and oxidative stress in the digestive tract (98–100).

Curcumin, found in turmeric, has been indicated to have anti-inflammatory effects in preclinical (101,102) and clinical studies, controlling symptoms such as abdominal pain, diarrhea, and inflammation in individuals with IBD (103–105). Resveratrol, found in grapes and berries, has also been shown to have anti-inflammatory and antioxidant properties. This polyphenol may favor beneficial bacteria in the gut, which may help alleviate colitis and decrease the number of pro-inflammatory pathogenic or opportunistic microbes (106–108). Clinical studies on isoflavone supplementation in IBD patients have also shown a positive correlation in maintaining the remissive state of the disease (109,110).

In addition, the various polyphenols mentioned, such as quercetin, curcumin, and resveratrol, have been observed to improve the inflammatory process in IBD by modulating the immune response. This results in a noticeable decrease in the levels of cytokines such as IFN-γ, TNF-α, IL-6, IL-1β, IL-8, IL-17, chemokines such as MIP-2 and MCP-1, and adhesion molecules such as ICAM-1. Additionally, polyphenols promote the inhibition of eicosanoid synthesis by reducing COX enzyme production, which can also contribute to their anti-inflammatory effects (111–114).

Indeed, phenolic compounds have many positive effects on human health, but they use have some limitations and challenges. Some phenolics are easily degraded during storage or processing due to auto-oxidation, epimerization, hydrolysis, and crystallization (115). Furthermore, their bioavailability (absorption, distribution, metabolism, and excretion) to

human organisms is poor due to physicochemical features like poor water dispersibility and metabolic changes during digestion. A delivery system is necessary to overcome these challenges and improve their bioefficacy in natural conditions. The nano-delivery system loaded with phenolic compounds is a strategy to enhance their efficacy and target delivery (116–118). These approaches aim to maintain the bioactivity of phenolics after oral administration by using nano-delivery systems that can specifically target the colon tissue (119). This can enhance the pharmacological action of phenolics and improve their effectiveness as a therapeutic alternative for IBD.

Nanoparticle-mediated active compound delivery systems for the treatment of IBD

Nanoparticle (NP)-mediated delivery systems for active compounds have emerged as a promising approach for treating IBD. NPs are nanoscale particles with dimensions typically ranging from 1 to 100 nanometers and can encapsulate and deliver active compounds specifically to inflamed sites in the gastrointestinal tract, thereby improving therapeutic efficacy and minimizing side effects (120).

Several types of nanoparticles can be used to transport actives into IBD, including liposomes, polymeric nanoparticles, solid lipid nanoparticles, and others. These systems can be ideated and developed by assigning various properties, such as size, surface charge, and surface functionalization, to optimize their drug delivery capability (121).

Actually, one of the main advantages of nanoparticle-mediated active delivery for IBD is the ability to improve drug stability and bioavailability. Many active compounds used in IBD treatment, such as corticosteroids and immunosuppressive drugs, are susceptible to degradation in the gastrointestinal environment (121). Encapsulating these compounds within nanoparticles can improve their stability, allowing for sustained and controlled action release at the target site. Nanoparticle-mediated drug delivery systems for IBD also provide the potential for combination therapy. Multiple active compounds with complementary mechanisms of action also can be encapsulated in the same nanoparticle, allowing for synergistic effects and improved treatment outcomes (122).

The development of nanoparticles targeting the colon has attracted the attention of researchers as a strategy for new formulations to treat UC due to their ability to accumulate in the inflamed colonic mucosa selectively (123,124). In addition, studies have shown that drug administration directed to the colon can reduce the dosage and minimize systemic absorption of active substances to avoid adverse effects (125,126). Furthermore, colon-targeted NPs exhibit

adhesion to inflamed colonic tissues, increase the systemic bioavailability of poorly absorbed active compounds, and favor the retention time of actives in the colon in models of experimental intestinal inflammation (127,128).

Nanoparticle systems have also been studied as a delivery method for phenolic compounds to improve their bioavailability and efficacy. These nanoparticles can protect phenolic compounds from degradation in the gastrointestinal tract and facilitate their absorption by the body (129,130). A study using chitosan nanoparticles loaded curcumin coated with Eudragit FS 30D investigated the anti-inflammatory effect it for treating IBD. The results showed that curcumin-loaded nanoparticles could reduce inflammation and improve mouse colitis symptoms (131). Some studies have investigated different types of nanoparticle systems associated with various phenolic compounds for treating intestinal disease, as summarized in Table 2.

Table 2. Application of phenolic-loaded nanocarriers in IBDs.

Phenolic compounds	Type of nanodelivery systems	Targets	Mechanism of action	Reference
Curcumin	Chitosan nanoparticles containing curcumin coated with Eudragit FS 30D	*In vivo* evaluation of the specific delivery system to the colon by scintigraphic scan	After 24 h of system administration, the maximum concentration of the system was found in the colon, followed by the small intestine, and only traces were found in the stomach; showing that the highest retention time of the NPs was in the colon for local effect.	(131)
Curcumin	A hyaluronic acid/zein complex was incorporated into alginate/ chitosan hydrogel microparticles with electrospray technology.	Stability tests in simulated gastrointestinal fluid, *in vitro* release tests and in an *in vivo* model of DSS-induced colitis in mice.	The system showed sustained release profiles of curcumin in simulated gastric fluid, while showing rapid release in simulated colonic fluid. Oral administration of the system significantly mitigated colitis symptoms in mice with DSS-induced UC by inhibiting the TLR4/NF-κB pathway.	(132)
EGCG (epigallocatechin-gallate)	Polymeric nanosystem for the delivery of small interfering RNAs (siRNAs) complexed with EGCG	Dextran sulfate sodium (DSS)-induced model in mice	The intrarectal administration of the obtained supramolecular showed significant decreases of TNF-α, prolyl hydroxylase 2 (PDH2), and inflammatory cell infiltration in the intestine	(133)
EGCG (epigallocatechin-gallate)	Ovalbumin nanoparticles with EGCG	*In vitro*: Raw 264.7 macrophages and *in vivo*: Dextran sulfate sodium (DSS)-induced model in mice	*In vitro*: Suppression of pro-inflammatory markers expressions, such as TNF-α, IL-6, and IL-12. *In vivo*: The treated group showed a smaller mucosal lesion, and almost no accumulation of inflammatory	(134)

			cells, when compared to the untreated DSS group.	
Apigenin	Metallic-based nanoparticles coated with hyaluronic acid (HA) to load apigenin	Dextran sulfate sodium (DSS)-induced model in mice	The oral gavage of NPs with apigenin displayed a better restoration of the damaged epithelial colon barrier, reduced inflammatory markers, and enhanced therapeutic effects against DSS-induced colitis mice	(135)
Resveratrol	Polymeric nanocarrier, formed with PLGA, galactosamine, and tween 80, was also applied to enhance the oral delivery of resveratrol	Oral bioavailability and in vitro anti-inflammatory activity were investigated in rats and LPS-induced RAW 264.7 cells	This formulation not only increased the intestinal crossing of the loaded drug, but also displayed promising anti-inflammatory effects in RAW 264.7 macrophages.	(136)
Resveratrol	Resveratrol-loaded PLGA nanoparticles targeted with folate	TNBS colonic inflammation induction	Pathological analysis of mouse intestinal sections showed that the nanocarrier system able to significantly inhibit inflammation and reduce neutrophil and lymphocyte accumulation. The system with folate demonstrated the greatest efficacy in suppressing colon inflammation.	(137)

1.2 METABOLIC SYNDROME

The first definition of metabolic syndrome was proposed by Dr. Gerald Reaven during the Banting Lecture in 1988. Dr. Reaven, an endocrinologist and researcher proposed the concept of "Syndrome X," which later came to be known as metabolic syndrome. During his lecture, Dr. Reaven highlighted the clustering of several metabolic risk factors that often occur together and increase the risk of cardiovascular disease and type 2 diabetes. These risk factors include insulin resistance, high blood pressure, high blood sugar levels, abnormal cholesterol levels (high triglycerides and low HDL cholesterol), and abdominal obesity (138).

However, the first organization to formally suggest diagnostic criteria for metabolic syndrome was the World Health Organization (WHO) in 1998. The WHO defined metabolic syndrome as a cluster of risk factors for cardiovascular disease and diabetes, including insulin resistance, impaired glucose tolerance or diabetes, high blood pressure, and obesity (specifically, increased waist circumference) (139,140).

In 2009, a joint meeting was held between the International Diabetes Federation (IDF) Task Force on Epidemiology and Prevention, National Heart, Lung, and Blood Institute (NHLBI),

American Heart Association (AHA), World Heart Federation, International Atherosclerosis Society, and International Association for the Study of Obesity to standardize the definitions and diagnostic criteria for metabolic syndrome in adults (Table 3). During this meeting, it was agreed that the diagnosis of metabolic syndrome would require the presence of at least three out of five metabolic alterations. It was also noted that waist circumference is a useful measure for screening, but specific cut-off points should be population-specific, considering factors such as ethnicity (141).

Table 3. Definitions and diagnostic criteria for metabolic syndrome in adults.

Component criteria	Definition
Waist circumference	The waist circumference cut-off points may vary based on population-specific guidelines.
Triglycerides	≥ 150 mg/dL (1.7 mmol/L) or drug treatment for elevated triglycerides
High-density lipoprotein (HDL) cholesterol	< 40 mg/dL (1.03 mmol/L) (men) or < 50 mg/dL (1.29 mmol/L) (women) or drug treatment for reduced HDL cholesterol
Blood pressure	Systolic blood pressure ≥ 130 mmHg or diastolic blood pressure ≥ 85mmHg or antihypertensive drug treatment in a patient with a history of hypertension
Fasting glucose	≥ 100 mg/dL (5.6 mmol/L) or drug treatment for elevated glucose

Source: Adapted from Alberti et al. 2009 (141).

Etiopathogenesis

The exact causes of metabolic syndrome are not fully comprehended, but it is believed to result from a combination of genetic, environmental, and lifestyle factors and their interactions (142,143). Genetic and epigenetic factors can play a role in the development of metabolic syndrome, as many susceptible genes and genetic variations can contribute to the phenotypic variation of this syndrome. However, lifestyle factors such as lack of physical activity, smoking habits, alcoholism, and unhealthy dietary patterns also play a significant role in developing metabolic syndrome (144).

Metabolic syndrome is a state of chronic low-grade inflammation arising from a complex interplay of various genetic and environmental factors. Insulin resistance, visceral adiposity (accumulation of fat around organs), atherogenic dyslipidemia (abnormal lipid profiles), hypertension and endothelial dysfunction (impairment of blood vessel lining), genetic susceptibility, hypercoagulable state (increased blood clotting tendency), and chronic stress are some of the factors that contribute to the development of metabolic syndrome (143).

Insulin resistance

Insulin resistance is a crucial feature of metabolic syndrome and is closely associated with its pathophysiology. Insulin is a hormone produced by the pancreas that helps regulate glucose metabolism. It promotes glucose uptake from the bloodstream into cells, which can be used for energy or stored for future use. In insulin resistance, cells in the body become less responsive to the action of insulin, resulting in decreased glucose uptake by cells. This leads to higher glucose levels in the bloodstream, known as hyperglycemia. In response to the high blood glucose levels, the pancreas produces more insulin to try to overcome the resistance, leading to hyperinsulinemia (high insulin levels in the blood) (142).

In physiological insulin signaling, insulin binds to its receptor, a ligand-activated tyrosine kinase. This binding leads to the phosphorylation of downstream substrates and activation of two parallel pathways: the phosphoinositide 3-kinase (PI3K)/protein kinase B (AKT) pathway and the mitogen-activated protein kinase (MAPK) pathway. These pathways are critical in regulating glucose metabolism, lipid metabolism, and cellular growth.

In insulin resistance, the PI3K-AKT pathway is affected, while the MAPK pathway is not. This results in an imbalance between these two pathways, leading to various metabolic abnormalities. The impaired PI3K-AKT pathway reduces endothelial nitric oxide (eNOS) production, contributing to endothelial dysfunction, a characteristic feature of metabolic syndrome (145). In addition, insulin resistance also decreases Glucose transporter type 4 (GLUT-4) translocation, which is the process by which insulin promotes glucose uptake into skeletal muscle and adipose tissue. This further contributes to impaired glucose uptake by skeletal muscle and fat, leading to hyperglycemia, a hallmark of diabetes mellitus often associated with metabolic syndrome (146).

On the other hand, the MAPK pathway remains unaffected in insulin resistance, leading to continued production of endothelin 1, a vasoconstrictor, and expression of vascular cell adhesion molecules. These changes promote inflammation and a mitogenic stimulus to vascular smooth muscle cells, which can contribute to the development of atherosclerosis. In summary, insulin resistance in metabolic syndrome leads to altered signaling pathways, with impaired PI3K-AKT and unaffected MAPK pathways (147). These changes result in endothelial dysfunction, reduced glucose uptake, and vascular abnormalities, collectively predisposing to atherosclerosis and other metabolic abnormalities associated with metabolic syndrome (148).

Additionally, AMP-activated protein kinase (AMPK) is an essential regulator of cellular energy homeostasis. It is a crucial enzyme that senses changes in cellular energy levels and responds by activating metabolic pathways that generate ATP and inhibiting pathways that consume ATP. AMPK is activated in response to cellular stress, such as energy depletion or oxidative stress. In insulin-resistant states, AMPK activity is often reduced, leading to dysregulated glucose and lipid metabolism (149,150).

Visceral adiposity

Visceral adiposity, or the accumulation of fat around the organs in the abdominal cavity, can lead to the release of various signaling molecules from adipose tissue. One of the main signaling pathways involved in visceral adiposity is the release of pro-inflammatory cytokines from adipose tissue. Adipocytes, or fat cells, secrete pro-inflammatory cytokines such as TNF-α, IL-6, and IL-1β, among others. These cytokines can activate signaling pathways that promote inflammation and impair insulin signaling (151,152).

In addition to cytokines, fatty tissue releases other signaling molecules known as adipokines, such as adiponectin and leptin. Adipokines are bioactive molecules secreted by adipocytes that can have pro-inflammatory and anti-inflammatory effects. For example, adiponectin is an anti-inflammatory adipokine that benefits insulin sensitivity (152). On the other hand, leptin is a hormone that regulates energy balance and appetite by acting as a signaling molecule to the brain. It helps control food intake and energy expenditure, allowing the body to balance the amount of energy consumed and the amount of energy expended (153). When adipose tissue increases in size, leptin levels increase and send a signal to the hypothalamus to reduce food intake and improve energy expenditure. Conversely, when fatty tissue decreases in size, leptin levels fall and send a signal to the hypothalamus to increase food intake and decrease energy expenditure (154). In obesity, the gene expression of the leptin receptor (Leptin-R) can be altered, leading to reduced tissue sensitivity to leptin (155).

Atherogenic dyslipidemia

Atherogenic dyslipidemia, characterized by elevated triglycerides and decreased high-density lipoprotein (HDL) cholesterol, is a common feature of metabolic syndrome and can contribute to forming plaques in arteries, leading to atherosclerosis. Several signaling pathways are involved in developing atherogenic dyslipidemia and its consequences on arterial health (156).

One of the critical signaling pathways involved in atherogenic dyslipidemia is the peroxisome proliferator-activated receptors (PPARs) pathway. PPARs are a group of nuclear receptors that

play a role in regulating lipid metabolism (157). Activation of PPARs can modulate the expression of genes implicated in lipid metabolism, including those that hold triglyceride synthesis, storage, and clearance. Dysregulation of PPAR signaling can result in increased triglyceride synthesis and impaired triglyceride clearance, leading to elevated triglyceride levels in circulation, a hallmark of atherogenic dyslipidemia (158).

Another important signaling pathway involved in atherogenic dyslipidemia is the lipoprotein lipase (LPL) pathway. LPL is an enzyme that plays a crucial role in the hydrolysis of triglycerides in circulating lipoproteins, such as very low-density lipoprotein (LDL) and chylomicrons. Therefore, impaired LPL activity or expression can result in decreased clearance of triglyceride-rich lipoproteins from circulation, leading to elevated triglyceride levels. Additionally, decreased hepatic lipase expression, another enzyme involved in lipoprotein metabolism, can contribute to atherogenic dyslipidemia (159).

The insulin signaling pathway also plays a role in atherogenic dyslipidemia. Insulin resistance, commonly associated with metabolic syndrome, can impair insulin signaling in adipose tissue and the liver, leading to increased hepatic production of LDL and decreased clearance of triglyceride-rich lipoproteins from circulation. This can result in elevated triglycerides and decreased HDL cholesterol levels (160).

Inflammation and oxidative stress, often present in metabolic syndrome, can also contribute to the development of atherogenic dyslipidemia. Inflammatory signaling pathways, such as NF-kB and MAPKs, can modulate the expression of genes involved in lipid metabolism and contribute to the dysregulation of lipoprotein metabolism. Oxidative stress can also impair lipid metabolism and contribute to the formation of atherogenic lipoprotein particles (160).

In the context of metabolic syndrome, atherogenic dyslipidemia involves complex interactions of various signaling pathways, including those related to PPARs, LPL, insulin, inflammation, and oxidative stress. Targeting these signaling pathways may be a potential therapeutic approach for managing atherogenic dyslipidemia and reducing the risk of atherosclerosis in individuals with metabolic syndrome.

Hypertension and endothelial dysfunction

Hypertension, high blood pressure, and endothelial dysfunction are standard metabolic syndrome components. Endothelial dysfunction refers to impaired function of the endothelium, the inner lining of blood vessels. Several signaling pathways are implicated in the relationship

between hypertension, endothelial dysfunction, and metabolic syndrome. These pathways include the nitric oxide pathway, reactive oxygen species pathway, inflammatory pathways, renin-angiotensin-aldosterone system pathway, insulin signaling pathway, and adipokine signaling pathway (161).

Genetic susceptibility

Based on the results of genome-wide studies and genetic association studies with metabolic syndrome, it is highly recommended to investigate further the genes that have shown significant associations with the disease, which are Low-Density Lipoprotein Receptor (LDLR); Glycogen Branching Enzyme 1 (GBE1); Interleukin 1 Receptor Type 1 (IL1R1); Transforming Growth Factor Beta 1 (TGFB); IL6; Collagen Type V Alpha 2 (COL5A2); Selectin E (SELE); Hepatic Lipoprotein Lipase (LIPC) (162,163). These genes are involved in several biological processes, such as cholesterol homeostasis, glycogen synthesis, inflammation, and plasma lipid regulation. In addition, dysregulation or mutations in these genes have been associated with familial hypercholesterolemia, apoptosis, neoplastic cell growth, osteopenia and osteoporosis, and accumulation of blood leukocytes at sites of inflammation (164).

It is important to note that all these factors are interconnected and can exacerbate each other, leading to a complex and multifactorial pathophysiology of metabolic syndrome. Therefore, understanding these underlying mechanisms can help develop effective treatment and management strategies for metabolic syndrome.

Treatment of Metabolic Syndrome

The treatment of metabolic syndrome typically involves a combination of lifestyle changes and medical interventions to address the underlying risk factors associated with the condition. The specific treatment plan may vary depending on the severity of the metabolic syndrome, individual health factors, and other medical conditions (165). Some common approaches to treating metabolic syndrome are:

1) Lifestyle changes: Lifestyle modifications are often the first line of treatment for metabolic syndrome. These may include a healthy diet, regular physical activity, and weight management.

2) Medications: Depending on the individual's health status and risk factors, medications may be prescribed to manage the underlying risk factors associated with metabolic syndrome. These may include statins, antihypertensive and antidiabetic drugs. Statin medications are commonly prescribed to lower low-density lipoprotein (LDL) cholesterol levels and reduce the risk of

cardiovascular disease in individuals with metabolic syndrome who have elevated cholesterol levels. Antihypertensive drugs, medications to lower blood pressure, such as angiotensin-converting enzyme (ACE) inhibitors, angiotensin II receptor blockers (ARBs), diuretics, or beta-blockers, may be prescribed to manage hypertension, which is often associated with metabolic syndrome. Antidiabetic medications, if an individual with metabolic syndrome has diabetes or prediabetes, medications such as metformin or other antidiabetic drugs may be prescribed to help manage blood sugar levels.

3) Management of other health conditions: Managing other medical conditions commonly associated with metabolic syndrome, such as sleep apnea, polycystic ovary syndrome (PCOS), and fatty liver disease, may also be a part of the treatment plan.

4) Regular monitoring: Regular monitoring of blood pressure, blood sugar levels, cholesterol levels, and other relevant health markers may be recommended to track progress and adjust the treatment plan as needed.

In summary, global weight control strategies include diet and lifestyle modifications to reduce calorie intake and increase physical activity. If these strategies are ineffective, the WHO recommends pharmacotherapy to block nutrient absorption, modulate fat metabolism, regulate adipose signals, and modulate satiety (3). Many drugs have been used to manage obesity, but most have been withdrawn due to their severe adverse effects and subsequent low therapeutic adherence (166).

Based on this issue, the search for alternative or complementary treatments to prevent obesity has led the general population and the scientific community to have a great interest in some medicinal plants (167). Generally, these plants have bioactive compounds such as phenolic compounds, flavonoids, alkaloids, and fatty acids, which can contribute to satiety, increased metabolism, and weight loss. Furthermore, it is believed that such plants' consumption can improve the human body's inflammatory, glycemic, and oxidative health and regulate insulin sensitivity, glucose homeostasis, and lipid metabolism (168). Therefore, it is necessary to study new sources of active compounds that can modulate molecular pathways and gene/protein expressions beneficially. These studies can lead to new compounds with anti-obesity, anti-diabetic, and anti-inflammatory properties that could be used as adjuvants in treating metabolic syndrome and its associated disorders.

Alternative and complementary therapies: Polyphenolics and Metabolic Syndrome

Plant extracts are rich in bioactive compounds, in which polyphenols stand out when it comes to their potential effects on symptoms of metabolic syndrome. This effect occur due to their antioxidant activity, ability to improve insulin resistance and modulation of the inflammatory response associated with obesity (169). Additionally, they have been found to preserve the altered function of the intestinal barrier and restore intestinal dysbiosis (170).

Polyphenols on Insulin Resistance

Polyphenols can restore insulin sensitivity and glucose uptake in skeletal muscle and adipocytes by activating AMPK and PI3K/AKT pathways. Burgess and colleagues found, through an experimental model of metabolic syndrome in pigs, that resveratrol decreased glucose levels 30 minutes after its administration. In addition, it increased the expression of insulin receptor substrate 1 (IRS-1) and AKT in liver tissue analyses. The analyses in skeletal muscle tissue also showed an increase in GLUT-4, PPAR-α, and PPAR-γ (171). Another study also found that polyphenols such as epigallocatechin-3-gallate (EGCG), present in green tea, activate the AKT pathway and improve insulin sensitivity in skeletal muscle and adipocytes (172).

Polyphenols on adipose tissue

Once adipose tissue has been expanded by hyperplasia, it becomes difficult for an obese individual to lose weight because adipocytes are highly resistant to apoptosis. Furthermore, as weight loss reduces adipocyte volume but not necessarily adipocyte number, it highlights the importance of preventing hyperplasia in the first place (173).

Polyphenols can act on adipose tissue by activating specific signaling pathways and enzymes that promote lipid oxidation, glucose uptake, and adipogenesis inhibition (172,174–176). For instance, green tea polyphenols, such as epigallocatechin gallate (EGCG), can activate the AMPK pathway and increase adipocyte fatty acid oxidation. This leads to decreased adipose tissue mass and improved insulin sensitivity (172). In addition, resveratrol has been shown to activate sirtuin 1 (SIRT1), a protein that regulates energy metabolism and promotes adipocyte differentiation (174). This effect may help to reduce adipose tissue inflammation and improve glucose metabolism. Furthermore, the flavonoid quercetin can inhibit adipocyte differentiation by downregulating several adipogenic genes, including PPAR-γ, C/EBPα, and SREBP-1c (175). Quercetin also exerts anti-inflammatory effects in adipose tissue by decreasing the production of pro-inflammatory cytokines such as TNF-α and IL-6 (176).

Polyphenols on dyslipidemia

Numerous studies have shown that polyphenols can reduce dyslipidemia by several mechanisms, such as inhibiting cholesterol absorption, modulating lipoprotein metabolism, decreasing inflammation and increasing antioxidant activity. Polyphenols such as EGCG, luteolin and quercetin can inhibit the absorption of cholesterol in the small intestine by reducing the activity of cholesterol transporters (177,178). Polyphenols can also modulate the metabolism of lipoproteins, which transport lipids in the blood. It has been studied that resveratrol can increase the activity of lipoprotein lipase (LPL), an enzyme that breaks down triglycerides in the blood, leading to decreased levels of triglycerides and LDL cholesterol (179,180).

The inflammation and oxidative stress also play a key role in the development of dyslipidemia and cardiovascular diseases. Polyphenols-rich extract can decrease inflammation by reducing the production of pro-inflammatory cytokines such as TNF-α and IL-6, and by increasing the production of anti-inflammatory cytokines (181,182). Polyphenols can act as antioxidants, scavenging free radicals and reducing oxidative stress in the body. Several clinical studies have investigated the effects of polyphenols on dyslipidemia, and the results have been promising (183). For example, a study in overweight and obese women found that daily consumption of a green tea extract containing EGCG for 6 weeks led to significant reductions in LDL cholesterol and triglyceride levels (184).

Polyphenols on gut microbiota and barrier function

Studies have provided evidence that polyphenols can protect against obesity by modulating gut microbiota composition and functionality while benefiting intestinal inflammation and barrier integrity. Polyphenols are proposed to help the microbiota by selectively targeting potentially harmful bacteria (185). A systematic review, which included a meta-analysis, showed that supplementation with polyphenols led to a significant increase in the abundance of *Lactobacillus* and *Bifidobacterium* by 220% and 56%, respectively. These two types of bacteria are considered beneficial for gut health. In addition to promoting the growth of beneficial bacteria, polyphenols were also found to inhibit the growth of harmful microbiota, such as *Clostridium histolyticum* and *Clostridium perfringens*. These two bacteria are common pathogenic microorganisms associated with various health problems (186).

An in vivo study investigating the effects of cactus extract from *Opuntia ficus-indica*, a vegetable traditionally consumed in Mexico and Southern United States, concluded that

Opuntia increased the abundance of *Bacteroidetes* and decreased that of *Firmicutes*. In addition, it was suggested that consumption of *Opuntia* extract promotes and maintains intestinal barrier function by increasing the mucosal layer and through increased occludin gene expression (187).

1.3 NOPAL CACTUS - *Nopalea cochenillifera*

Nopalea cochenillifera Salm-Dyck (NC) (Figure 5), commonly known as the cochineal cactus, nopal cactus, "*Palma forrageira*" or "*Palma doce ou miúda*" in Portuguese, is a native cactus species from Mexico but is now widely distributed in Northeastern Brazil as well as in different parts of the world (16). NC is a small cactus with a very branched stem. Its cladode weighs about 350 g, is almost 25 cm long, obovate, and bright green. The flowers of NC are found in the red, pink, orange, or yellow colors, and their corollas may remain half-closed during the cycle. The fruit is a purple-colored berry that is edible and commonly used in Mexican cuisine. When compared to other cactus species, the NC is considered more palatable and more manageable because it does not contain thorns in its structure (16).

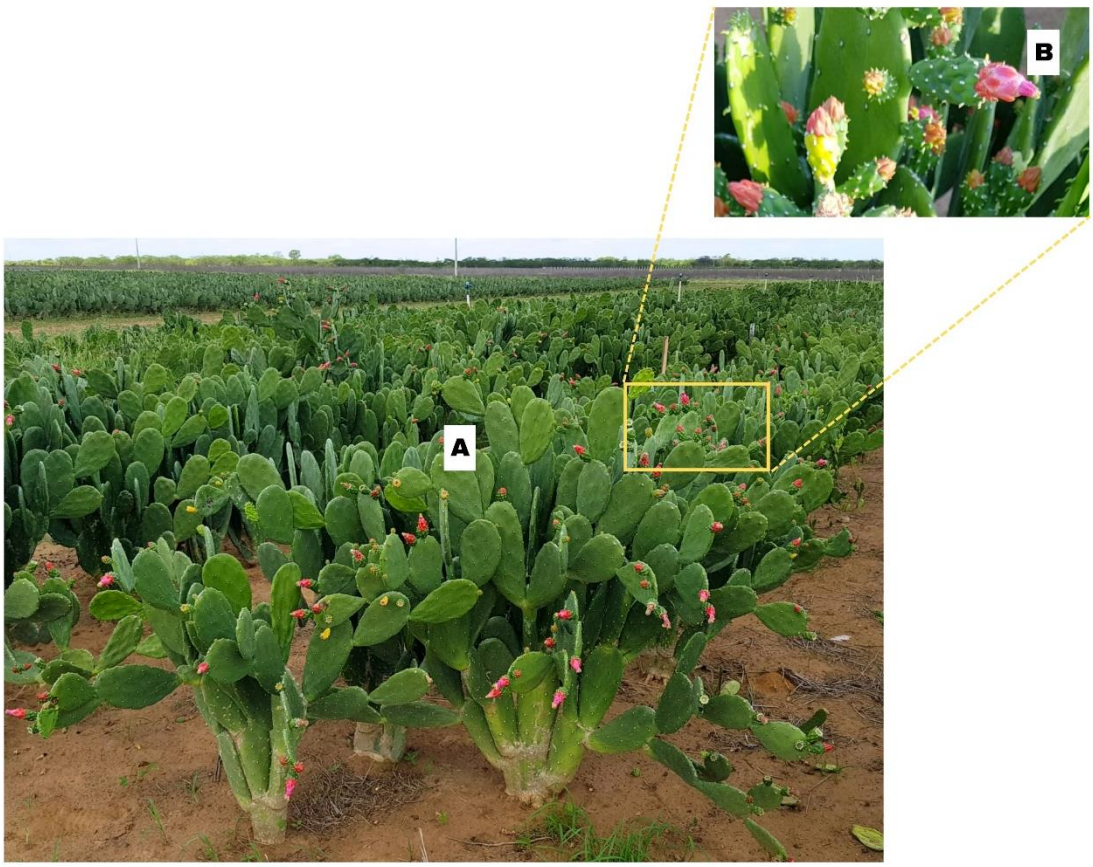

Figure 4. Pictures of *Nopalea cochenillifera* (L) Salm Dyck. A – cladode; B – fruit.

N. cochenillifera uses the photosynthetic pathway Crassulacean Acid Metabolism (CAM), a specialized adaptation that allows it to survive in water-limited environments. CAM plants open their stomata at night to take in CO_2 and fix it into an organic acid, which is stored in the vacuoles of the cells. Then, during the day, the stomata close to prevent water loss, and the organic acid is broken down to release the CO_2 for use in photosynthesis. This allows the plant to conserve water by avoiding excessive transpiration during the day when temperatures are high, and humidity is low (188,189). In summary, the CAM photosynthetic pathway in the NC is an adaptation that enables the plant to survive in arid environments by reducing water loss through transpiration while still fixing carbon for photosynthesis.

NC has been traditionally used as a food source for both animals and humans in Brazil and many other countries worldwide. The fruits and cladodes of NC are often rich in nutrients, such as vitamins, minerals, and fibers. They can be eaten fresh or processed into various products, such as juice, jellies, gels, liquid sweeteners, pickles, jams, sauces, etc. In addition, the young cladodes can be consumed boiled, grilled, or pickled and used in various dishes, such as salads, soups, and stews (16).

NC has become a good food source for humans and animals in regions with severe climatic conditions, such as drought-prone areas, where other species may have difficulty growing. NC is well adapted to these conditions and can provide a reliable food source for humans and animals (190). Thus, investigations on cactus chemical components and nutritional values have become the research subject in diverse scientific fields.

It is worth mentioning that NC represents a good plant choice for cultivation in the Northeast region of Brazil due to its resistance in drought season, its management being accessible, and because it can assist in the sustainable development of the region through the establishment of the entire productive chain to obtain raw material to be applied as active ingredient in pharmaceuticals or foods.

Chemical composition of *Nopalea cochenillifera*

The chemical composition of NC can vary depending on factors such as the cultivation area, age of the cladode, and growing conditions. However, in general, NC is known for having high water content and minerals such as calcium, magnesium, potassium, and iron, which can be important for human and animal nutrition. Soluble carbohydrates, such as glucose and fructose, are also present in NC, which can provide a source of energy. NC is also a good source of

vitamin C and vitamin A, which have antioxidant properties and have important functions (16,189–191).

There is scarce information on the physical-chemical and nutritional characterization of NC, as well as its bioactive compounds. Regarding secondary metabolites, the varieties grown in Northeast Brazil of *Nopalea* genus are sources of compounds such as steroids and phenolic compounds (15,19,20,189).

Using histochemical reactions, the presence of flavonoids were detected in ethanolic extract of NC (23), and in another study in the ethanolic extract obtained from the fresh cladodes of NC also was quantitatively determined the presence of phenols and flavonoids expressed in gallic acid and rutin equivalents/g extract, respectively (192). Studies have reported a presence of flavonoids in the rainy seasons, detected by Shinoda's reactions (193,194). Matos et al. and Fabela-Illescas et al. (15,195), also identified some phenolic compounds through liquid chromatography. Table 4 summarizes the phytochemical studies performed on parts of the species *N. cochenillifera*.

Table 4. Summary of phytochemical and chemical screenings already reported for the species *N. cochenillifera* (NC).

Plant part	Solvent and Extraction method	Analysis	Results	References
Cladodes	-	Histochemical tests	Flavonoids were detected, through the potassium hydroxide and hydrochloric acid reagents, by the development of yellow color in histological sections of the plant.	(23)
Fresh cladodes	Ethanol extract (Maceration)	Dosage of flavonoids using rutin as a standard solution of aluminum chloride in methanol.	29.62% ± 1,356 of total polyphenol gallic acid equivalents/g. 7.63% ± 0,075 of flavonoid rutin equivalents/g extract.	(192)
Cladodes	Ethanol (95%) extract (Maceration by 8 days)	Chemical prospection: Steroids were detected by the Liebermann-Burchard reaction; flavonoids detected by of Shinoda reaction e Taubouk. Determining total phenolics content and total flavonoid content by spectrophotometric method using the Folin-Ciocateau reagent and aluminum chloride methanolic solution, respectively.	NC contain flavonoids and steroids independent of the cultivars analyzed or the period (dry and rainy).	(193,194,196)
Cladodes	Fresh cladodes subjected to	UPLC-QTOF-MS^{E}	Tryptophan; quercetin-3-*O*-2’’,6’’-	(195)

	a bath with liquid N_2, lyophilized, ground and submitted to the accelerated solvent extraction (ASE) system with 70:30 ethanol/ water (v/v) at the temperature of 80 ºC.		dirhamnosillglucosídeo; isorhamnetin-glucosyl-dirhamnoside; isorhamnetin-3-*O*-rhamnosyl hexoside; isorhamnetin-3-*O*-triglucoside.	
Cladodes	Dry cladodes and ground in a mill (flour)	Quantification of phenolic acids by HPLC	Determined the content of soluble and hydrolysable polyphenols, 207.92 and 647.99 mg, respectively. Identified of the presence of six phenolic acids (gallic, ferulic, chlorogenic, p-coumaric, syringic, and neochlorogenic were identified)	(15)

Ethnobotany and pharmacological activity

In traditional medicine, this species is used to treat urinary problems, "cooling", high cholesterol levels, hypertension, kidney problems, urinary problems, and diabetes (18). Although an ethnobotanical study also points to *N. cochenillifera* as one of the main plants reported in Mexico as hypoglycemic, the traditional preparation form cited uses the plant as Steam raw (17).

Previous preclinical studies have reported scientific evidence that this plant showed potential antibiotic and antifungal activities in vitro assays (20,192,197) and decreased the blood glucose level in an *in vivo* study (21). Furthermore, regarding the anti-inflammatory effect, the oral administration of the hydroethanolic extract of *N. cochenillifera* cladodes showed significant anti-inflammatory activity in the rat granuloma induction method (23). Table 5 summarizes the pre-clinical pharmacological studies conducted with the species *N. cochenillifera*.

Table 5. Summary of pre-clinical pharmacological studies already reported for the species *N. cochenillifera* (NC).

Plant part	Extract/ Fraction/ compound	Test/ Pharmacological activity	Results	References
Fresh and dry cladodes	Hexanic fraction; chloroformic fraction; ethanolic fraction	*In vitro* - antibacterial and antifungal activity	Activity antimicrobial activity against *Escherichia coli*, *Salmonella enterica* and *Candida albicans*.	(20)
Fresh cladodes	Ethanol extract (Maceration)	*In vitro* - Antibacterial activity	NC showed good antibacterial activity and showed an inhibitory activity against microorganisms tested (*Escherichia coli, Salmonella typhi, Micrococcus, Klebsiella*	(192)

			pneumoniae, Staphylococcus aureus, Candida albicans, Candida glabrata, Prototheca zopffi, Cryptococcus neormans, Saccharomyces cervisiae e Malassezia furfur).	
Cladodes and fruits fresh	Extract methanolic and chloroform	*In vitro* - Antimicrobial activity	Methanolic extract was found to be an effective against the microbes: *E. coli, Bacillus subtilis, Staphylococcus aureus, Pseudomonas aeruginosa Candida albican C.glabrata C.haemulonii C.Tropicalis*. Maximum activity was observed against *E. coli, B. Subtilis and, C.albican* and *C.glabrata* at 40mg/ml.	(197)
Cladodes	Ethanol (95%) extract (Maceration by 8 days)	*In vitro* - Cytotoxic activity	Inhibitory effect on the growth of cancer cells (HCT116 cells (human rectal colon rectal), SF-295 (human glioblastoma) and OVCAR-8 (human ovarian cancer)	(193)
Cladodes	hydroethanolic extract	*In vivo* - Anti-inflammatory activity (granuloma induction in rats)	The animals treated with the extract showed 53.5 % inhibition formation of granulomatous tissue while the positive control group showed 58.5%, confirming a significant anti-inflammatory activity.	(23)
Fresh cladodes	Methanolic extract	*In vivo* - Antihyperglycaemic effect	NC showed a significantly reduced postprandial glycaemia in rats but did not markedly inhibit α-glucosidase and had a low antioxidant effect in the ABTS test.	(21)

Clinical studies on using *N. cochenillifera* must be more extensive and limited. There is, in fact, only one study on the effects of NC on humans. Fabela-Illescas et al. (22) conducted a clinical trial with 20 patients, out of which ten were diabetic, and the remaining had hypertension overweight, and obesity. The treatment administered to all patients was a fresh *N. cochenillifera* beverage, which consisted of a mixture of 50 g of NC cladode with 250 mL of water, was taken daily for 30 days. The results of the study showed significant improvements in several parameters. There was a significant decrease in waist circumference, weight, and systolic and diastolic blood pressure in patients who received the *N. cochenillifera* preparation. However, there were no statistically significant changes in glucose levels. On the other hand, significant values were found for glycated hemoglobin, an indicator of long-term blood sugar control in people with diabetes. It's important to note that this study had a small sample size of only 20 patients and was conducted over a relatively short duration of 30 days.

In view of this, the aim this study was evaluated the anti-inflammatory effect of free extract and nanosystem containing the NCE *in vivo* models of intestinal inflammation and metabolic syndrome. In addition, another aim of the study was characterized the chromatographic profile and the total phenolic and flavonoid compounds

II. HYPOTHESIS & AIM

Inflammatory bowel diseases (IBD) and metabolic syndrome (MS) are two increasingly common health conditions worldwide, particularly in developed countries (1–3). IBD, including Crohn's disease and ulcerative colitis, are chronic diseases that affect the gastrointestinal tract and can cause symptoms such as rectal bleeding, mucous or bloody diarrhea, abdominal pain, fatigue, and weight loss (4). Metabolic syndrome, conversely, is a set of medical conditions, including abdominal obesity, high blood pressure, elevated blood sugar levels, and dyslipidemia (5).

Both are multifactorial and complex diseases whose etiopathology involves genetic, environmental, and behavioral factors. In the case of IBD, it is believed that the interaction between intestinal microbiota, the immune system, and environmental factors may play an important role in their development. Additionally, factors such as smoking, stress, and prolonged use of nonsteroidal anti-inflammatory drugs (NSAIDs) may also contribute to the development of IBD (6,7).

Just like IBD, metabolic syndrome is also associated with chronic inflammation implicated in its pathogenesis. The set of risk factors, such as abdominal obesity, insulin resistance, high blood pressure, and dyslipidemia, increases the risk of developing cardiovascular diseases, such as heart attack and stroke (8). Chronic inflammation occurs when the body's immune system is persistently activated, leading to the continuous production of pro-inflammatory cytokines and chronic inflammation. Treatment of metabolic syndrome often involves reducing chronic inflammation through lifestyle changes, such as a healthy diet, regular physical exercise, stress management, and medications to control blood pressure, reduce blood sugar levels, and lower cholesterol and triglyceride levels. Although IBD and metabolic syndrome are different conditions, they may be related to specific individuals, and a better understanding of chronic inflammation may help develop more effective treatments for both diseases (9).

Clinical evidence has shown that using isolated phenolics or phenolic-rich extracts in combination with medications already used for treating IBD and in cases of metabolic syndrome, they have improved patient quality of life (10,11). Polyphenols are secondary metabolites produced by plants that possess antioxidant and anti-inflammatory properties, making them effective in preventing and treating these diseases. Their remarkable anti-inflammatory and antioxidant capacity is due to multiple action targets, such as inhibition of production or action of pro-inflammatory mediators, or even the strong influence they can exert on the intestinal microbiota (12–14).

In this scenario, the cactus *Nopalea cochenillifera*, popularly known as prickly pear or sweet cactus, is a good source of anti-inflammatory bioactive compounds. Its cladodes are rich in polysaccharides and polyphenols (15) and have been widely used for agricultural, food, and medicinal purposes (16). It is traditionally used as an anti-inflammatory and curative in treating diseases such as high cholesterol, high blood pressure, kidney and urinary problems, and in treating diabetes (17,18). Previous studies have reported the potential antibiotic and antifungal activity of *Nopalea in vitro* assays (19,20). In addition, glucose levels were reduced *in vivo* studies (21) and in a pilot clinical trial (22). Regarding the anti-inflammatory effect, oral administration of the hydroethanolic extract of *N. cochenillifera* cladodes demonstrated significant anti-inflammatory activity in granuloma models and gastric ulcer induction in rodents (23,24).

The polyphenols present in *N. cochenillifera* extract are already considered a promising source of bioactive agents. However, when it comes to inflammatory bowel diseases, targeting these active ingredients in the colon region and reducing the concentrations of plant extracts required to achieve pharmacological activity are still challenges to be overcome. Developing drug delivery systems capable of transporting active substances from the extract to the colon tissue is a promising alternative to improve oral bioavailability and prolong retention in the colon. Nanotechnology systems have shown interesting and promising properties in this regard, such as improving stability, solubility, and bioavailability of natural compounds, enabling control of the release of bioactive compounds, and reducing the doses and frequencies of administration (25–27). Strategies involving the encapsulation of *N. cochenillifera* extract and directing its release to the colon region can enhance its effectiveness and reduce the therapeutic dose required.

Considering the bioactive potential of *N. cochenillifera*, it is relevant to highlight that this species is an excellent choice for developing inputs due to its adaptation to the northeastern region of Brazil and the presence of established crops in the area. This enables the creation of a complete productive chain in the country, from cultivation to the final production, which can positively impact the local economy, such as job creation and promoting sustainable development in the region. In this context, this proposal seeks to support the development of new active ingredient to pharmaceutical or food products.

AIM

This work aimed to conduct a phytochemical study of *Nopalea cochenillifera* hydroethanolic extract and evaluate its toxicity and efficacy in vivo models of intestinal inflammation and metabolic syndrome. In addition, this work aimed to develop and characterize a nanoparticulate system loaded with the extract of N. cochenillifera and to evaluate the pharmacological effect of the extract free (NCE) and associated with nanoparticles (NPE)

The specific objectives are:

1. Physicochemical characterize the *N. cochenillifera* extract, determine the content of total phenolic and flavonoid compounds, and the chromatographic profile by high-performance liquid chromatography-mass spectrometry (HPLC-MS).
2. Evaluate the acute oral toxicity of NCE in rats.
3. Evaluate the intestinal anti-inflammatory effect of different doses of NCE in an experimental intestinal inflammation model induced by 2,4-dinitro-benzene sulfonic acid (DNBS) in rats.
4. Develop, characterize, and evaluate the effects of a nanoparticulate system loaded with NCE in an experimental intestinal inflammation model induced by sodium dextran sulfate in mice.
5. Evaluate the effect of NCE in an experimental model of metabolic syndrome induced by a high-fat diet in mice.

III. MATERIAL & METHODS

3.1 Reagents

Unless otherwise stated, most of the chemicals used were purchased from Sigma-Aldrich Chemical (São Paulo, Brazil; Madrid, Spain).

The following reagents were used to obtain the nanoparticles: The methyl methacrylate copolymer Eudragit® S100 (EUD S100) was purchased from (Evonik, Darmstadt, Germany). Poloxamer 407 (POL 407, Kolliphor® 407, Mw = 12,600 Da) and Rhodamine B were purchased from Sigma-Aldrich (St. Louis, MO, USA). Ethanol (EtOH) was purchased from Labsynth (São Paulo, Brazil). Finally, purified water (1.3 $\mu S.cm^{-1}$) was obtained using reverse osmosis equipment OS50 LX (Gehaka, SP, Brazil). All reagents were of analytical grade.

3.2 Plant Material

The cladodes of *N. cochenillifera* were harvested in May 2019 at the experimental station "Rommel Mesquita de Farias, belonging to the Empresa de Pesquisa Agropecuária do Rio Grande do Norte S/A" (EMPARN) in the Parnamirim city, Rio Grande do Norte state, Brazil (geographical coordinates: 05°55′30″ S – 35°11′20″ W) (Figure 6). The cladodes collected were young, with a dark green color and direct exposure to sunlight, and without flowers or fruits. Harvest was in the rainy season.

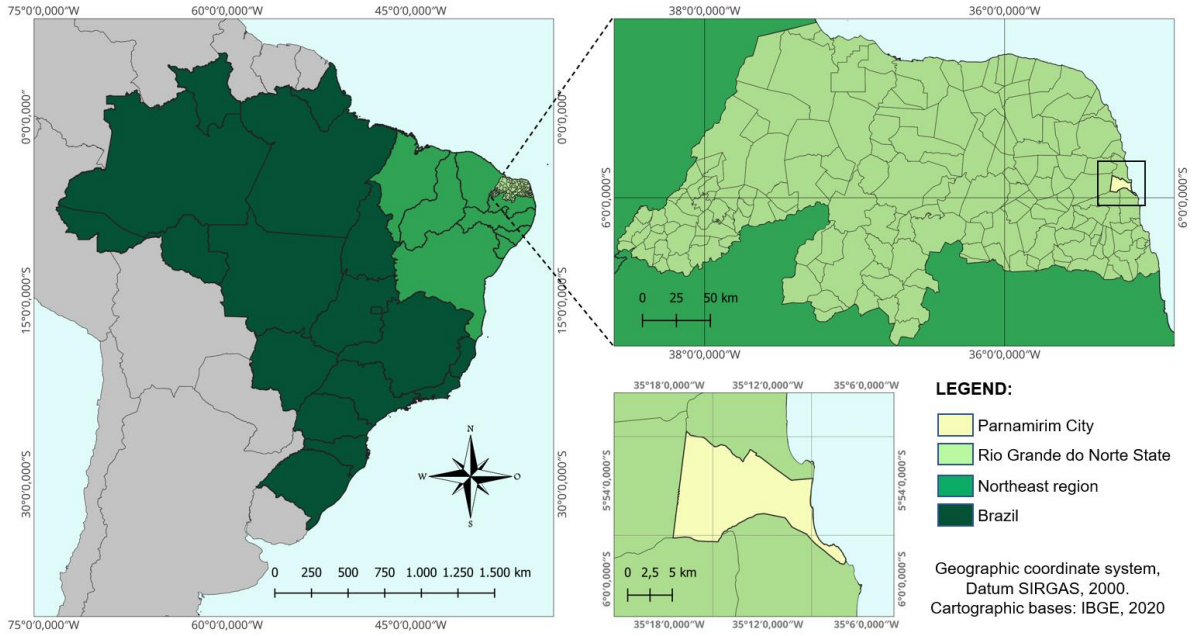

Figure 6. Location of the Parnamirim city in the Rio Grande do Norte state, Brazil. Coordinate System Geocentric Reference System for the Americas: SIRGAS, 2000. Cartographic bases: Brazilian Institute of Geography and Statistics (IBGE).

The identification of the plant was made by a biologist MSc. Alan de Araújo Roque, a voucher specimen (No. 3702), was deposited at the herbarium of the Bioscience Center of the Federal University of Rio Grande do Norte. The research was authorized by the National System for the Management of Genetic Heritage and Associated Traditional Knowledge (SISGEN) process No. A5DB251. The accepted name plant was published on the Internet; http://www.worldfloraonline.org/taxon/wfo-0000378923. Accessed on: 25 Mar 2023, possessing as a synonym *Opuntia cochenillifera* (L.) Mill. (WFO, 2023) (198).

3.3 Preparation of *Nopalea cochenillifera* Extract (NCE)

Immediately after harvesting, the fresh cladodes were processed. They were dried at 50 °C in a circulating air oven for eight days and then ground in a knife mill. The raw material was extracted, by the maceration method (48 h), using as a solvent ethanol: water (70:30, *v/v*) in a proportion of 1:10 solvent (g/mL). The extract was filtered, and the remaining raw material was extracted again for 24 h. This process was repeated two times to obtain a satisfactory extraction yield. At the end of the process, the three extractions were pooled, resulting in the *N. cochenillifera* hydroethanolic extract (NCE). The organic phase was evaporated under reduced pressure using a rotavapor (Büchi®) with a temperature below 40 °C and finally lyophilized and stored at 4 °C (Figure 7).

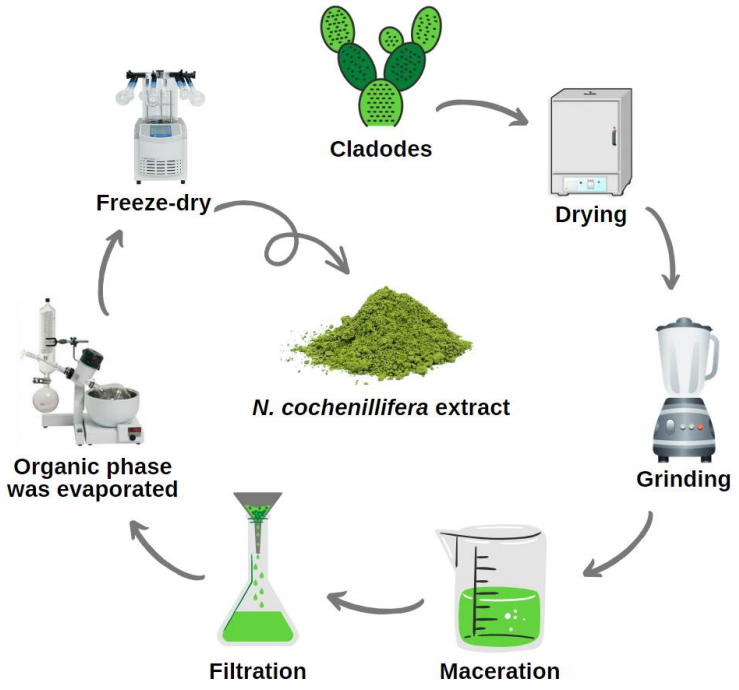

Figure 7. Preparation of *Nopalea cochenillifera* extract.

3.4 Physicochemical Analysis of *Nopalea cochenillifera* Extract

The physical-chemical analysis of the NCE was performed in the Nutrition Laboratory of the *Escola Agrícola de Jundiaí (EAJ) – Universidade Federal do Rio Grande do Norte (UFRN)*, Brazil. The NCE was evaluated for moisture content (%), ash (%), ether extract (%), crude fiber (%), protein (%), pH, and titratable acidity were determined as recommended by AOAC (2020) (199). The analyses were performed in triplicate in three independent experiments (three replicates and each one was analyzed in triplicate).

The pH analysis was determined using 5 g of NCE diluted in 50 mL of distilled water with a portable electronic pH meter (KASVI®). Titratable acidity was determined by the potentiometric method in a solution prepared with 1 g of the NCE in 50 mL of distilled water and then titrated with 0.1 M sodium hydroxide solution until the pH became basic. To determine the moisture (AOAC method 925.10), weighed 1.0 g of NCE and taken to an oven with air circulation and renewal at 105 °C for 16 h (TECNAL® TE-394/2-MP).

Regarding the percentage of ashes, we weighed 1.0 g of NCE in the crucible. Then, to determine the ashes percentage took crucible taken to the muffle furnace (Quimis Q-318M24) until reaching a temperature of 600 °C for 4 h (AOAC method 942.05). To determine the ether extract, extraction was performed in a Soxhlet-type apparatus. Next, the crude fiber content of the extract was determined by the method of digesting the material in 0.255N H_2SO_4 solution for 40 min, followed by 0.313N NaOH for another 40 min (AOAC method 973.18). Finally, the Kjeldahl method (AOAC method 950.36) was employed for protein analysis, involving three main steps: digestion of the extract in sulfuric acid with a catalyst, distillation of the resulting ammonia into a receiver solution, and quantification of the released ammonia through titration with a standard solution.

The content of total carbohydrates was calculated by compositional difference according to the following equation (200):

$$\text{Total carbohydrates (g/100 g)} = 100 - (\text{moisture} + \text{proteins} + \text{ether extract} + \text{ash})$$

3.5 Determination of Total Phenolic and Flavonoid Content

The total phenolic content (TPC) of NCE was determined based on the Folin–Ciocalteu reagent method (28). Initially, a curve of the gallic acid standard in dimethyl sulfoxide (DMSO) was constituted at different concentrations (1.25, 2.5, 5, 10, 20, 40, 60 and 80 μg/mL). The blank

contained 25 µL of H_2O and the Folin-Ciocalteu reagent (125 µL) without NCE. Briefly, in a 96-well plate, 25 µL of sample solution was added at 2 mg/mL with 125 µL of Folin–Ciocalteu reagent freshly diluted to 1:10 (*v/v*) with distilled H_2O. After, an amount of 100 µL of the solution was mixed with 100 µL of a 7.5% Na_2CO_3 solution; the mixture was then left for 30 min in the dark, and the absorbance was measured in a microplate reader (Epoch-Biotek®, Winooski, Vermont, United States of America) at 765 nm. After that, the TPC was calculated as mg of gallic acid equivalent (GAE) per g of the sample (mg of GAE/g). The analyses were performed in triplicate in three independent experiments (analyzed three replicates, and each one was in triplicate).

The aluminum chloride colorimetric method determined total flavonoid content (TFC) (29). First, a standard curve of quercetin in DMSO was constructed at different concentrations (2.5, 5, 10, 20, 40, 60, and 80 µg/mL). The blank was constituted of 50 µL of H_2O and $AlCl_3$ in the absence of NCE. Then, a 50 µL sample of each extract (2 mg/mL) was mixed with 160 µL of ethanol (P.A.), 20 µL of aluminum chloride solution (1.8% *w/v*), and 20 µL of sodium acetate (8.2% *w/v*). The mixture was left at room temperature in the dark for 40 min. The absorbance was measured at 415 nm using an ELISA microplate reader after subtracting the blank reading value and compared with a calibration curve. The TFC was calculated as mean ± SD and expressed as mg quercetin equivalent per g sample (mg QE/g sample). Analyses were performed in triplicate in three independent experiments (analyzed three replicates, each in triplicate).

3.6 Phytochemical Analysis by HPLC-ESI-MS^n of *Nopalea cochenillifera* Extract

The sample was prepared from 1.0 mg of the NCE in 1.0 mL of MeOH: H2O (50:50, *v/v*) and filtered using a 0.45 µm PVDF filter. HPLC-ESI-MS^n analysis was performed using high-performance liquid chromatography equipment (Shimadzu®, Kyoto, Japan) consisting of an automatic injector (Accela AS), two pumps (LC-20AD), an autosampler (SIL-20AHT) and a system controller (CBM-20A) and an Ion Trap mass spectrometer amazon-SL (Bruker Daltonics®), with the electrospray ionization (ESI) source operated in positive and negative mode. The chromatographic conditions were performed at room temperature using a C_{18} reversed-phase column (Kromasil®, 150 mm × 4.6 mm d.i., 5 µm). The elution method adopted for NCE was a linear gradient with a mobile phase composed of water acidified with 0.1% formic acid (eluent A) and methanol (eluent B) from 5 to 100% (B) in 60 min. The injection volume for the analysis was 20 µL, and the flow rate was 600 µL/min. The MS parameters were

optimized for the performance of the analysis as follows: HV End plate offset of −500 V, nebulizer of 40 psi, dry gas (N_2) with the flow of 8.0 L/min, dry temperature of 300 °C and capillary voltage of −4500 V. Monitored the acquisition range of the mass analysis from *m/z* 150–1200 and recorded every 0.2 s. The fragmentation experiments were performed by collision-induced dissociation (CID) running in auto MS^n (intelligent fragmentation) for MS^2 and MS^3 acquisition and with a fragmentation amplitude of 1.0 V. For precursors selection in MS^2 and MS^3 experiments, the most intense ions were isolated above the absolute threshold of 25,000 and 2500, respectively, and a relative intensity threshold of 5%. The data were acquired and processed using the Bruker Compass Data Analysis software (Version 4.0, Billerica, MA, United States).

For metabolite annotation, first convert data HPLC-ESI-MS^n to mzML format in MSConvert software (ProteoWizard). Then MS^2 spectra were searched against the Library Search dereplication workflow on the Global Natural Products Social Molecular Networking (GNPS) platform (201). The matches obtained were manually verified by comparison with other databases [Dictionary of Natural Products (DNP, 2013)] and LOTUS [https://lotus.naturalproducts.net/ (accessed on 16 November 2022)] (202), as well as data previously reported in the literature. Additionally, a similar procedure was done for those spectra that did not find a match with the MS data library.

3.7 Preparation and characterization of Nanoparticles

The nanoparticulate system was obtained and characterized in collaboration with Prof. Dr. Arnóbio Antônio da Silva Junior and PhD student Thayse Silva Medeiros at the Pharmaceutical Technology (TecBioFar — UFRN).

Preparation of nanoparticles

Blank nanoparticles (NPB) and extract-loaded nanoparticles (NPE) were prepared by the nanoprecipitation method (34,35). The organic phase (OP) (6 mL) containing 0.75% (*w*/*v*) of polymer (EUD S100) was solubilized in ethanol: water 9:1 (*v*/*v*). To NPE, NC-extract in a 1:10 ratio (NC: EUD S100) was solubilized in an organic phase. The organic solution was then transferred dropwise (at an output flux of 1.0 $mL.min^{-1}$) into 14 mL of aqueous phase (AP) containing a stabilizer (POL 407) at a concentration of 0.25% (*w/v*) under constant magnetic stirring (720 rpm) at 25 °C. The solvent evaporation step was performed at 25 °C, and the nanoparticles remained stirring overnight to slow the diffusion of organic solvent. After this

period, the samples were taken to rotary evaporation (model V-700, Buchi®) to altogether remove any residual organic solvent (Figure 8).

In addition, to obtain the fluorescence-labeled nanoparticles, rhodamine B was added in the organic phase to get a 1:100 Rhodamine: EUD S100 (*w/w*) ratio, following the same experimental protocol. All experimentations were performed in triplicate, and the data are expressed as mean ± standard deviation (SD).

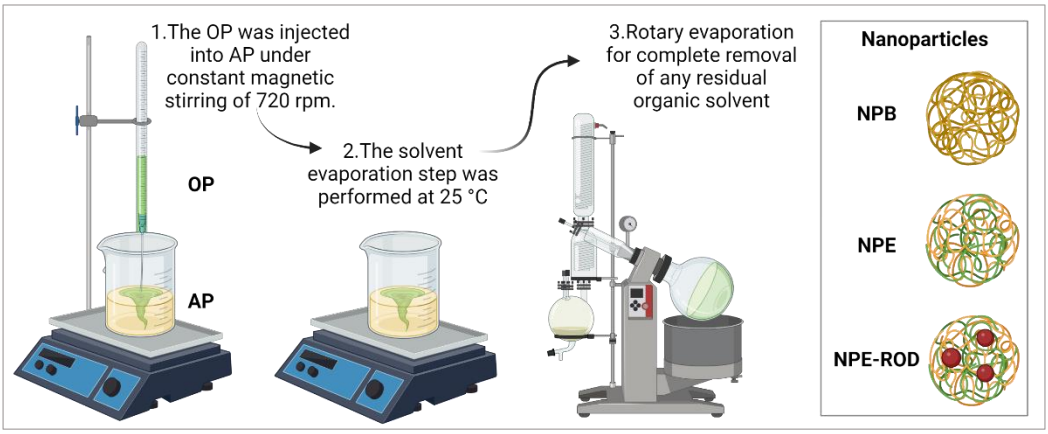

Figure 8. Preparation of nanoparticles. Organic phases (OP); Aqueous phases (AP); Blank nanoparticles without extract (NPB) and extract-loaded nanoparticles (NPE) and fluorescence-labeled nanoparticles with rhodamine B (NPE-ROD).

Particle size, Polydispersity Index and Zeta Potential measurements

The determination of the average particle diameter and polydispersity index (PdI) was performed by the Dynamic Light Scattering technique (Nano ZS Zetasizer, Malvern Instruments Corp., Malvern, UK), at a temperature of 25 ± 2° C, at 633 nm and detection angle of 173°. The samples were diluted in purified water at a 1:10 *v/v* ratio. Determined the zeta potential of the nanoparticles by analyzing the electrophoretic mobility of the suspended particles using the same equipment at 25 ± 2 °C. The samples were appropriately diluted in purified water at a 1:10 *v/v* ratio. Experimental values are given as the mean ± SD for the experiments carried out in triplicate for each sample.

Entrapment Efficiency (EE)

The entrapment efficiency was determined using an indirect method, where the nanoparticles containing extract were centrifuged at 16.9 RCF (g) for 60 min at 4 °C using an ultra-centrifugal filter (Sartorius®, Vivaspin 2, Ultra-15 MWCO 100 kDa). Then, the supernatant was collected and quantified using a spectrophotometer (Evolution 60S UV-visible, Thermo Fisher Scientific,

USA) for the content of total phenolic compounds at a wavelength of 765 nm, using the straight-line equation generated by a previously prepared analytical curve, methodology described in the topic 3.5.

The analysis was performed in triplicate from three independent experiments, and the incorporation efficiency of total phenolics in the formulation was calculated according to the following equation:

$$EE\ (\%) = \left(\frac{Total\ phenolics - free - Phenolics\ in\ supernatant}{Total\ phenolics} \right) x100$$

Scanning Electron Microscopy (SEM) and Atomic Force Microscopy (AFM)

SEM and AFM imaging were performed to analyze the morphology of the nanoparticles. For the SEM analyses, a drop of the suspension was spread, fixed on a conductive adhesive surface, and covered with approximately 20 nm of gold in a BAL-TEC sputter coater (Bal-Tec, Scotia, USA), model SCD 005. After drying for 24h in the desiccator, image reading was performed using a FEG-SEM (Zeiss, Auriga®). To observe the shape of the nanoparticles by atomic force microscopy, the samples were dried under a desiccator for 24 h and then analyzed using an AFM (SPM-9700, Shimadzu, Tokyo, Japan) at 25° C in a non-contact cantilever, 1 Hz.

Attenuated Total Reflectance - Fourier Transform Infrared (ATR-FTIR)

The interaction between the chemical constituents of the NC-extract and EUD S100 nanoparticles was investigated using an ATR-FTIR spectrophotometer Shimadzu IR Affinity-1 (Shimadzu, Tokyo, Japan). Before the analysis, the colloidal dispersion of nanoparticles was submitted to a freeze-dryer process performed using a Christ Alpha 1-2 LD freeze-dryer (Martin Christ Gefriertrocknungsanlagen GmbH, Osterode am Harz, Germany). The spectra were obtained at 20 scans with a resolution of 4 cm^{-1} (4000 and 500 cm^{-1}) for each component (NC-extract, EUD S100, and POL 407), as well as the nanoparticles (NPB and NPE).

Physicochemical Stability

The physical stability study was performed for blank nanoparticles (NPB) and extract-loaded nanoparticles (NPE). The analyses were done during the 30 days by evaluating the mean diameter, zeta potential, and polydispersity index according to techniques described in the previous items. The dispersions were hermetically sealed and stored at 5 ± 2 °C.

3.8 In vitro study

Cell internalization performance test of Nanoparticles containing N. cochenillifera extract and rhodamine (NPE-ROD)

HCT-116 human colon cancer cells were seeded into 8-well culture chambers and glass microscope slide at a density of 8×10^3 cells. After cells reached 80% confluence, the treatment with NPE-ROD was performed at a concentration of 10 µg/mL after dilution in Dulbecco's modified eagle medium (DMEM), supplemented with 10% FBS, 1% of penicillin–streptomycin, 1% of amphotericin-B and 1% of L-glutamine. The control group received only DMEM. The cells were evaluated at 12 h, 24 h, and 48 h. After incubation, cells were washed with PBS, fixed with 4% paraformaldehyde for 20 min, and washed again with PBS. Last, the slides were mounted with a mounting medium containing 4,6-diamidino2-phenylindole (DAPI) for cell nucleus marking. Images were acquired using a confocal laser scanning microscope (CLSM) (Leica TCS-SP5 II) in the *Centro de Instrumentación científica* (CIC) of the University of Granada.

3.9 In vivo studies

The studies described in items 9.1 and 9.2 were executed at the Bioterium of the *Centro de Biociências-UFRN*, Brazil. Female Wistar rats (200 ± 20 g, 8 weeks old) were used. Rodents were acclimated for 7 days before experimentation, housed under standard environment conditions at 20–25 °C and 12 h dark/light cycle, and had free access to potable water (ad libitum) and standard food. The experimental protocol of the study was approved by the Committee for Ethics in Animal Experimentation of the UFRN under protocol n° 176.027/2019 (ANNEX II) following the guidelines of the National Council for the Control of Animal Experimentation (CONCEA).

The studies described in items 3.9.3 and 3.9.4 were executed at *Centro de Instrumentación Científica (CIC) de la Universidad de Granada (UGR)*, Spain. This research was submitted and approved by the Ethics Committee on Animal Experimentation (CEEA) of the University of Granada (Spain) with protocol No. 28/03/2016/30. The studies followed the "Guide for the Care and Use of Laboratory Animals" promulgated by the National Institute of Health. All the animals were housed in Makrolon cages, with food and water ad libitum, under standard environmental conditions: the temperature at 24 ± 1 °C, 12 hours light/dark cycle. Every effort was made to reduce the number of animals used and to minimize their suffering.

3.9.1 Acute toxicity

The acute toxicity by the oral route of the NCE was performed following the criteria recommended by the OECD, 2001 (30). The animals were randomly divided into two groups (n = 6 per group). The control group received distilled water orally, and the NCE group received a limited dose at 2000 mg/kg of the NCE by oral route.

Behavioral Evaluation (Hippocratic Screening and Open Field Test) and Motor (Rotarod Test)

After administration, the animals of all groups were observed with special attention in the first minutes (0, 5, 10, 15, 30, 60, 120, and 240) and 24 h after administration. Then, the behavioral evaluation was followed daily for 14 days. The analysis method applied was the Hippocratic screening, which considers the excitatory behavioral and inhibitory criteria and general activity such as defecation, diarrhea, urination, piloerection, and death (203). In addition, body mass and feed consumption were also evaluated throughout the experiment.

On days 1, 7, and 14 after the administration of the NCE, the animals were submitted to behavioral testing using the open field apparatus to analyze the exploratory activity of the animals (maximum time of 5 min for each animal). On the same days (1, 7, and 14), the animals were placed on the rotating bar of the rotarod apparatus at a constant speed of 10 rpm. After 1 min of training, the time the animal remained on the bar was recorded (maximum time of 3 min) by the method described by Pereira et al. (204) with few adaptations.

Evaluation of Hematological, Biochemical and Anatomopathological Parameters

On the 15th day, the animals were anesthetized with 10% ketamine and 2% xylazine (50 mg/kg; 10 mg/kg, intraperitoneal route), and blood was collected by cardiac puncture to perform hematological and biochemical tests: glucose, triglycerides, total cholesterol (CHOL), urea, creatinine (CREA), albumin (ALB), aspartate aminotransferase (AST) and alanine aminotransferase (ALT), as analytical quality control of the analysis of lipemia and degree of hemolysis were performed. The biochemical assays were performed using standardized commercial diagnostic kits from ByoSys® and Kovalent® in a biochemical analyzer. For hematological analysis: Erythrocytes, hematocrit (HCT), hemoglobin (HGB), mean corpuscular volume (MCV), mean corpuscular hemoglobin (MCH) and mean corpuscular hemoglobin concentration (MCHC), leukocytes and platelets were then determined.

The organs (liver, kidney, and spleen) were collected, and their absolute weights were measured. The relative weight of these organs was obtained using the formula: organ mass/ponderal mass × 100. The organs were analyzed macroscopically and microscopically.

3.9.2 Dinitrobenzene sulfonic acid (DNBS)-induced colitis in rats

Colitis induction was conducted according to Morris et al. (31), with minor modifications (205). Female Wistar rats were randomized into six groups (n = 8): The control group (non-colitis), DNBS group (were not treated after colitis induction), sulfasalazine (SSZ; received 250 mg/kg), and NCE (received 100, 200 or 300 mg/kg), as described in Table 6.

Table 6. Experimental groups: Dinitrobenzene sulfonic acid (DNBS)-induced acute colitis assay.

Group	Treatment
Control	Non-colitis group received intracolonic instillation of 0.9% normal saline only
DNBS	Not treated after colitis induction
SSZ	Received the drug sulfasalazine 250 mg/kg administered by oral gavage
NCE 100	Received 100 mg/kg of *N. cochenillifera* extract administered by oral gavage
NCE 200	Received 200 mg/kg of *N. cochenillifera* extract administered by oral gavage
NCE 300	Received 300 mg/kg of *N. cochenillifera* extract administered by oral gavage

SSZ: (sulfasalazine); NCE (*Nopalea cochenillifera* extract).

The animals received treatments 3 days before and 2 days after colitis induction. On day 4, under light anesthesia at doses of 50 mg/kg of ketamine and 5 mg/kg of xylazine by an intraperitoneal route and fasting overnight, animals kept in head-down positions were given 0.25 mL DNBS (25 mg dissolved in 50% (*v/v*) ethanol solution) through a Teflon cannula (2 mm diameter) inserted 8 cm into the anus. Rats from the control group intracolonically received 0.5 mL of 0.9% saline. The vehicle (water; control groups) or NCE or sulfasalazine were orally administered for 12, 24, and 48 h after the colitis induction. All animals 72 h after the induction with DNBS were euthanized with anesthetic overdoses of ketamine (225 mg/kg) and xylazine (30 mg/kg) by an intraperitoneal route (Figure 9).

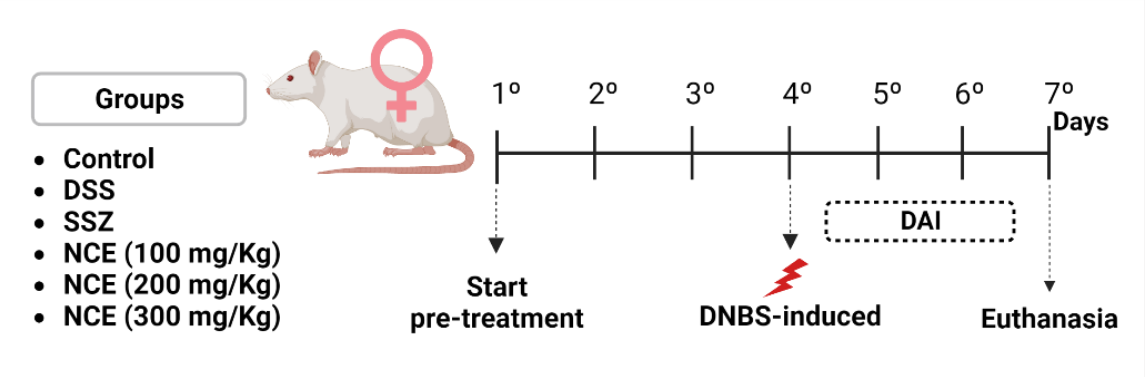

Figure 9. Experimental design in the DNBS-induced colitis in rats. DNBS (Dinitrobenzene sulfonic acid); SSZ (sulfasalazine); NCE (*N. cochenillifera* extract); DAI (Disease activity index)

The disease activity index (IAD) was evaluated by body weight variation, presence of rectal bleeding, and stool consistency, a methodology adapted from Cooper et al., (206) and Berberat et al. (207) (Table 7).

Table 7. Disease activity index (DAI) score used to evaluate the DNBS-induced.

Score (0-4)	Weight loss (%)	Stool consistency	Rectal bleeding
0	None	Normal	Absent
1	1-10	Slight loss of consistency	Slight (+)
2	10-15	Moderate loss of consistency	Moderate (++)
3	15-20	Pasty	Intense (+++)
4	>20	Diarrhea	Very intense (++++)

Adapted from Cooper et al. (206) and Berberat et al. (207)

In this assay, the colons were opened longitudinally, photographed, and macroscopic damage was assessed according to Bell et al. (1995) (208), with scores ranging from (0) normal colon (no damage); (2) ulceration without hyperemia or wall thickening; (3) ulceration with flash point; (4) two sites or more of ulceration and/or inflammation; (5) large inflammation zones and ulceration with an extension greater than 1 cm and (6–10) for large areas of tissue damage and for damage with an extension greater than 2 cm, with 1 point being added for each additional centimeter of tissue injury. Finally, the length and weight of the colon were measured.

Representative samples of the inflamed area were collected and fixed in buffered formaldehyde for histological and immunohistochemical studies. Colonic samples also were frozen at -80 °C for RT-qPCR, myeloperoxidase (MPO), malondialdehyde (MDA), and cytokine production analyses.

3.9.3 Dextran sulfate sodium (DSS)-induced colitis in mice

Male C57BL/6J mice (7-9 weeks old) obtained from Charles River Laboratories (Lyon, France) were randomly divided into five groups (n = 10): Control (non-colitis group), DSS (colitis group), NPB (Blank nanoparticles), NCE (*N. cochenillifera* extract 200 mg/kg) and NPE (extract-loaded nanoparticles), as described in Table 8.

Table 8. Experimental groups: Dextran sulfate sodium (DSS)-induced acute colitis assay.

Group	Treatment
Control	Non-colitis group
DSS	Not treated after colitis induction
NPB	Received nanoparticles without extract administered by oral gavage
NCE	Received 200 mg/Kg of *N. cochenillifera* extract administered by oral gavage
NPE	Received 4mg/Kg of extract-loaded nanoparticles administered by oral gavage

NPB (Blank nanoparticles); NCE (*Nopalea cochenillifera* extract); NPE (extract-loaded nanoparticles).

The animals received pre-treatments in the first two weeks of the trial. On day 15, colitis induction was initiated by adding 3% (*w*/*v*) DSS (36-50 KDa, MP Biomedicals) to the animals drinking water for five consecutive days, except in the healthy group, which received only water. All mice were fed standard rodent chow and water (with or without DSS) *ad libitum* throughout the experimental period. The dose chosen for this trial was based on the results obtained in a previously performed study (described in topic 3.9.2). The disease activity index (DAI) was evaluated from the first day of induction with DSS (day 15) until the sixth day after induction (day 20). Mice were euthanized on day 21 (Figure 10). The DAI was evaluated by body weight variation, presence of rectal bleeding and stool consistency (32) (Table 9).

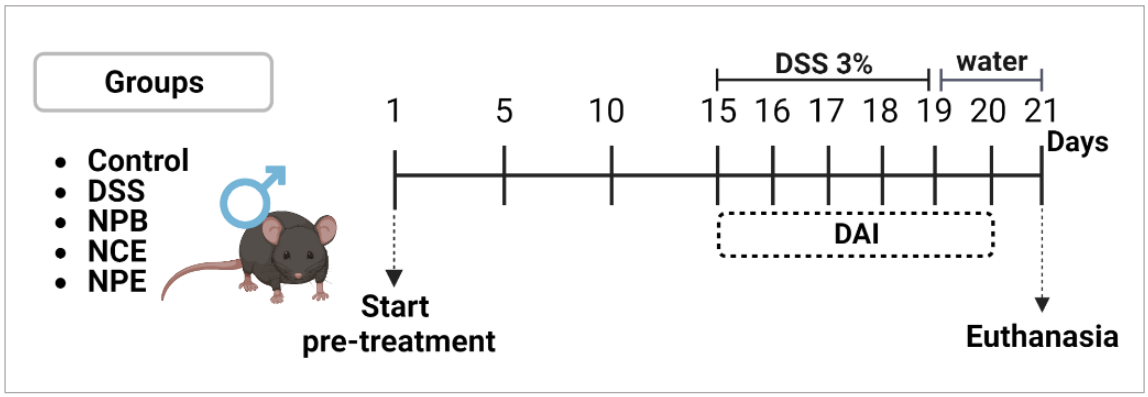

Figure 10. Experimental design in the DSS-induced colitis in mice. DSS (dextran sulfate sodium); NPB (Blank nanoparticles); NCE (*Nopalea cochenillifera* extract); NPE (extract-loaded nanoparticles); DAI (Disease activity index).

Table 9. Disease activity index (DAI) score used to evaluate the DSS-induced.

Score (0-4)	Weight loss (%)	Stool consistency	Rectal bleeding
0	None	Normal	Absent
1	1-5	Mucous traces	Perianal blood traces
2	5-10	Loose stools	Blood traces on stools
3	10-20	Diarrhea	Bleeding
4	>20	Gross diarrhea	Gross bleeding

Adapted from Garrido-Mesa et al. (32).

After the euthanasia of the animals, the colon was dissected near the ileocecal valve, weighed (g), and its length (cm) was measured under a constant load (2 g) to determine the weight/length ratio (g/cm) of the colon. Subsequently, intestinal explants were collected to measure cytokine production (methodology described in item 3.9.3.2). Colon tissue samples were also collected and fixed in buffered formaldehyde for histological studies. Finally, parts of the fragments were frozen at -80 °C for RT-qPCR analysis.

3.9.3.1 Intestinal permeability

Four hours before being euthanized, mice from different experimental groups (n = 4) received a FITC-Dextran solution administered by oral gavage (350 mg/Kg). Soon after, blood samples were collected by cardiac puncture and centrifuged at 4 °C and 3000 rpm (4000×g) for 10 minutes. Plasma was diluted (1:50) in PBS (pH 7.4) and analyzed for FITC-Dextran concentration with a fluorescence Spectrophotometer (Fluorostart, BMG Labtechnologies, Offenburg, Germany) at an excitation wavelength of 485 nm and an emission wavelength of 535 nm. Standard curves were obtained by diluting FITC-dextran in PBS (33).

3.9.3.1 Colonic explant culture and cytokine determination by ELISA

Immediately after euthanasia, three circular fragments were collected from the distal, medial, and proximal portions of the colon tissue using a punch biopsy (Miltex). The samples were placed in cell culture plates with the mucosal part facing up and incubated in DMEM at 37 °C (33). After 24 hours, the supernatants were collected (n = 8 per group). The levels of pro-inflammatory cytokines (IL-1β and MIP-2) present in the supernatant were measured using enzyme-linked immunosorbent assay (ELISA) with kits purchased from PeproTech (PeproTech EC Ltd, London, UK), according to manufacturer's instructions.

3.9.4 Metabolic Syndrome Study - Diet-Induced

Male C57BL/6J mice (5 weeks old) obtained from Charles River Laboratories (Lyon, France) were randomly divided into four groups (n = 10): SD control, SD-NCE, HFD control, and HFD-NCE, as described in Table 10.

Table 10. Experimental groups: Diet-induced metabolic syndrome assay.

Group	Treatment
SD control	Standard Diet + Vehicle
SD-NCE (200 mg/kg)	Standard Diet + *N. cochenillifera* extract administered by oral gavage
HFD control	High-fat Diet + Vehicle
HFD-NCE (200 mg/kg	High-fat Diet + *N. cochenillifera* extract administered by oral gavage

SD (Standard diet); HFD (High-fat diet); NCE (*Nopalea cochenillifera* extract).

Mice were fed with either a standard chow diet (13% calories from fat, 20% calories from protein, and 67% calories from carbohydrates) (Global diet 2014; Harlan Laboratories, Barcelona, Spain) or a high-fat diet (HFD) with 60% of its caloric content derived from fat (Purified diet 230 HF; Scientific Animal Food & Engineering, Augy, France). NCE was dissolved in 0.1 mL of water and administered daily by oral gavage. The control groups also received the same volume of the vehicle (water) used daily to administer the extract. Treatments followed for 10 weeks, and the mice body weight and food and water intake were measured regularly twice a week (36) (Figure 11).

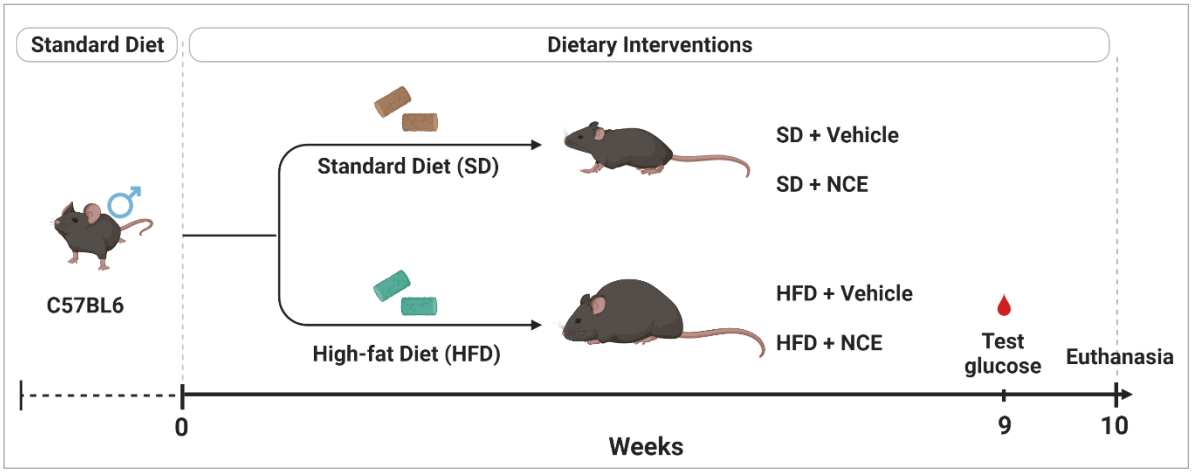

Figure 11. Experimental design in the mouse model of diet-induced metabolic syndrome. SD (Standard Diet); HFD (High-fat Diet); NCE (*N. cochenillifera* extract).

The energy intake was calculated by multiplying the amount of diet consumed by each animal per day (measured in g/day/animal) by the energy density of the respective diet and expressed in kcal/g mouse weight/day. Furthermore, the energy efficiency was determined by computing

the ratio between the final weight gain and the total energy intake throughout the entire experimental period, expressed in g/kcal.

Glucose tolerance test

One week before the mice were euthanized, a glucose-tolerance test was performed on mice that were food deprived for 8 h. The mice received a 50% glucose solution in water at a dose of 2 g/kg of body weight by intraperitoneal route. Blood samples were collected from the tail vein, and blood glucose was measured at time 0 (minutes before injection administration) and 60, 0, 15, 30, 60, 120, and 180 minutes after the glucose administration. The blood glucose levels were measured using a portable glucometer (Contour XT, Ascensia Diabetes Care, S.L., Barcelona, Spain).

Plasma determinations

At the end of the 10th week of treatment, the mice were anesthetized, and blood samples were collected by cardiac puncture. The samples were centrifuged for 20 minutes at 5000×g at 4°C, and the plasma was frozen at -80°C. Plasma glucose, insulin, LDL (low-density lipoprotein)-cholesterol, and HDL (high-density lipoprotein)-cholesterol concentrations were measured by colorimetric methods using Spinreact kits (Spinreact, S.A., Girona, Spain).

Morphological variables

Liver, abdominal, epididymis, and brown fat were removed, cleaned, and weighed. Liver and fat weight indices were calculated by dividing their weights by the tibia length. Afterward, all tissue samples were frozen in liquid nitrogen and stored at -80 °C.

3.9.5 Thiobarbituric acid reactive substance (TBARS) Assay

To assess lipid oxidation in liver tissue, we measured the levels of 2-thiobarbituric acid-reactive substances (TBARS) using an extraction method with thiobarbituric acid (TBA) dissolved in dimethyl sulfoxide (DMSO) and trichloroacetic acid at 10% (w/v) in water, along with 1,1,3,3-tetramethoxypropane dissolved in ethanol. This method allowed us to indirectly measure the levels of malondialdehyde (MDA), a breakdown product of lipid peroxidation, based on its ability to react with TBA and form TBARS, a pink chromogen measured at 535 nm. TBARS levels were expressed as µM/mg of protein in the liver tissue. The protein content of the samples was determined using the bicinchoninic acid assay (BCA) colorimetric method with bovine serum albumin (BSA) as the standard.

3.9.6 Determination of myeloperoxidase (MPO) activity

MPO activity following the technique described by Krawisz et al. (209). Next, the homogenates were subjected to a triple freeze-thaw process for approximately 3 hours and then subjected to the action of a sonicator (Schuster L 200 Ultrasonic Washer) for 5 minutes without the presence of light. Next, aliquots were centrifuged (2000×g at 4 °C for 20 minutes), and the supernatant was stored at -80°C until analysis. For the assay, 50 µL of the resulting supernatant from colonic tissue aliquots and 150 µL of chromogenic reagent (composed of o-dianisidine dihydrochloride with hydrogen peroxide) were added to a 96-well plate, resulting in the formation of a chromophore that has a maximum absorbance of 450 nm, which was quantified using a microplate reader (Mindray MR-96A). Results were expressed as units of MPO per gram of wet tissue (U/g), with one unit of MPO activity defined as the amount of MPO that degrades 1 mmol of hydrogen peroxide per minute at 25 °C.

3.9.7 Determination of malondialdehyde (MDA) levels in the intestine

MDA content was determined by the method described by Esterbauer and Cheeseman (210). First, colonic tissue samples (n = 8) were homogenized (homogenizer Marconi MA1102, SP, Brazil) with 20 mM Tris hydrochloride buffer (pH = 7.4; 1:5 *w*/*v*) and centrifuged at 2500× *g* at 4 °C for 10 min. Then, the supernatants were assayed with chromogenic reagent (1-methyl-2-phenylindole 10.3 mM in 3:1 acetonitrile) and HCl (37%) for 40 min at 45 °C and centrifuged again (2500× *g* at 4 °C for 5 min). Finally, the reading was performed at 492 nm in a microplate reader (Mindray MR-96, SP, Brazil), and calculated its content by interpolation on a standard curve with 1,1,3,3-tetra ethoxy propane (10 mM). The results were expressed as nmol/g tissue (181).

3.9.8 Measurement of Cytokine Production in the Intestine

Intestinal tissue (n = 8) was homogenized (homogenizer Marconi MA1102, SP, Brazil) with PBS and centrifuged (3500× *g* at 4 °C for 10 min). Cytokine levels in the supernatant resulting from centrifugation were evaluated using kit protocols (Sigma-Aldrich, São Paulo, Brazil), and standard capture and detection antibodies for IL-1β, TNF-α and IL-10. Cytokine levels were determined at an absorbance of 450 nm (expressed in ng/g) by ELISA (Mindray MR-96, SP, Brazil), performed using the method described by Da Silva et al. (211).

3.9.9 Analysis of gene expression by RT-qPCR

RNA extraction

Colon tissue samples collected in the DNBS-induced colitis study (described in item 9.2 of this section) were homogenized. First, RNA was extracted from colonic tissue using the Trizol reagent (Intvitrogen™, Waltham, MA, USA). And then, RNA was isolated using the total SV Total RNA isolation system (Promega Corporation®, Southampton, UK), following the manufacturer's specifications.

For colon tissue samples were homogenized using a Precellys 24 tissue homogenizer (Bertin Technologies, Montigny-Le bretonneux, France), and then RNA was isolated using the RNeasy® Mini Kit (Qiagen, Hilden, Germany), following the manufacturer's instructions. The extracted RNA was measured with a NanoDrop™ 2000 spectrophotometer (ThermoFisher Scientific, Waltham, MA, USA).

RNA retrotranscription

For cDNA synthesis, 2 µg - 5 µg of total RNA per sample was reverse transcribed into cDNA using the oligo(dT) primers (Promega, Southampton, UK) or Kit High-Capacity cDNA Reverse Transcription (Applied Biosystems, USA), following the manufacturer's instructions.

Gene expression analysis by quantitative PCR (qPCR)

The resulting cDNA was amplified using MasterMix qPCR Syber Green (PCR Biosystems Ltd) and primers (Forward-Reverse/FW-RV) (Table 11). The gene expression was normalized using the housekeeping glyceraldehyde-3-phosphate dehydrogenase (GAPDH) and beta-actin (β-actin) gene as the internal control. Relative gene expression was calculated using the ΔΔCt method and expressed as fold-change compared with the control group.

Table 11. Primer sequences used in PCR assays.

Gene	Primer sequence 5'- 3'	Organism	Annealing T (ºC)
GAPDH	FW: CCATCACCATCTTCCAGGAG RV: CCTGCTTCACCACCTTCTTG	Mouse	60
β-actin	FW: CGCACTGCCGCATCCTCT RV: GTCGAAGAGAGCCTCGG	Rats	58
AMPK	FW: GACTTCCTTCACAGCCTCATC RV: CGCGCGACTATTCAAAGACATACG	Mouse	60
GLUT-4	FW: TCAGAAGACAAGATCACCGGA RW: GCTGGTGTGACTGTAAGTGGG	Mouse	59
ICAM-1	FW: GAGGAGGTGAATGTATAAGTTATG RV: GGATGTGGAGGAGCAGAG	Mouse	60

IL-1β	FW: TGATGAGAATGACCTGTTCT RV: CTTCTTCAAAGATGAAGGAAA	Mouse	57
IL-6	FW: TAGTCCTTCCTACCCCAATTTCC RV: TTGGTCCTTAGCCACTCCTTC	Mouse	59
iNOS	FW: GTTGAAGACTGAGACTCTGG RV: GACTAGGCTACTCCGTGGA	Mouse	56
Leptin-R	FW: GCTATTTTGGGAAGATGT RV: TGCCTGGGCCTCTATCTC	Mouse	60
MAPK-1	FW: CCCAAGTGATGAGCCCATTG RV: GGTAAGTCGTCCAGCTCCATGT	Rats	58
MCP-1	FW: AGCCAACTCTCACTGAAG RV: TCTCCAGCCTACTCATTGF	Mouse	55
MIP-2	FW: CAGTGAGCTGCGCTGTCCAATG RV: CAGTTAGCCTTGCCTTTGTTCAG	Mouse	65
MUC-1	FW: GCAGTCCTCAGTGGCACCTC RV: CACCGTGGGCTACTGGAGAG	Mouse	60
MUC-2	FW: GCAGTCCTCAGTGGCACCTC RV: CACCGTGGGGCTACTGGAGAG	Rats	60
MUC-3	FW: CGTGGTCAACTGCGAGAATGG RV: CGGCTCTATCTCTACGCTCTCC	Mouse	65
NF-KB P65	FW: TCTGCTTCCAGGTGACAGTG RV: ATCTTGAGCTCGGCAGTGTT	Rats	58
OCLN	FW: ACGGACCCTGACCACTATGA RV: TCAGCAGCAGCCATGTACTC	Mouse	64
PPAR-α	FW: AGGCTGTAAGGGCTTCTTTCG RV: GGCATTTGTTCCGGTTCTTC	Mouse	62
PPAR-γ	FW:CATGGTGCCTTCGCTGAT RV:CAATGGCCATGAGGGAGTTA	Mouse	60
TLR-4	FW: GCCTTTCAGGGAATTAAGCTCC RV: AGATCAACCGATGGACGTGTAA	Mouse	65
TNF-α	FW: AACTAGTGGTGCCAGCCGAT RV: CTTCACAGAGCAATGACTCC	Mouse	56
ZO-1	FW: GGGGCCTACACTGATCAAGA RV: TGGAGATGAGGCTTCTGCTT	Mouse	56

3.10 Western blot

Liver samples (n = 6) were homogenized, and protein concentrations were measured (BCA Protein Assay Kit, Pierce Biotechnology, Rockford, IL, USA). 100 μg of protein were separated on 12% sodium dodecyl sulfate-polyacrylamide gel electrophoresis (SDS-PAGE, 12%) (Beyotime Biotechnology, Jiangsu, China) and transferred to a polyvinylidene fluoride (PVDF) membrane (GE Healthcare Life Sciences, Chicago, IL, USA). The membranes were blocked with 3% BSA and incubated at 4 °C overnight in primary antibodies: AMPK (1:1000 dilution), pAMPK (1:1000 dilution), PI3K (1:500 dilution), pPI3K (1:500), and β-actin (1:1000 dilution) served as the internal reference (Santa Cruz Biotechnology, Heidelberg, Germany, sc-47778). After 3 consecutive washes, the membranes were incubated for 2 h with secondary antibodies (Abcam, Cambridge, UK). Signal development was performed with the clarity western ECL substrate (Bio-Rad, Hercules, CA, USA) and signal acquisition using a ChemiDoc image system (Bio-Rad, Hercules, CA, USA). The quantification of bands was performed by

densitometric analysis using ImageJ Fiji software (Free Software Foundation Inc., Boston, MA, USA) (212).

3.11 Histological studies

Representative samples of colonic tissue, liver, and fat (n = 5 per group) were collected and fixed in 4% paraformaldehyde, dehydrated in ethanol solutions, and embedded in paraffin. Subsequently, colonic sections with 4-5 μm thickness were obtained with a microtome and stained with hematoxylin and eosin (H&E).

Specifically, the histochemical staining of mucins was carried out in the samples from the DSS-induced colitis study (described in item 9.3 of this section). Sections were first incubated in alcian blue (1%) in acetic acid (3%) for 30 min prior to conventional H&E staining.

Histological sections were evaluated for the degree of leukocyte infiltration and its distribution in the colonic tissue (Score 1-6), following criteria pre-established by Zea-Iriarte et al. (213) or the degree of edema, inflammatory cell infiltration, presence of ulceration, and state of the crypts were evaluated (Score 0-59), following criteria pre-established by Garrido-Mesa et al. (32). Additionally, the adipocyte size of the fat samples collected from the mouse-induced metabolic syndrome assay (described in item 9.4 of this section) was measured and analyzed using Fiji (advanced distribution of ImageJ) imaging software with the Adiposoft v1.16 plugin.

Immunohistochemical analysis was performed on the colon samples collected in the DNBS-induced colitis study (described in section 9.2 of this section). The histological sections were deparaffinized, rehydrated, washed in 0.3% Triton X-100 in phosphate buffer, and incubated with endogenous peroxidase (3% hydrogen peroxide). The sections were incubated overnight at 4 °C in the presence of primary antibodies (Santa Cruz Biotechnology, Dallas, TX, USA): NF-κB p65 (1:100) and COX-2 (1:500). The sections were carefully rinsed with phosphate buffer and incubated in the presence of secondary antibody streptavidin/HRP-conjugated (Biocare Medical, Concord, CA, USA) for 30 min. Immunoreactive cells were visualized by colorimetric detection following the protocol provided by the manufacturer (TrekAvidin-HRP Label + Kit Biocare Medical). Determination of the immunostaining intensity of the cells was determined by an adaptation of the protocol described by Guerra et al. (214).

3.12 Statistical Analysis

All data are represented as the mean ± SEM. Differences between means were tested for statistical significance using one-way ANOVA followed by Tukey's test. Non-parametric data (score) were expressed as the median (range) and were analyzed using the Mann–Whitney test for histological studies.

As for the experimental data related to obtaining and characterizing the nanoparticles, they were presented with the mean values ± standard deviation. Initially, a normality test was performed, followed by the test t-student for paired analyses of two means or the one-way analysis of variance (ANOVA), followed by the Tukey test when applicable.

All statistical analyses were performed using GraphPad 6.0 software (GraphPad Software Inc., La Jolla, CA, USA) with statistical significance set at $p < 0.05$.

IV. RESULTS

The results obtained from the experiments were sequentially presented in this section, arranged in the order of their execution.

4.1 Physicochemical and phytochemical analysis of *Nopalea cochenillifera* Extract

The physicochemical analysis results of NCE, including pH, molar acidity, moisture, ashes, ether extract, crude fiber, protein, and total carbohydrates, are presented in Table 12. Notably, NCE has a high carbohydrate content (67.863 ± 0.00) and a significant content of phenolics (67.85 ± 0.04) but a low lipid content (2.78 ± 0.69). The total phenolic and flavonoid contents were expressed in gallic acid (GAE) and quercetin equivalent (QE) (mg) per gram of dry extract with a mean value equal to 67.85 mg GAE per g and 46.16 mg QE per g, respectively. The yield of dry extract was 4.48% (Table 13).

Table 12. Physicochemical analysis of *N. cochenillifera* hydroethanolic extract (NCE).

Parameters	Values
pH	4.50 ± 0.04
Molar acidity (g/100 g)	4.40 ± 0.00
Moisture (g/100 g)	12.98 ± 0.51
Ashes (g/100 g)	0.002 ± 0.00
Ether extract (g/100 g)	2.78 ± 0.69
Crude fiber (g/100 g)	63.85 ± 7.32
Protein (g/100 g)	16.36 ± 0.35
Total carbohydrates (g/100 g)	67.86 ± 0.00

Experimental results analyzed in triplicate. Data expressed as mean ± standard deviation.

Table 13. Total phenolic and flavonoid content of *N. cochenillifera* extract (NCE).

Extract	Total phenolics [1] (mg GAE/g)	Total flavonoids [2] (mg QE/g)	Yeld
Nopalea cochenillifera hydroethanolic extract	67.85 ± 0.04	46.16 ± 0.03	4%

[1] Gallic acid equivalent milligrams (GAE) per hundred grams of extract (mg GAE/g); [2] Quercetin equivalent milligrams (QE) per hundred grams of extract (mg QE/g); Experimental results analyzed in triplicate. Data expressed as mean ± standard deviation.

The chromatographic profile analysis was performed through HPLC-ESI-MS^n in the negative and positive ionization mode (Figure 12), allowing the characterization of saccharides, organic acids, phenolic acids, and flavonoids.

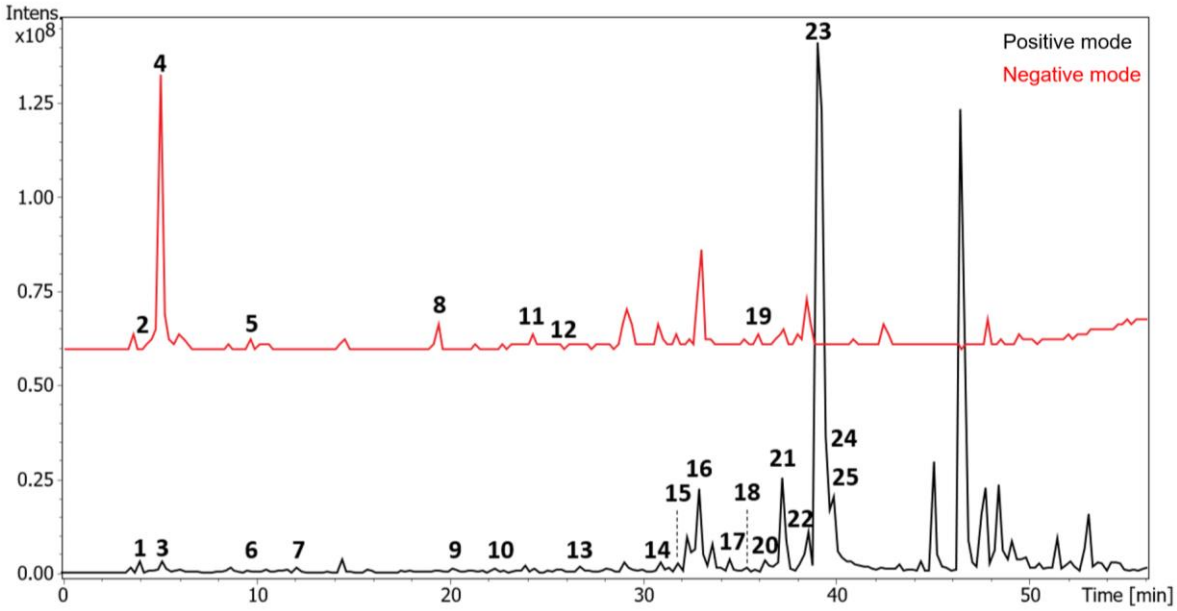

Figure 12. HPLC-ESI-MS/MS chromatogram of *N. cochenillifera* extract in the negative mode and positive mode.

The compounds were characterized based on assignments of their mass spectra, using the precursor ion, fragment ions, and comparing the fragmentation patterns with molecules provided by the GNPS library and described in the literature. The putative identification of these compounds is summarized in Table 14. Each compound was assigned a number following the sequence of its retention time.

Table 14. Annotated compounds in the *N. cochenillifera* hydroethanolic extract by HPLC-ESI-MS^n

.N.	Rt (min)	Adduct	MS (*m/z*)	MS^2 (*m/z*)	MS^3 (*m/z*)	Metabolite	References
1	4.47	$[M+Cl]^-$	377	**341**	281, 179, 161	dihexose (maltose or sucrose)	TRIPODO et al., 2018.
2	4.71	$[M-H]^-$	195	177, 159, **129**	101, 85, 57	gluconic acid	LIU et al., 2010.
3	4.95	$[M+Cl]^-$	539	**503**, 341	341, 323	trihexose (raffinose)	TIKUNOV et al., 2010.
4	5.17	$[M+Cl]^-$	377	**341**	281, 179, 161	dihexose (maltose or sucrose)	TRIPODO et al., 2018.
5	9.32	$[M-H]^-$	191	173, **111**	67	citric acid	YAKUBU et al., 2021.
6	9.69	$[M+H]^+$	135	**117**, 99	99, 71	malic acid	ABU-REIDAH et al., 2015.
7	12.19	$[M+H]^+$	284	**152**	135, 128, 110	guanosine	TUYTTEN et al., 2005.
8	19.50	$[M-H]^-$	447	429, 403, **315**, 297,	269, 195, 163, 153, 119	dihydroxybenzoic acid *O*-pentose-hexose	HAN et al., 2008

				207, 177, 163			
9	21.42	$[M-H]^-$	447	**315**	153, 123	dihydroxybenzoic acid *O*-pentose-hexose	HAN et al., 2008
10	22.46	$[M+H]^+$	195	**177**	163, 145, 117	ferulic acid	BEN-SAID et al., 2017
11	24.36	$[M-H]^-$	355	295, 265, 235, 217, **193**, 175, 160, 134	178, 149, 134	ferulic acid *O*-hexose	BEN-SAID et al., 2017
12	25.75	$[M-H]^-$	355	217, **193**, 175	178, 149, 134	ferulic acid *O*-hexose	BEN-SAID et al., 2017
13	27.53	$[M+H]^+$	169	**137**	109, 93, 81	vanillic acid	HAYUN et al., 2020.
14	30.98	$[M+H]^+$	757	611, 465, **303**	285, 257, 229, 165, 153	quercetin-*O*-hexose-deoxyhexose	LIN, HARNLY 2007.
15	31.89	$[M+H]^+$	476	**314**	177, 145	feruloyltyramine-*O*-hexose	GENG et al., 2017
16	32.98	$[M+H]^+$	771	625, 479, 463, 427, **317**, 302	302, 285, 274, 257, 153	methylquercetin-*O*-hexose-deoxyhexose-deoxyhexose	LIN, HARNLY 2007.
17	34.32	$[M+H]^+$	562	386, **314**	177, 145	feruloyltyramine-*O*-(malonyl)-hexose	NIKOLIĆ et al., 2013.
18	35.19	$[M+H]^+$	611	593, 465, **303**	285, 257, 229, 165	quercetin-*O*-hexose-deoxyhexose (rutin)	SPINOLA et al., 2015
19	36.56	$[M-H]^-$	445	**283**	268	hydroxymethoxy-isoflavone-*O*-hexose	LIN, HARNLY 2007
20	37.27	$[M+H]^+$	461	**299**	284, 266	hydroxy-dimethoxy-isoflavone-*O*-hexose	LIN, HARNLY 2007
21	37.46	$[M+H]^+$	314	**177**, 145, 117	145, 117	feruloyltyramine	NIKOLIĆ et al., 2013.
22	38.15	$[M+H]^+$	595	449, **287**	269, 258, 241, 231, 213, 197, 165, 153, 121	kaempferol-*O*-hexose-deoxyhexose	LIN, HARNLY 2007
23	38.60	[M+H]+	625	479, **317**, 302	302, 285, 229, 165, 153	methylquercetin-*O*-hexose-deoxyhexose	LIN, HARNLY 2007
24	38.83	$[M+H]^+$	547	**299**, 284, 266	284, 266	hydroxydimethoxy-isoflavone-*O*-(malonyl)-hexose	LIN, HARNLY 2007
25	39.91	$[M+H]^+$	547	**299**, 284, 266	284, 266, 239	hydroxydimethoxy-isoflavone-*O*-(malonyl)-hexose	LIN, HARNLY 2007

(a) In bold are the precursor ions of MS^n experiments.

The sugar portion of the *O*-glycosylated compounds was determined by analysis of fragmentation pathways of the precursor ions in the positive and negative mode, such as the cleavage of saccharide residues, leading to characteristic neutral losses of 132 (pentose), 146 (deoxyhexose), and 162 Da (hexose) (215,216). MS/MS spectra analysis of the precursor ions $[M+H]^+$ at m/z 757 (**14**), 771 (**16**), 611 (**18**), 595 (**22**), and 625 (**23**) showed characteristic fragmentations of the flavonoids *O*-glycosylated with sequential losses of deoxyhexose and hexose moiety, which led to the formation of the product ions Y_0^+ at m/z 287 and m/z 303, found to be associated with the flavonol aglycones of kaempferol and quercetin, respectively. In addition, second-order fragmentation for compounds **16** and **23** resulted in neutral losses of 15 and 32 Da, corresponding to CH_3 and CH_3OH, respectively (217,218).

The precursor ions $[M+H]^+$ at *m/z* 447 (**19**), 461 (**20**), and 547 (**24** and **25**) showed a fragmentation pattern similar to flavonoids due to the loss of sugar residues, which resulted in the formation of Y_0^+ ions at *m/z* 285 (**19**) and at *m/z* 299 (**20**, **24** and **25**) and the radical elimination of methyl groups. This fragmentation pattern, which agrees with reports published in the literature, implies the presence of methoxylated isoflavones (219). The second-order fragmentation of compounds **24** and **25** resulted in a characteristic loss of 248 Da [M+H−86−162]+, indicating an acylation at the glycosyl residue assigned to the malonyl hexose group (215).

The analysis of the MS/MS mass spectra recorded for the precursor ions at m/z 476 (**15**), 562 (**17**), and 314 (**21**) showed representative fragmentation patterns of the amides of hydroxycinnamic. The second-order mass spectra of these ions showed similar characteristic losses of 137 Da and the fragment at *m/z* 177, corresponding to the tyramine and the ferulic acid residue, respectively (220,221). Other organic compounds were also observed, including several organic acids (compounds **2**, **5,** and **6**), benzoic acids (compounds **8**–**9** and **13**), and hydroxycinnamic acid and their derivatives (compounds **10**–**12**). (Table 14).

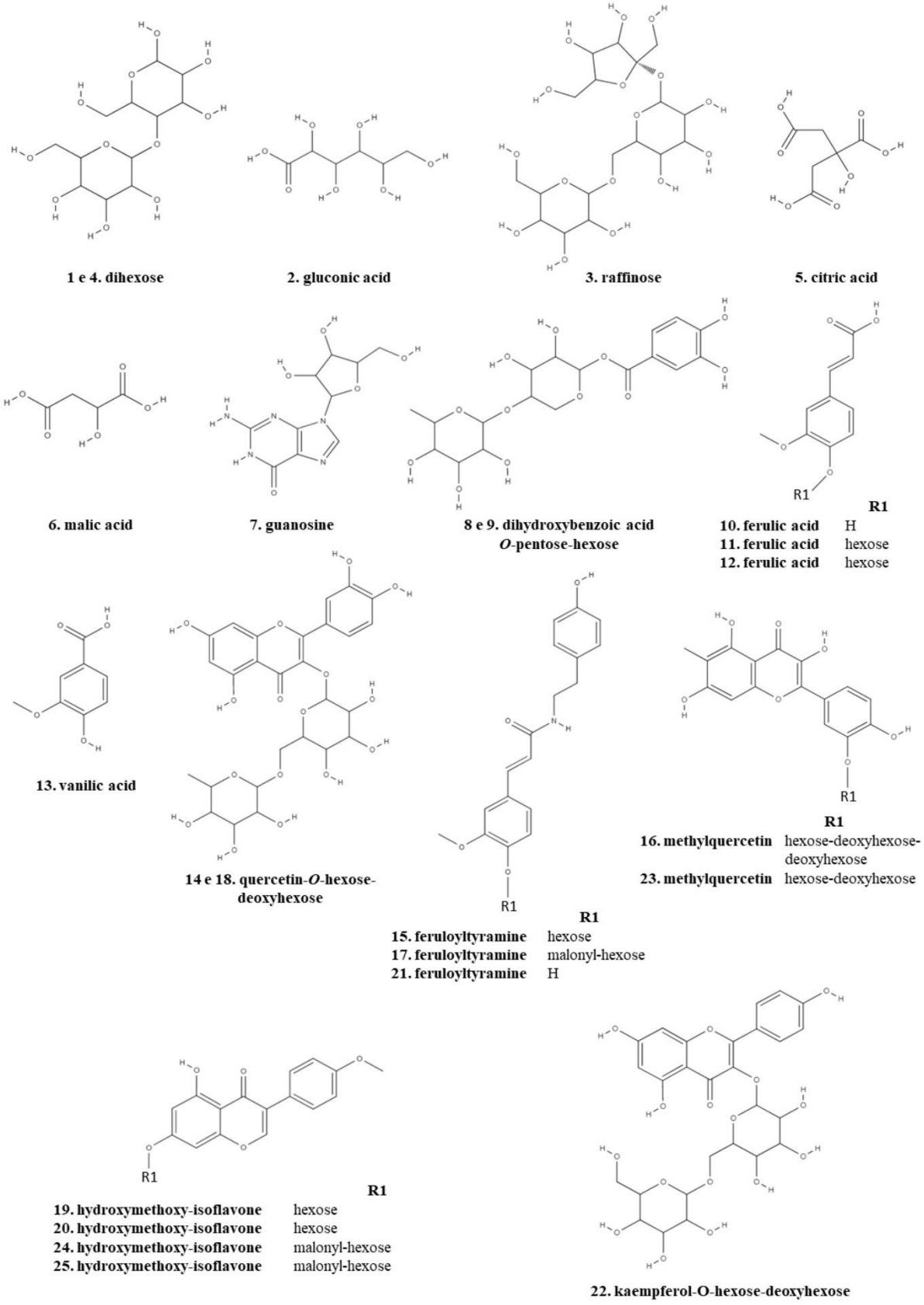

Figure 13. Structures of the compounds characterized in the *N. cochenillifera* extract.

4.2 Acute Toxicity

In the acute toxicity test, no mortality was observed in the experimental group that received an oral administration of NCE at a dose of 2000 mg/kg for a short period of 48 h and a prolonged period of 14 days. The animals survived until the end of the observation period. Body weight and feed consumption did not change during the 14 days compared to the control group (Figure 14).

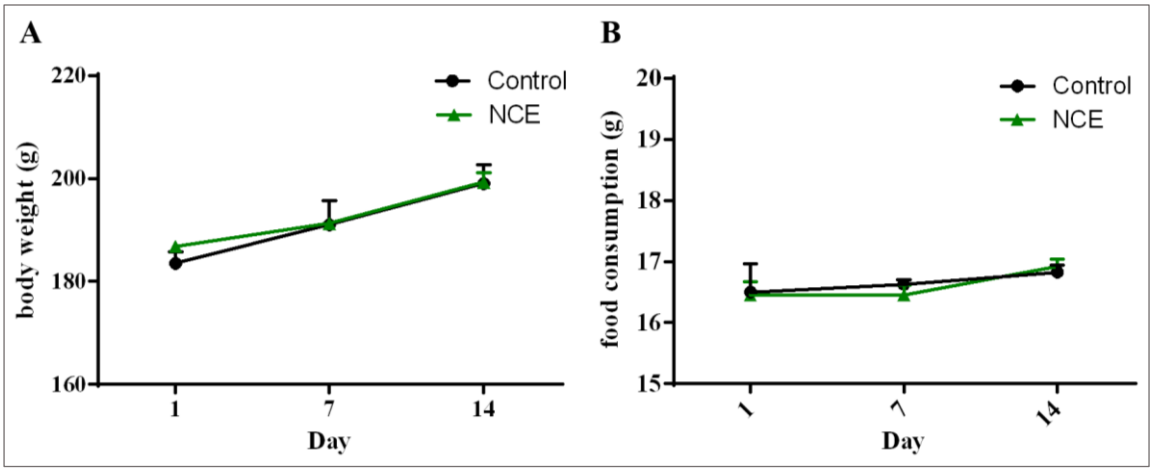

Figure 14. Relative body weight (**A**) and food consumption (**B**) of female rats treated with a single dose (2000 mg/kg) of *Nopalea cochenillifera* extract (NCE) observed for 14 days. Data are expressed as Mean ± SEM (*n* = 6/group). No statistical differences were detected between the treated group and the control group.

Table 15 presents the results of biochemical and hematological tests. NCE administration did not induce adverse effects related to toxicity concerning variation in body weight, general behavior, relative organ weights, and hematological and biochemical parameters of the animals in the treated group compared to the control group. For comparison purposes, the specialized literature recommends appropriate standardizing values for healthy animals from each animal house/laboratory, respecting local characteristics (222,223).

Table 15. Biochemical and hematological parameters of female rats treated with a single oral dose (2000 mg/kg) of *Nopalea cochenillifera* extract (NCE).

Biochemical Parameters			
Parameters	**Control^{ns}**	**NCE^{ns} (2000 mg/kg)**	**Reference Wistar (Females)**
Glucose (mg/dL)	159 ± 5.39	151 ± 9.26	53–172
Triglycerides (mg/dL)	48 ± 9.91	54 ± 5.26	23–138
Total Cholesterol (mg/dL)	69 ± 5.55	62 ± 3.33	54–96
Urea (mg/dL)	36 ± 5.55	33 ± 5.26	24–49
Creatinine (mg/dL)	0.6 ± 0.05	0.5 ± 0.08	0.3–1.1

Albumin (mg/dL)	2.9 ± 0.09	3.0 ± 0.04	1.3–3.8
AST (U/L)	99 ± 2.90	86 ±8.53	51–211
ALT (U/L)	50 ± 0.69	52 ± 0.55	32–62
Hematological parameters			
Erythrocytes (x10^6/µL)	7.53 ± 5.39	7.28 ± 9.26	5.21–8.83
Hemoglobin (g/dL)	13.7 ± 2.20	13.40 ± 1.13	11.1–17.10
Hematocrit (%)	44 ± 2.95	43.00 ± 2.43	27.00–49.00
MCV (fL)	51.27 ± 1.55	49.86 ± 4.36	45.00–56.70
MCH (pg)	18.41 ± 1.95	20.06 ± 1.06	16.60–22.80
MCHC (g/dL)	30.74 ± 0.12	31.35 ± 0.98	30.40–43.90
Leukocytes (cell/µL)	6400 ± 1920	5900 ± 1150	2300–9900
Platelets (x10^6/µL)	904 ± 96	1.025 ± 89	760–1.310

AST: aspartate aminotransferase, ALT: alanine aminotransferase, MCV: Mean Corpuscular Volume, MCHC: Mean Corpuscular Hemoglobin, MCHC: Mean Corpuscular Hemoglobin Concentration. ns: not significant. Data are expressed as Mean ± SEM (*n* = 6/group). No statistical differences were detected between the treated group and the control group.

No changes were observed between groups in the Hippocratic screening. The open-field test showed no significant difference in ambulation, rearing behavior, and grooming activities when comparing the control group to those treated with NCE. On day 7, there was an increase in the frequency of standing up in the group treated with the 2000 mg/kg dose of NCE. An increase in the number of defecations was also observed in the treated group during the experiment (Table 15).

In evaluating the motor activity of the animals employing the dwell time (seconds) on the rotating bar of the rotarod apparatus, no significant differences were recorded between the control group and the treated animals. The data are presented in Table 16.

Table 16. Behavioral evaluation in the open field test and motor activity evaluation in the rotarod test in rats on days 1, 7 and 14 post-treatment with *N. cochenillifera* extract (NCE) in a single oral dose (2000 mg/kg).

Open Field Test			
Parameters	**Day**	**Control**	**NCE (2000 mg/kg)**
Total distance traveled (cm)	1	230.80 ± 3.93	250.20 ± 5.54
	7	240.20 ± 2.15	220.20 ± 4.76
	14	260.80 ± 3.50	250.80 ± 4.52
Rearing or climbing behavior (count)	1	14.20 ± 2.25	16.40 ± 8.40
	7	12.32 ± 5.28	12.20 ± 4.38
	14	16.00 ± 6.06	19.6 ± 4.76

Grooming (count)	1	8.60 ± 1.95	9.60 ± 2.91
	7	7.00 ± 2.80	8.74 ± 2.67
	14	7.65 ± 1.54	9.80 ± 2.96
Number of defecations	1	1.00 ± 1.00 [a]	3.80 ± 1.00 [b]
	7	1.60 ± 1.02 [a]	3.80 ± 0.98 [b]
	14	0.80 ± 0.53 [a]	4.20 ± 2.00 [b]
Rotarod test			
Staying Time (seconds)	1	180.0 ± 0.00	179.6 ± 0.40
	7	180.0 ± 0.00	179.0 ± 1.00
	14	180.0 ± 0.00	180.0 ± 0.00

Values represent the mean ± SEM (*n* = 6/group). Different letters differ statistically.

The relative weights of the organs displayed no statistically significant distinctions between the animals that received NCE doses and those in the control group. Therefore, the relative weights of the liver, spleen, kidneys, heart, and lungs were unaffected by the acute administration of NCE at a dose of 2000 mg/kg (Table 17). Additionally, no external morphological modifications were noted in the texture or color of these organs compared to the control group.

Table 17. Relative weight of the organs of the rats in the control group and treated with *N. cochenillifera* extract (NCE) in a single oral dose (2000 mg/kg).

Relative Organ Weight (g/100 g body weight)		
Organ	**Control[ns]**	**NCE[ns] (2000 mg/kg)[ns]**
Liver	3.80 ± 0.12	4.10 ± 0.02
Spleen	0.28 ± 0.03	0.30 ± 0.04
Kidneys	0.90 ± 0.03	0.87 ± 0.04
Heart	0.35 ± 0.01	0.37 ± 0.02
Lung	0.42 ± 0.09	0.42 ± 0.20

ns: not significant. Data are expressed as Mean ± SEM (n = 6/group). No statistical differences were detected between the treated group and the control group.

In the microscopic analysis of the organs (liver, kidneys, and spleen) performed with the control group and with the animals treated with NCE (2000 mg/kg), no abnormalities were found, and the organs analyzed presented normal architecture, suggesting that there were no morphological changes (Figure 15).

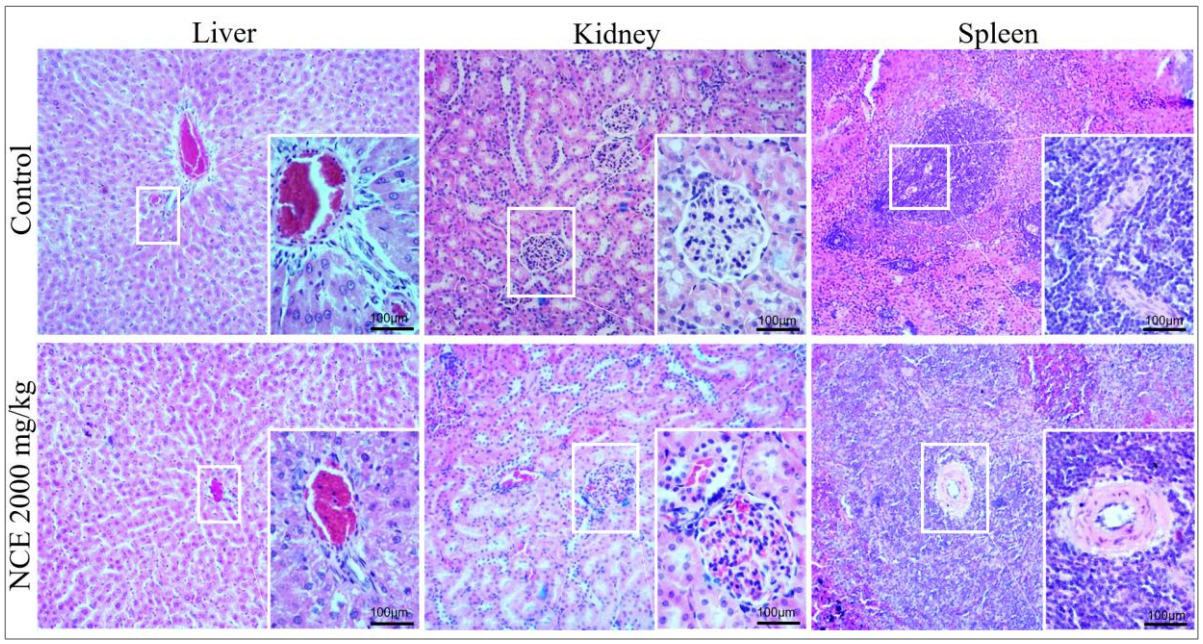

Figure 15. Photomicrographs of histopathological analyses of the liver, kidneys, and spleen (eosin-hematoxylin stain; 10× and 40× magnification) of tissues from rats in the control group and treated with *N. cochenillifera* extract (NCE) in a single oral dose (2000 mg/kg) after 14 days.

4.3 Effect of *Nopalea cochenillifera* extract on DNBS-Induced colitis in rats

The Disease Activity Index (DAI), Macroscopic Score and Weight/Colonic Length Ratio

The DNBS group showed important characteristics related to IBD, evidenced throughout the experiment, such as a loss of body weight, blood in the perianal region, and altered stool consistency, represented in parameters evaluated in the DAI (Figure 16A). Pre-treatment with NCE 100, 200, and 300 mg/kg or SSZ 250 mg/kg promoted a significant improvement in the DAI values when compared to the DNBS group ($p < 0.05$) (Figure 16A).

The body weights of all control and DNBS group rats were measured daily. The change in body weight from day 1 to day 6 is shown in Figure 16B. The baseline of the weight change was the mean weight of the first day (Day 1). The difference in weight loss was observed from day 5 onward in the SSZ and NCE-treated groups at doses of 200 and 300 mg/kg compared to the DNBS group.

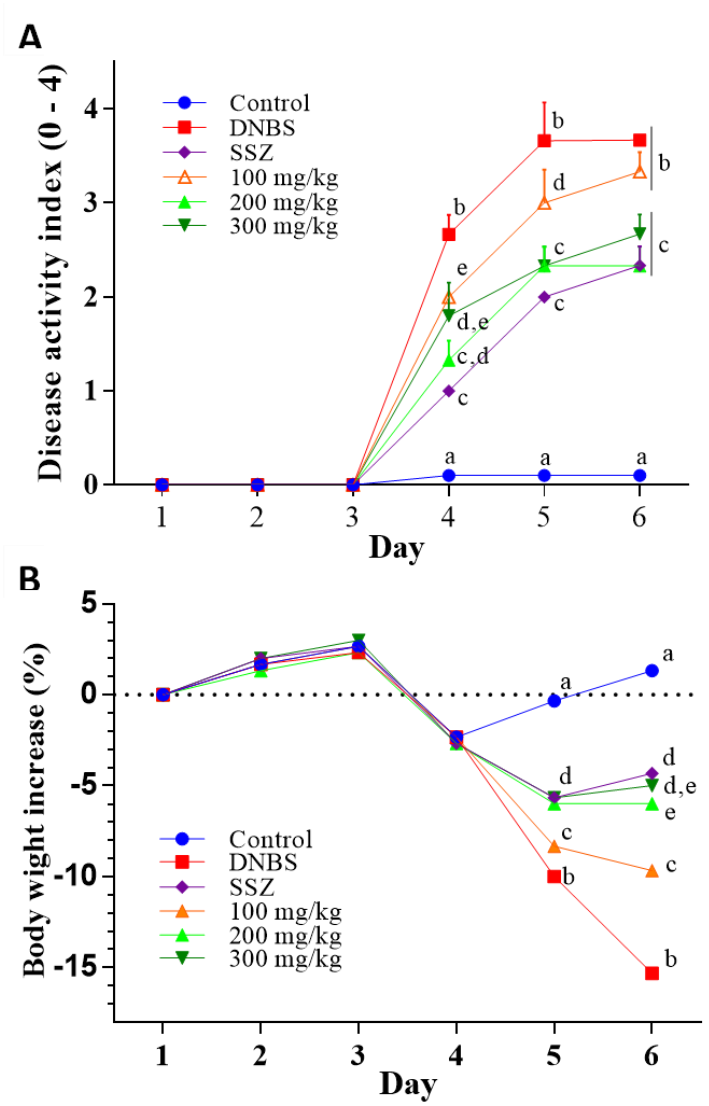

Figure 16. Effect of treatments with *N. cochenillifera* extract (NCE) (100, 200 and 300 mg/kg) and sulfasalazine (SSZ) (250 mg/kg) on colitis induced in rats by 2.4-Dinitrobenzene sulfonic acid (DNBS). (A) disease activity index and (B) weight loss. Data are expressed as means ± SEM. Groups with a different letter differ statistically ($p < 0.05$).

The macroscopic colonic damage observed in the DNBS control group was characterized by large areas of tissue damage, with the presence of ulcerations and thickening of the intestinal wall (Figure 17A) leading to a mean macroscopic damage score of 9.0 (Figure 17B), also represented by the weight/length of the intestine (Figure 17C).

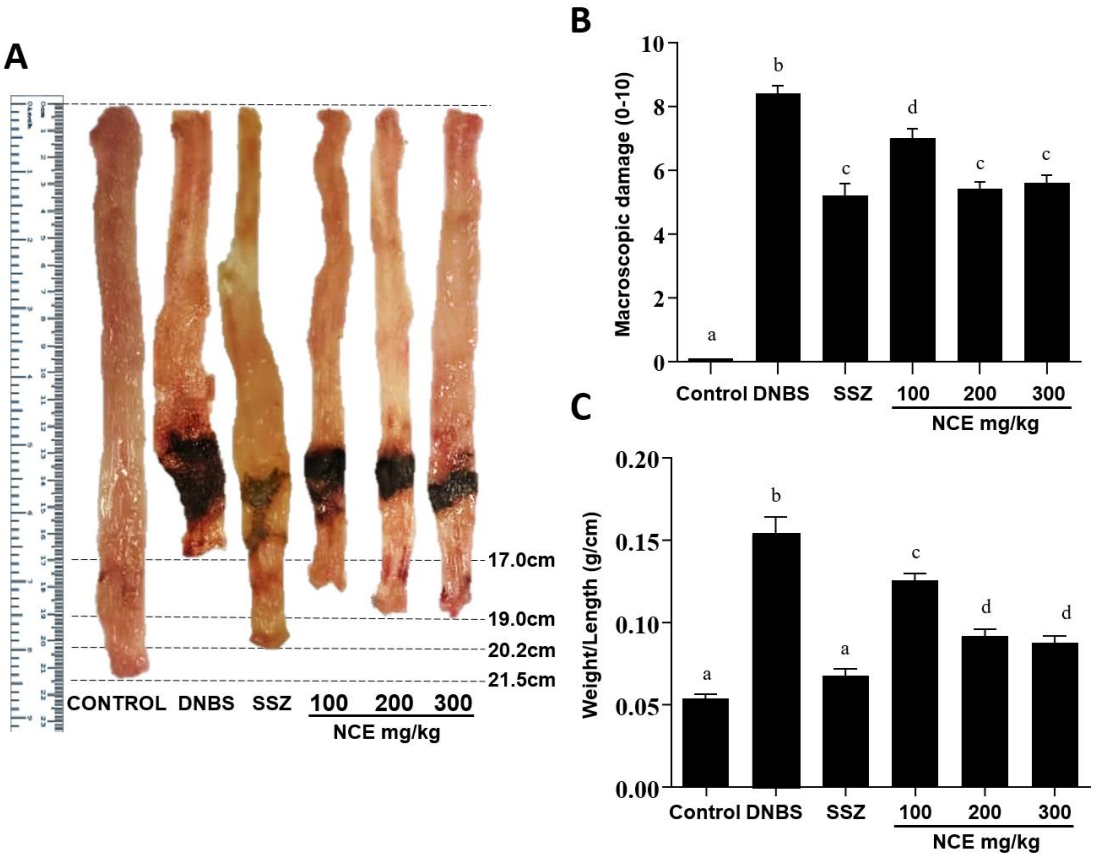

Figure 17. Effect of treatments with *N. cochenillifera* extract (NCE) (100, 200 and 300 mg/kg) and sulfasalazine (SSZ) (250 mg/kg) on colitis induced in rats by 2.4-Dinitrobenzene sulfonic acid (DNBS). (**A**) Colon damage; (**B**) macroscopic damage score; (**C**) weight/length ratio. Data are expressed as means ± SEM. Groups with a different letter differ statistically ($p < 0.05$).

Effect of N. cochenillifera extract on cytokine levels, oxidative stress and gene expression of inflammation markers

The malondialdehyde (MDA) levels significantly decreased in the colonic tissue samples of the SSZ group and NCE-treated rats at 100, 200, and 300 mg/kg compared to the DNBS group can be seen in Figure 18.

To verify whether treatment with NCE might cause an effect on reducing neutrophil infiltration into the intestinal mucosal layer, myeloperoxidase (MPO) activity was measured in the colonic tissue. As shown in Figure 18, the colitis induced significant recruitment of intestinal neutrophils. These parameters were significantly reduced in the SSZ and NCE-treated groups at doses of 200 and 300 mg/kg.

TNF-α levels were significantly increased in the DNBS group and remained at baseline levels in the control group. On the other hand, it reduced in the SSZ group ($p < 0.05$) and all groups treated with NCE, compared to the DNBS group. The pre-treatment revealed that NCE at 200

and 300 mg/kg doses significantly reduced IL-1β levels. However, NCE at a 100 mg/kg dose did not differ statistically from the DNBS group. IL-10 levels were significantly increased in the SSZ group and the treatment with NCE at doses of 200 and 300 mg/kg compared to the DNBS group, and in NCE (100 mg/kg), no significant increase was observed ($p < 0.05$) (Figure 18).

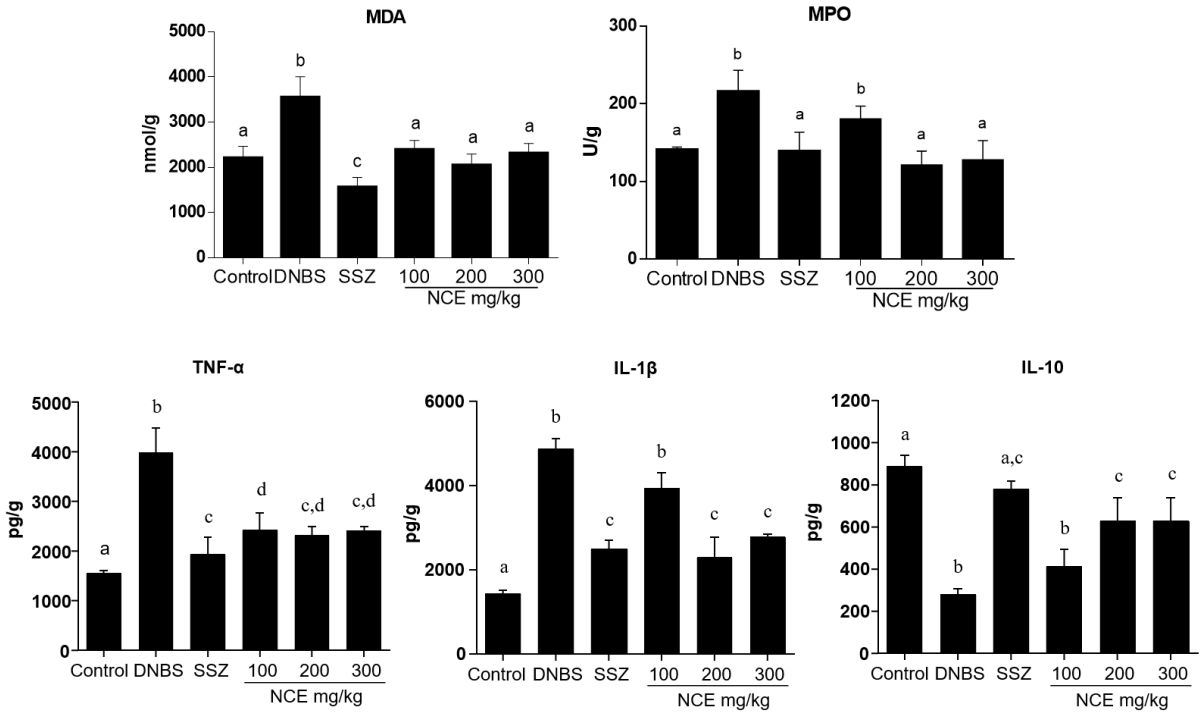

Figure 18. Effect of *N. cochenillifera* extract (NCE) (100, 200 and 300 mg/kg) and sulfasalazine (SSZ) (250 mg/kg) on colonic. Malondialdehyde (MDA) levels; myeloperoxidase activity and cytokines levels: tumor necrosis factor alpha (TNF-α), interleukin-1beta (IL-1β), and interleukin 10 (IL-10). Data are expressed as means ± SEM. Groups with a different letter differ statistically ($p < 0.05$).

The quantitative real-time polymerase chain reaction (qPCR) experiment for the DNBS group exhibited an increased mRNA expression of MAPK1 (ERK2) and NF-κB-p65 compared to the healthy group. In addition, DNBS-induced colonic damage showed decreases in gene expression of MUC-2 and ZO-1 when compared to the healthy group. The SSZ and NCE groups decreased the mRNA expression of MAPK1/ERK2 and NF-κB p65. The data demonstrated increased mRNA expression for MUC-2 and ZO-1 in the groups treated with SSZ and NCE at doses of 200 and 300 mg/kg ($p < 0.05$) compared to the DNBS group (Figure 19).

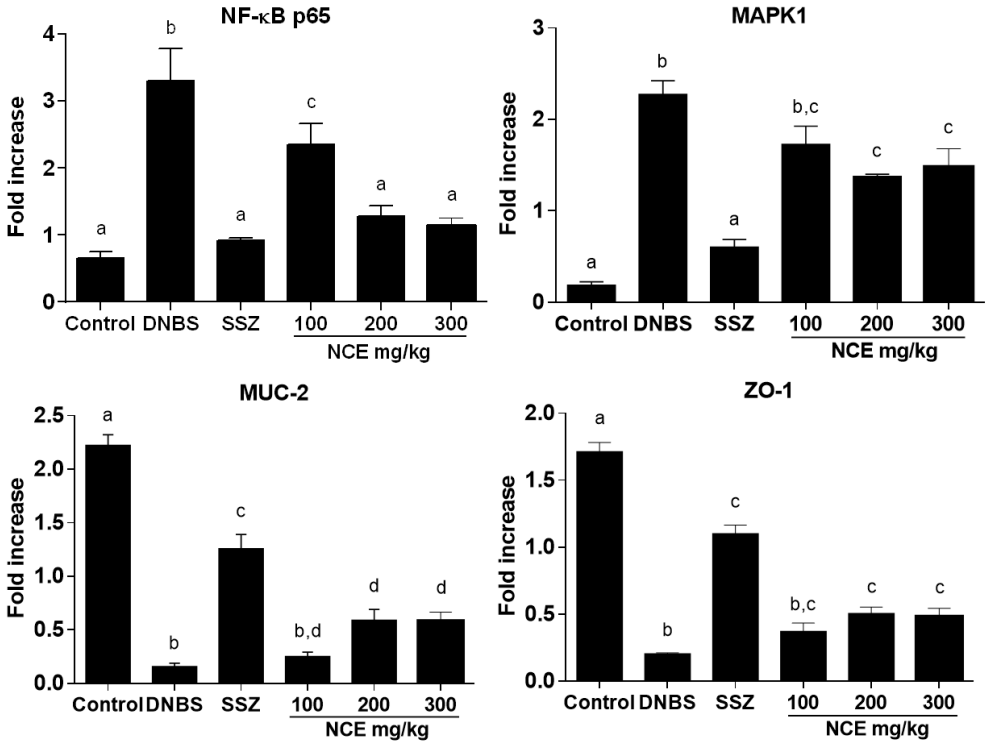

Figure 19. Effect of *N. cochenillifera* extract (NCE) (100, 200 and 300 mg/kg) and sulfasalazine (SSZ) (250 mg/kg) on the gene expression of mitogen-activated protein kinase 1 (MAPK1/ERK2), nuclear factor kappa B p65 (NF-κB p65), zonula occludens type I (ZO-1) and mucin type II (MUC-2) in colonic tissue of the experimental trial of colitis induced by 2,4-dinitrobenzene sulfonic acid (DNBS) in rats. Data are expressed as means ± SEM. Groups with a different letter differ statistically ($p < 0.05$).

Histological and immunohistochemical analysis

According to the results of the histological analyses of the colon samples, the treatment with NCE has a positive impact on reducing inflammation and promoting the regeneration of the intestinal mucosa. The DNBS group displayed severe inflammation, with intense infiltration of polymorphonuclear cells and ulceration of the intestinal mucosa, leading to loss of basal membrane integrity (as shown in Figure 20B). On the other hand, the SSZ group and the groups receiving NCE at doses of 200 and 300 mg/kg showed moderate inflammatory infiltration, and the intestinal mucosa was observed to be in the regeneration process (as shown in Figures 20E and 20F). Furthermore, the histological analysis revealed a statistically significant difference in the histopathological scores for the SSZ group ($p < 0.05$; Figure 20G) and all the groups treated with NCE compared to the DNBS group.

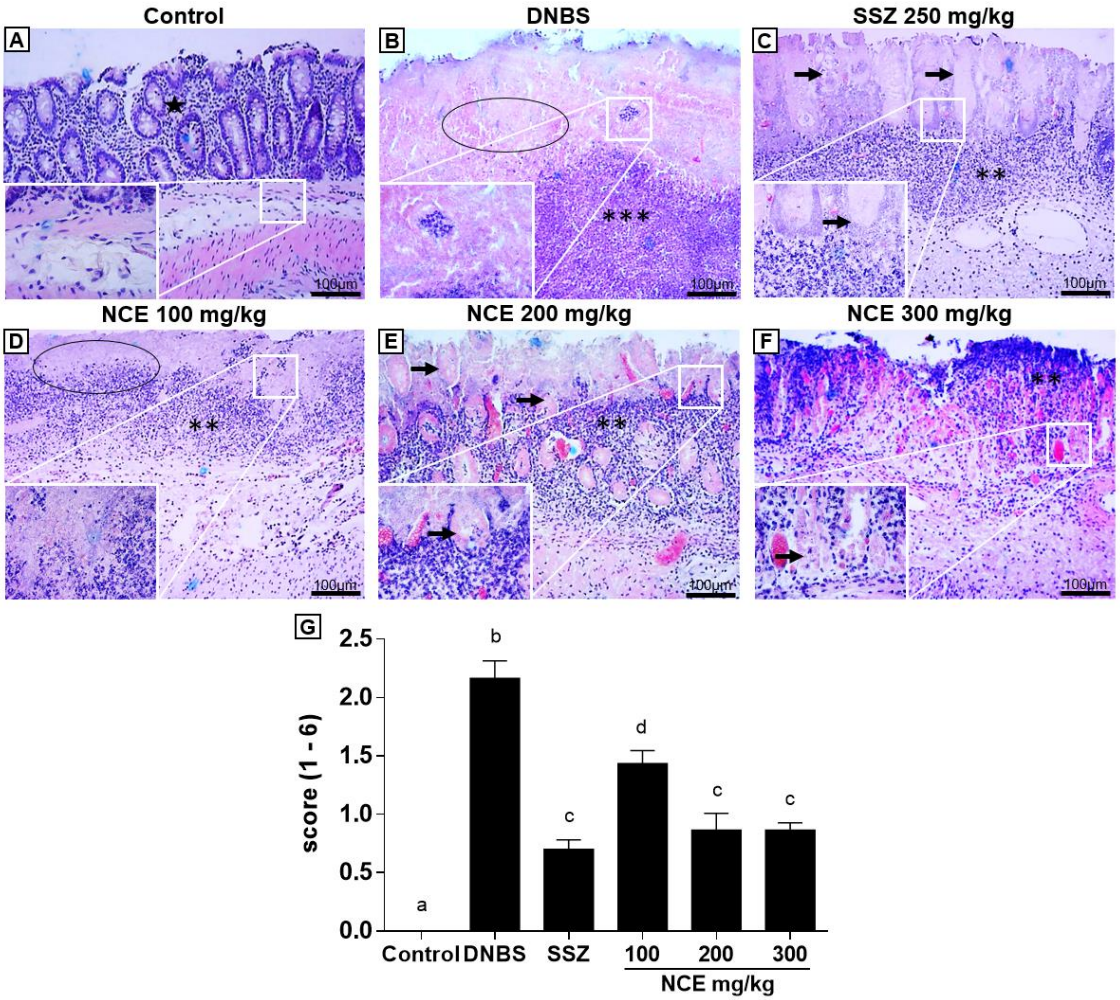

Figure 20. Histopathological analyses of representative colonic tissue (longitudinal section) using Hematoxylin/Eosin staining. Groups represented: Control group (**A**), DNBS group (**B**), Sulfasalazine (SSZ) (250 mg/kg) (**C**) and NCE—*N. cochenillifera* extract (100, 200 and 300 mg/kg) (**D**–**F**) and histopathological score (**G**). The figure represents microscopic damage assessment (10× and 40× magnification). Normal intestinal layers (star), inflammatory cell infiltrate intense (***) and moderate (**), total mucosal ulceration (circle), Initial mucosal regeneration (arrow). Data are expressed as means ± SEM. Groups with a different letter differ statistically ($p < 0.05$).

Figure 21 depicts the immunohistochemical staining of NF-κB p65 and COX-2 in colonic tissue samples. In the control group, there was no observed expression of NF-κB p65 or COX-2 positive cells. However, the administration of DNBS increased the expression of NF-κB p65 and COX-2 in the colon tissue compared to the control group (as shown in Figure 20). In contrast, administering sulfasalazine and NCE at 200 and 300 mg/kg doses reduced the expression of NF-κB p65 and COX-2 positive cells compared to the DNBS group ($p < 0.05$, as depicted in Figure 21).

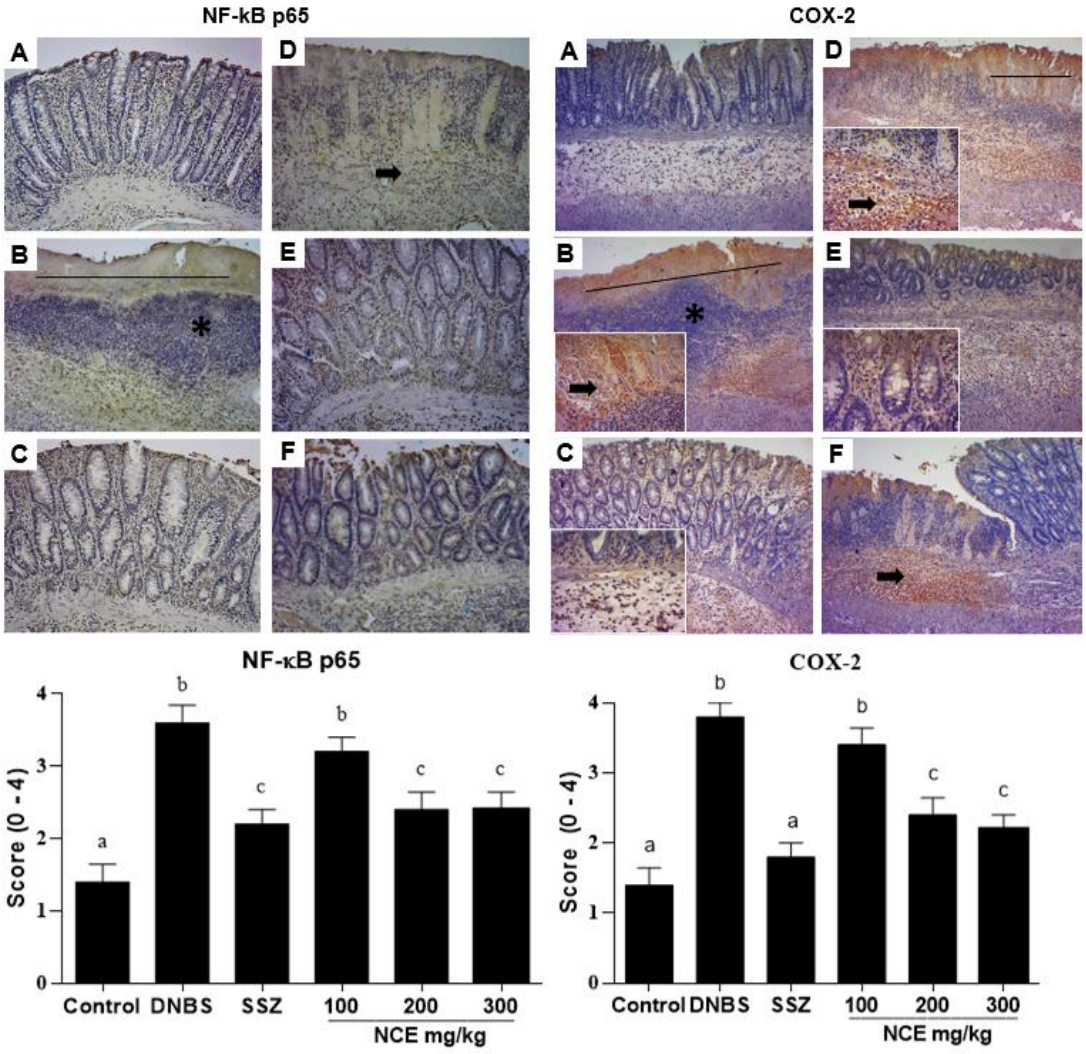

Figure 21. Immunohistochemical analyses of representative colonic tissue (longitudinal section). NF-κB p65 and COX-2 and their respective immunohistochemical scores. Groups represented: Control group (**A**), DNBS group (**B**), Sulfasalazine (SSZ) (250 mg/kg) (**C**) and NCE—*N. cochenillifera* extract (100, 200 and 300 mg/kg) (**D**–**F**). The figure represents a microscopic damage assessment (10× and 40× magnification), the lines indicate diffuse active colitis with intense antibody reactivity, the asterisks represent dense infiltrate of inflammatory cells and arrows indicate antibody reactivity. Data are expressed as means ± SEM. Groups with a different letter differ statistically ($p < 0.05$).

4.4 Preparation, Characterization and Entrapment Efficiency of Nanoparticles (NPB and NPE)

The characterization of NC-nanoparticles (NPE) and blank nanoparticles (NPB) is described in Table 18. For both NPB and NPE, the average particle size was less than 100 nm, with unimodal distribution (PdI < 0.2), and significant differences were not observed ($p > 0.05$) for size and PdI data between the two samples. The entrapment efficiency (EE) for NPE was determined using an indirect method of phenolics dosage. The data show an EE close to 100% (99.15 ± 0.3%) (Table 18).

Table 18. Physicochemical properties of the nanoparticle blanks (NPB) and extract-loaded nanoparticles (NPE), immediately after obtaining the systems and incorporation efficiency of NPE (*n* = 3). PdI (polydispersity index), nm (nanometer), standard deviation (SD), millivolt (mV).

	Diameter (nm) ± SD	PdI (nm) ± SD	Zeta Potential (mV) ± SD	EE (%)
NPB	68.88 ± 1.711	0,134 ± 0,011	-25.1 ± 1.80	-
NPE	76.45 ± 2.246	0.165 ± 0.011	-15.8 ± 2.61	99.15 ± 0.3

Fourier transform infrared spectroscopy (FTIR - ATR) analysis

The spectra of the extract, the polymers, and the NPB and NPE are shown in Figure 22. The leading bands were observed at 3330, 2920, 1620, and 1440 cm^{-1}, and the most intense at 1044 cm^{-1}. In the spectrum of the nanoparticle system loaded with the extract (NPE), the signals from the extract practically disappear, leaving only the signals related to the polymer Eudragit S100. Note the broadening of a band at 1440 cm^{-1} in the NPE spectrum that was identified in the NPB (Figure 22).

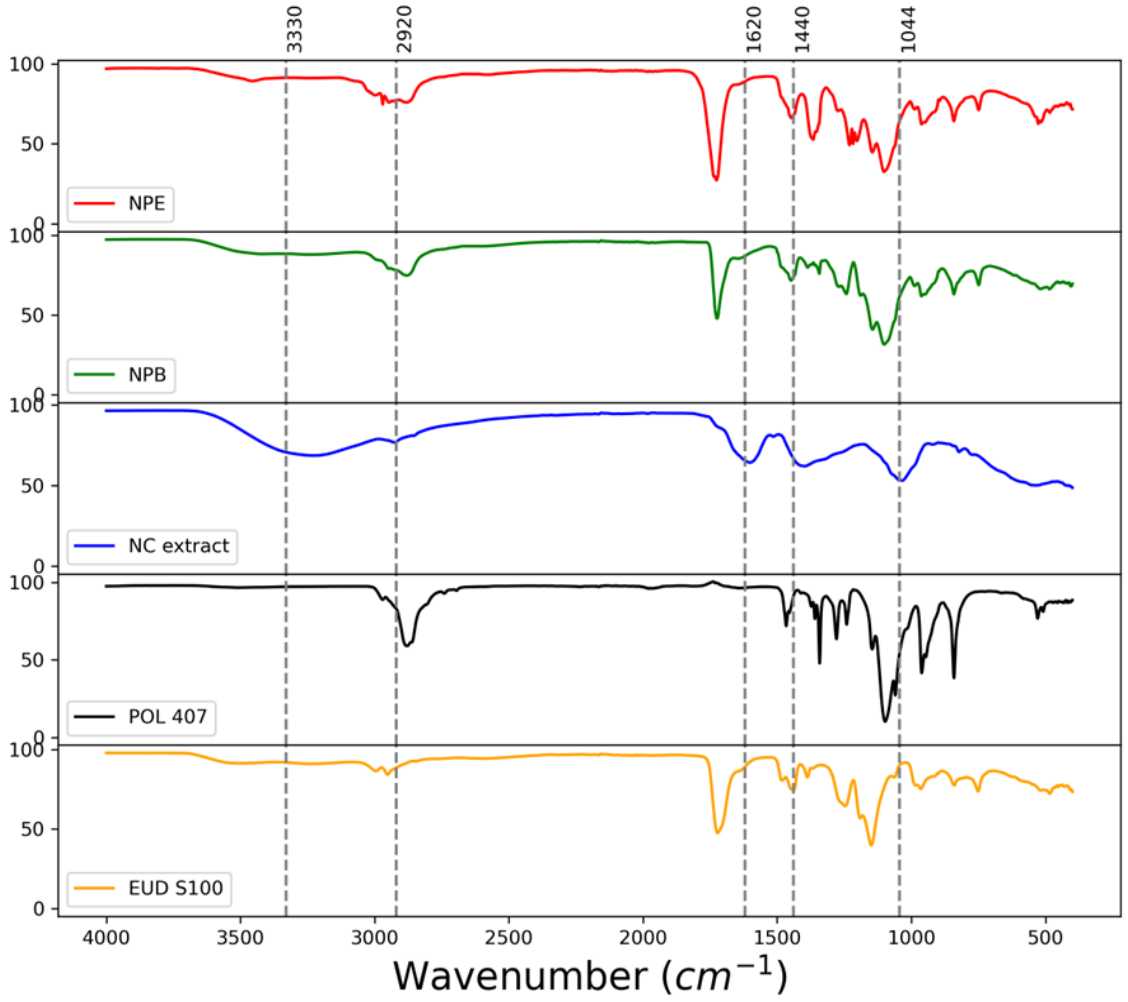

Figure 22. Fourier transform infrared spectra (FTIR) for individual excipient and for the active: extract-loaded nanoparticles (NPE), nanoparticle blanks (NPB), *N. cochenillifera* extract (NCE), Poloxamer 407 (POL 407) and Eudragit® S100 (EUD S100).

Morphological analysis of the nanoparticles

Figure 23 demonstrates 2D and 3D AFM images, SEM images, and particle size distribution charts. Microscopic analyses were carried out to observe the morphology and appearance of the particles, such as shape and surface. It can be seen from the images that both NPB and NPE have a spherical shape and a smooth and intact surface. A narrow distribution is observed with the size distribution charts, which corroborates the obtained PdI values.

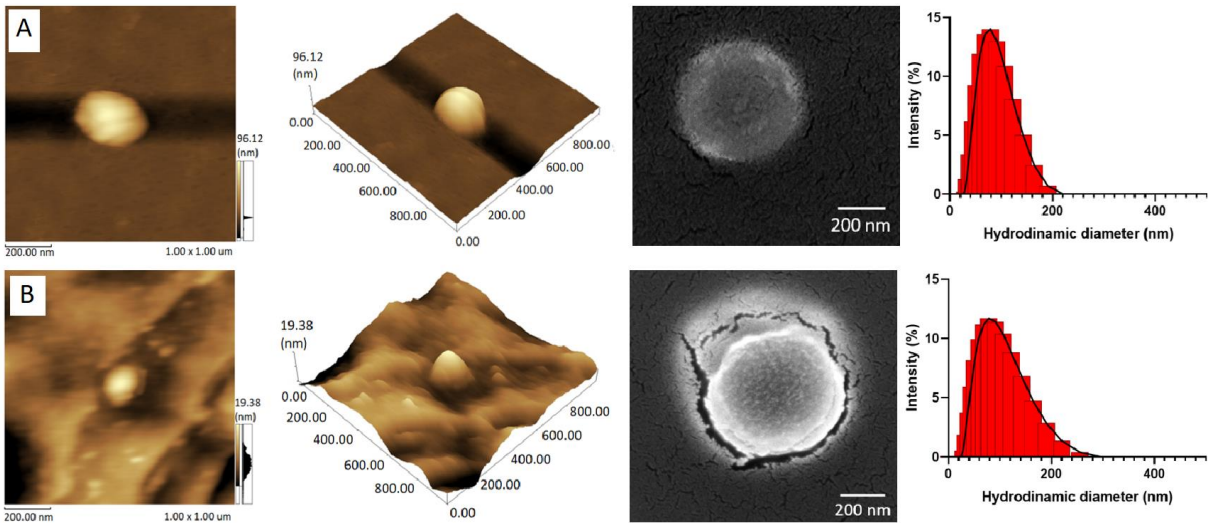

Figure 23. Nanoparticles morphology in 2D and 3D topographic images obtained by AFM, SEM images and distribution of particles, respectively. (**A**) EUD S100 nanoparticles blanks – NPB; (**B**) EUD S100 extract-loaded nanoparticles (NPE).

Stability study of Nanoparticles

Over 30 days, the systems were stored in the refrigerator at 4 ± 2 ºC, and their stability was evaluated on changes in particle size, polydispersity index (PdI), and zeta potential (ZP). No changes were identified in the parameters analyzed during the study time, both for the white nanoparticles and those loaded with NCE (Figure 24, Table 19). This result suggests the physical stability of the colloidal systems.

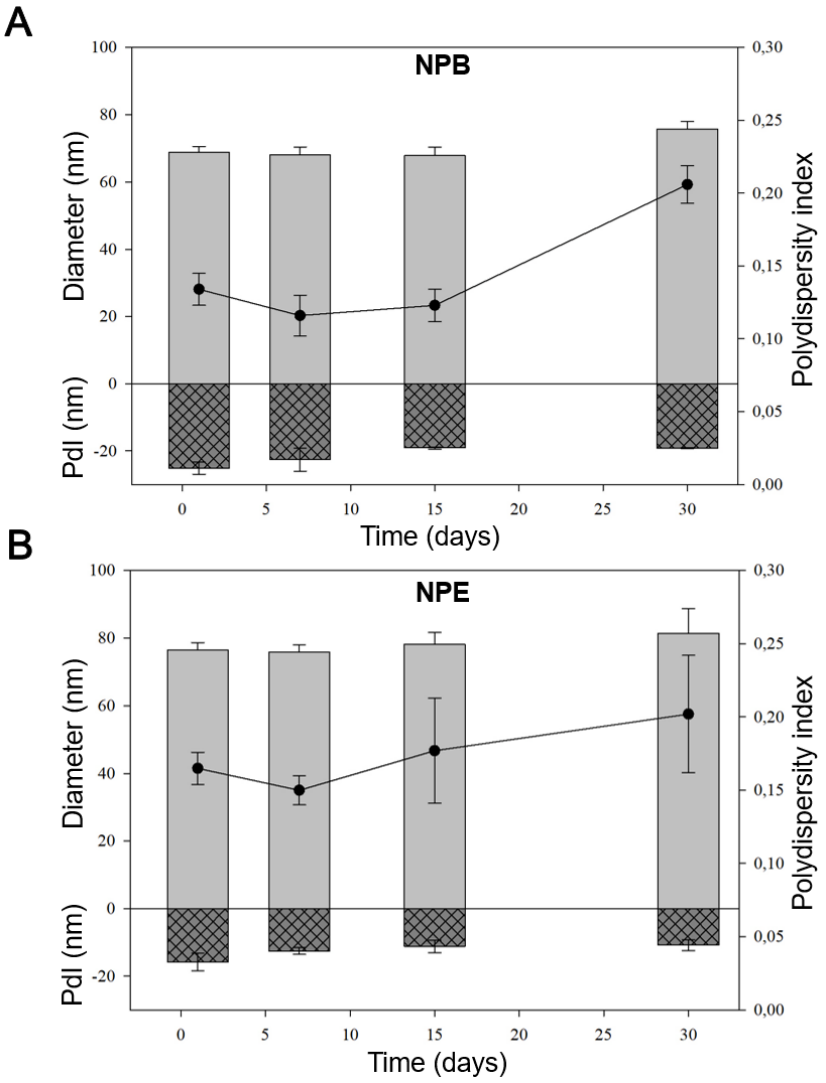

Figure 24. Stability study of (A) nanoparticle blanks (NPB) and (B) extract-loaded nanoparticles (NPE). Values of particle size (diameter), zeta potential and polydispersity index (PdI) according to storage time, 30 days at 4 ± 2 °C (mean ± standard deviation; *n* = 3).

Table 19. Values referring to the stability study of (A) blank nanoparticles (NPB) and (B) extract-loaded nanoparticles (NPE). Values of particle size (diameter), zeta potential (ZP) and polydispersity index (PdI) according to storage time, 30 days at 4 ± 2 °C (mean ± standard deviation; *n* = 3).

	NPB			NPE		
Day	**Diameter (nm)**	**ZP (mV)**	**PdI (nm)**	**Diameter (nm)**	**ZP (mV)**	**PdI (nm)**
1	68.88 ± 1,71	-25.1 ± 1,80	0.13 ± 0.01	76.45 ± 2,25	-15.8 ± 2,61	0.16 ± 0.01
7	68.03 ± 2,42	-22.6 ± 3,43	0.12 ± 0.01	75.80 ± 2,23	-12.5 ± 1,06	0.15 ± 0.01
15	67.91 ± 2,50	-19.1 ± 0.3	0.12 ± 0.01	78.18 ± 3,48	-11.2 ± 1,78	0.18 ± 0.04
30	75.72 ± 2,32	-19.2 ± 0.2	0.21 ± 0.01	81.38 ± 7,40	-10.8 ± 1,60	0.20 ± 0.04

4.5 Internalization assay with extract-loaded nanoparticles (NPE) in HCT-116 cells

Through the confocal microscopy images performed on HCT-116 cells at three different incubation times with the nanoparticles associated with the *N. cochenillifera* extract (NPE), it was possible to observe the rhodamine fluorescent marker (red staining) around the nucleus of

HCT-116 cells from the first incubation time (12 hours) (Figure 25B). As observed in Figures 25C and 25D, the fluorescence did not increase in the other incubation times (24 h and 48 h). In Figure 25A, it is possible to observe the cell nucleus stained with the marker DAPI (blue staining) when the cells were subjected to DMEM alone. By observing the images, it is possible to suggest that NPE can cross the plasma membrane of the cells and concentrate in the cell cytoplasm.

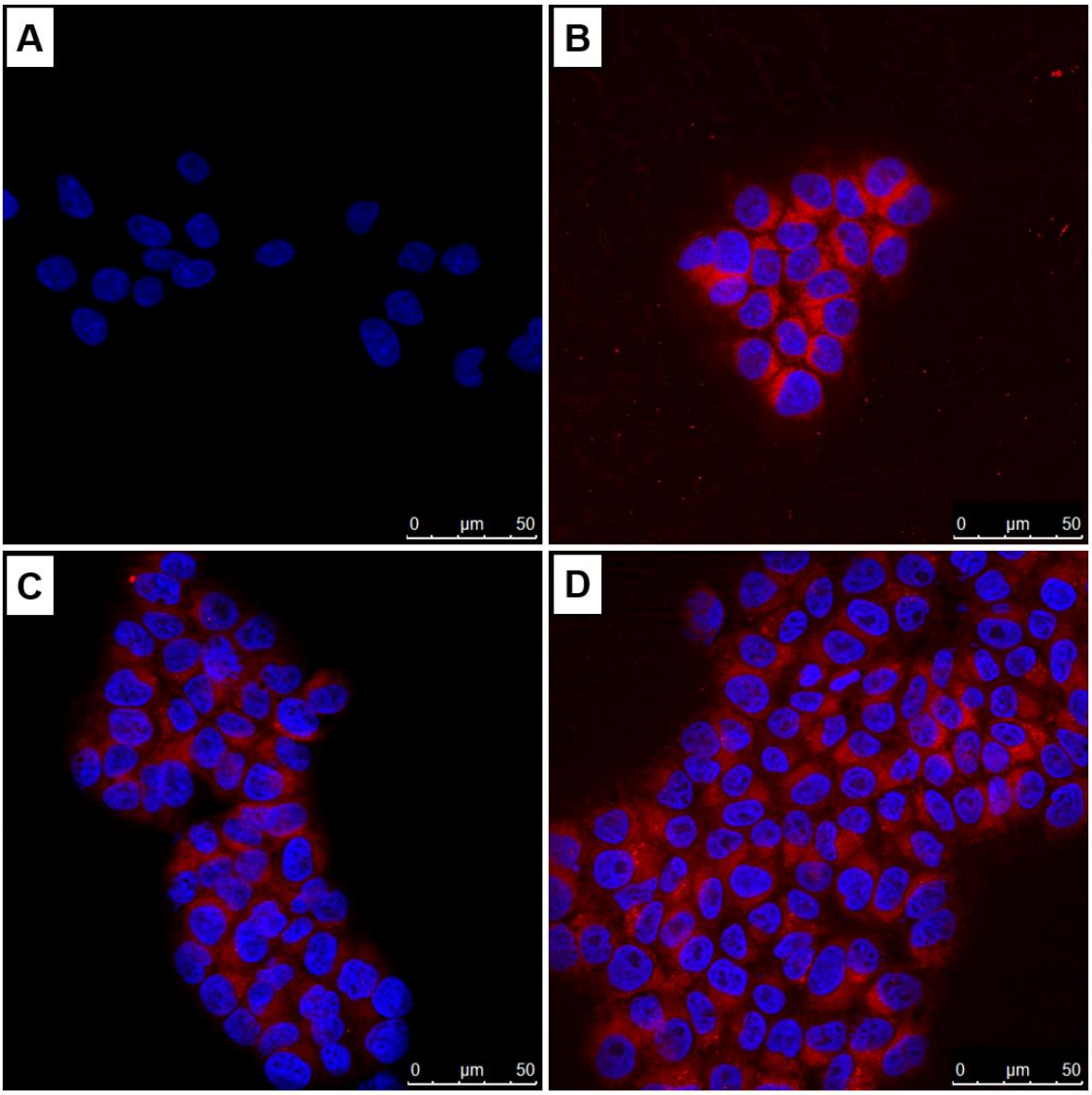

Figure 25. Confocal images of HCT-116 cells incubated with DMEM (**A**) and with extract-loaded nanoparticles (NPE) at different incubation times, after 12 h (**B**), 24 h (**C**) and 48 h (**D**). Rhodamine fluorescent marker (red staining). DAPI marker (blue staining). *Scale bars*, 50 µm.

4.6 Effect of *Nopalea cochenillifera* extract (NCE) and Extract-loaded nanoparticles (NPE) on DSS-Induced colitis in mice

The Disease Activity Index (DAI) and Weight/Colonic Length Ratio

The effects of NCE and NPE were evaluated in mice with colitis induced with 3% DSS, administered orally for 5 consecutive days. On the first day after induction of colitis with DSS, the observation of parameters for evaluation of the disease activity index (DAI) was recorded (Figure 26A). The group without colitis showed an irrelevant variation in the parameters evaluated. In contrast, ingestion of DSS caused a significant increase in DAI ($p < 0.05$; vs. control group) in the mice in the DSS group and the groups receiving the treatments. However, mice with DSS-induced colitis treated with NCE and NPE showed a significant recovery starting on day 4 and maintained the reduction until day 6 and the last day when compared to the DSS and NPB group (Figure 26A) ($p < 0.05$; vs. DSS).

In the macroscopic analysis (Figure 26B), it is possible to notice a shortening in the colon length of the animals in the DSS and NPB groups compared to the control group. This shortening was lessened in the groups treated with NCE and NPE ($p < 0.05$; vs. DSS). The colonic weight/length ratio values were significantly higher in the DSS and NPB groups than in the NCE and NPE-treated groups (Figure 26C).

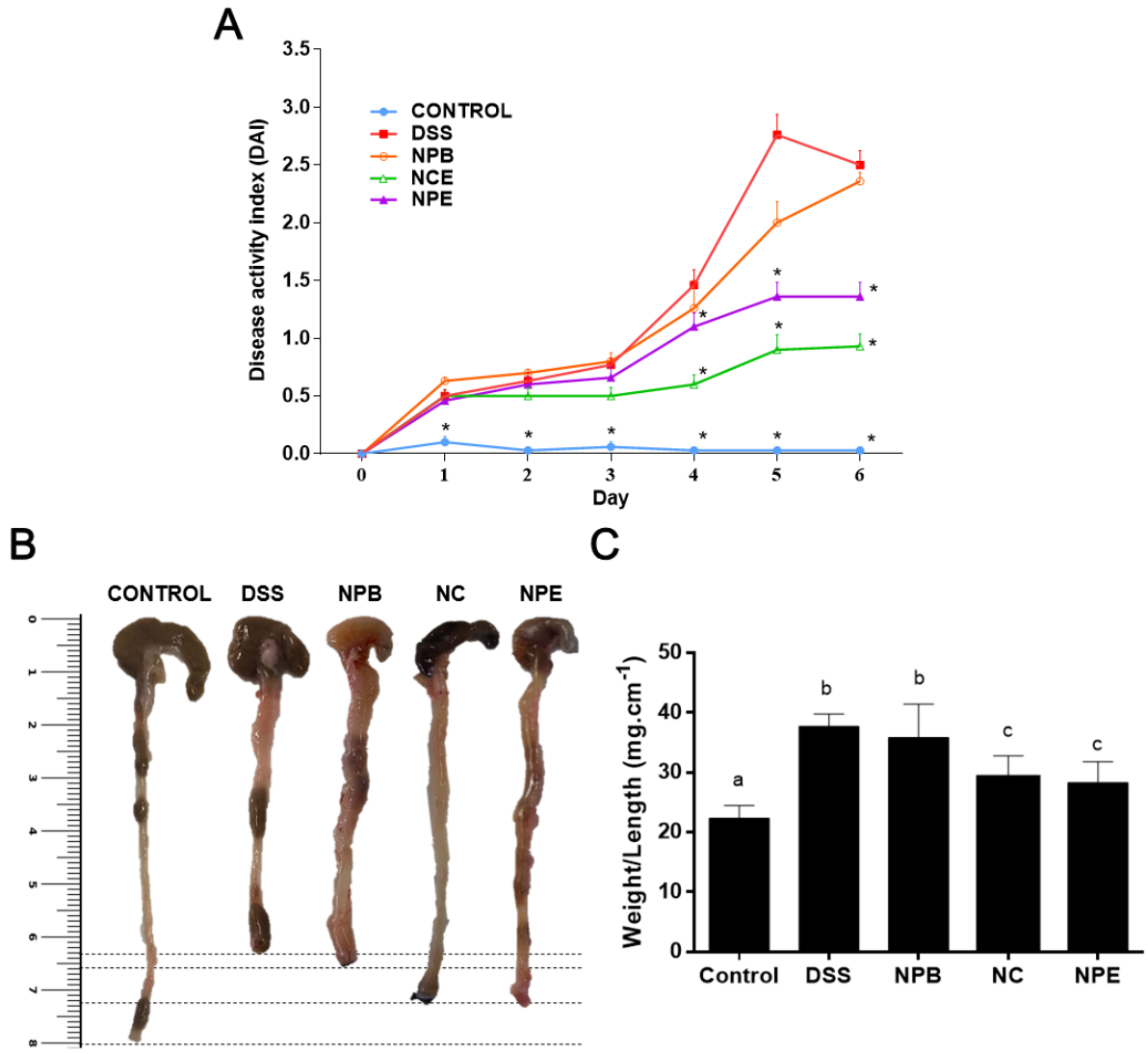

Figure 26. Evaluation of the disease activity index (DAI) (**A**). Colonic representation (**B**) and colon length/weight ratio (**C**). Groups: Control; Dextran sulfate sodium (DSS); Extract of *N. cochenillifera* (NCE); Extract-loaded nanoparticles (NPE) and blank nanoparticles (NPB). Parametric data are expressed as mean ± SEM (n = 10). Statistical differences analyzed by two-way ANOVA followed by Tukey's multiple comparisons test. Different letters indicate significant differences between groups ($p < 0.05$).

Effect of NCE and NPE on gene expression of inflammation and oxidative stress markers

The production of inflammation mediators was significantly altered ($p < 0.05$) in the DSS and NPB group compared to the control group and treated with NCE and NPE (Figure 26). The NCE and NPE reduced the mRNA expression in almost all the inflammation markers evaluated (TNF-α, IL-1β, IL-6, TLR-4, MIP-2, and MCP-1), as well as the adhesion molecule ICAM-1, the same result was observed for the marker iNOS. However, the analyses performed with the markers IL-6 in the group treated with NPB did not show statistical significance compared to the NPE group (Figure 27).

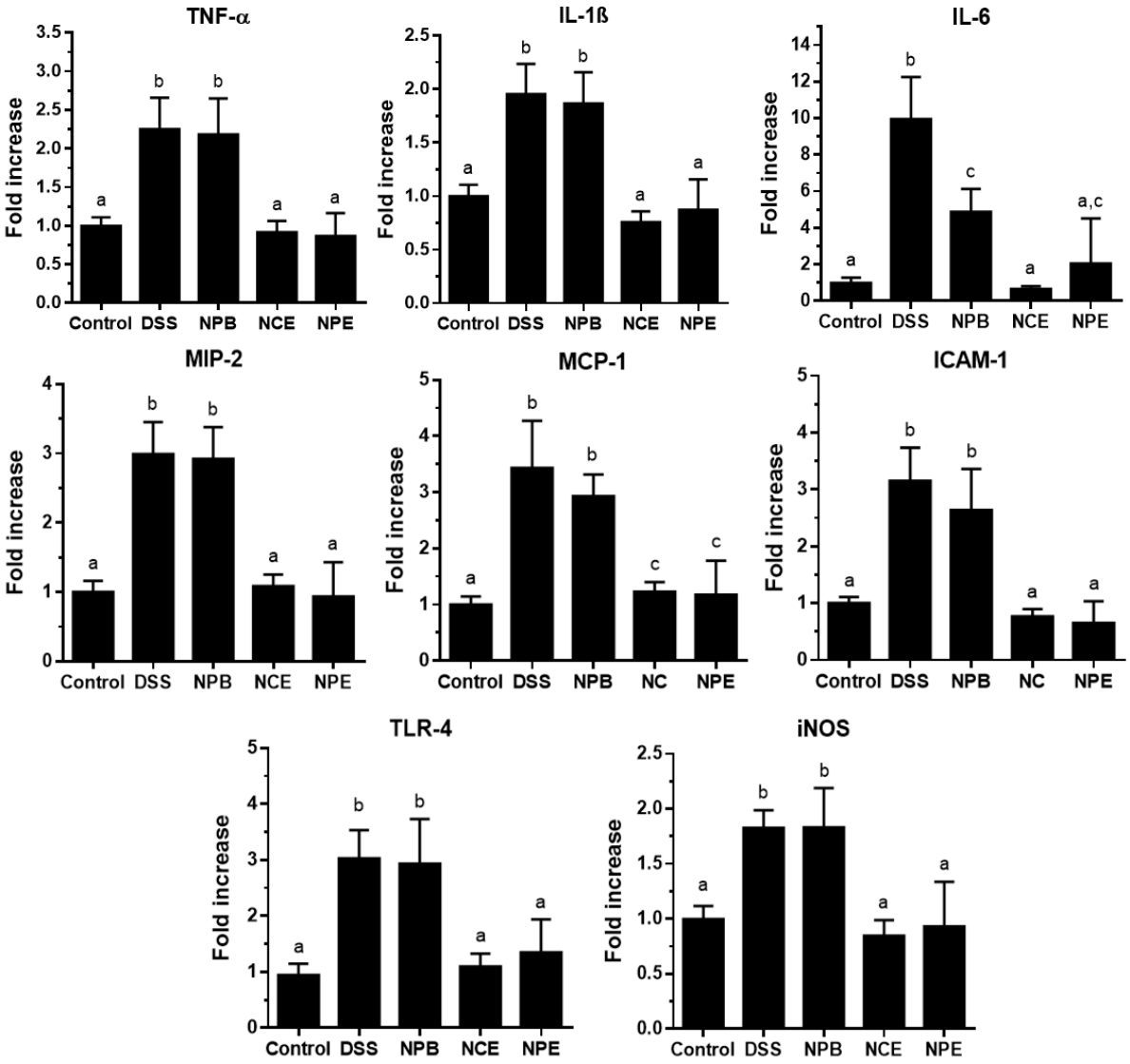

Figure 27. Effect of *N. cochenillifera* extract (NC) and Extract-loaded nanoparticles (NPE) on gene expression of TNF-α, IL-1β, IL-6, TLR-4, MIP-2, MCP-1, ICAM-1 and iNOS, was quantified by real-time PCR. Dextran sulfate sodium (DSS); blank nanoparticles (NPB). Data are expressed as mean ± SEM (n = 8). Statistical differences analyzed by two-way ANOVA followed by Tukey's multiple comparisons test. Different letters indicate significant differences between groups ($p < 0.05$).

Effect of NCE and NPE on intestinal permeability

In the case of markers involved in barrier maintenance and protection of the intestinal mucosa, the DSS caused a significant negative regulation (down-regulation) ($p < 0.05$) in the gene expression of ZO-1, OCLN, and MUC-3. In contrast, the treatment with NCE and NPE promoted an up-regulation of the gene expression of ZO-1 and MUC-3 significantly when compared with DSS and NPB groups ($p < 0.05$; Figure 28). RT-qPCR data indicated that the NPE treatment showed no increase in OCLN gene expression compared to the DSS and NPB groups, showing no statistically significant difference ($p > 0.05$; Figure 28).

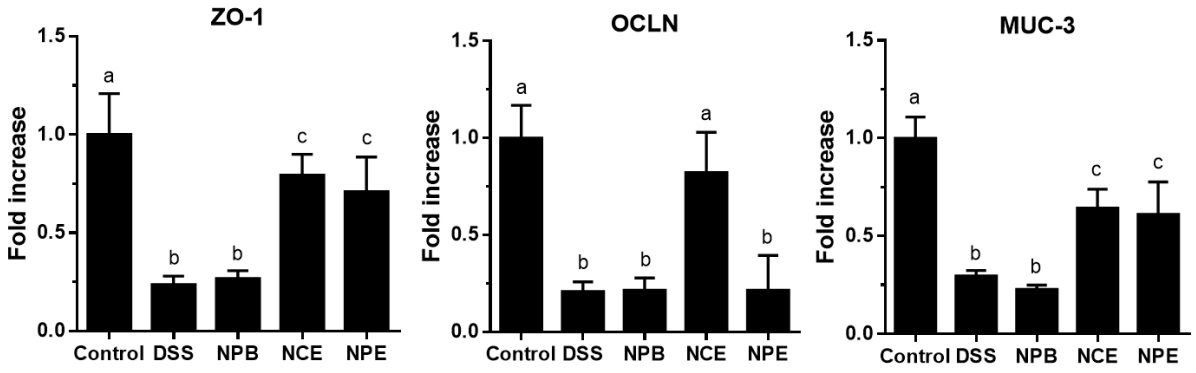

Figure 28. Effect of *N. cochenillifera* extract (NC) and Extract-loaded nanoparticles (NPE) on gene expression of the epithelial integrity markers: Zonula occludens-1 (ZO-1), Occludin (OCLN) and Mucin type 3 (MUC-3), was quantified by real-time PCR. Dextran sulfate sodium (DSS); blank nanoparticles (NPB). Data are expressed as mean ± SEM (n = 8). Statistical differences analyzed by two-way ANOVA followed by Tukey's multiple comparisons test. Different letters indicate significant differences between groups (*$p < 0.05$).

NCE and NPE increased intestinal functionality by improving intestinal permeability, which was investigated using FITC-dextran. The levels of FITC-dextran detected in the plasma of mice in the DSS groups were significantly higher than those in the control group mice, which agrees with the DSS-induced alteration of the epithelial barrier function. However, the animals treated with NCE and NPE significantly reduced the amount of FITC-dextran in plasma ($p <$ 0.05). In this result, despite the difference between the doses of extract administered in each group, no significant difference was observed between the NCE and NPE groups (Figure 29A).

Microscopically, DSS-induced colitis was characterized by inflammatory infiltration and ulcerations in the colonic mucosa, and these observations were more present in the DSS and NPB groups (Figure 29B). The colon damage in the mice in the groups treated with NCE and NPE was significantly reduced, including improved histological structure through reduced epithelial disintegration, reduced inflammatory cell infiltration and presence of goblet cells, and increased mucins (Figure 29B). In this experiment, a microscopic examination of the colon of the DSS and NPB group revealed compromised tissue architecture, as demonstrated by high histological damage scores.

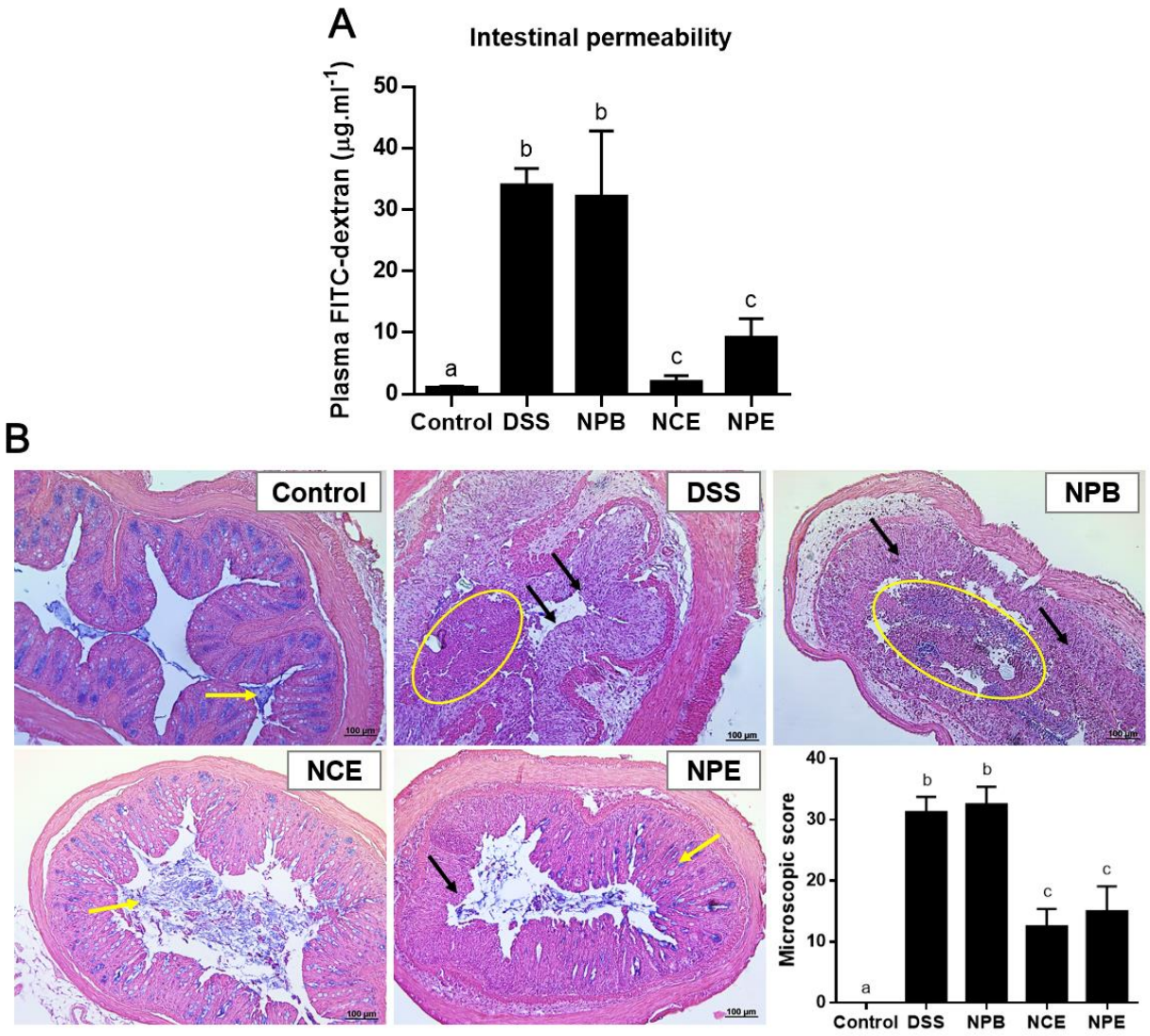

Figure 29. Effect of *N. cochenillifera* extract (NCE) and Extract-loaded nanoparticles (NPE) on intestinal permeability in colitic mice. Intestinal permeability measurement by the FITC-dextran assay *in vivo* (**A**); Histological sections of colon in transverse direction and stained with alcian blue (mucins) and hematoxylin/eosin (**B**); *Scale bars*, 100 µm. (n = 5). Dextran sulfate sodium (DSS); blank nanoparticles (NPB). The yellow arrow indicates the presence of goblet cells and increased mucins; black arrows represent areas of epithelial disintegration and the loss of goblet cells; circles indicate inflammatory infiltration. Data are expressed as mean ± SEM. Statistical differences analyzed by two-way ANOVA followed by Tukey's multiple comparisons test. Different letters indicate significant differences between groups ($p < 0.05$).

Effect of NCE and NPE on mucosal explants

The cytokine IL-1β produced by cultures of colon mucosal explants from mice with DSS-induced colitis was significantly lower in the control and the NCE- and NPE-treated groups compared to the DSS and NPB groups. In addition, NCE and NPE treatments also showed a tendency to decrease MIP-2 levels. However, these differences were not statistically significant compared to the DSS group ($p > 0.05$; Figure 30).

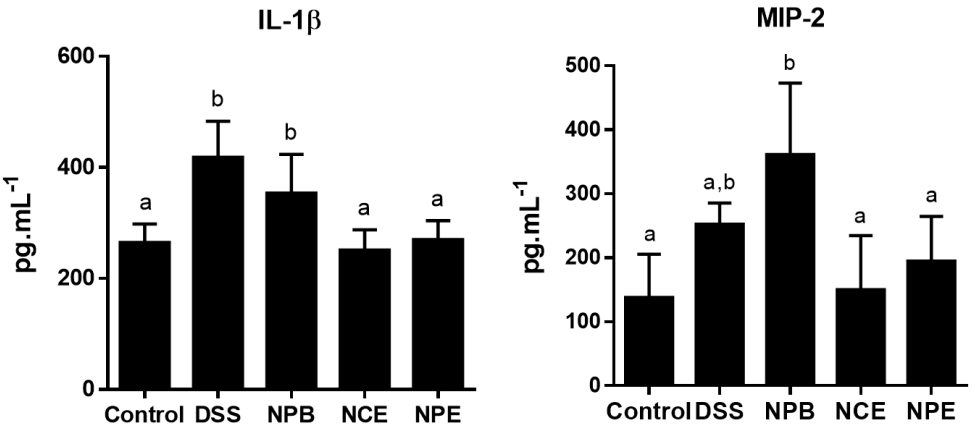

Figure 30. Cytokine levels (IL-1β and MIP-2) measured by ELISA in supernatants of colon fragments from mice from each experimental group incubated for 24 h in DMEM medium. Dextran sulfate sodium (DSS); *N. cochenillifera* extract (NCE); Extract-loaded nanoparticles (NPE) and blank nanoparticles (NPB). Data are expressed as mean ± SEM (n = 8). Statistical differences analyzed by two-way ANOVA followed by Tukey's multiple comparisons test. Different letters indicate significant differences between groups (*$p < 0.05$).

Effects of *N. cochenillifera* extract (NCE) on diet-induced metabolic syndrome assay in mice

Lipid Peroxidation Determination

The thiobarbituric acid reactive substances (TBARS) fluorometric assay is a widely used technique for detecting the presence of MDA. In this method, MDA reacts with thiobarbituric acid to produce chromogenic products, which can be measured using a colorimetric plate reader. In the NCE group, a significant reduction in TBARS was found compared to the HFD control group, suggesting that daily NCE of 200 mg/kg reduces oxidative stress caused by HFD (Figure 31).

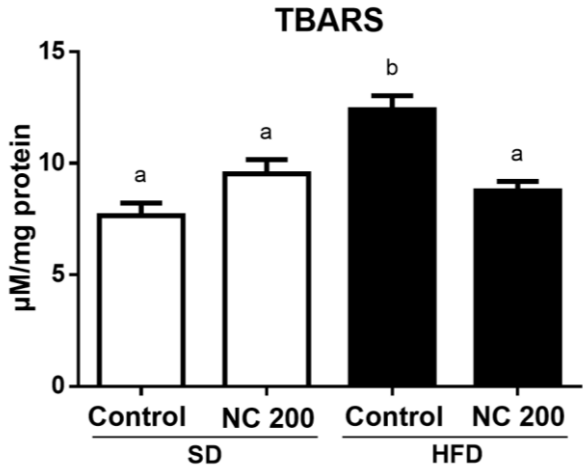

Figure 31. Effects of *N. cochenillifera* extract (NCE) on TBARS production in liver lysates. Standard diet (SD); High fat diet (HFD). Data are expressed as means ± SEM (n = 10). Groups with different letters statistically different ($p < 0.05$).

Body weight, glucose tolerance test and plasma biochemical profile

The HFD-fed group showed a more significant increase in body weight than the group fed a standard diet, as predicted. However, daily administration of NCE to the HFD-fed mice resulted in a significant reduction in weight gain starting from day 20 (Figure 32A). However, this reduction in weight gain was not attributed to a decrease in energy intake, as the energy intake was similar among the groups that received an HFD (as shown in Figure 32B). Instead, the treated groups exhibited a lower weight gain-to-energy intake ratio than the HFD-fed mice that did not receive the treatment. This observation indicates that NCE may reduce feed efficiency (as indicated in Figure 32C).

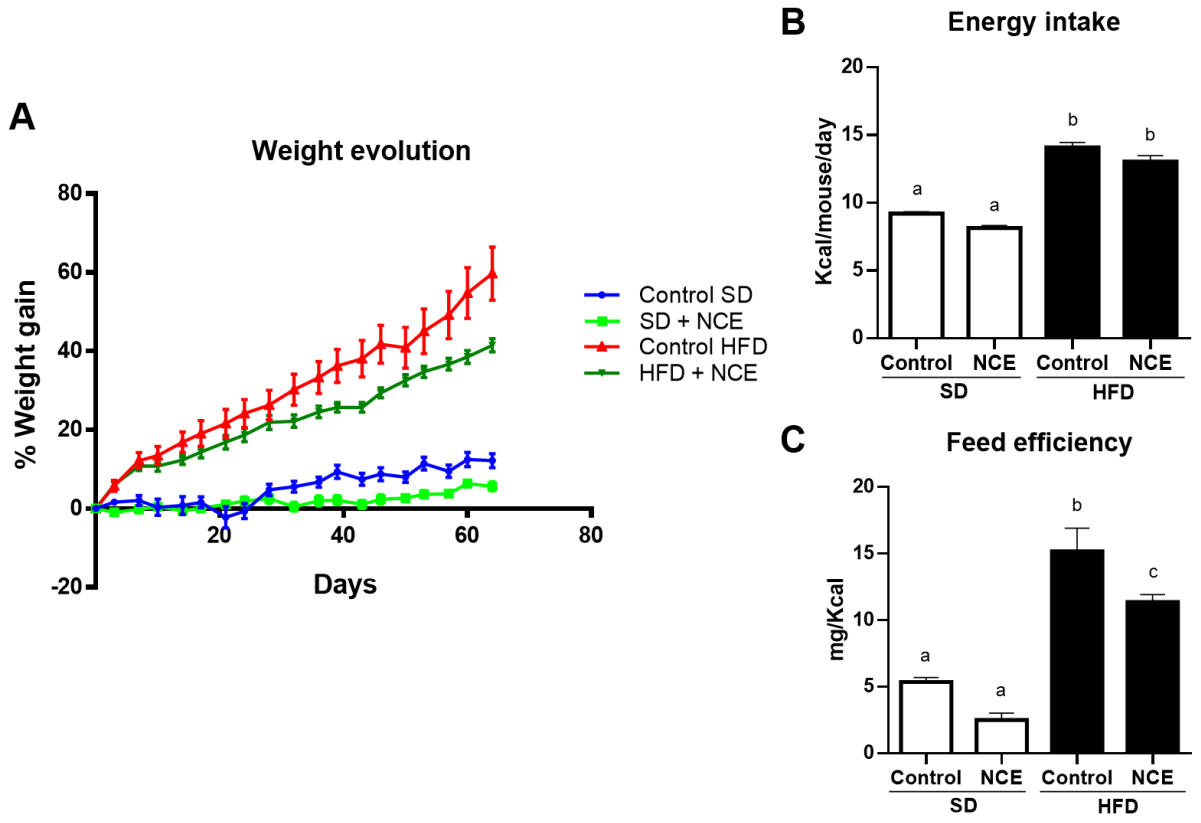

Figure 32. Effects of *N. cochenillifera* extract (NCE) on: Body weight evolution (**A**), energy intake (**B**) and energy efficiency (**C**). Standard diet (SD); High fat diet (HFD). Data are expressed as means ± SEM (n = 10). Groups with different letter statistically different ($p < 0.05$).

The groups of obese mice exhibited considerably higher peaks of glucose levels compared to the non-obese groups. However, treatment of obese mice with *N. cochenillifera* extract showed a significant decrease in plasma glucose levels compared to the untreated group fed with HFD, starting from 60 minutes onwards (Figure 33A). This led to a significant reduction in the area under the curve (AUC), as illustrated in Figure 33B.

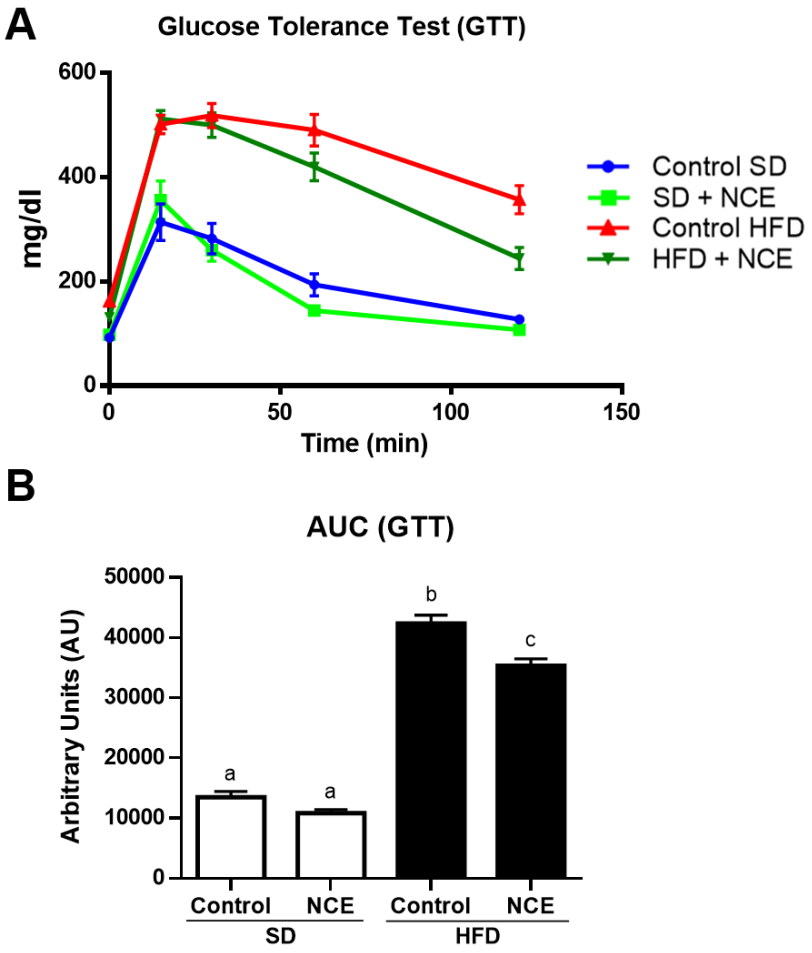

Figure 33. Effects of *N. cochenillifera* extract (NCE) on: (**A**) Glucose tolerance test and (**B**) area under the curve (AUC). Standard diet (SD); High fat diet (HFD). Data are expressed as means ± SEM (n=10). Groups with different letter statistically different ($p < 0.05$).

After euthanasia, biochemical measurements were performed in the plasma of the rats. The results showed that the HFD-fed group had higher fasting plasma glucose levels than the non-obese mice fed a standard diet (SD). However, administering the NCE extract to obese mice significantly reduced their plasma glucose levels, as shown in Figure 34A. Additionally, the HFD-fed mice showed hypercholesterolemia and increased LDL-cholesterol and HDL-cholesterol levels compared to the non-obese mice fed a standard diet. However, the total cholesterol levels were significantly decreased in the groups fed the HFD and treated with NCE (Figure 34B). The administering of the NCE extract to obese mice also resulted in a significant reduction in plasma LDL levels, as indicated in Figure 34C. There was no significant difference in HDL levels between the treated and untreated groups fed HFD, as shown in Figure 34D.

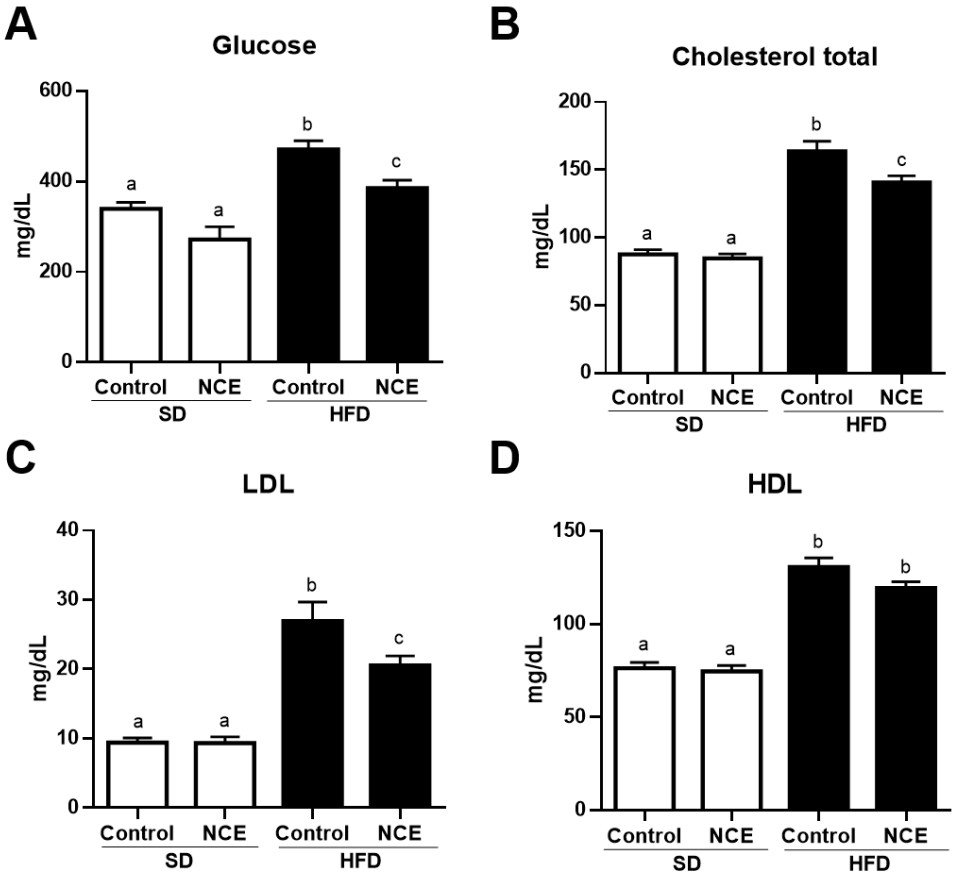

Figure 34. Effects of *N. cochenillifera* extract (NCE) on plasma of mice subjected to standard diet (SD) or high fat diet (HFD) after 10 weeks of treatment with NCE (200 mg/kg) or vehicle (Control group) in: Glucose (**A**); Cholesterol total (**B**); LDL (**C**) and HDL (**D**). Data are expressed as means ± SEM (n=10). Groups with different letters differ statistically (P< 0.05).

As expected, HFD-fed and untreated mice showed heavier fat deposits (abdominal, epididymal, and brown fat) than those fed the standard diet and those fed HFD and treated with NCE (Figure 35A-C). In addition, liver weight was increased in the rats in the control group and fed HFD compared to the rats fed the standard diet. NCE administration resulted in a statistically significant reduction in liver weight in the HFD-fed animals (Figure 35D). There were no significant differences in spleen weight between the groups tested (Figure 35E).

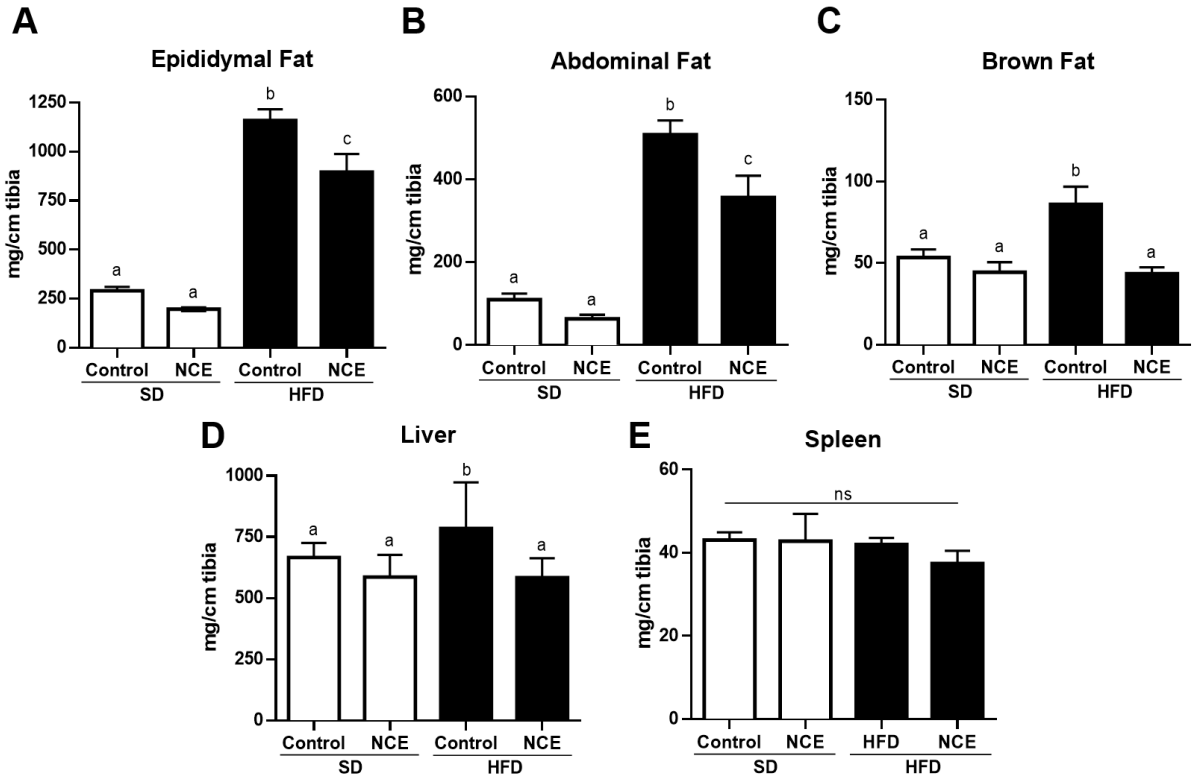

Figure 35. Effects of *N. cochenillifera* extract (NCE) on plasma of mice subjected to standard diet (SD) or high fat diet (HFD) after 10 weeks of treatment with NCE (200 mg/kg) or vehicle (Control group) in: Glucose (A); Cholesterol total (**B**); LDL (**C**) and HDL (**D**). Data are expressed as means ± SEM (n=10). Groups with different letters differ statistically (P< 0.05).

The histological analysis of epididymal fat tissue from the untreated HFD-fed mice showed evidence of adipocyte hypertrophy compared to the standard diet-fed mice (Figure 36). However, this hypertrophy was significantly reduced in obese mice that were treated with NCE. Consequently, there was a decrease in the area and perimeter of the adipocytes, as shown in Figure 36.

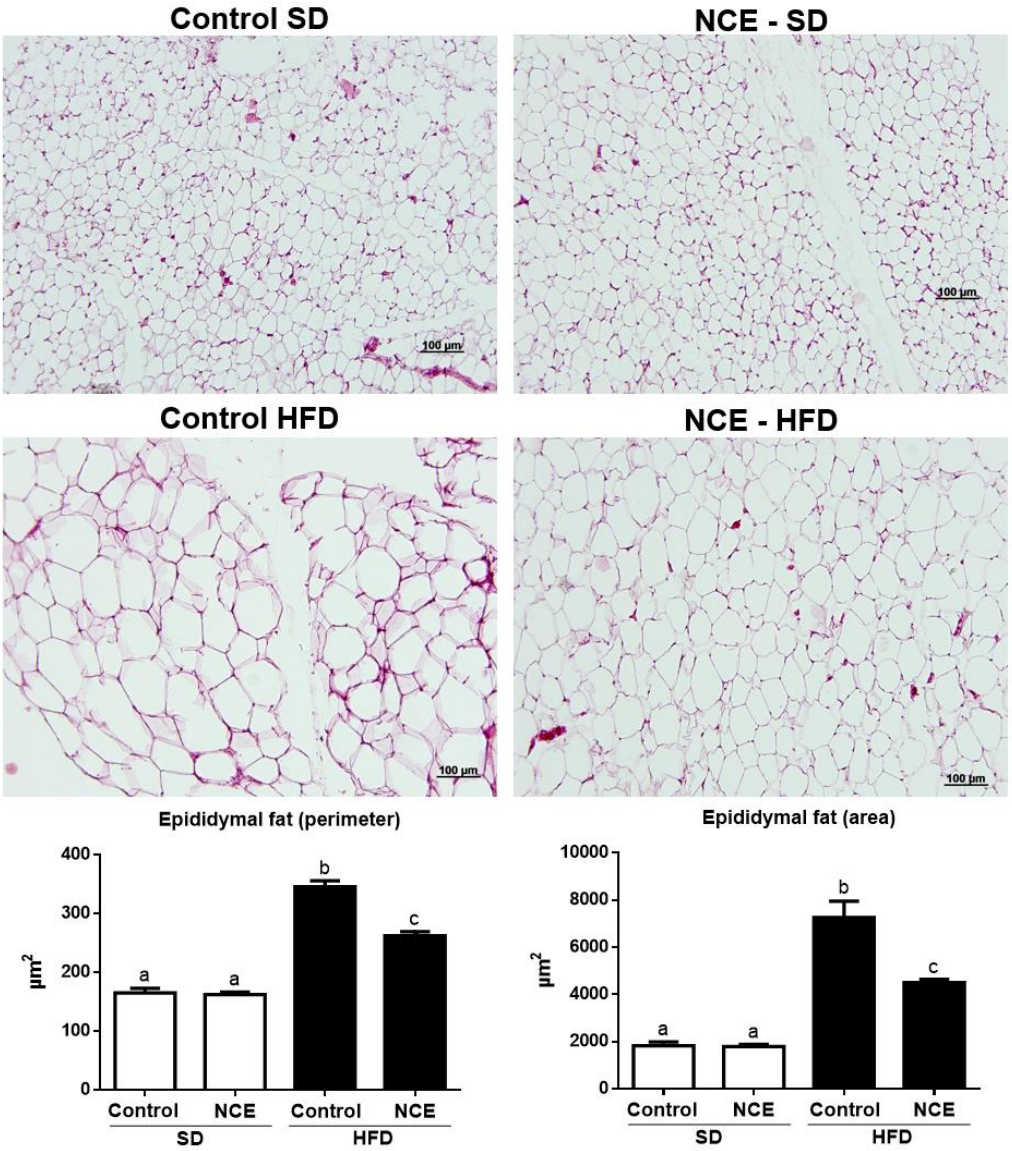

Figure 36. Effects of *N. cochenillifera* extract (NCE) administration on epididymal adipose tissue, analyzed by hematoxylin and eosin staining (scale bar = 100 µm) and on area/perimeter of epididymal adipocytes. Standard diet (SD); High fat diet (HFD). Data are expressed as means ± SEM (n = 10). Groups with different letters differ statistically ($p < 0.05$).

Effects of N. cochenillifera on gene expression markers

The mRNA levels of common hepatic inflammatory markers such as TNF-α were investigated and showed a significant reduction in their expression after NCE administration (Figure 37A). Conversely, the administration of NCE increased the expression of AMPK and GLUT-4 in the liver, as depicted in Figures 37B and 37C.

Leptin-R expression was decreased in the liver of HFD-fed mice. However, NCE treatment suggests an increase in the expression of this marker (Figure 37D). In addition, the HFD-fed and untreated group showed a significant decrease in PPARα expression in liver samples compared with other groups (Figure 37E). In contrast, the group fed HFD and treated with NCE

showed similar results to mice fed the standard diet. On the other hand, PPAR-γ gene expression was not significantly altered between all groups. (Figure 37F).

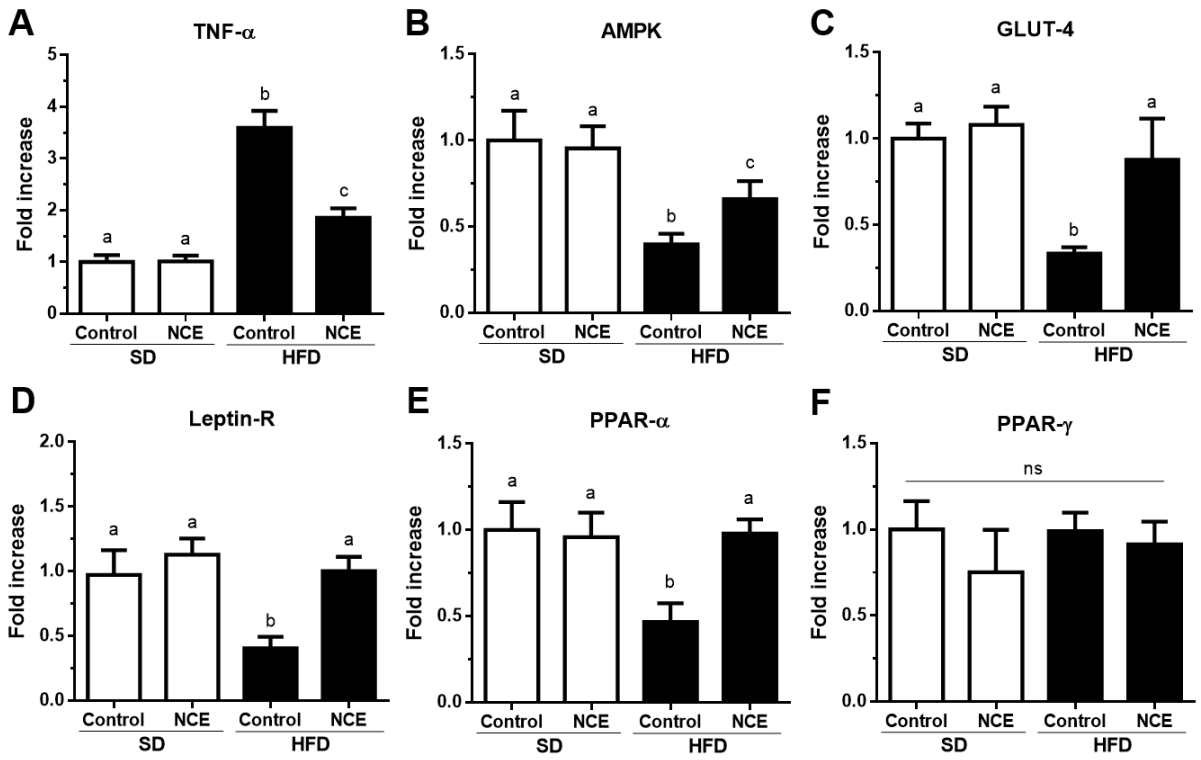

Figure 37. Effect of *N. cochenillifera* extract (NC) on gene expression in liver tissue. TNF-α, AMPK, GLUT-4, Leptin-R, PPAR-α and PPAR-y, was quantified by real-time PCR. Standard diet (SD); High fat diet (HFD). Data are expressed as mean ± SEM (n = 8). Statistical differences analyzed by two-way ANOVA followed by Tukey's multiple comparisons test. Different letters indicate significant differences between groups (*$p < 0.05$).

In mice fed a high-fat diet, the function of the intestinal epithelial barrier is compromised, leading to a decrease in the expression of various proteins associated with intestinal integrity, such as ZO-1, MUC-1, and MUC-3, as compared to mice fed a normal diet. This finding is consistent with the results of our current study. However, administration of NCE to mice fed a high-fat diet resulted in an up-regulation of ZO-1 and MUC-3 markers (as shown in Figures 38A and 38C). Notably, no statistically significant difference in MUC-1 gene expression was observed between the experimental groups in this study (Figure 38B).

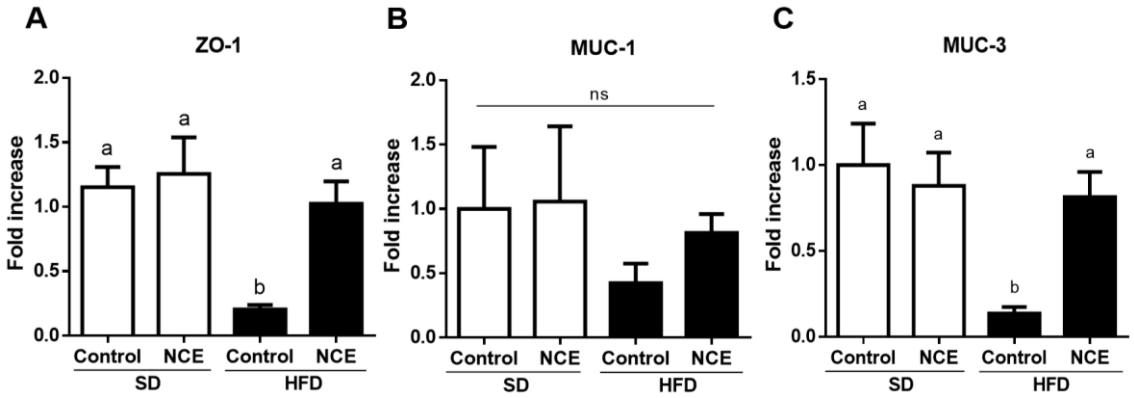

Figure 38. Effect of *N. cochenillifera* extract (NCE) on gene expression in colonic tissue. zonula occludens (ZO-1) and Mucins (MUC-1 and MUC-3) was quantified by real-time PCR. Standard diet (SD); High fat diet (HFD). Data are expressed as mean ± SEM (n = 8). Statistical differences analyzed by two-way ANOVA followed by Tukey's multiple comparisons test. Different letters indicate significant differences between groups (*$p < 0.05$).

Effects of N. cochenillifera on protein expression in liver

Figures 39 and 40 showed the levels of PI3K and AMPK markers in the liver of mice fed with either a high-fat diet (HFD) or a standard diet, as analyzed by Western blot. The liver of mice on HFD displayed a decrease in the expression of PI3K and AMPK compared to those on the standard diet groups. However, upon administration of NCE to the HFD-fed mice, an increase in the expression of these proteins was observed in the liver. The findings are presented as the density ratio relative to β-actin.

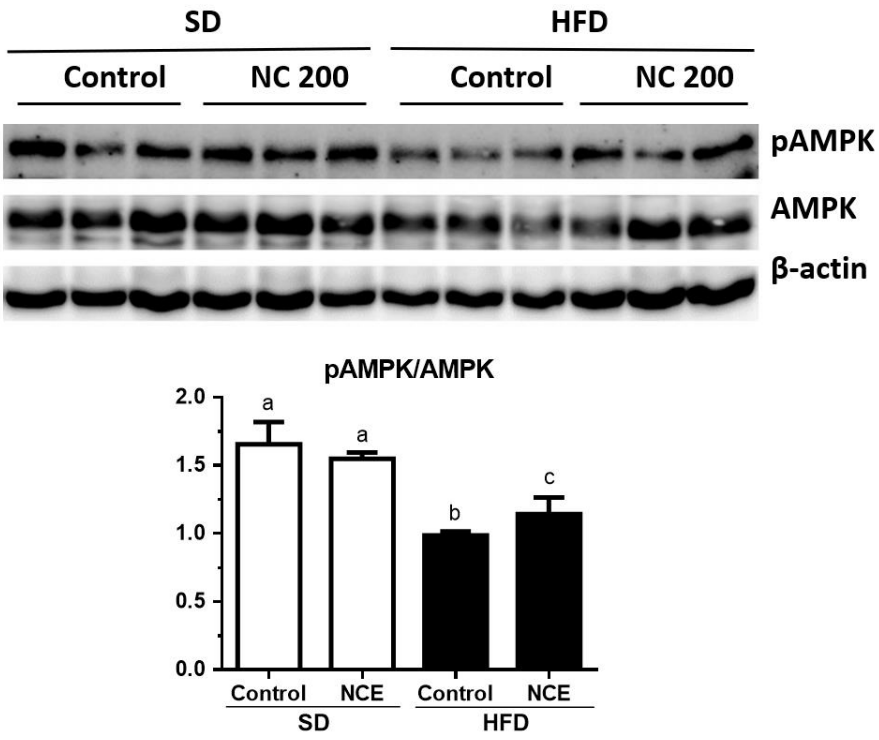

Figure 39. Effects of *N cochenillifera* extract (NCE) administration on: AMPK gene expression and pAMPK/AMPK ratio evaluated by Western blot. Standard diet (SD); High fat diet (HFD). Data are expressed as means ± SEM (n = 6). Groups with different letters statistically differ ($p < 0.05$).

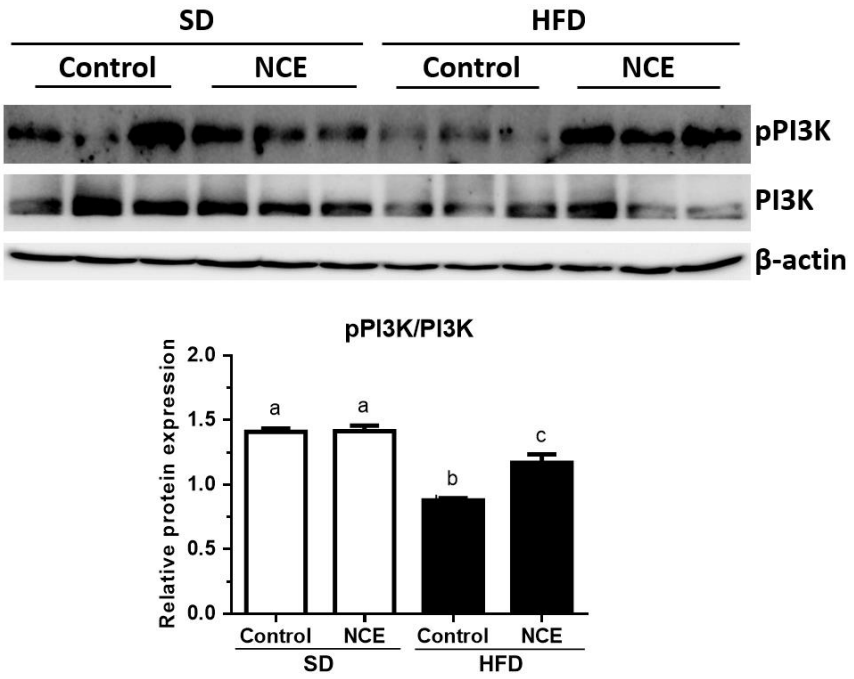

Figure 40. Effects of *N cochenillifera* extract (NCE) administration on: PI3K gene expression and pPI3K/PI3K ratio evaluated by Western blot. Standard diet (SD); High fat diet (HFD). Data are expressed as means ± SEM (n = 6). Groups with different letters statistically differ ($p < 0.05$).

V. DISCUSSION

PART I

The physicochemical and phytochemical characterization of Nopalea cochenillifera extract identifies the presence of beneficial compounds to intestinal health

The physicochemical characterization of the *N. cochenillifera* extract (NCE) demonstrated a substantial proportion of crude fiber and a considerable content of carbohydrates. These outcomes are consistent with a prior investigation conducted by Silva et al. (224). In addition, Lima et al. (225) also revealed that NCE harvested in Paraíba, Brazil, had a high total carbohydrate content (66.80% of fresh raw material).

The determination of phytochemical content in a raw material (dry extract) is an essential quality parameter to ensure the reproducibility of therapeutic effects (226). Gallic acid and quercetin equivalent (mg) per gram of dry extract were used to express TPC and TFC in NCE, with an average value of 67.85 mg GAE/g and 46.16 mg QE/g of dry extract obtained from NCE cladodes. These values exceeded those previously reported by Alves et al. (2017) (194), who assessed TPC and TFC in ethanolic extracts of *Opuntia* and *Nopalea*, obtaining 5.41 mg GAE/g and 2.7 mg QE/g, respectively, from samples collected from different cultivars during the rainy season. Fabela-Illescas et al. (15) found a content of 6.47 mg of polyphenols equivalent/g of gallic acid and 2.08 mg of rutin equivalent/g of flavonoid in *N. cochenillifera* cladode flour. In this last study, the low value of TFC can be explained because the authors analyze the flour instead an extract.

Differences in phenolic and flavonoid content observed in studies may be related to environmental factors such as light, water stress, rainy season, salinity, low temperatures, and nutrient deficiency, which can affect plant metabolism, leading to changes in secondary metabolic processes and concentrations of secondary metabolites (227). The extraction method and solvent used are also important, as they can be selective in extracting certain metabolites (228). TPC and TFC per gram of *N. cochenillifera* hydroethanolic extract represent a quality control parameter that may be associated with the preclinical pharmacological effect found in this study, thereby ensuring consistency and reproducibility of the raw material (229).

The phytochemical profile of NCE was characterized through HPLC-ESI-MS^n analysis. By dereplicating negative and positive HPLC-ESI-MS^n data and by comparison of data with GNPS public libraries, literature information, and fragmentation pattern study (MS^2 and MS^3 experiments), we could characterize 25 metabolites present in NCE. Partial results corroborate with Fabella-Illescas et al. (15), who identified and quantified the first-time phenolic

compounds such as acid gallic, acid ferulic, acid chlorogenic, acid *p*-coumaric, acid siring, and acid neo-chlorogenic in samples of *N. cochenillifera* cladodes flour through HPLC. However, to our knowledge, this is the first dereplication study and description of isoflavones for this species. The presence of isoflavones is almost entirely restricted to the *Fabaceae* subfamily of the *Leguminosae* family, but they are also occasionally found in some other families (230).

It is possible to associate the anti-colitis effect observed in preclinical studies with the phytochemical content found in NCE. To strengthen our findings, clinical studies about flavonoid supplementation in patients with IBD have demonstrated a positive correlation in maintaining remissive disease status (109,110).

Nopalea cochenillifera extract did not produce toxic effects in rats after acute treatment

Changes in the weights of organs are sensitive indicators of toxicity and physiological disruptions in studies on toxicity (231,232). In the same way, evaluating hematological parameters is a common approach for assessing the potential toxicity of drug compounds and botanical extracts (233). Hematopoietic system changes are more predictive of human toxicity when data is extrapolated from animal investigations (234). Additionally, alterations in platelet counts can signal hemostatic imbalances and suggest the possibility of thromboembolic complications (235).

In the acute toxicity assay, administration of NCE at a single dose of 2000 mg/kg did not impact spontaneous locomotor activity or behavioral parameters, as evidenced by no alterations in total distance traveled, lifting, and grooming. Additionally, there were no observed changes in motor coordination, as indicated by consistent performance on the rotarod test across all evaluated days. Although there was an increase in the number of defecations in the group of animals treated with NCE, this parameter was not considered indicative of anxiety, as it did not correlate with the other behavioral parameters analyzed.

The acute in vivo toxicity study was the first report for this species, and it is considered important safety data for further studies. The NCE can be considered of low acute toxicity according to the class method recommended by OECD 423 (OECD, 2001) (30) and fits in Type 5 (substance with LD50 higher than 2000 mg/kg and less than 5000 mg/kg) because there were no signs of general toxicity such as changes in water and feed consumption, body weight, hematological and biochemical parameters. There were no behavioral changes and no deaths observed during the whole experimental period. Furthermore, the extract did not cause morphological changes in the organs investigated microscopically.

Nopalea cochenillifera extract attenuates intestinal inflammation by DNBS in rats

Following the preclinical safety assessments, this study proceeded to investigate the anti-inflammatory effect of *N. cochenillifera* extract, as this species is a good raw material source of fibers, polysaccharides, and polyphenols (15). These compounds possess anti-inflammatory and antioxidant properties that could explain their ability to attenuate intestinal inflammation, as demonstrated in preclinical and clinical studies (236,237). Therefore, we decided to investigate the anti-colitis effect of NCE in this study. Of note, this is the first report linking *N. cochenillifera* to inflammatory bowel diseases.

The induction of intestinal inflammation through the in vivo model of DNBS causes acute inflammation in the colon that replicates clinical features and an inflammatory response similar to Crohn's disease in humans. This leads to symptoms such as weight loss, diarrhea, and bloody stool, which serve as parameters used to assess the disease activity index (DAI) in animals (238). Administration of sulfasalazine and NCE resulted in significantly lower DAI and reduced weight loss on all days following colitis induction. The colitis groups exhibited a substantial loss in body weight, indicating the progression of severe colitis, but the treatments alleviated this weight loss. Furthermore, the NCE exhibited a reduction in the ratio of colonic weight (mg) to length (cm), which indirectly indicates edema and inflammation. This reduction was accompanied by a decrease in macroscopic damage, highlighting the beneficial effect of NCE treatment.

IBD is are characterized by the hyperactivation of the intestinal immune system, resulting in chronic inflammation and the release of inflammatory cytokines that exacerbate tissue damage. A histopathological hallmark of IBD is the infiltration of immune cells, particularly neutrophils, into the affected area. These immune cells are recruited to the intestinal mucosa and contribute to the inflammatory response by producing inflammatory cytokines and reactive oxygen species (ROS). In addition, the enzyme MPO is secreted by both neutrophils and monocytes, further contributing to the inflammatory process (239). Markers of oxidative damage, such as MPO, are elevated in the mucosa of patients with IBD, and their reduction indicates a decrease in inflammation of the damaged tissue. The present study demonstrated that animals treated with NCE exhibited a significant decrease in MPO activity, which supports the histological analyses that revealed a reduction in the infiltration of inflammatory cells.

In preclinical experimental models and IBD in humans, the intestinal inflammatory process, which leads to the induction of oxidative stress, has been associated with a significant increase

in MDA in intestinal tissue. The MDA is a byproduct of lipid peroxidation that activates pro-inflammatory cytokines and contributes to the inflammatory response (240). The ability of NCE to improve intestinal inflammation induced by DNBS may be attributed to its antioxidant properties, which can be largely attributed to the presence of phenolic compounds. Some research has shown that phenolic compounds, such as those found in NCE, can scavenge radicals and act as antioxidants (99).

IBD is characterized by an upregulation of inflammatory mediators that contribute to the initiation and persistence of inflammation in the gastrointestinal tract. These mediators include pro-inflammatory cytokines like IL-1β, IL-6, and IL-17, as well as TNF-α, prostaglandins, and nitric oxide (NO) (82). Thus, polyphenolic compounds have been shown to possess anti-inflammatory properties due to their ability to downregulate the expression of pro-inflammatory molecules, particularly IL-1β, IL-6, TNF-α, and COX-2. These molecules are known to play a significant role in the pathogenesis of IBD, and their suppression by polyphenols may contribute to the beneficial effects observed in treating this condition (241). Furthermore, NCE was observed to increase the levels of IL-10, an anti-inflammatory cytokine that is often used as a marker for the evolution of intestinal inflammation. In IBD, IL-10 levels typically increase only at the time of disease evolution, and the ability of NCE to promote IL-10 production suggests a potential mechanism for its anti-inflammatory effects in the context of DNBS-induced colitis (242,243). However, an increase in IL-10 was observed in the groups treated with the 200 and 300 mg/kg doses of NCE shortly after the period of disease activation by DNBS (3 days).

The beneficial effects of NCE in experimental models of DNBS-induced colitis also may be attributed to its ability to modulate the NF-κB p65/MAPK signaling pathway, which plays a crucial role in regulating inflammatory gene expression. NF-κB p65 is a key transcription factor in macrophages and is responsible for inducing the expression of various inflammatory genes, including IL-1β, TNF-α, and COX-2, the activation of the NF-κB signaling pathway by DNBS leads to increased expression of these pro-inflammatory cytokines, exacerbating intestinal inflammation (244). In addition, activating inflammatory cytokines such as IL-1β and TNF-α can stimulate the MAPK signaling pathway, including ERK1/2, p38 MAPK, and JNK. These pathways are closely linked with IBD, and their dysregulation can contribute to the progression of intestinal inflammation (245,246). Therefore, by modulating the NF-κB and MAPK pathways, NCE may effectively alleviate inflammation in DNBS-induced colitis.

The observed decrease in colonic levels of pro-inflammatory cytokines (IL-1β and TNF-α) in this study may be attributed to the presence of phenolic compounds, including those derived from kaempferol, quercetin, and ferulic acid, identified in NCE. These compounds can potentially inhibit the activation of the p65 NF-κB pathway, thus mitigating inflammation in DNBS-induced colitis (247–249). Gallic acid was shown to increase IκB in human gastric carcinoma cells, inhibiting NF-κB activity and the pro-inflammatory cascade (250). In another study involving experimental colitis by DSS-induced in mice, isoflavones were found to promote the inhibition of NF-κB in colon tissues (251). Thus, we can hypothesize that the bioactive compounds in NCEs may act synergistically on the same pathway. In this study, a downregulation in both gene and protein expression of NF-κB was observed in the SSZ and NCE groups.

The DNBS-induced colitis model in rodents disrupts the integrity and function of intestinal cells, leading to the breakdown of tight epithelial junctions and imbalances in paracellular permeability. Specifically, the untreated DNBS group exhibited lower gene expression of intestinal epithelial barrier markers (MUC-2 and ZO-1), while SSZ and NCE increased the expression of these markers. MUC-2 is essential for protecting the intestinal mucosa, and its dysfunction or reduced expression is associated with IBD pathogenesis, as it impairs protection against pathogenic bacterial invasion and colonization (252). ZO-1 is part of a subgroup of proteins that make up the tight junctions of the intestinal epithelium. The increase in its expression is an important factor in reducing the intestinal inflammatory process in IBD (253). A study using a human colorectal adenocarcinoma cell line indicated that polyphenols could modulate the expression of MUC-2 and ZO-1, which can help protect the epithelial barrier function of cells exposed to chemical agents (254).

Our studies have reinforced the hypothesis about the benefits of NCE in intestinal inflammation, demonstrating its effects in rats with DNBS-induced inflammation, especially at doses of 200 and 300 mg/kg. Phenolic compounds, such as those present in NCE, are known to have many positive effects on human health but also have limitations and challenges. They are easily degraded during storage or processing due to auto-oxidation, epimerization, hydrolysis, and crystallization (115). Additionally, they may undergo metabolic changes during digestion. This research aimed to develop a nanoparticle system loaded with *N. cochenillifera* extract to achieve a more specific delivery of active compounds to the colonic tissue, increase therapeutic efficacy, improve bioavailability and stability, and reduce the bioactive dose. The free and

nanoparticle-loaded extract also was evaluated in another in vivo model of DSS-induced inflammation.

Nanoparticles loaded with N. cochenillifera extract showed high encapsulation efficiency and stability for 30 days.

The nanoparticles showed a mean particle size of 76.45 nm and a negative zeta potential. Nano-sized particles can contribute to increasing the absorption and retention of metabolites of interest load-nanoparticles since they are more easily absorbed by immune system cells present in active inflammation. Lamprecht et al. and Sharma et al. (255,256), developed lipid nanoparticles containing curcumin (size less than 200 nm) and evaluated the in vivo absorption of the drug-free and incorporated into the nanoparticles by the gastrointestinal tract after oral administration, and were able to observe that the concentration of curcumin in the inflamed tissues of the colon was higher when carried by nanosystems.

The zeta potential consists of the difference between the electric potential at the shear surface of the colloid particle and the electric potential of the dispersant, which can be determined by evaluating the velocity of the charged species moving toward the electrode in the presence of an external electric field (257,258). For this analysis, the values were -25.1 ± 1.80 and -15.8 ± 2.61 for NPB and NPE, respectively. The difference in the surface charges of these particles can be explained by the high presence of phenolic acids in NCE. In addition, studies have shown that the expression of transferrin is increased in the membrane of colonocytes in IBD patients and colitis-induced rats (259). This overexpression of transferrin can lead to an accumulation of positively charged ions, such as iron, on the surface of the intestinal epithelium (260–262). This, in turn, may favor the formation of electrostatic interactions between this protein and nanoparticles with negative ZP, increasing the retention of NPE in the inflamed colon tissues.

The data show an entrapment efficiency (EE) close to 100% (99.15 ± 0.3%), which can be explained by the intermolecular interactions between the phenolic compounds present in the extract and the EUDRAGIT S100 (EUD S100) polymer. Phenolic compounds can form several types of interactions with the polymer via non-covalent forces, such as hydrogen bonding, electrostatic interactions, hydrophobic interactions, or π–π stacking. Multiple interactions can occur in forming the same nanosystem, especially in self-assembly techniques such as nanoprecipitation, used in developing NPE (11,263). EUD S100 has carbonyls (-C=O) and hydroxyls (-OH) that favor the formation of hydrogen bonds with phenolic compounds, such as ferulic acid, rutin, vanillic acid and other abundant flavonoids in NCE that have hydrogen

donor and acceptor groups, in addition to hydrophobic interactions between the methyl groups (-CH_3) present in their polymer chain and the carbon chains of these metabolites (264). Previous studies reported high encapsulation of phenolics compounds in polymeric nanoparticles. For example, Sulfikkarali et al. (265) incorporated the compound naringenin into Eudragit E nanoparticles and obtained almost 90% EE (265). In another study, Alves et al. (34) prepared Eudragit EPO nanoparticles containing *Passiflora edulis* f. *flavicarpa* extract and used isoorientin as a phytochemical marker for quantification, obtaining 100% EE. These results corroborate with our findings and demonstrate the influence of intermolecular interactions of the used polymer with the metabolites of NCE.

The identification of some functional groups present in the chemical structure of *N. cochenillifera* was performed by FTIR spectroscopy, which provides a "chemical fingerprint" of the compounds present in the molecule by means of the frequency of absorption of the bond present in the functional groups. It was observed that the behaviors in the spectra were also similar to those found in other related investigations (266–270). The broad absorption band at around 3330 cm^{-1} is attributed to OH stretching relative to alcohol and carboxylic acid commonly involved in intermolecular OH bonding and corroborates with the analyses performed by Ferreira et al. (267) and Rodrıguez-González et al. (269) in mucilage from *Nopalea* and *Opuntia* species, respectively. This band may also indicate the presence of OH groups, characteristic of phenolic acids, flavonoids, and other phenolic derivatives (34). At 2920 cm^{-1}, a discrete band was observed associated with the vibrations of -CH and -CH_2 groups (268,269). Next, a band was seen at 1625 cm^{-1}, followed by another at 1440 cm^{-1} corresponding to the carboxylic ion (group COO-) (269). The most intense signal at 1044 cm^{-1} é indicative of the presence of polysaccharides and corresponds to the CC and CO vibrations.

In the spectrum of the nanoparticle system loaded with the extract (NPE), the signals from the extract practically disappear, leaving only the signals related to the polymer Eudragit S100. However, the broadening of a band at 1440 cm^{-1} in the NPE spectrum and not identified in the NPB may indicate some interaction between Eudragit S100 and the polysaccharides present in the extract. Furthermore, the NCE concentration is lower than the other components, so its characteristic bands appear less intensely in NPE. Furthermore, the subtly appearance of NCE in the NPE spectrum indicates its incorporation into nanoparticles, corroborating the findings in the EE evaluation.

About the stability study, two main mechanisms can explain the physical stability demonstrated by nanoparticles in colloidal suspensions in aqueous media: I) electrostatic repulsion, where the classical DLVO (Derjaguin–Landau–Verwey–Overbeek) theory is applied, and ZP is a parameter used to predict suspension stability. The higher the ZP, the more stable the suspension is; II) steric stabilization, which occurs through non-ionic amphiphilic stabilizers that provide a solvation effect (271). In this study, the physical stability of the nanoparticles over the storage period can be explained by the steric stabilization promoted by the stabilizer used in the preparation of the formulations, poloxamer 407, which is a triblock copolymer, amphiphilic and non-ionic (272) and, at the concentration used, was able to prevent the aggregation of nanoparticles (35).

NPs are gaining increasing attention for potential application in inflammatory bowel diseases; consequently, studying their interaction with intestinal mucosal cells is important (12,273). A study using Eudragit S100 and chitosan-based nanoparticles as drug carriers for the treatment of colorectal cancer via oral administration found that the nanoparticulate system showed cellular internalization and an efficacy of 8 to 10% after 48 hours of treatment in the HCT 116 cell line, signifying an even distribution of the drug within the cells (274). In addition, a uniform distribution of NPB within the cells was observed, indicating excellent cell uptake for the strain tested (275).

Nopalea cochenillifera extract (NC) and Extract-loaded nanoparticles (NPE) attenuates intestinal inflammation by DSS in mice

The DSS-induced colitis model is widely used for IBD research because of its fast, straightforward, and reproducible nature. DSS facilitates the entry of bacteria and antigens into the mucosa, leading to local inflammation. This model is well-suited for investigating events resulting from temporary mucosal homeostasis failure and provides valuable insights into the mechanisms driving intestinal inflammation and mucosal recovery after the initial injury (276), At the same time, DNBS acts as a hapten by binding to autologous or microbial proteins in the colon, making them immunogenic (277).

As well as in the induction of intestinal inflammation by DNBS, parameters such as weight loss and excretion of diarrhea and bloody stools are indicators of the severity of intestinal inflammation caused by DSS-induced colitis (276). Our results indicated an overall improvement in DSS-induced adverse effects in the group treated with NCE and NPE. The dose of the extract administered in this trial was 200 mg/kg (The best dose effect presented in the

trial with DNBS was considered). In the case of NPE, the dose of extract administered was 50x lower; considering the concentration of extract incorporated into the nanoparticulate system, the animals in this group received a dose of 4 mg/kg. No significant differences were observed between NCE and NPE in evaluating DAI and colon weight/length ratio.

Studies conducted with EUD S100 nanoparticles as carriers of actives for treating intestinal inflammation in preclinical models showed marked improvements over drugs administered in free form (278,279). Gugulothu et al. (279) developed EUD S100 nanoparticles loaded with celecoxib and curcumin and evaluated their efficacy in mice with TNBS-induced ulcerative colitis. Nanoparticles loaded proved more effective than celecoxib or curcumin alone, as they achieved effects similar to the conventional dose at a 50% lower concentration. In another study, Beloqui et al. (280) developed nanoparticles of PLGA/EUD S100 loaded curcumin for the treatment of inflammatory bowel diseases, evaluated the curcumin release profile at different pH, and were able to observe that the molecule was released more (90%) at pH 7.2 which is in line with the pH of the colon. EUD S100 promoted colon-specific drug delivery, and the accumulation of curcumin in the colon was confirmed by in vivo studies.

These results indicate that with a dose 50x lower, the NPE promotes a treatment efficacy equal to the NCE. Incorporating the nanoparticles makes it possible to reduce the administered dose and maintain the desired therapeutic effect. Such success may have been obtained by the internalization of NPs inside the cells (281), by the accumulation of NPs in the colon by electrostatic interactions with abundant proteins in the inflamed tissue (282) and by the colon-specific delivery promoted by the pH-sensitive polymer EUD S100 (283). The data prove the relevance of incorporating the extract into EUD S100 nanoparticles.

Based on our findings, NCE and NPE have been found to promote intestinal barrier integrity in mice with DSS-induced colitis. Furthermore, histopathological analyses suggest that therapy with NCE extract in both free and nanoparticulate form may accelerate recovery after DSS exposure. To support this hypothesis, we observed that colon tissue samples from mice treated with NCE and NPE showed a significant increase in the relative mRNA expression levels of intestinal epithelial integrity regulators (ZO-1, OCCLUDIN, and MUC-3). Overall, NCE was found to regulate the expression of these genes, maintaining them at levels similar to those of the control group, effectively alleviating the barrier disruption caused by DSS.

NCE and NPE also reduce inflammatory and oxidative responses in colitic mice. As well as DNBS, the DSS is toxic to intestinal epithelial cells, leading to an acute inflammatory response.

The damage caused to the intestinal epithelium leads to increased mucosal permeability and, consequently, the entry of microorganisms and their derivatives into the intestinal mucosa. Thus microorganisms and their derivatives can penetrate through the loosened tight epithelial junctions, activating intestinal macrophages, which secrete inflammatory cytokines, including TNF-α, IL-1β, and IL-6 (284,285). Chemokines act in recruiting other immune cells, such as dendritic cells, T cells, B cells, and neutrophils that aggravate colon inflammation (286). The presence of MCP-1 is thought to be responsible for invading monocytes and polymorphonuclears into inflamed tissue (287). MIP-2 also mediates neutrophil recruitment to sites of injury or infection and modulates immune and inflammatory responses (288).

MIP-2 synthesis is also regulated at the transcriptional level by signaling through the Toll-like receptors (TLRs) in response to various pathogens (289). The decreased expression of TLR-4 in our findings corroborates with the decreased expression of MIP-2 and the observation of increased intestinal mucosal integrity in the NCE and NPE-treated groups. Consequently, lower expression of intercellular adhesion molecules is visualized since positive regulation of ICAM-1 in IBD may lead to increased adhesion and retention of polymorphonuclear cells on the apical intestinal epithelial cell (290).

These results corroborate with the DNBS inflammatory induction assay, in which NCE also decreased the expression of inflammatory cytokines such as IL-1β and TNF-α and showed protective effects on the gastrointestinal mucosa in experimental models of DSS-induced intestinal inflammation. This research provides a better understanding and elucidation of the molecular mechanisms of action of *N. cochenillifera* extract in a free and nanoparticle-associated form on intestinal inflammation. Furthermore, it may encourage further research on applying nanoformulation to provide therapeutic actives compounds for treating IBD.

PART II

N. cochenillifera extract reduces body weight and improves the lipid profile of mice subjected to a high fat diet

N. cochenillifera has been traditionally used to treat dyslipidemia and hyperglycemia, among other conditions (22,23). However, few studies support its efficacy and investigate the possible mechanisms involved. According to the results obtained in this study, NCE has been found to be effective in reducing body weight in an experimental model of metabolic syndrome induced by the consumption of a high-fat diet in mice, with a significant reduction observed from the 20th day of treatment onwards.

This effect was confirmed by analyzing the weight of the fat deposits at the end of the experimental period. The treatment with NCE significantly reduced epididymal fat, abdominal fat, and brown fat. The weight reduction effect observed in the HFD-fed group treated with NCE was also demonstrated by histological analysis of the epididymal fat of mice. Adipocytes of mice HFD-fed treated with NCE were significantly smaller than those of the untreated HFD group. These results suggest a positive effect of NCE on reducing fat deposits, as a decrease in adipocyte size is equivalent to a reduction in lipid accumulation. The treatment with NC extract also significantly reduced the plasma levels of total cholesterol and LDL cholesterol in HFD-fed mice that received treatment. This effect supports that NC is an alternative therapy in several countries to reduce cholesterol levels (22,23). No statistically significant difference was observed in HDL levels between the control and NCE-treated groups.

The weight reduction by NCE treatment confirms what was observed in the studies of Fabela-Illescas et al. (22). This effect may be due to the high content of phenolic compounds present in NCE. Several studies conducted with phenolic-rich extracts have shown to reduce weight and fat accumulation in a rat model of high-fat diet-induced obesity (291–293).

Additionally, NCE has demonstrated a significant effect in reducing liver weight in obese mice. Non-alcoholic fatty liver disease occurs when excess fat is stored in the liver, and this pathology is strongly related to metabolic syndrome (294). Thus, it would be expected that the obese group would have a heavier liver due to the accumulation of excess fat in the liver, which is exactly what was observed. In contrast, the group fed HFD and treated with NCE showed similar median liver weight to healthy animals. Thus, NCE could be involved in improving the non-alcoholic fatty liver condition associated with metabolic syndrome. However, further studies would be needed to evaluate this effect.

The reduction in body weight caused by NCE not only seems to be related to an effect at the level of reducing fat deposition in tissues, but it may also be triggering this effect by increasing the expression of the leptin receptor (a hormone involved in satiety). The peptide hormone leptin regulates food intake and body weight, as well as being involved in lipolysis. Leptin is synthesized and secreted by white adipose tissue cells and acts on target cells by binding to its receptor (Leptin-R). Leptin resistance is characterized by a reduction in satiety, so excessive food intake tends to occur, leading to an increase in body weight. Leptin resistance is also caused by a decrease in leptin receptor expression (155); therefore, by increasing leptin receptor expression, NCE could be exerting a sensitizing effect in relation to this hormone, triggering a greater sense of satiety and therefore, less food intake, thus reducing body weight. It would be

interesting to elucidate whether NCE achieves its weight-reducing effects by influencing lipid metabolism (increasing lipid catabolism) or reducing food intake (stimulating satiety), or whether it exerts its effect using both mechanisms.

According to the results obtained in this study, the last option seems to be the most favorable, so NCE exerts its body weight reduction effect through both mechanisms. This option is supported by the significant increase in leptin R expression when HFD-fed mice are treated with NCE and, simultaneously, by the increase in peroxisome proliferator-activated receptor alpha (PPARα) expression in this same group. PPARα is a nuclear receptor expressed in tissues with the high oxidative activity that plays a central role in regulating glycolipid metabolism (295). PPARγ is highly expressed in adipose tissue, where it accelerates the uptake of fatty acids into adipocytes and increases insulin sensitivity, thereby reducing the flow of fatty acids to the liver (296). However, no significant differences in the expression of this marker were observed in the liver samples of the analyzed groups.

N. cochenillifera extract reduces glycemic levels and insulin resistance

Based on the results obtained in this study, treatment with NCE improves the glucose profile of HFD-fed mice, as reflected in the significant reduction in fasting plasma glucose levels. Regarding insulin resistance, NCE improves this pathology, as demonstrated by the glucose tolerance test. It was found that NCE significantly reduced plasma glucose levels compared to the HFD control group from 60 minutes, resulting in a significant reduction in the area under the curve (AUC). The improvement of insulin resistance and glycemic profile by NCE observed in this study is in line with previous studies suggesting that this plant has activity in controlling diabetes (22,23). This also confirms what was observed in a pre-clinical study conducted by Magaña-Cerino et al. (21).

Insulin physiological signaling occurs after insulin binds to its receptor, a ligand-activated tyrosine kinase. This binding results in the tyrosine phosphorylation of various substrates and the activation of two parallel pathways: the PI3K-AKT and the MAPK pathways. In insulin resistance, the PI3K-AKT pathway is affected, while the MAPK pathway is not. This leads to an imbalance between the two parallel pathways. Inhibiting the PI3K-AKT pathway reduces endothelial NO production, resulting in endothelial dysfunction and a decrease in GLUT-4 translocation, leading to a decrease in glucose uptake by skeletal muscle and fat. In contrast, the MAPK pathway is not affected, and it continues to produce endothelin 1, express vascular cell adhesion molecules, and stimulate mitogenic activity in vascular smooth muscle cells.

Consequently, insulin resistance leads to vascular abnormalities predisposing individuals to atherosclerosis (113).

The effect of NCE against insulin resistance, according to the results obtained, is mediated by the modulation of the expression of the proteins pI3K and AMPK in their active (phosphorylated) forms. In this sense, the expression of p-PI3K in HFD-fed mice was reduced but showed recovery in the group treated with NCE. Additionally, treatment with NCE induced a significant recovery in the gene expression of GLUT-4. The AMPK gene and protein expression increase was also observed in the liver samples of mice HDF-fed and treated with NCE. The activation of AMPK increases the activation of IRS-1 mediated by S6K and the phosphorylation of Akt, thus increasing sensitivity to insulin signaling (297).

N. cochenillifera extract can promote improved intestinal permeability

The dysbiosis associated with obesity leads to increased damage to enterocytes and, therefore, intestinal permeability increases. The intestinal mucus, in turn, is composed of highly glycosylated proteins released by intestinal goblet cells, which also belong to the epithelial barrier (298). Previous studies have observed a decrease in the thickness of the intestinal mucus in mice fed a high-fat diet (299), which may favor bacterial translocation or the passage of bacterial substances responsible for endotoxemia observed in patients with metabolic syndrome and which leads to a situation of subclinical chronic inflammation (300).

According to the results obtained in this study, treatment with NCE appears to restore levels of intestinal mucus in obese mice treated, as observed through the increased gene expression of MUC-3 in colon samples of the group treated with NCE, as well as demonstrated more significant expression of one of the tight junction proteins ZO-1, suggesting an improvement in intestinal mucosal integrity. In this way, we could conclude that NCE exerts a protective effect against intestinal permeability associated with obesity. Furthermore, this intestinal protective effect of NC is consistent with previous studies that suggest that this plant has gastroprotective activity (22–24).

N. cochenillifera extract can reduce oxidative stress in liver tissue

Many studies have revealed that a high-fat diet causes oxidative stress in most experimental models and patients with clinical conditions. To determine a possible antioxidant effect of NCE, liver samples were collected, and TBARS levels were evaluated. TBARS are produced during oxidative stress, which is induced by lipid peroxidation. MDA is the best-known specific

TBARS and is considered a promising biomarker of oxidative damage caused by free radicals in the process of oxidative stress (181). The TBARS assay confirmed the *in vivo* antioxidant effect of the NCE. Thus, the administration of NCE in obese mice significantly reduced TBARS values, meaning that NCE restored the antioxidant status in treated obese animals. Due to the richness of NCE in antioxidant compounds (phenolic and flavonoid compounds), it makes sense to think that its antioxidant effects are due to these compounds.

CONCLUSION

In the analysis of *N. cochenillifera* extract by HPLC-ESI-MS, it was possible to determine the chromatographic profile of the hydroethanolic extract obtained from the cladodes of the species *Nopalea cochenillifera*, 25 compounds were characterized, being predominant the presence of phenolics. The content of total phenols and flavonoids in the extract was 67.85% and 46.16%, respectively.

Regarding the effects of NCE in the DNBS model of intestinal inflammation and of NCE and NPE in the DSS model, it was observed that both showed preventive and anti-inflammatory effects through the reduction of disease activity index score and macroscopic and microscopic damage in the colon. Furthermore, through molecular analyses, it was possible to observe that NCE and NPE decreased levels of inflammatory and oxidative mediators and promoted negative regulation of the expression of genes in important inflammatory and oxidative pathways. In addition, NCE and NPE contributed to improving epithelial integrity, as evidenced by barrier marker analyses and histological techniques. The free and nanoparticle-associated extract presented similar results. However, the dose of NCE administered by NPE was 50x lower in the DSS induction assay.

In the diet-induced metabolic syndrome assays, NCE showed an improvement in the metabolic profile of obese mice, as well as a significant reduction in body weight gain. Furthermore, these effects were associated with an improvement in systemic inflammatory status. Different mechanisms seem to be involved, highlighting the possible immunomodulatory effects of phenolics, as these compounds can have beneficial effects in regulating genes involved in metabolic, inflammatory, and oxidative stress processes. However, further studies are needed to fully understand the underlying mechanisms.

The preclinical results indicate that free NCE or incorporated into nanoparticles is beneficial in preventing induced colitis and metabolic syndrome. Therefore, the results of this study support future investigations into the therapeutic potential of *N. cochenillifera* extract in treating the intestinal inflammation and metabolic syndrome and can be seen as a promising bioactive ingredient for the development of an herbal medicine or functional supplement innovative useful in the complementary treatment of these diseases.

REFERENCES

1. Kaplan GG, Windsor JW. The four epidemiological stages in the global evolution of inflammatory bowel disease. Nat Rev Gastroenterol Hepatol [Internet]. 2021 Jan 8;18(1):56–66. Available from: https://www.nature.com/articles/s41575-020-00360-x
2. Saklayen MG. The Global Epidemic of the Metabolic Syndrome. Curr Hypertens Rep [Internet]. 2018 Feb 26;20(2):12. Available from: http://link.springer.com/10.1007/s11906-018-0812-z
3. WHO Regional office for Europe. WHO European Regional Obesity Report 2022 [Internet]. 2022. 1–220 p. Available from: http://apps.who.int/bookorders.
4. Saeid Seyedian S, Nokhostin F, Dargahi Malamir M. A review of the diagnosis, prevention, and treatment methods of inflammatory bowel disease. J Med Life [Internet]. 2019 Apr;12(2):113–22. Available from: https://medandlife.org/wp-content/uploads/JMedLife-12-113.pdf
5. Cornier M-A, Dabelea D, Hernandez TL, Lindstrom RC, Steig AJ, Stob NR, et al. The Metabolic Syndrome. Endocr Rev [Internet]. 2008 Dec 1;29(7):777–822. Available from: https://academic.oup.com/edrv/article/29/7/777/2354985
6. Abegunde AT, Muhammad BH, Bhatti O, Ali T. Environmental risk factors for inflammatory bowel diseases: Evidence based literature review. World J Gastroenterol [Internet]. 2016;22(27):6296. Available from: http://www.wjgnet.com/1007-9327/full/v22/i27/6296.htm
7. Krela-Kaźmierczak I, Zakerska-Banaszak O, Skrzypczak-Zielińska M, Łykowska-Szuber L, Szymczak-Tomczak A, Zawada A, et al. Where Do We Stand in the Behavioral Pathogenesis of Inflammatory Bowel Disease? The Western Dietary Pattern and Microbiota—A Narrative Review. Nutrients [Internet]. 2022 Jun 17;14(12):2520. Available from: https://www.mdpi.com/2072-6643/14/12/2520
8. Ginsberg HN, MacCallum PR. The Obesity, Metabolic Syndrome, and Type 2 Diabetes Mellitus Pandemic: Part I. Increased Cardiovascular Disease Risk and the Importance of Atherogenic Dyslipidemia in Persons With the Metabolic Syndrome and Type 2 Diabetes Mellitus. J Cardiometab Syndr [Internet]. 2009 Mar;4(2):113–9. Available from: https://onlinelibrary.wiley.com/doi/10.1111/j.1559-4572.2008.00044.x
9. Rochlani Y, Pothineni NV, Kovelamudi S, Mehta JL. Metabolic syndrome: pathophysiology, management, and modulation by natural compounds. Ther Adv Cardiovasc Dis [Internet]. 2017 Aug 22;11(8):215–25. Available from: http://journals.sagepub.com/doi/10.1177/1753944717711379
10. Hagan M, Hayee BH, Rodriguez-Mateos A. (Poly)phenols in Inflammatory Bowel Disease and Irritable Bowel Syndrome: A Review. Molecules [Internet]. 2021 Mar 25;26(7):1843. Available from: https://www.mdpi.com/1420-3049/26/7/1843
11. Qi Y, Li J, Nie Q, Gao M, Yang Q, Li Z, et al. Polyphenol-assisted facile assembly of bioactive nanoparticles for targeted therapy of heart diseases. Biomaterials [Internet]. 2021 Aug;275:120952. Available from: https://linkinghub.elsevier.com/retrieve/pii/S0142961221003082
12. Chen F, Liu Q, Xiong Y, Xu L. Current Strategies and Potential Prospects of Nanomedicine-Mediated Therapy in Inflammatory Bowel Disease. Int J Nanomedicine [Internet]. 2021 Jun;Volume 16:4225–37. Available from: https://www.dovepress.com/current-strategies-and-potential-prospects-of-nanomedicine-mediated-th-peer-reviewed-fulltext-article-IJN
13. Ambriz-Perez DL, Leyva-Lopez N, Gutierrez-Grijalva EP, Heredia JB. Phenolic compounds: Natural alternative in inflammation treatment. A Review. Yildiz F, editor. Cogent Food Agric [Internet]. 2016 Jan 11;2(1). Available from: https://www.cogentoa.com/article/10.1080/23311932.2015.1131412
14. Rahman MM, Rahaman MS, Islam MR, Rahman F, Mithi FM, Alqahtani T, et al. Role of Phenolic Compounds in Human Disease: Current Knowledge and Future Prospects. Molecules [Internet]. 2021 Dec 30;27(1):233. Available from: https://www.mdpi.com/1420-3049/27/1/233
15. Fabela-Illescas HE, Castro-Mendoza MP, Montalvo-González E, Anaya-Esparza LM, Vargas-Torres A, Betanzos-Cabrera G, et al. Bioactive compounds identification and physicochemical characterization from Nopalea cochenillifera (L.) Salm-Dyck cladodes flour. Biotecnia [Internet]. 2022 Feb 23;24(1):46–54. Available from: http://biotecnia.unison.mx/index.php/biotecnia/article/view/1519
16. Araújo DF de S, de Oliveira MEG, de Carvalho POAA, Tavares E de A, Guerra GCB, Queiroga R de CR do E, et al. Food Plants in the Caatinga. In Springer; 2021. p. 225–50. Available from: https://link.springer.com/10.1007/978-3-030-69139-4_11
17. Andrade-Cetto A, Heinrich M. Mexican plants with hypoglycaemic effect used in the treatment of diabetes. J Ethnopharmacol [Internet]. 2005 Jul;99(3):325–48. Available from: https://linkinghub.elsevier.com/retrieve/pii/S0378874105003004

18. Lans CA. Ethnomedicines used in Trinidad and Tobago for urinary problems and diabetes mellitus. J Ethnobiol Ethnomed [Internet]. 2006 Dec 13;2(1):45. Available from: https://ethnobiomed.biomedcentral.com/articles/10.1186/1746-4269-2-45
19. Necchi RMM, Alves IA, Alves SH, Manfron MP. In vitro antimicrobial activity, total polyphenols and flavonoids contents of Nopalea cochenillifera (L.) Salm-Dyck (Cactaceae). In 2015.
20. Gomez-Flor R, Tamez-Guer P, Tamez-Guer R, Rodriguez- C, Monreal-Cu E, Hauad-Marr LA, et al. In vitro Antibacterial and Antifungal Activities of Nopalea cochenillifera Pad Extracts. Am J Infect Dis [Internet]. 2006 Jan 1;2(1):1–8. Available from: http://www.thescipub.com/abstract/?doi=ajidsp.2006.1.8
21. Magaña-Cerino JM, Guzmán TJ, Soto-Luna IC, Betanzos-Cabrera G, Gurrola-Díaz CM. Cladodes from Nopalea cochenillifera (L.) Salm-Dyck (Cactaceae) attenuate postprandial glycaemia without markedly influencing α-glucosidase activity. Nat Prod Res [Internet]. 2022 Feb 16;36(4):1105–8. Available from: https://www.tandfonline.com/doi/full/10.1080/14786419.2020.1851223
22. Fabela-Illescas HE, Ávila-Domínguez R, Hernández-Pacheco A, Ariza Ortega JA, Betanzos-Cabrera G. Effect of a beverage made from cactus pear (Nopalea cochenillifera (L) SALM-DYCK) ina rural population of hidalgo, México; a pilot clinical trial. Nutr Hosp. 2015 Dec;32(6):2710–4.
23. Necchi R, Maki T, Canto G, Moresco R, Dalmora S, Manfron M. Antiinflammatory Activity and Biochemical Parameters of the Ethanol Extract of Nopalea cochenillifera (L.) Salm-Dyck (Cactaceae). Lat Am J Pharm. 2011;30.
24. da Silva ECS, Guerra GC, de Araújo ERD, Schlamb J, Silva V, Tavares E de A, et al. Phenolic-rich extract from Nopalea cochenillifera attenuates gastric lesion induced in experimental model through inhibiting oxidative stress, modulating inflammatory markers and cytoprotective effect. Food Funct [Internet]. 2023; Available from: http://pubs.rsc.org/en/Content/ArticleLanding/2023/FO/D2FO03735A
25. Abbas S, Karangwa E, Bashari M, Hayat K, Hong X, Sharif HR, et al. Fabrication of polymeric nanocapsules from curcumin-loaded nanoemulsion templates by self-assembly. Ultrason Sonochem [Internet]. 2015 Mar;23:81–92. Available from: https://linkinghub.elsevier.com/retrieve/pii/S1350417714003125
26. Neves MA, Hashemi J, Prentice C. Development of novel bioactives delivery systems by micro/nanotechnology. Curr Opin Food Sci [Internet]. 2015 Feb;1:7–12. Available from: https://linkinghub.elsevier.com/retrieve/pii/S221479931400006X
27. Pateiro M, Gómez B, Munekata PES, Barba FJ, Putnik P, Kovačević DB, et al. Nanoencapsulation of Promising Bioactive Compounds to Improve Their Absorption, Stability, Functionality and the Appearance of the Final Food Products. Molecules [Internet]. 2021 Mar 11;26(6):1547. Available from: https://www.mdpi.com/1420-3049/26/6/1547
28. Dantas-Medeiros R, Zanatta AC, de Souza LBFC, Fernandes JM, Amorim-Carmo B, Torres-Rêgo M, et al. Antifungal and Antibiofilm Activities of B-Type Oligomeric Procyanidins From Commiphora leptophloeos Used Alone or in Combination With Fluconazole Against Candida spp. Front Microbiol [Internet]. 2021 Feb 22;12. Available from: https://www.frontiersin.org/articles/10.3389/fmicb.2021.613155/full
29. Sousa EO, Miranda CMBA, Nobre CB, Boligon AA, Athayde ML, Costa JGM. Phytochemical analysis and antioxidant activities of Lantana camara and Lantana montevidensis extracts. Ind Crops Prod [Internet]. 2015 Aug;70:7–15. Available from: https://linkinghub.elsevier.com/retrieve/pii/S0926669015001855
30. OCDE Guideline for the testing of chemicals. Test No. 425: Acute Oral Toxicity: Up-and-Down Procedure [Internet]. Paris, France: OECD; 2001. (OECD Guidelines for the Testing of Chemicals, Section 4). Available from: https://www.oecd-ilibrary.org/environment/test-no-425-acute-oral-toxicity-up-and-down-procedure_9789264071049-en
31. Morris GP, Beck PL, Herridge MS, Depew WT, Szewczuk MR, Wallace JL. Hapten-induced model of chronic inflammation and ulceration in the rat colon. Gastroenterology [Internet]. 1989 Mar;96(3):795–803. Available from: https://linkinghub.elsevier.com/retrieve/pii/0016508589909049
32. Garrido-Mesa J, Rodríguez-Nogales A, Algieri F, Vezza T, Hidalgo-Garcia L, Garrido-Barros M, et al. Immunomodulatory tetracyclines shape the intestinal inflammatory response inducing mucosal healing and resolution. Br J Pharmacol [Internet]. 2018 Dec;175(23):4353–70. Available from: https://onlinelibrary.wiley.com/doi/10.1111/bph.14494
33. Hidalgo-Garcia L, Molina-Tijeras JA, Huertas-Peña F, Ruiz-Malagón AJ, Diez-Echave P, Vezza T, et al. Intestinal mesenchymal cells regulate immune responses and promote epithelial regeneration in vitro and in dextran sulfate sodium-induced experimental colitis in mice. Acta Physiol [Internet]. 2021 Oct 21;233(2). Available from: https://onlinelibrary.wiley.com/doi/10.1111/apha.13699
34. Alves JSF, Silva AM dos S, da Silva RM, Tiago PRF, de Carvalho TG, de Araújo Júnior RF, et al. In Vivo Antidepressant Effect of Passiflora edulis f. flavicarpa into Cationic Nanoparticles: Improving

Bioactivity and Safety. Pharmaceutics [Internet]. 2020 Apr 21;12(4):383. Available from: https://www.mdpi.com/1999-4923/12/4/383

35. dos-Santos-Silva E, Alves-Silva MF, de Medeiros JS, dos Santos-Cavalcante R, Cornélio AM, Fernandes-Pedrosa MF, et al. Colloidal properties of self-assembled cationic hyperbranched-polyethyleneimine covered poly lactide-co-glycolide nanoparticles: Exploring modified release and cell delivery of methotrexate. J Mol Liq [Internet]. 2020 Oct;315:113721. Available from: https://linkinghub.elsevier.com/retrieve/pii/S0167732220314689
36. Toral M, Gómez-Guzmán M, Jiménez R, Romero M, Sánchez M, Utrilla MP, et al. The probiotic Lactobacillus coryniformis CECT5711 reduces the vascular pro-oxidant and pro-inflammatory status in obese mice. Clin Sci [Internet]. 2014 Jul 1;127(1):33–45. Available from: https://portlandpress.com/clinsci/article/127/1/33/87050/The-probiotic-Lactobacillus-coryniformis-CECT5711
37. Alatab S, Sepanlou SG, Ikuta K, Vahedi H, Bisignano C, Safiri S, et al. The global, regional, and national burden of inflammatory bowel disease in 195 countries and territories, 1990–2017: a systematic analysis for the Global Burden of Disease Study 2017. Lancet Gastroenterol Hepatol [Internet]. 2020 Jan;5(1):17–30. Available from: https://linkinghub.elsevier.com/retrieve/pii/S2468125319303334
38. Albuquerque IC de, Cherao AA da S, Barbosa RC das N, Meinicke PT, Boarini LR, Daher BL. Epidemiologia das doenças inflamatórias intestinais em um serviço terciário do estado de São Paulo. J Coloproctology [Internet]. 2018 Oct;38:140. Available from: https://linkinghub.elsevier.com/retrieve/pii/S2237936318304118
39. Le Berre C, Ananthakrishnan AN, Danese S, Singh S, Peyrin-Biroulet L. Ulcerative Colitis and Crohn's Disease Have Similar Burden and Goals for Treatment. Clin Gastroenterol Hepatol [Internet]. 2020 Jan;18(1):14–23. Available from: https://linkinghub.elsevier.com/retrieve/pii/S1542356519307384
40. Ananthakrishnan AN. Environmental Triggers for Inflammatory Bowel Disease. Curr Gastroenterol Rep [Internet]. 2013 Jan 8;15(1):302. Available from: http://link.springer.com/10.1007/s11894-012-0302-4
41. Khor B, Gardet A, Xavier RJ. Genetics and pathogenesis of inflammatory bowel disease. Nature [Internet]. 2011 Jun 15;474(7351):307–17. Available from: http://www.nature.com/articles/nature10209
42. Lees CW, Barrett JC, Parkes M, Satsangi J. New IBD genetics: common pathways with other diseases. Gut [Internet]. 2011 Dec 1;60(12):1739–53. Available from: https://gut.bmj.com/lookup/doi/10.1136/gut.2009.199679
43. Liu JZ, van Sommeren S, Huang H, Ng SC, Alberts R, Takahashi A, et al. Association analyses identify 38 susceptibility loci for inflammatory bowel disease and highlight shared genetic risk across populations. Nat Genet [Internet]. 2015 Sep 20;47(9):979–86. Available from: https://www.nature.com/articles/ng.3359
44. Karban A. Effect of smoking on inflammatory bowel disease: Is it disease or organ specific. World J Gastroenterol [Internet]. 2007;13(15):2150. Available from: http://www.wjgnet.com/1007-9327/13/2150.asp
45. Kondamudi PK, Malayandi R, Eaga C, Aggarwal D. Drugs as causative agents and therapeutic agents in inflammatory bowel disease. Acta Pharm Sin B [Internet]. 2013 Sep;3(5):289–96. Available from: https://linkinghub.elsevier.com/retrieve/pii/S2211383513000609
46. Axelrad JE, Cadwell KH, Colombel J-F, Shah SC. The role of gastrointestinal pathogens in inflammatory bowel disease: a systematic review. Therap Adv Gastroenterol [Internet]. 2021 Jan 31;14:175628482110044. Available from: http://journals.sagepub.com/doi/10.1177/17562848211004493
47. Narula N, Wong ECL, Dehghan M, Mente A, Rangarajan S, Lanas F, et al. Association of ultra-processed food intake with risk of inflammatory bowel disease: prospective cohort study. BMJ [Internet]. 2021 Jul 14;n1554. Available from: https://www.bmj.com/lookup/doi/10.1136/bmj.n1554
48. Vasseur P, Dugelay E, Benamouzig R, Savoye G, Lan A, Srour B, et al. Dietary Patterns, Ultra-processed Food, and the Risk of Inflammatory Bowel Diseases in the NutriNet-Santé Cohort. Inflamm Bowel Dis [Internet]. 2021 Jan 1;27(1):65–73. Available from: https://academic.oup.com/ibdjournal/article/27/1/65/5736007
49. Papoutsopoulou S, Satsangi J, Campbell BJ, Probert CS. Review article: impact of cigarette smoking on intestinal inflammation-direct and indirect mechanisms. Aliment Pharmacol Ther [Internet]. 2020 Jun;51(12):1268–85. Available from: https://onlinelibrary.wiley.com/doi/10.1111/apt.15774
50. Jones DP, Richardson TG, Davey Smith G, Gunnell D, Munafò MR, Wootton RE. Exploring the Effects of Cigarette Smoking on Inflammatory Bowel Disease Using Mendelian Randomization. Crohn's Colitis 360 [Internet]. 2020 Jan 1;2(1). Available from: https://academic.oup.com/crohnscolitis360/article/doi/10.1093/crocol/otaa018/5803495
51. Chen B-C, Weng M-T, Chang C-H, Huang L-Y, Wei S-C. Effect of smoking on the development and outcomes of inflammatory bowel disease in Taiwan: a hospital-based cohort study. Sci Rep [Internet].

2022 May 10;12(1):7665. Available from: https://www.nature.com/articles/s41598-022-11860-y
52. Mark-Christensen A, Lange A, Erichsen R, Frøslev T, Esen BÖ, Sørensen HT, et al. Early-Life Exposure to Antibiotics and Risk for Crohn's Disease: A Nationwide Danish Birth Cohort Study. Inflamm Bowel Dis [Internet]. 2022 Mar 2;28(3):415–22. Available from: https://academic.oup.com/ibdjournal/article/28/3/415/6275621
53. Koloski NA, Bret L, Radford-Smith G. Hygiene hypothesis in inflammatory bowel disease: A critical review of the literature. World J Gastroenterol [Internet]. 2008;14(2):165. Available from: http://www.wjgnet.com/1007-9327/full/v14/i2/165.htm
54. Forbes JD, Van Domselaar G, Bernstein CN. The Gut Microbiota in Immune-Mediated Inflammatory Diseases. Front Microbiol [Internet]. 2016 Jul 11;7. Available from: http://journal.frontiersin.org/Article/10.3389/fmicb.2016.01081/abstract
55. Frank DN, St. Amand AL, Feldman RA, Boedeker EC, Harpaz N, Pace NR. Molecular-phylogenetic characterization of microbial community imbalances in human inflammatory bowel diseases. Proc Natl Acad Sci [Internet]. 2007 Aug 21;104(34):13780–5. Available from: https://pnas.org/doi/full/10.1073/pnas.0706625104
56. Andoh A, Kuzuoka H, Tsujikawa T, Nakamura S, Hirai F, Suzuki Y, et al. Multicenter analysis of fecal microbiota profiles in Japanese patients with Crohn's disease. J Gastroenterol [Internet]. 2012 Dec 11;47(12):1298–307. Available from: http://link.springer.com/10.1007/s00535-012-0605-0
57. Qin J, Li R, Raes J, Arumugam M, Burgdorf KS, Manichanh C, et al. A human gut microbial gene catalogue established by metagenomic sequencing. Nature [Internet]. 2010 Mar;464(7285):59–65. Available from: http://www.nature.com/articles/nature08821
58. Stojanov S, Berlec A, Štrukelj B. The Influence of Probiotics on the Firmicutes/Bacteroidetes Ratio in the Treatment of Obesity and Inflammatory Bowel disease. Microorganisms [Internet]. 2020 Nov 1;8(11):1715. Available from: https://www.mdpi.com/2076-2607/8/11/1715
59. Khan I, Ullah N, Zha L, Bai Y, Khan A, Zhao T, et al. Alteration of Gut Microbiota in Inflammatory Bowel Disease (IBD): Cause or Consequence? IBD Treatment Targeting the Gut Microbiome. Pathogens [Internet]. 2019 Aug 13;8(3):126. Available from: https://www.mdpi.com/2076-0817/8/3/126
60. PASSOS M do CF, MORAES-FILHO JP. INTESTINAL MICROBIOTA IN DIGESTIVE DISEASES. Arq Gastroenterol [Internet]. 2017 Jul 6;54(3):255–62. Available from: http://www.scielo.br/scielo.php?script=sci_arttext&pid=S0004-28032017000300255&lng=en&tlng=en
61. Becker C, Neurath MF, Wirtz S. The Intestinal Microbiota in Inflammatory Bowel Disease. ILAR J [Internet]. 2015 Aug 31;56(2):192–204. Available from: https://academic.oup.com/ilarjournal/article-lookup/doi/10.1093/ilar/ilv030
62. Im E, Riegler FM, Pothoulakis C, Rhee SH. Elevated lipopolysaccharide in the colon evokes intestinal inflammation, aggravated in immune modulator-impaired mice. Am J Physiol Liver Physiol [Internet]. 2012 Aug 15;303(4):G490–7. Available from: https://www.physiology.org/doi/10.1152/ajpgi.00120.2012
63. Selvamani S, Mehta V, Ali El Enshasy H, Thevarajoo S, El Adawi H, Zeini I, et al. Efficacy of Probiotics-Based Interventions as Therapy for Inflammatory Bowel Disease: A Recent Update. Saudi J Biol Sci [Internet]. 2022 May;29(5):3546–67. Available from: https://linkinghub.elsevier.com/retrieve/pii/S1319562X22001206
64. Quaranta G, Guarnaccia A, Fancello G, Agrillo C, Iannarelli F, Sanguinetti M, et al. Fecal Microbiota Transplantation and Other Gut Microbiota Manipulation Strategies. Microorganisms [Internet]. 2022 Dec 7;10(12):2424. Available from: https://www.mdpi.com/2076-2607/10/12/2424
65. Paramsothy S, Kamm MA, Kaakoush NO, Walsh AJ, van den Bogaerde J, Samuel D, et al. Multidonor intensive faecal microbiota transplantation for active ulcerative colitis: a randomised placebo-controlled trial. Lancet [Internet]. 2017 Mar;389(10075):1218–28. Available from: https://linkinghub.elsevier.com/retrieve/pii/S0140673617301824
66. Santino A, Scarano A, De Santis S, De Benedictis M, Giovinazzo G, Chieppa M. Gut Microbiota Modulation and Anti-Inflammatory Properties of Dietary Polyphenols in IBD: New and Consolidated Perspectives. Curr Pharm Des [Internet]. 2017 Jun 20;23(16). Available from: http://www.eurekaselect.com/149866/article
67. Cundra L, Saadeh M, Vallabhaneni M, Houston K, D'Souza S, Johnson DA. Dietary Modulation of the Gut Microbiome in Inflammatory Bowel Disease. Recent Prog Nutr [Internet]. 2022 Apr 28;2(3):1–1. Available from: https://lidsen.com/journals/rpn/rpn-02-03-019
68. Vancamelbeke M, Vermeire S. The intestinal barrier: a fundamental role in health and disease. Expert Rev Gastroenterol Hepatol [Internet]. 2017 Sep 2;11(9):821–34. Available from: https://www.tandfonline.com/doi/full/10.1080/17474124.2017.1343143
69. Vindigni SM, Zisman TL, Suskind DL, Damman CJ. The intestinal microbiome, barrier function, and immune system in inflammatory bowel disease: a tripartite pathophysiological circuit with implications

for new therapeutic directions. Therap Adv Gastroenterol [Internet]. 2016 Jul 22;9(4):606–25. Available from: http://journals.sagepub.com/doi/10.1177/1756283X16644242

70. Kim YS, Ho SB. Intestinal Goblet Cells and Mucins in Health and Disease: Recent Insights and Progress. Curr Gastroenterol Rep [Internet]. 2010 Oct 13;12(5):319–30. Available from: http://link.springer.com/10.1007/s11894-010-0131-2
71. Chelakkot C, Ghim J, Ryu SH. Mechanisms regulating intestinal barrier integrity and its pathological implications. Exp Mol Med [Internet]. 2018 Aug 16;50(8):1–9. Available from: https://www.nature.com/articles/s12276-018-0126-x
72. Tornavaca O, Chia M, Dufton N, Almagro LO, Conway DE, Randi AM, et al. ZO-1 controls endothelial adherens junctions, cell–cell tension, angiogenesis, and barrier formation. J Cell Biol [Internet]. 2015 Mar 16;208(6):821–38. Available from: https://rupress.org/jcb/article/208/6/821/38104/ZO1-controls-endothelial-adherens-junctions
73. Neurath MF. Cytokines in inflammatory bowel disease. Nat Rev Immunol [Internet]. 2014 May 22;14(5):329–42. Available from: http://www.nature.com/articles/nri3661
74. Cario E. Innate immune signalling at intestinal mucosal surfaces: a fine line between host protection and destruction. Curr Opin Gastroenterol [Internet]. 2008 Nov;24(6):725–32. Available from: http://journals.lww.com/00001574-200811000-00014
75. Opitz CA, Litzenburger UM, Lutz C, Lanz T V., Tritschler I, Köppel A, et al. Toll-Like Receptor Engagement Enhances the Immunosuppressive Properties of Human Bone Marrow-Derived Mesenchymal Stem Cells by Inducing Indoleamine-2,3-dioxygenase-1 via Interferon-β and Protein Kinase R. Stem Cells [Internet]. 2009 Apr 1;27(4):909–19. Available from: https://academic.oup.com/stmcls/article/27/4/909-919/6402178
76. Huang Y, Chen Z. Inflammatory bowel disease related innate immunity and adaptive immunity. Am J Transl Res. 2016;8(6):2490–7.
77. Palomino DCT, Marti LC. Chemokines and immunity. Einstein (São Paulo) [Internet]. 2015 Sep;13(3):469–73. Available from: http://www.scielo.br/scielo.php?script=sci_arttext&pid=S1679-45082015000300469&lng=en&tlng=en
78. Silva FAR, Rodrigues BL, Ayrizono M de LS, Leal RF. The Immunological Basis of Inflammatory Bowel Disease. Gastroenterol Res Pract [Internet]. 2016;2016:1–11. Available from: https://www.hindawi.com/journals/grp/2016/2097274/
79. Marshall JS, Warrington R, Watson W, Kim HL. An introduction to immunology and immunopathology. Allergy, Asthma Clin Immunol [Internet]. 2018 Sep 12;14(S2):49. Available from: https://aacijournal.biomedcentral.com/articles/10.1186/s13223-018-0278-1
80. Medzhitov R. Recognition of microorganisms and activation of the immune response. Nature [Internet]. 2007 Oct 17;449(7164):819–26. Available from: http://www.nature.com/articles/nature06246
81. Abreu MT. Toll-like receptor signalling in the intestinal epithelium: how bacterial recognition shapes intestinal function. Nat Rev Immunol [Internet]. 2010 Feb;10(2):131–44. Available from: http://www.nature.com/articles/nri2707
82. Andrade AWL, Guerra GCB, de Souza Araújo DF, de Araújo Júnior RF, de Araújo AA, de Carvalho TG, et al. Anti-Inflammatory and Chemopreventive Effects of Bryophyllum pinnatum (Lamarck) Leaf Extract in Experimental Colitis Models in Rodents. Front Pharmacol [Internet]. 2020 Jul 29;11. Available from: https://www.frontiersin.org/article/10.3389/fphar.2020.00998/full
83. Kaiko GE, Horvat JC, Beagley KW, Hansbro PM. Immunological decision-making: how does the immune system decide to mount a helper T-cell response? Immunology [Internet]. 2008 Mar;123(3):326–38. Available from: https://onlinelibrary.wiley.com/doi/10.1111/j.1365-2567.2007.02719.x
84. Thakur A, Mikkelsen H, Jungersen G. Intracellular Pathogens: Host Immunity and Microbial Persistence Strategies. J Immunol Res [Internet]. 2019 Apr 14;2019:1–24. Available from: https://www.hindawi.com/journals/jir/2019/1356540/
85. Kawai T, Akira S. Signaling to NF-κB by Toll-like receptors. Trends Mol Med [Internet]. 2007 Nov;13(11):460–9. Available from: https://linkinghub.elsevier.com/retrieve/pii/S1471491407001840
86. Hayden MS, Ghosh S. Signaling to NF-κB. Genes Dev [Internet]. 2004 Sep 15;18(18):2195–224. Available from: http://genesdev.cshlp.org/lookup/doi/10.1101/gad.1228704
87. Baumgart DC, Sandborn WJ. Inflammatory bowel disease: clinical aspects and established and evolving therapies. Lancet [Internet]. 2007 May;369(9573):1641–57. Available from: https://linkinghub.elsevier.com/retrieve/pii/S014067360760751X
88. Neurath MF. Current and emerging therapeutic targets for IBD. Nat Rev Gastroenterol Hepatol [Internet]. 2017 May 1;14(5):269–78. Available from: http://www.nature.com/articles/nrgastro.2016.208
89. Cai Z, Wang S, Li J. Treatment of Inflammatory Bowel Disease: A Comprehensive Review. Front Med

[Internet]. 2021 Dec 20;8. Available from: https://www.frontiersin.org/articles/10.3389/fmed.2021.765474/full
90. Iacucci M, de Silva S, Ghosh S. Mesalazine in Inflammatory Bowel Disease: A Trendy Topic Once Again? Can J Gastroenterol [Internet]. 2010;24(2):127–33. Available from: http://www.hindawi.com/journals/cjgh/2010/586092/
91. Bruscoli S, Febo M, Riccardi C, Migliorati G. Glucocorticoid Therapy in Inflammatory Bowel Disease: Mechanisms and Clinical Practice. Front Immunol [Internet]. 2021 Jun 3;12. Available from: https://www.frontiersin.org/articles/10.3389/fimmu.2021.691480/full
92. Adamina M, Bonovas S, Raine T, Spinelli A, Warusavitarne J, Armuzzi A, et al. ECCO Guidelines on Therapeutics in Crohn's Disease: Surgical Treatment. J Crohn's Colitis [Internet]. 2020 Feb 10;14(2):155–68. Available from: https://academic.oup.com/ecco-jcc/article/14/2/155/5631809
93. Rubin DT, Ananthakrishnan AN, Siegel CA, Sauer BG, Long MD. ACG Clinical Guideline: Ulcerative Colitis in Adults. Am J Gastroenterol [Internet]. 2019 Mar 27;114(3):384–413. Available from: https://journals.lww.com/00000434-201903000-00010
94. Lichtenstein GR, Loftus E V, Isaacs KL, Regueiro MD, Gerson LB, Sands BE. ACG Clinical Guideline: Management of Crohn's Disease in Adults. Am J Gastroenterol [Internet]. 2018 Apr;113(4):481–517. Available from: https://journals.lww.com/00000434-201804000-00010
95. H. Al Mamari H. Phenolic Compounds: Classification, Chemistry, and Updated Techniques of Analysis and Synthesis. In 2022. Available from: https://www.intechopen.com/chapters/77604
96. Machado AP da F, Geraldi MV, do Nascimento R de P, Moya AMTM, Vezza T, Diez-Echave P, et al. Polyphenols from food by-products: An alternative or complementary therapy to IBD conventional treatments. Food Res Int [Internet]. 2021 Feb;140:110018. Available from: https://linkinghub.elsevier.com/retrieve/pii/S0963996920310437
97. Kumar S, Pandey AK. Chemistry and Biological Activities of Flavonoids: An Overview. Sci World J [Internet]. 2013;2013:1–16. Available from: http://www.hindawi.com/journals/tswj/2013/162750/
98. Farzaei M, Rahimi R, Abdollahi M. The Role of Dietary Polyphenols in the Management of Inflammatory Bowel Disease. Curr Pharm Biotechnol [Internet]. 2015 Feb 2;16(3):196–210. Available from: http://www.eurekaselect.com/openurl/content.php?genre=article&issn=1389-2010&volume=16&issue=3&spage=196
99. Kaulmann A, Bohn T. Bioactivity of Polyphenols: Preventive and Adjuvant Strategies toward Reducing Inflammatory Bowel Diseases—Promises, Perspectives, and Pitfalls. Oxid Med Cell Longev [Internet]. 2016;2016:1–29. Available from: http://www.hindawi.com/journals/omcl/2016/9346470/
100. Lyu Y-L, Zhou H-F, Yang J, Wang F-X, Sun F, Li J-Y. Biological Activities Underlying the Therapeutic Effect of Quercetin on Inflammatory Bowel Disease. Subramanian VS, editor. Mediators Inflamm [Internet]. 2022 Jul 23;2022:1–8. Available from: https://www.hindawi.com/journals/mi/2022/5665778/
101. Lubbad A, Oriowo MA, Khan I. Curcumin attenuates inflammation through inhibition of TLR-4 receptor in experimental colitis. Mol Cell Biochem [Internet]. 2009 Feb 11;322(1–2):127–35. Available from: http://link.springer.com/10.1007/s11010-008-9949-4
102. Billerey-Larmonier C, Uno JK, Larmonier N, Midura AJ, Timmermann B, Ghishan FK, et al. Protective effects of dietary curcumin in mouse model of chemically induced colitis are strain dependent. Inflamm Bowel Dis [Internet]. 2008 Jun;14(6):780–93. Available from: https://academic.oup.com/ibdjournal/article/14/6/780-793/4654533
103. Singla V, Pratap Mouli V, Garg SK, Rai T, Choudhury BN, Verma P, et al. Induction with NCB-02 (curcumin) enema for mild-to-moderate distal ulcerative colitis — A randomized, placebo-controlled, pilot study. J Crohn's Colitis [Internet]. 2014 Mar;8(3):208–14. Available from: https://academic.oup.com/ecco-jcc/article-lookup/doi/10.1016/j.crohns.2013.08.006
104. Lang A, Salomon N, Wu JCY, Kopylov U, Lahat A, Har-Noy O, et al. Curcumin in Combination With Mesalamine Induces Remission in Patients With Mild-to-Moderate Ulcerative Colitis in a Randomized Controlled Trial. Clin Gastroenterol Hepatol [Internet]. 2015 Aug;13(8):1444-1449.e1. Available from: https://linkinghub.elsevier.com/retrieve/pii/S1542356515001585
105. Holt PR, Katz S, Kirshoff R. Curcumin Therapy in Inflammatory Bowel Disease: A Pilot Study. Dig Dis Sci [Internet]. 2005 Nov;50(11):2191–3. Available from: http://link.springer.com/10.1007/s10620-005-3032-8
106. Cui X, Jin Y, Hofseth AB, Pena E, Habiger J, Chumanevich A, et al. Resveratrol Suppresses Colitis and Colon Cancer Associated with Colitis. Cancer Prev Res [Internet]. 2010 Apr 1;3(4):549–59. Available from: https://aacrjournals.org/cancerpreventionresearch/article/3/4/549/48763/Resveratrol-Suppresses-Colitis-and-Colon-Cancer
107. Alrafas HR, Busbee PB, Nagarkatti M, Nagarkatti PS. Resveratrol modulates the gut microbiota to prevent murine colitis development through induction of Tregs and suppression of Th17 cells. J Leukoc Biol [Internet]. 2019 Jul 25;106(2):467–80. Available from:

https://academic.oup.com/jleukbio/article/106/2/467/6935814
108. Zhang L, Xue H, Zhao G, Qiao C, Sun X, Pang C, et al. Curcumin and resveratrol suppress dextran sulfate sodium-induced colitis in mice. Mol Med Rep [Internet]. 2019 Feb 20; Available from: http://www.spandidos-publications.com/10.3892/mmr.2019.9974
109. Glabska D, Guzek D, Grudzińska D, Lech G. Influence of dietary isoflavone intake on gastrointestinal symptoms in ulcerative colitis individuals in remission. World J Gastroenterol [Internet]. 2017;23(29):5356. Available from: http://www.wjgnet.com/1007-9327/full/v23/i29/5356.htm
110. Skolmowska D, Głąbska D, Guzek D, Lech G. Association between Dietary Isoflavone Intake and Ulcerative Colitis Symptoms in Polish Caucasian Individuals. Nutrients [Internet]. 2019 Aug 17;11(8):1936. Available from: https://www.mdpi.com/2072-6643/11/8/1936
111. Ko S-J, Bu Y, Bae J, Bang Y, Kim J, Lee H, et al. Protective Effect of Laminaria japonica with Probiotics on Murine Colitis. Mediators Inflamm [Internet]. 2014;2014:1–10. Available from: http://www.hindawi.com/journals/mi/2014/417814/
112. Shimizu M. Multifunctions of dietary polyphenols in the regulation of intestinal inflammation. J Food Drug Anal [Internet]. 2017 Jan;25(1):93–9. Available from: https://linkinghub.elsevier.com/retrieve/pii/S1021949816301958
113. Vezza T, Algieri F, Rodríguez-Nogales A, Garrido-Mesa J, Utrilla MP, Talhaoui N, et al. Immunomodulatory properties of Olea europaea leaf extract in intestinal inflammation. Mol Nutr Food Res [Internet]. 2017 Oct;61(10):1601066. Available from: https://onlinelibrary.wiley.com/doi/10.1002/mnfr.201601066
114. Zhang P, Jiao H, Wang C, Lin Y, You S. Chlorogenic Acid Ameliorates Colitis and Alters Colonic Microbiota in a Mouse Model of Dextran Sulfate Sodium-Induced Colitis. Front Physiol [Internet]. 2019 Mar 27;10. Available from: https://www.frontiersin.org/article/10.3389/fphys.2019.00325/full
115. Thakur L, Ghodasra U, Patel N, Dabhi M. Novel approaches for stability improvement in natural medicines. Pharmacogn Rev [Internet]. 2011;5(9):48. Available from: http://www.phcogrev.com/article/2011/5/9/1041030973-784779099
116. Krupkova O, Ferguson SJ, Wuertz-Kozak K. Stability of (−)-epigallocatechin gallate and its activity in liquid formulations and delivery systems. J Nutr Biochem [Internet]. 2016 Nov;37:1–12. Available from: https://linkinghub.elsevier.com/retrieve/pii/S0955286316000243
117. Garavand F, Jalai-Jivan M, Assadpour E, Jafari SM. Encapsulation of phenolic compounds within nano/microemulsion systems: A review. Food Chem [Internet]. 2021 Dec;364:130376. Available from: https://linkinghub.elsevier.com/retrieve/pii/S0308814621013820
118. Tang D-W, Yu S-H, Ho Y-C, Huang B-Q, Tsai G-J, Hsieh H-Y, et al. Characterization of tea catechins-loaded nanoparticles prepared from chitosan and an edible polypeptide. Food Hydrocoll [Internet]. 2013 Jan;30(1):33–41. Available from: https://linkinghub.elsevier.com/retrieve/pii/S0268005X12001002
119. Rakotondrabe TF, Fan M-X, Muema FW, Guo M-Q. Modulating Inflammation-Mediated Diseases via Natural Phenolic Compounds Loaded in Nanocarrier Systems. Pharmaceutics [Internet]. 2023 Feb 19;15(2):699. Available from: https://www.mdpi.com/1999-4923/15/2/699
120. Yang C, Merlin D. Nanoparticle-Mediated Drug Delivery Systems For The Treatment Of IBD: Current Perspectives. Int J Nanomedicine [Internet]. 2019 Nov;Volume 14:8875–89. Available from: https://www.dovepress.com/nanoparticle-mediated-drug-delivery-systems-for-the-treatment-of-ibd-c-peer-reviewed-article-IJN
121. Zhang M, Merlin D. Nanoparticle-Based Oral Drug Delivery Systems Targeting the Colon for Treatment of Ulcerative Colitis. Inflamm Bowel Dis [Internet]. 2018 Jun 8;24(7):1401–15. Available from: https://academic.oup.com/ibdjournal/article/24/7/1401/4999330
122. Lamprecht A, Yamamoto H, Takeuchi H, Kawashima Y. Nanoparticles Enhance Therapeutic Efficiency by Selectively Increased Local Drug Dose in Experimental Colitis in Rats. J Pharmacol Exp Ther [Internet]. 2005 Oct;315(1):196–202. Available from: http://jpet.aspetjournals.org/lookup/doi/10.1124/jpet.105.088146
123. El-Maghawry E, Tadros MI, El-Kheshen SA, Abd-Elbary A. Eudragit®-S100 Coated PLGA Nanoparticles for Colon Targeting of Etoricoxib: Optimization and Pharmacokinetic Assessments in Healthy Human Volunteers. Int J Nanomedicine [Internet]. 2020 Jun;Volume 15:3965–80. Available from: https://www.dovepress.com/eudragitreg-s100-coated-plga-nanoparticles-for-colon-targeting-of-etor-peer-reviewed-article-IJN
124. Li D, Yang M, Xu H, Zhu M, Zhang Y, Tian C, et al. Nanoparticles for oral delivery: targeted therapy for inflammatory bowel disease. J Mater Chem B [Internet]. 2022;10(31):5853–72. Available from: http://xlink.rsc.org/?DOI=D2TB01190E
125. Naeem M, Bae J, A. Oshi M, Kim M-S, Moon HR, Lee BL, et al. Colon-targeted delivery of cyclosporine A using dual-functional Eudragit® FS30D/PLGA nanoparticles ameliorates murine experimental colitis. Int J Nanomedicine [Internet]. 2018 Feb;Volume 13:1225–40. Available from:

https://www.dovepress.com/colon-targeted-delivery-of-cyclosporine-a-using-dual-functional-eudrag-peer-reviewed-article-IJN

126. Wang Q-S, Wang G-F, Zhou J, Gao L-N, Cui Y-L. Colon targeted oral drug delivery system based on alginate-chitosan microspheres loaded with icariin in the treatment of ulcerative colitis. Int J Pharm [Internet]. 2016 Dec;515(1–2):176–85. Available from: https://linkinghub.elsevier.com/retrieve/pii/S037851731630936X
127. Brusini R, Varna M, Couvreur P. Advanced nanomedicines for the treatment of inflammatory diseases. Adv Drug Deliv Rev [Internet]. 2020;157:161–78. Available from: https://linkinghub.elsevier.com/retrieve/pii/S0169409X20300946
128. Youshia J, Lamprecht A. Size-dependent nanoparticulate drug delivery in inflammatory bowel diseases. Expert Opin Drug Deliv [Internet]. 2016 Feb 4;13(2):281–94. Available from: http://www.tandfonline.com/doi/full/10.1517/17425247.2016.1114604
129. Yang B, Dong Y, Wang F, Zhang Y. Nanoformulations to Enhance the Bioavailability and Physiological Functions of Polyphenols. Molecules [Internet]. 2020 Oct 10;25(20):4613. Available from: https://www.mdpi.com/1420-3049/25/20/4613
130. Borges A, de Freitas V, Mateus N, Fernandes I, Oliveira J. Solid Lipid Nanoparticles as Carriers of Natural Phenolic Compounds. Antioxidants [Internet]. 2020 Oct 15;9(10):998. Available from: https://www.mdpi.com/2076-3921/9/10/998
131. Raj PM, Raj R, Kaul A, Mishra AK, Ram A. Biodistribution and targeting potential assessment of mucoadhesive chitosan nanoparticles designed for ulcerative colitis via scintigraphy. RSC Adv [Internet]. 2018;8(37):20809–21. Available from: http://xlink.rsc.org/?DOI=C8RA01898G
132. Zhang C, Wang X, Xiao M, Ma J, Qu Y, Zou L, et al. Nano-in-micro alginate/chitosan hydrogel via electrospray technology for orally curcumin delivery to effectively alleviate ulcerative colitis. Mater Des [Internet]. 2022 Sep;221:110894. Available from: https://linkinghub.elsevier.com/retrieve/pii/S0264127522005160
133. Shen W, Wang Q, Shen Y, Gao X, Li L, Yan Y, et al. Green Tea Catechin Dramatically Promotes RNAi Mediated by Low-Molecular-Weight Polymers. ACS Cent Sci [Internet]. 2018 Oct 24;4(10):1326–33. Available from: https://pubs.acs.org/doi/10.1021/acscentsci.8b00363
134. Gou S, Chen Q, Liu Y, Zeng L, Song H, Xu Z, et al. Green Fabrication of Ovalbumin Nanoparticles as Natural Polyphenol Carriers for Ulcerative Colitis Therapy. ACS Sustain Chem Eng [Internet]. 2018 Oct 17;6(10):12658–67. Available from: https://pubs.acs.org/doi/10.1021/acssuschemeng.8b01613
135. Lv F, Zhang Y, Peng Q, Zhao X, Hu D, Wen J, et al. Apigenin-Mn(II) loaded hyaluronic acid nanoparticles for ulcerative colitis therapy in mice. Front Chem [Internet]. 2022 Jul 22;10. Available from: https://www.frontiersin.org/articles/10.3389/fchem.2022.969962/full
136. Siu F, Ye S, Lin H, Li S. Galactosylated PLGA nanoparticles for the oral delivery of resveratrol: enhanced bioavailability and in vitro anti-inflammatory activity. Int J Nanomedicine [Internet]. 2018 Jul;Volume 13:4133–44. Available from: https://www.dovepress.com/galactosylated-plga-nanoparticles-for-the-oral-delivery-of-resveratrol-peer-reviewed-article-IJN
137. Naserifar M, Hosseinzadeh H, Abnous K, Mohammadi M, Taghdisi SM, Ramezani M, et al. Oral delivery of folate-targeted resveratrol-loaded nanoparticles for inflammatory bowel disease therapy in rats. Life Sci [Internet]. 2020 Dec;262:118555. Available from: https://linkinghub.elsevier.com/retrieve/pii/S0024320520313084
138. Kaplan NM. The deadly quartet. Upper-body obesity, glucose intolerance, hypertriglyceridemia, and hypertension. Arch Intern Med [Internet]. 1989 Jul 1;149(7):1514–20. Available from: http://archinte.ama-assn.org/cgi/doi/10.1001/archinte.149.7.1514
139. Vasques ACJ, Rosado LEFPL, Alfenas R de CG, Geloneze B. Análise crítica do uso dos índices do Homeostasis Model Assessment (HOMA) na avaliação da resistência à insulina e capacidade funcional das células-beta pancreáticas. Arq Bras Endocrinol Metabol [Internet]. 2008 Feb;52(1):32–9. Available from: http://www.scielo.br/scielo.php?script=sci_arttext&pid=S0004-27302008000100006&lng=pt&tlng=pt
140. Matthews DR, Hosker JP, Rudenski AS, Naylor BA, Treacher DF, Turner RC. Homeostasis model assessment: insulin resistance and ?-cell function from fasting plasma glucose and insulin concentrations in man. Diabetologia [Internet]. 1985 Jul;28(7):412–9. Available from: http://link.springer.com/10.1007/BF00280883
141. Alberti KGMM, Eckel RH, Grundy SM, Zimmet PZ, Cleeman JI, Donato KA, et al. Harmonizing the Metabolic Syndrome. Circulation [Internet]. 2009 Oct 20;120(16):1640–5. Available from: https://www.ahajournals.org/doi/10.1161/CIRCULATIONAHA.109.192644
142. Roberts CK, Hevener AL, Barnard RJ. Metabolic Syndrome and Insulin Resistance: Underlying Causes and Modification by Exercise Training. In: Comprehensive Physiology [Internet]. Wiley; 2013. p. 1–58. Available from: https://onlinelibrary.wiley.com/doi/10.1002/cphy.c110062

143. Fahed G, Aoun L, Bou Zerdan M, Allam S, Bou Zerdan M, Bouferraa Y, et al. Metabolic Syndrome: Updates on Pathophysiology and Management in 2021. Int J Mol Sci [Internet]. 2022 Jan 12;23(2):786. Available from: https://www.mdpi.com/1422-0067/23/2/786
144. Carson C, Lawson HA. Epigenetics of metabolic syndrome. Physiol Genomics [Internet]. 2018 Nov 1;50(11):947–55. Available from: https://www.physiology.org/doi/10.1152/physiolgenomics.00072.2018
145. Huang X, Liu G, Guo J, Su Z. The PI3K/AKT pathway in obesity and type 2 diabetes. Int J Biol Sci [Internet]. 2018;14(11):1483–96. Available from: http://www.ijbs.com/v14p1483.htm
146. Wang T, Wang J, Hu X, Huang X, Chen G-X. Current understanding of glucose transporter 4 expression and functional mechanisms. World J Biol Chem [Internet]. 2020 Nov 27;11(3):76–98. Available from: https://www.wjgnet.com/1949-8454/full/v11/i3/76.htm
147. Xu J, Zou M-H. Molecular Insights and Therapeutic Targets for Diabetic Endothelial Dysfunction. Circulation [Internet]. 2009 Sep 29;120(13):1266–86. Available from: https://www.ahajournals.org/doi/10.1161/CIRCULATIONAHA.108.835223
148. Muniyappa R, Yavuz S. Metabolic actions of angiotensin II and insulin: A microvascular endothelial balancing act. Mol Cell Endocrinol [Internet]. 2013 Sep;378(1–2):59–69. Available from: https://linkinghub.elsevier.com/retrieve/pii/S0303720712003115
149. Long YC. AMP-activated protein kinase signaling in metabolic regulation. J Clin Invest [Internet]. 2006 Jul 3;116(7):1776–83. Available from: http://www.jci.org/cgi/doi/10.1172/JCI29044
150. Towler MC, Hardie DG. AMP-Activated Protein Kinase in Metabolic Control and Insulin Signaling. Circ Res [Internet]. 2007 Feb 16;100(3):328–41. Available from: https://www.ahajournals.org/doi/10.1161/01.RES.0000256090.42690.05
151. Balistreri CR, Caruso C, Candore G. The Role of Adipose Tissue and Adipokines in Obesity-Related Inflammatory Diseases. Mediators Inflamm [Internet]. 2010;2010:1–19. Available from: http://www.hindawi.com/journals/mi/2010/802078/
152. Chait A, den Hartigh LJ. Adipose Tissue Distribution, Inflammation and Its Metabolic Consequences, Including Diabetes and Cardiovascular Disease. Front Cardiovasc Med [Internet]. 2020 Feb 25;7. Available from: https://www.frontiersin.org/article/10.3389/fcvm.2020.00022/full
153. Martelli D, Brooks VL. Leptin Increases: Physiological Roles in the Control of Sympathetic Nerve Activity, Energy Balance, and the Hypothalamic–Pituitary–Thyroid Axis. Int J Mol Sci [Internet]. 2023 Jan 31;24(3):2684. Available from: https://www.mdpi.com/1422-0067/24/3/2684
154. Münzberg H, Morrison CD. Structure, production and signaling of leptin. Metabolism [Internet]. 2015 Jan;64(1):13–23. Available from: https://linkinghub.elsevier.com/retrieve/pii/S0026049514002923
155. Obradovic M, Sudar-Milovanovic E, Soskic S, Essack M, Arya S, Stewart AJ, et al. Leptin and Obesity: Role and Clinical Implication. Front Endocrinol (Lausanne) [Internet]. 2021 May 18;12. Available from: https://www.frontiersin.org/articles/10.3389/fendo.2021.585887/full
156. Manoria PC, Chopra HK, Parashar SK, Dutta AL, Pinto B, Mullasari A, et al. The nuances of atherogenic dyslipidemia in diabetes: Focus on triglycerides and current management strategies. Indian Heart J [Internet]. 2013 Dec;65(6):683–90. Available from: https://linkinghub.elsevier.com/retrieve/pii/S0019483213003349
157. Tyagi S, Sharma S, Gupta P, Saini A, Kaushal C. The peroxisome proliferator-activated receptor: A family of nuclear receptors role in various diseases. J Adv Pharm Technol Res [Internet]. 2011;2(4):236. Available from: http://www.japtr.org/text.asp?2011/2/4/236/90879
158. Wang Y-X. PPARs: diverse regulators in energy metabolism and metabolic diseases. Cell Res [Internet]. 2010 Feb 26;20(2):124–37. Available from: http://www.nature.com/articles/cr201013
159. Kumari A, Kristensen KK, Ploug M, Winther A-ML. The Importance of Lipoprotein Lipase Regulation in Atherosclerosis. Biomedicines [Internet]. 2021 Jul 6;9(7):782. Available from: https://www.mdpi.com/2227-9059/9/7/782
160. Tangvarasittichai S. Oxidative stress, insulin resistance, dyslipidemia and type 2 diabetes mellitus. World J Diabetes [Internet]. 2015;6(3):456. Available from: http://www.wjgnet.com/1948-9358/full/v6/i3/456.htm
161. Gallo G, Volpe M, Savoia C. Endothelial Dysfunction in Hypertension: Current Concepts and Clinical Implications. Front Med [Internet]. 2022 Jan 20;8. Available from: https://www.frontiersin.org/articles/10.3389/fmed.2021.798958/full
162. Kissebah AH, Sonnenberg GE, Myklebust J, Goldstein M, Broman K, James RG, et al. Quantitative trait loci on chromosomes 3 and 17 influence phenotypes of the metabolic syndrome. Proc Natl Acad Sci [Internet]. 2000 Dec 19;97(26):14478–83. Available from: https://pnas.org/doi/full/10.1073/pnas.97.26.14478
163. McCarthy JJ, Meyer J, Moliterno DJ, Newby LK, Rogers WJ, Topol EJ. Evidence for substantial effect modification by gender in a large-scale genetic association study of the metabolic syndrome among

coronary heart disease patients. Hum Genet [Internet]. 2003 Dec 1;114(1):87–98. Available from: http://link.springer.com/10.1007/s00439-003-1026-1

164. Gotoda T. Genetic susceptibility to metabolic syndrome. Nippon rinsho Japanese J Clin Med. 2004;62(6):1037–44.
165. Dobrowolski P, Prejbisz A, Kuryłowicz A, Baska A, Burchardt P, Chlebus K, et al. Metabolic syndrome – a new definition and management guidelines A joint position paper by the Polish Society of Hypertension, Polish Society for the Treatment of Obesity, Polish Lipid Association, Polish Association for Study of Liver, Polish Society of F. Arch Med Sci [Internet]. 2022 Aug 30;18(5):1133–56. Available from: https://www.archivesofmedicalscience.com/Metabolic-syndrome-a-new-definition-and-management-guidelines-nA-joint-position-paper,152921,0,2.html
166. Tak YJ, Lee SY. Anti-Obesity Drugs: Long-Term Efficacy and Safety: An Updated Review. World J Mens Health [Internet]. 2021;39(2):208. Available from: https://wjmh.org/DOIx.php?id=10.5534/wjmh.200010
167. Mopuri R, Islam MS. Medicinal plants and phytochemicals with anti-obesogenic potentials: A review. Biomed Pharmacother [Internet]. 2017 May;89:1442–52. Available from: https://linkinghub.elsevier.com/retrieve/pii/S0753332216328177
168. Sandoval V, Sanz-Lamora H, Arias G, Marrero PF, Haro D, Relat J. Metabolic Impact of Flavonoids Consumption in Obesity: From Central to Peripheral. Nutrients [Internet]. 2020 Aug 10;12(8):2393. Available from: https://www.mdpi.com/2072-6643/12/8/2393
169. Williamson G, Sheedy K. Effects of Polyphenols on Insulin Resistance. Nutrients [Internet]. 2020 Oct 14;12(10):3135. Available from: https://www.mdpi.com/2072-6643/12/10/3135
170. Zhang S, Xu M, Zhang W, Liu C, Chen S. Natural Polyphenols in Metabolic Syndrome: Protective Mechanisms and Clinical Applications. Int J Mol Sci [Internet]. 2021 Jun 6;22(11):6110. Available from: https://www.mdpi.com/1422-0067/22/11/6110
171. Burgess TA. Improving Glucose Metabolism With Resveratrol in a Swine Model of Metabolic Syndrome Through Alteration of Signaling Pathways in the Liver and Skeletal Muscle. Arch Surg [Internet]. 2011 May 1;146(5):556. Available from: http://archsurg.jamanetwork.com/article.aspx?doi=10.1001/archsurg.2011.100
172. Jang H-J, Ridgeway SD, Kim J. Effects of the green tea polyphenol epigallocatechin-3-gallate on high-fat diet-induced insulin resistance and endothelial dysfunction. Am J Physiol Metab [Internet]. 2013 Dec 15;305(12):E1444–51. Available from: https://www.physiology.org/doi/10.1152/ajpendo.00434.2013
173. Longo M, Zatterale F, Naderi J, Parrillo L, Formisano P, Raciti GA, et al. Adipose Tissue Dysfunction as Determinant of Obesity-Associated Metabolic Complications. Int J Mol Sci [Internet]. 2019 May 13;20(9):2358. Available from: https://www.mdpi.com/1422-0067/20/9/2358
174. Costa C dos S, Rohden F, Hammes TO, Margis R, Bortolotto JW, Padoin AV, et al. Resveratrol Upregulated SIRT1, FOXO1, and Adiponectin and Downregulated PPARγ1–3 mRNA Expression in Human Visceral Adipocytes. Obes Surg [Internet]. 2011 Mar 26;21(3):356–61. Available from: http://link.springer.com/10.1007/s11695-010-0251-7
175. YUN-SOO S, OK-HWA K, SUNG-BAE K, SU-HYUN M, DA-HYE K, DA-WUN Y, et al. Quercetin prevents adipogenesis by regulation of transcriptional factors and lipases in OP9 cells. Int J Mol Med [Internet]. 2015 Jun;35(6):1779–85. Available from: https://www.spandidos-publications.com/10.3892/ijmm.2015.2185
176. Rivera L, Morón R, Sánchez M, Zarzuelo A, Galisteo M. Quercetin Ameliorates Metabolic Syndrome and Improves the Inflammatory Status in Obese Zucker Rats. Obesity [Internet]. 2008 Sep;16(9):2081–7. Available from: http://doi.wiley.com/10.1038/oby.2008.315
177. Nekohashi M, Ogawa M, Ogihara T, Nakazawa K, Kato H, Misaka T, et al. Luteolin and Quercetin Affect the Cholesterol Absorption Mediated by Epithelial Cholesterol Transporter Niemann–Pick C1-Like 1 in Caco-2 Cells and Rats. Beh C, editor. PLoS One [Internet]. 2014 May 23;9(5):e97901. Available from: https://dx.plos.org/10.1371/journal.pone.0097901
178. Feng J, Yang J, Chang Y, Qiao L, Dang H, Luo K, et al. Caffeine-free hawk tea lowers cholesterol by reducing free cholesterol uptake and the production of very-low-density lipoprotein. Commun Biol [Internet]. 2019 May 8;2(1):173. Available from: https://www.nature.com/articles/s42003-019-0396-4
179. Yashiro T, Nanmoku M, Shimizu M, Inoue J, Sato R. Resveratrol increases the expression and activity of the low density lipoprotein receptor in hepatocytes by the proteolytic activation of the sterol regulatory element-binding proteins. Atherosclerosis [Internet]. 2012 Feb;220(2):369–74. Available from: https://linkinghub.elsevier.com/retrieve/pii/S0021915011010756
180. Akbari M, Tamtaji OR, Lankarani KB, Tabrizi R, Dadgostar E, Haghighat N, et al. The effects of resveratrol on lipid profiles and liver enzymes in patients with metabolic syndrome and related disorders: a systematic review and meta-analysis of randomized controlled trials. Lipids Health Dis [Internet]. 2020 Dec 17;19(1):25. Available from: https://lipidworld.biomedcentral.com/articles/10.1186/s12944-020-

1198-x
181. Ruiz-Malagón AJ, Rodríguez-Sojo MJ, Hidalgo-García L, Molina-Tijeras JA, García F, Pischel I, et al. The Antioxidant Activity of Thymus serpyllum Extract Protects against the Inflammatory State and Modulates Gut Dysbiosis in Diet-Induced Obesity in Mice. Antioxidants [Internet]. 2022 May 28;11(6):1073. Available from: https://www.mdpi.com/2076-3921/11/6/1073
182. Li Y, Rahman SU, Huang Y, Zhang Y, Ming P, Zhu L, et al. Green tea polyphenols decrease weight gain, ameliorate alteration of gut microbiota, and mitigate intestinal inflammation in canines with high-fat-diet-induced obesity. J Nutr Biochem [Internet]. 2020 Apr;78:108324. Available from: https://linkinghub.elsevier.com/retrieve/pii/S0955286319302748
183. Feldman F, Koudoufio M, Desjardins Y, Spahis S, Delvin E, Levy E. Efficacy of Polyphenols in the Management of Dyslipidemia: A Focus on Clinical Studies. Nutrients [Internet]. 2021 Feb 19;13(2):672. Available from: https://www.mdpi.com/2072-6643/13/2/672
184. Huang L-H, Liu C-Y, Wang L-Y, Huang C-J, Hsu C-H. Effects of green tea extract on overweight and obese women with high levels of low density-lipoprotein-cholesterol (LDL-C): a randomised, double-blind, and cross-over placebo-controlled clinical trial. BMC Complement Altern Med [Internet]. 2018 Dec 6;18(1):294. Available from: https://bmccomplementalternmed.biomedcentral.com/articles/10.1186/s12906-018-2355-x
185. Wang X, Qi Y, Zheng H. Dietary Polyphenol, Gut Microbiota, and Health Benefits. Antioxidants [Internet]. 2022 Jun 20;11(6):1212. Available from: https://www.mdpi.com/2076-3921/11/6/1212
186. Ma G, Chen Y. Polyphenol supplementation benefits human health via gut microbiota: A systematic review via meta-analysis. J Funct Foods [Internet]. 2020 Mar;66:103829. Available from: https://linkinghub.elsevier.com/retrieve/pii/S1756464620300530
187. Sánchez-Tapia M, Aguilar-López M, Pérez-Cruz C, Pichardo-Ontiveros E, Wang M, Donovan SM, et al. Nopal (Opuntia ficus indica) protects from metabolic endotoxemia by modifying gut microbiota in obese rats fed high fat/sucrose diet. Sci Rep [Internet]. 2017 Jul 5;7(1):4716. Available from: https://www.nature.com/articles/s41598-017-05096-4
188. Tongerlo E, Trouwborst G, Hogewoning SW, Ieperen W, Dieleman JA, Marcelis LFM. Crassulacean acid metabolism species differ in the contribution of C 3 and C 4 carboxylation to end of day CO 2 fixation. Physiol Plant [Internet]. 2021 May 22;172(1):134–45. Available from: https://onlinelibrary.wiley.com/doi/10.1111/ppl.13312
189. da Silva ECS, Bernardo Guerra GC, de Araújo ERD, Schlamb J, da Silva VC, de Aragão Tavares E, et al. Phenolic-rich extract of Nopalea cochenillifera attenuates gastric lesions induced in experimental models through inhibiting oxidative stress, modulating inflammatory markers and a cytoprotective effect. Food Funct [Internet]. 2023;14(7):3242–58. Available from: http://xlink.rsc.org/?DOI=D2FO03735A
190. Silva RR, Sampaio EVSB. Palmas forrageiras Opuntia fícus-indica e Nopalea cochenillifera: sistemas de produção e usos | Opuntia fícus-indica and Nopalea cochenillifera cacti:production systems and uses. Rev Geama [Internet]. 2016;1(2):151–161. Available from: https://journals.ufrpe.br/index.php/geama/article/view/504
191. Siqueira MCB, Chagas JCC, Monnerat JPIS, Monteiro CCF, Mora-Luna RE, Felix SB, et al. Cactus Cladodes Opuntia or Nopalea and By-Product of Low Nutritional Value as Solutions to Forage Shortages in Semiarid Areas. Animals [Internet]. 2022 Nov 17;12(22):3182. Available from: https://www.mdpi.com/2076-2615/12/22/3182
192. Necchi R, Alves IA, Alves SH, Manfron M. In vitro antimicrobial activity, total polyphenols, and flavonoids contents of Nopalea cochenillifera (L.) Salm-Dyck (Cactaceae). Res Pharm. 2012;2:1–7.
193. Francisco ALA, Albericio P de A, Riselane de LAB, Djalma C dos S. Study of the variability, correlation and importance of chemical and nutritional characteristics in cactus pear (Opuntia and Nopalea). African J Agric Res [Internet]. 2016 Aug 4;11(31):2882–92. Available from: http://academicjournals.org/journal/AJAR/article-abstract/E969FD559817
194. ALVES FAL, ANDRADE AP de, BRUNO R de LA, SILVA MG de V, SOUZA M de FV de, SANTOS DC dos. Seasonal variability of phenolic compounds and antioxidant activity in prickly pear cladodes of Opuntia and Nopalea genres. Food Sci Technol [Internet]. 2017 Oct 26;37(4):536–43. Available from: http://www.scielo.br/scielo.php?script=sci_arttext&pid=S0101-20612017000400536&lng=en&tlng=en
195. Matos TK, Guedes J, Alves Filho E, Luz L, Lopes GS, do Nascimento R, et al. Integrated UPLC-HRMS, Chemometric Tools, and Metabolomic Analysis of Forage Palm (Opuntia spp. and Nopalea spp.) to Define Biomarkers Associated with Non-Susceptibility to Carmine Cochineal (Dactylopius opuntiae). J Braz Chem Soc [Internet]. 2021; Available from: http://jbcs.sbq.org.br/audiencia_pdf.asp?aid2=11152&nomeArquivo=2020-0560AR.pdf
196. Francisco ALA, Albericio P de A, Riselane de LAB, Maria G de VS, Maria de FV de S, Claudia P, et al. Genetic diversity and seasonal chemical profile by 1H NMR and cytotoxic activity in Opuntia and

Nopalea genres. J Med Plants Res [Internet]. 2016 Oct 25;10(40):732–47. Available from: http://academicjournals.org/journal/JMPR/article-abstract/E010AA961417
197. Suryawanshi PR, Vidyasagar GM. Antimicrobial Activity of Opuntia cochenillifera (L.) Mill Fruit and Cladode Extracts. In 2016.
198. WFO (2023). Nopalea cochenillifera (L.) Salm-Dyck [Internet]. [cited 2022 Mar 25]. Available from: http://www.worldfloraonline.org/taxon/wfo-0000378923
199. AOAC. Official Methods of Analysis. Vol. 46, American Journal of Public Health and the Nations Health. 1956. p. 916–916.
200. Terra J, Antunes AM, Bueno MIMS, Prado MA. Um método verde, rápido e simples para determinar o valor energético de farinhas e cereais matinais. Quim Nova [Internet]. 2010;33(5):1098–103. Available from: http://www.scielo.br/scielo.php?script=sci_arttext&pid=S0100-40422010000500017&lng=pt&nrm=iso&tlng=pt
201. Wang M, Carver JJ, Phelan V V, Sanchez LM, Garg N, Peng Y, et al. Sharing and community curation of mass spectrometry data with Global Natural Products Social Molecular Networking. Nat Biotechnol [Internet]. 2016 Aug 9;34(8):828–37. Available from: https://www.nature.com/articles/nbt.3597
202. Rutz A, Sorokina M, Galgonek J, Mietchen D, Willighagen E, Gaudry A, et al. The LOTUS initiative for open knowledge management in natural products research. Elife [Internet]. 2022 May 26;11. Available from: https://elifesciences.org/articles/70780
203. Malone MH, Robichaud RC. A Hippocratic screen for pure or crude drug materials. In 1962.
204. Pereira JR, da Fonseca AG, de Sena Fernandes LL, Furtado AA, da Silva VC, da Veiga Júnior VF, et al. Toxicological and pharmacological effects of pentacyclic triterpenes rich fraction obtained from the leaves of Mansoa hirsuta. Biomed Pharmacother [Internet]. 2022 Jan;145:112478. Available from: https://linkinghub.elsevier.com/retrieve/pii/S0753332221012646
205. Gálvez J, Garrido M, Merlos M, Torres MI, Zarzuelo A. Intestinal anti-inflammatory activity of UR-12746, a novel 5-ASA conjugate, on acute and chronic experimental colitis in the rat. Br J Pharmacol [Internet]. 2000 Aug;130(8):1949–59. Available from: http://doi.wiley.com/10.1038/sj.bjp.0703505
206. Cooper HS, Murthy SN, Shah RS, Sedergran DJ. Clinicopathologic study of dextran sulfate sodium experimental murine colitis. Lab Invest [Internet]. 1993;69(2):238—249. Available from: http://europepmc.org/abstract/MED/8350599
207. Berberat PO, A-Rahim YI, Yamashita K, Warny MM, Csizmadia E, Robson SC, et al. Heme Oxygenase-1-Generated Biliverdin Ameliorates Experimental Murine Colitis. Inflamm Bowel Dis [Internet]. 2005 Apr;11(4):350–9. Available from: https://academic.oup.com/ibdjournal/article/11/4/350-359/4683951
208. Bell CJ, Gall DG, Wallace JL. Disruption of colonic electrolyte transport in experimental colitis. Am J Physiol Liver Physiol [Internet]. 1995 Apr 1;268(4):G622–30. Available from: https://www.physiology.org/doi/10.1152/ajpgi.1995.268.4.G622
209. Krawisz JE, Sharon P, Stenson WF. Quantitative assay for acute intestinal inflammation based on myeloperoxidase activity. Gastroenterology [Internet]. 1984 Dec;87(6):1344–50. Available from: https://linkinghub.elsevier.com/retrieve/pii/0016508584902026
210. Esterbauer H, Cheeseman KH. Determination of aldehydic lipid peroxidation products: Malonaldehyde and 4-hydroxynonenal. In: Methods Enzymol [Internet]. 1990. p. 407–21. Available from: https://linkinghub.elsevier.com/retrieve/pii/007668799086134H
211. da Silva V, de Araújo A, Araújo D, Lima M, Vasconcelos R, de Araújo Júnior R, et al. Intestinal Anti-Inflammatory Activity of the Aqueous Extract from Ipomoea asarifolia in DNBS-Induced Colitis in Rats. Int J Mol Sci [Internet]. 2018 Dec 12;19(12):4016. Available from: http://www.mdpi.com/1422-0067/19/12/4016
212. Schindelin J, Arganda-Carreras I, Frise E, Kaynig V, Longair M, Pietzsch T, et al. Fiji: an open-source platform for biological-image analysis. Nat Methods [Internet]. 2012 Jul 28;9(7):676–82. Available from: http://www.nature.com/articles/nmeth.2019
213. Zea-Iriarte W-L, Makiyama K, Goto S, Murase K, Urata Y, Sekine I, et al. Impairment of Antioxidants in Colonic Epithelial Cells Isolated from Trinitrobenzene Sulphonic Acid-Induced Colitis Rats Protective Effect of Rebamipide. Scand J Gastroenterol [Internet]. 1996 Jan 8;31(10):985–92. Available from: http://www.tandfonline.com/doi/full/10.3109/00365529609003118
214. Guerra GCB, de Menezes MSS, de Araújo AA, de Araújo Júnior RF, de Medeiros CACX. Olmesartan Prevented Intra-articular Inflammation Induced by Zymosan in Rats. Biol Pharm Bull [Internet]. 2016;39(11):1793–801. Available from: https://www.jstage.jst.go.jp/article/bpb/39/11/39_b16-00296/_article
215. Cuyckens F, Claeys M. Mass spectrometry in the structural analysis of flavonoids. J Mass Spectrom [Internet]. 2004 Jan;39(1):1–15. Available from: https://onlinelibrary.wiley.com/doi/10.1002/jms.585
216. Dantas-Medeiros R, Furtado AA, Zanatta AC, Torres-Rêgo M, Guimarães Lourenço EM, Ferreira Alves JS, et al. Mass spectrometry characterization of Commiphora leptophloeos leaf extract and preclinical

evaluation of toxicity and anti-inflammatory potential effect. J Ethnopharmacol [Internet]. 2021 Jan;264:113229. Available from: https://linkinghub.elsevier.com/retrieve/pii/S0378874120331111

217. Justesen U. Collision-induced fragmentation of deprotonated methoxylated flavonoids, obtained by electrospray ionization mass spectrometry. J Mass Spectrom [Internet]. 2001 Feb;36(2):169–78. Available from: https://onlinelibrary.wiley.com/doi/10.1002/jms.118
218. Zanatta AC, Mari A, Masullo M, Zeppone Carlos I, Vilegas W, Piacente S, et al. Chemical metabolome assay by high-resolution Orbitrap mass spectrometry and assessment of associated antitumoral activity of Actinocephalus divaricatus. Rapid Commun Mass Spectrom [Internet]. 2018 Feb 15;32(3):241–50. Available from: https://onlinelibrary.wiley.com/doi/10.1002/rcm.8034
219. Lin L-Z, Lu S, Harnly JM. Detection and Quantification of Glycosylated Flavonoid Malonates in Celery, Chinese Celery, and Celery Seed by LC-DAD-ESI/MS. J Agric Food Chem [Internet]. 2007 Feb 1;55(4):1321–6. Available from: https://pubs.acs.org/doi/10.1021/jf0624796
220. Geng P, Harnly JM, Sun J, Zhang M, Chen P. Feruloyl dopamine-O-hexosides are efficient marker compounds as orthogonal validation for authentication of black cohosh (Actaea racemosa)—an UHPLC-HRAM-MS chemometrics study. Anal Bioanal Chem [Internet]. 2017 Apr 3;409(10):2591–600. Available from: http://link.springer.com/10.1007/s00216-017-0205-1
221. Li Z, Zhao C, Zhao X, Xia Y, Sun X, Xie W, et al. Deep Annotation of Hydroxycinnamic Acid Amides in Plants Based on Ultra-High-Performance Liquid Chromatography–High-Resolution Mass Spectrometry and Its In Silico Database. Anal Chem [Internet]. 2018 Dec 18;90(24):14321–30. Available from: https://pubs.acs.org/doi/10.1021/acs.analchem.8b03654
222. Lima CM, Lima AK, Melo MGD, Dória GAA, Serafini MR, Albuquerque-Júnor RLC, et al. Valores de referência hematológicos e bioquímicos de ratos (Rattus novergicus linhagem Wistar) provenientes do biotério da Universidade Tiradentes. Sci Plena [Internet]. 2014 Apr 7;10(3 SE-). Available from: https://www.scientiaplena.org.br/sp/article/view/1784
223. Spinelli MO, Motta MC, Cruz RJ, Godoy CMSC. Intervalos de referência para alguns parâmetros hematológicos de animais criados e mantidos pelo Biotério da Faculdade de Medicina da Universidade de São Paulo. Acta Sci Heal Sci [Internet]. 2014 Mar 6;36(1):1. Available from: http://periodicos.uem.br/ojs/index.php/ActaSciHealthSci/article/view/14541
224. Silva APG da, Souza CCE de, Ribeiro JES, Santos MCG dos, Pontes AL de S, Madruga MS. CARACTERÍSTICAS FÍSICAS, QUÍMICAS E BROMATOLÓGICAS DE PALMA GIGANTE (Opuntia ficus-indica) E MIÚDA (Nopalea cochenillifera) ORIUNDAS DO ESTADO DA PARAÍBA. Rev Bras Tecnol Agroindustrial [Internet]. 2015 Dec 10;9(2). Available from: https://periodicos.utfpr.edu.br/rbta/article/view/1616
225. Lima VR do N, Silva ÁGF da, Cruz RRP, Barbosa L da S, Junior NR da S, Sales GNB, et al. Nopalea cochenillifera Biomass as Bioadsorbent in Water Purification. Water [Internet]. 2021 Jul 22;13(15):2012. Available from: https://www.mdpi.com/2073-4441/13/15/2012
226. Klein-Junior LC, de Souza MR, Viaene J, Bresolin TMB, de Gasper AL, Henriques AT, et al. Quality Control of Herbal Medicines: From Traditional Techniques to State-of-the-art Approaches. Planta Med [Internet]. 2021 Oct 19;87(12/13):964–88. Available from: http://www.thieme-connect.de/DOI/DOI?10.1055/a-1529-8339
227. Akula R, Ravishankar GA. Influence of abiotic stress signals on secondary metabolites in plants. Plant Signal Behav [Internet]. 2011 Nov;6(11):1720–31. Available from: http://www.tandfonline.com/doi/abs/10.4161/psb.6.11.17613
228. Abubakar A, Haque M. Preparation of medicinal plants: Basic extraction and fractionation procedures for experimental purposes. J Pharm Bioallied Sci [Internet]. 2020;12(1):1. Available from: https://journals.lww.com/10.4103/jpbs.JPBS_175_19
229. Cobaleda-Velasco M, Alanis-Bañuelos R, Almaraz N, Rojas-López M, Gonzalez L, Ávila-Reyes J, et al. Phenolic profiles and antioxidant properties of Physalis angulata L. as quality indicators [Perfiles fenólicos y propiedades antioxidantes de extractos de Physalis angulata L. como indicadores de calidad]. J Pharm Pharmacogn Res. 2017;5:114–28.
230. Reynaud J, Guilet D, Terreux R, Lussignol M, Walchshofer N. Isoflavonoids in non-leguminous families: an update. Nat Prod Rep [Internet]. 2005;22(4):504. Available from: http://xlink.rsc.org/?DOI=b416248j
231. Teo S, Stirling D, Thomas S, Hoberman A, Kiorpes A, Khetani V. A 90-day oral gavage toxicity study of d-methylphenidate and d,l-methylphenidate in Sprague–Dawley rats. Toxicology [Internet]. 2002 Oct;179(3):183–96. Available from: https://linkinghub.elsevier.com/retrieve/pii/S0300483X02003384
232. Michael B, Yano B, Sellers RS, Perry R, Morton D, Roome N, et al. Evaluation of Organ Weights for Rodent and Non-Rodent Toxicity Studies: A Review of Regulatory Guidelines and a Survey of Current Practices. Toxicol Pathol [Internet]. 2007 Aug 6;35(5):742–50. Available from: http://journals.sagepub.com/doi/10.1080/01926230701595292

233. Ibrahim MB, Sowemimo AA, Sofidiya MO, Badmos KB, Fageyinbo MS, Abdulkareem FB, et al. Sub-acute and chronic toxicity profiles of Markhamia tomentosa ethanolic leaf extract in rats. J Ethnopharmacol [Internet]. 2016 Dec;193:68–75. Available from: https://linkinghub.elsevier.com/retrieve/pii/S0378874116304597
234. Olson H, Betton G, Robinson D, Thomas K, Monro A, Kolaja G, et al. Concordance of the Toxicity of Pharmaceuticals in Humans and in Animals. Regul Toxicol Pharmacol [Internet]. 2000 Aug;32(1):56–67. Available from: https://linkinghub.elsevier.com/retrieve/pii/S0273230000913990
235. OSEI-BIMPONG A, McLEAN R, BHONDA E, LEWIS SM. The use of the white cell count and haemoglobin in combination as an effective screen to predict the normality of the full blood count. Int J Lab Hematol [Internet]. 2012 Feb 24;34(1):91–7. Available from: https://onlinelibrary.wiley.com/doi/10.1111/j.1751-553X.2011.01365.x
236. Yang W, Zhao P, Li X, Guo L, Gao W. The potential roles of natural plant polysaccharides in inflammatory bowel disease: A review. Carbohydr Polym [Internet]. 2022 Feb;277:118821. Available from: https://linkinghub.elsevier.com/retrieve/pii/S014486172101208X
237. Vezza T, Rodríguez-Nogales A, Algieri F, Utrilla M, Rodriguez-Cabezas M, Galvez J. Flavonoids in Inflammatory Bowel Disease: A Review. Nutrients [Internet]. 2016 Apr 9;8(4):211. Available from: http://www.mdpi.com/2072-6643/8/4/211
238. Morampudi V, Bhinder G, Wu X, Dai C, Sham HP, Vallance BA, et al. DNBS/TNBS Colitis Models: Providing Insights Into Inflammatory Bowel Disease and Effects of Dietary Fat. J Vis Exp [Internet]. 2014 Feb 27;(84). Available from: https://www.jove.com/t/51297/dnbs/tnbs-colitis-models-providing-insights-into-inflammatory-bowel-disease-and-effects-of-dietary-fat
239. Chami B, Martin NJJ, Dennis JM, Witting PK. Myeloperoxidase in the inflamed colon: A novel target for treating inflammatory bowel disease. Arch Biochem Biophys [Internet]. 2018 May;645:61–71. Available from: https://linkinghub.elsevier.com/retrieve/pii/S000398611830119X
240. Draper HH, Hadley M. [43] Malondialdehyde determination as index of lipid Peroxidation. In 1990. p. 421–31. Available from: https://linkinghub.elsevier.com/retrieve/pii/007668799086135I
241. Roudsari NM, Lashgari N-A, Momtaz S, Farzaei MH, Marques AM, Abdolghaffari AH. Natural polyphenols for the prevention of irritable bowel syndrome: molecular mechanisms and targets; a comprehensive review. DARU J Pharm Sci [Internet]. 2019 Dec 4;27(2):755–80. Available from: http://link.springer.com/10.1007/s40199-019-00284-1
242. Mitsuyama K, Tomiyasu N, Takaki K, Masuda J, Yamasaki H, Kuwaki K, et al. Interleukin-10 in the Pathophysiology of Inflammatory Bowel Disease: Increased Serum Concentrations During the Recovery Phase. Mediators Inflamm [Internet]. 2006;2006:1–7. Available from: http://www.hindawi.com/journals/mi/2006/026875/abs/
243. Ljuca F, Gegic A, Salkic NN, Pavlovic-Calic N. Circulating Cytokines Reflect Mucosal Inflammatory Status in Patients with Crohn's Disease. Dig Dis Sci [Internet]. 2010 Aug 16;55(8):2316–26. Available from: http://link.springer.com/10.1007/s10620-009-1016-9
244. Liu B, Li S, Sui X, Guo L, Liu X, Li H, et al. Root Extract of Polygonum cuspidatum Siebold & Zucc. Ameliorates DSS-Induced Ulcerative Colitis by Affecting NF-kappaB Signaling Pathway in a Mouse Model via Synergistic Effects of Polydatin, Resveratrol, and Emodin. Front Pharmacol [Internet]. 2018 Apr 11;9. Available from: http://journal.frontiersin.org/article/10.3389/fphar.2018.00347/full
245. Coskun M, Olsen J, Seidelin JB, Nielsen OH. MAP kinases in inflammatory bowel disease. Clin Chim Acta [Internet]. 2011 Mar;412(7–8):513–20. Available from: https://linkinghub.elsevier.com/retrieve/pii/S0009898110007710
246. Chen X, Chen W, He Y, Zhang Y, Chen C, Zhu Z, et al. The p38 MAPK and NF-κB Pathways are Involved in Cyclic Compressive Force-induced IL-6 Secretion in MLO-Y4 Cells. Brazilian Arch Biol Technol [Internet]. 2018;61. Available from: http://www.scielo.br/scielo.php?script=sci_arttext&pid=S1516-89132018000100437&tlng=en
247. Nair MP, Mahajan S, Reynolds JL, Aalinkeel R, Nair H, Schwartz SA, et al. The Flavonoid Quercetin Inhibits Proinflammatory Cytokine (Tumor Necrosis Factor Alpha) Gene Expression in Normal Peripheral Blood Mononuclear Cells via Modulation of the NF-κβ System. Clin Vaccine Immunol [Internet]. 2006 Mar;13(3):319–28. Available from: https://journals.asm.org/doi/10.1128/CVI.13.3.319-328.2006
248. Shanmugam M, Tharmaraj R, Murugaraj M. P, Asokan M, Ram B. S. Modulating Effect of Ferulic Acid on NF-kB, COX-2 and VEGF Expression Pattern During 7, 12-Dimethylbenz(a)anthracene Induced Oral Carcinogenesis. Open Nutraceuticals J [Internet]. 2014 Sep 26;7(1):33–8. Available from: http://benthamopen.com/ABSTRACT/TONUTRAJ-7-33
249. Giacomarra M, Mangano A, Montana G. The anti-inflammatory activity of ferulic acid on NF-κB depends on Keap1. LOJ Phar Cli Res. 2020;2(2).
250. Ho H-H, Chang C-S, Ho W-C, Liao S-Y, Wu C-H, Wang C-J. Anti-metastasis effects of gallic acid on

gastric cancer cells involves inhibition of NF-κB activity and downregulation of PI3K/AKT/small GTPase signals. Food Chem Toxicol [Internet]. 2010 Aug;48(8–9):2508–16. Available from: https://linkinghub.elsevier.com/retrieve/pii/S0278691510003984

251. Shen J, Li N, Zhang X. Daidzein Ameliorates Dextran Sulfate Sodium-Induced Experimental Colitis in Mice by Regulating NF-κB Signaling. J Environ Pathol Toxicol Oncol [Internet]. 2019;38(1):29–39. Available from: http://www.dl.begellhouse.com/journals/0ff459a57a4c08d0,4b309b253eb144f8,09ff16a8457417f2.html
252. Cobo ER, Kissoon-Singh V, Moreau F, Chadee K. Colonic MUC2 mucin regulates the expression and antimicrobial activity of β-defensin 2. Mucosal Immunol [Internet]. 2015 Nov;8(6):1360–72. Available from: https://linkinghub.elsevier.com/retrieve/pii/S1933021922010133
253. Kuo W-T, Zuo L, Turner J. THE TIGHT JUNCTION PROTEIN ZO-1 REGULATES MITOTIC SPINDLE ORIENTATION TO ENABLE EFFICIENT MUCOSAL REPAIR. Inflamm Bowel Dis [Internet]. 2021 Jan 21;27(Supplement_1):S28–S28. Available from: https://academic.oup.com/ibdjournal/article/27/Supplement_1/S28/6105506
254. Carrasco-Pozo C, Morales P, Gotteland M. Polyphenols Protect the Epithelial Barrier Function of Caco-2 Cells Exposed to Indomethacin through the Modulation of Occludin and Zonula Occludens-1 Expression. J Agric Food Chem [Internet]. 2013 Jun 5;61(22):5291–7. Available from: https://pubs.acs.org/doi/10.1021/jf400150p
255. Lamprecht A, Schäfer U, Lehr C-M. Size-Dependent Bioadhesion of Micro- and Nanoparticulate Carriers to the Inflamed Colonic Mucosa. Pharm Res [Internet]. 2001;18(6):788–93. Available from: https://doi.org/10.1023/A:1011032328064
256. Sharma M, Sharma S, Wadhwa J. Improved uptake and therapeutic intervention of curcumin via designing binary lipid nanoparticulate formulation for oral delivery in inflammatory bowel disorder. Artif Cells, Nanomedicine, Biotechnol [Internet]. 2019 Dec 4;47(1):45–55. Available from: https://www.tandfonline.com/doi/full/10.1080/21691401.2018.1543191
257. Bhattacharjee S. DLS and zeta potential – What they are and what they are not? J Control Release [Internet]. 2016 Aug;235:337–51. Available from: https://linkinghub.elsevier.com/retrieve/pii/S0168365916303832
258. Gaikwad VL, Choudhari PB, Bhatia NM, Bhatia MS. Characterization of pharmaceutical nanocarriers: in vitro and in vivo studies. In: Nanomaterials for Drug Delivery and Therapy [Internet]. Elsevier; 2019. p. 33–58. Available from: https://linkinghub.elsevier.com/retrieve/pii/B9780128165058000163
259. Harel E, Rubinstein A, Nissan A, Khazanov E, Nadler Milbauer M, Barenholz Y, et al. Enhanced Transferrin Receptor Expression by Proinflammatory Cytokines in Enterocytes as a Means for Local Delivery of Drugs to Inflamed Gut Mucosa. Dalmasso G, editor. PLoS One [Internet]. 2011 Sep 6;6(9):e24202. Available from: https://dx.plos.org/10.1371/journal.pone.0024202
260. Jubeh TT, Nadler-Milbauer M, Barenholz Y, Rubinstein A. Local treatment of experimental colitis in the rat by negatively charged liposomes of catalase, TMN and SOD. J Drug Target [Internet]. 2006 Jan 8;14(3):155–63. Available from: http://www.tandfonline.com/doi/full/10.1080/10611860600648429
261. Jubeh TT, Barenholz Y, Rubinstein A. Differential Adhesion of Normal and Inflamed Rat Colonic Mucosa by Charged Liposomes. Pharm Res [Internet]. 2004 Mar;21(3):447–53. Available from: http://link.springer.com/10.1023/B:PHAM.0000019298.29561.cd
262. Tirosh B, Khatib N, Barenholz Y, Nissan A, Rubinstein A. Transferrin as a Luminal Target for Negatively Charged Liposomes in the Inflamed Colonic Mucosa. Mol Pharm [Internet]. 2009 Aug 3;6(4):1083–91. Available from: https://pubs.acs.org/doi/10.1021/mp9000926
263. Wang X, Fan Y, Yan J, Yang M. Engineering polyphenol-based polymeric nanoparticles for drug delivery and bioimaging. Chem Eng J [Internet]. 2022 Jul;439:135661. Available from: https://linkinghub.elsevier.com/retrieve/pii/S1385894722011615
264. Higashi K, Hayashi H, Yamamoto K, Moribe K. The effect of drug and EUDRAGIT® S 100 miscibility in solid dispersions on the drug and polymer dissolution rate. Int J Pharm [Internet]. 2015 Oct;494(1):9–16. Available from: https://linkinghub.elsevier.com/retrieve/pii/S0378517315301058
265. Sulfikkarali N, Krishnakumar N, Manoharan S, Nirmal RM. Chemopreventive Efficacy of Naringenin-Loaded Nanoparticles in 7,12-dimethylbenz(a)anthracene Induced Experimental Oral Carcinogenesis. Pathol Oncol Res [Internet]. 2013 Apr 12;19(2):287–96. Available from: http://link.springer.com/10.1007/s12253-012-9581-1
266. Brito FAL de, Araújo YP de, Marcelino AS de AN, Ferreira NL, Fonseca KS, Brito AMSS, et al. Preparation and characterization of a biodegradable film from cactus Nopalea sp. J Prof Assoc Cactus Dev [Internet]. 2022 Aug 22;24:185–202. Available from: https://jpacd.org/jpacd/article/view/507
267. Ferreira NL, Fonseca KS, Pinheiro JC, Marcelino ASAN, Araújo YP, Souza JFN, et al. Effect of wet and dry periods on the yield of mucilage extracted from the prickly pear cactus clone 'Miúda' [Nopalea

cochenillifera (L.) Salm-Dyck]. Acta Hortic [Internet]. 2022 Sep;(1343):355–60. Available from: https://www.actahort.org/books/1343/1343_45.htm

268. Gheribi R, Puchot L, Verge P, Jaoued-Grayaa N, Mezni M, Habibi Y, et al. Development of plasticized edible films from Opuntia ficus-indica mucilage: A comparative study of various polyol plasticizers. Carbohydr Polym [Internet]. 2018 Jun;190:204–11. Available from: https://linkinghub.elsevier.com/retrieve/pii/S0144861718302431
269. Rodríguez-González S, Martínez-Flores HE, Chávez-Moreno CK, Macías-Rodríguez LI, Zavala-Mendoza E, Garnica-Romo MG, et al. Extraction and Characterization of Mucilage From Wild Species of O puntia. J Food Process Eng [Internet]. 2014 Jun;37(3):285–92. Available from: https://onlinelibrary.wiley.com/doi/10.1111/jfpe.12084
270. Dadashpour M, Firouzi-Amandi A, Pourhassan-Moghaddam M, Maleki MJ, Soozangar N, Jeddi F, et al. Biomimetic synthesis of silver nanoparticles using Matricaria chamomilla extract and their potential anticancer activity against human lung cancer cells. Mater Sci Eng C [Internet]. 2018 Nov;92:902–12. Available from: https://linkinghub.elsevier.com/retrieve/pii/S0928493117341875
271. Wu L, Zhang J, Watanabe W. Physical and chemical stability of drug nanoparticles. Adv Drug Deliv Rev [Internet]. 2011 May;63(6):456–69. Available from: https://linkinghub.elsevier.com/retrieve/pii/S0169409X11000172
272. Jaquilin P J R, Oluwafemi OS, Thomas S, Oyedeji AO. Recent advances in drug delivery nanocarriers incorporated in temperature-sensitive Pluronic F-127–A critical review. J Drug Deliv Sci Technol [Internet]. 2022 Jun;72:103390. Available from: https://linkinghub.elsevier.com/retrieve/pii/S1773224722003008
273. Nedelcu A, Mosteanu O, Pop T, Mocan T, Mocan L. Recent Advances in Nanoparticle-Mediated Treatment of Inflammatory Bowel Diseases. Appl Sci [Internet]. 2021 Jan 5;11(1):438. Available from: https://www.mdpi.com/2076-3417/11/1/438
274. Sood A, Dev A, Mohanbhai SJ, Shrimali N, Kapasiya M, Kushwaha AC, et al. Disulfide-Bridged Chitosan-Eudragit S-100 Nanoparticles for Colorectal Cancer. ACS Appl Nano Mater [Internet]. 2019 Oct 25;2(10):6409–17. Available from: https://pubs.acs.org/doi/10.1021/acsanm.9b01377
275. Gupta A, Sood A, Dhiman A, Shrimali N, Singhmar R, Guchhait P, et al. Redox responsive poly(allylamine)/eudragit S-100 nanoparticles for dual drug delivery in colorectal cancer. Biomater Adv [Internet]. 2022 Dec;143:213184. Available from: https://linkinghub.elsevier.com/retrieve/pii/S2772950822004617
276. Eichele DD, Kharbanda KK. Dextran sodium sulfate colitis murine model: An indispensable tool for advancing our understanding of inflammatory bowel diseases pathogenesis. World J Gastroenterol [Internet]. 2017 Sep 7;23(33):6016–29. Available from: http://www.wjgnet.com/1007-9327/full/v23/i33/6016.htm
277. Barone M, Chain F, Sokol H, Brigidi P, Bermúdez-Humarán LG, Langella P, et al. A Versatile New Model of Chemically Induced Chronic Colitis Using an Outbred Murine Strain. Front Microbiol [Internet]. 2018 Mar 27;9. Available from: http://journal.frontiersin.org/article/10.3389/fmicb.2018.00565/full
278. Qelliny MR, Aly UF, Elgarhy OH, Khaled KA. Budesonide-Loaded Eudragit S 100 Nanocapsules for the Treatment of Acetic Acid-Induced Colitis in Animal Model. AAPS PharmSciTech [Internet]. 2019 Aug 26;20(6):237. Available from: http://link.springer.com/10.1208/s12249-019-1453-5
279. Gugulothu D, Kulkarni A, Patravale V, Dandekar P. pH-Sensitive Nanoparticles of Curcumin–Celecoxib Combination: Evaluating Drug Synergy in Ulcerative Colitis Model. J Pharm Sci [Internet]. 2014 Feb;103(2):687–96. Available from: https://linkinghub.elsevier.com/retrieve/pii/S002235491530722X
280. Beloqui A, Coco R, Memvanga PB, Ucakar B, des Rieux A, Préat V. pH-sensitive nanoparticles for colonic delivery of curcumin in inflammatory bowel disease. Int J Pharm [Internet]. 2014 Oct;473(1–2):203–12. Available from: https://linkinghub.elsevier.com/retrieve/pii/S0378517314004992
281. Asfour MH, Mohsen AM. Formulation and evaluation of pH-sensitive rutin nanospheres against colon carcinoma using HCT-116 cell line. J Adv Res [Internet]. 2018 Jan;9:17–26. Available from: https://linkinghub.elsevier.com/retrieve/pii/S2090123217301078
282. Bak A, Ashford M, Brayden DJ. Local delivery of macromolecules to treat diseases associated with the colon. Adv Drug Deliv Rev [Internet]. 2018 Nov;136–137:2–27. Available from: https://linkinghub.elsevier.com/retrieve/pii/S0169409X1830259X
283. Patra CN, Priya R, Swain S, Kumar Jena G, Panigrahi KC, Ghose D. Pharmaceutical significance of Eudragit: A review. Futur J Pharm Sci [Internet]. 2017 Jun;3(1):33–45. Available from: https://linkinghub.elsevier.com/retrieve/pii/S2314724516301273
284. Perše M, Cerar A. Dextran Sodium Sulphate Colitis Mouse Model: Traps and Tricks. J Biomed Biotechnol [Internet]. 2012;2012:1–13. Available from: http://www.hindawi.com/journals/bmri/2012/718617/

285. Papadakis KA, Targan SR. Role of Cytokines in the Pathogenesis of Inflammatory Bowel Disease. Annu Rev Med [Internet]. 2000 Feb;51(1):289–98. Available from: https://www.annualreviews.org/doi/10.1146/annurev.med.51.1.289
286. Kany S, Vollrath JT, Relja B. Cytokines in Inflammatory Disease. Int J Mol Sci [Internet]. 2019 Nov 28;20(23):6008. Available from: https://www.mdpi.com/1422-0067/20/23/6008
287. Deshmane SL, Kremlev S, Amini S, Sawaya BE. Monocyte Chemoattractant Protein-1 (MCP-1): An Overview. J Interf Cytokine Res [Internet]. 2009 Jun;29(6):313–26. Available from: http://www.liebertpub.com/doi/10.1089/jir.2008.0027
288. Qin C-C, Liu Y-N, Hu Y, Yang Y, Chen Z. Macrophage inflammatory protein-2 as mediator of inflammation in acute liver injury. World J Gastroenterol [Internet]. 2017;23(17):3043. Available from: http://www.wjgnet.com/1007-9327/full/v23/i17/3043.htm
289. De Filippo K, Henderson RB, Laschinger M, Hogg N. Neutrophil Chemokines KC and Macrophage-Inflammatory Protein-2 Are Newly Synthesized by Tissue Macrophages Using Distinct TLR Signaling Pathways. J Immunol [Internet]. 2008 Mar 15;180(6):4308–15. Available from: https://journals.aai.org/jimmunol/article/180/6/4308/75987/Neutrophil-Chemokines-KC-and-Macrophage
290. Sumagin R, Brazil JC, Nava P, Nishio H, Alam A, Luissint AC, et al. Neutrophil interactions with epithelial-expressed ICAM-1 enhances intestinal mucosal wound healing. Mucosal Immunol [Internet]. 2016 Sep;9(5):1151–62. Available from: https://linkinghub.elsevier.com/retrieve/pii/S1933021922007620
291. Flavel M, Ellis TP, Stahl L, Begg D, Smythe J, Ilag LL, et al. Polyphenol Rich Sugarcane Extract Reduces Body Weight in C57/BL6J Mice Fed a High Fat, High Carbohydrate Diet. Appl Sci [Internet]. 2021 Jun 2;11(11):5163. Available from: https://www.mdpi.com/2076-3417/11/11/5163
292. Collins B, Hoffman J, Martinez K, Grace M, Lila MA, Cockrell C, et al. A polyphenol-rich fraction obtained from table grapes decreases adiposity, insulin resistance and markers of inflammation and impacts gut microbiota in high-fat-fed mice. J Nutr Biochem [Internet]. 2016 May;31:150–65. Available from: https://linkinghub.elsevier.com/retrieve/pii/S0955286316000346
293. Li A, Wang J, Kou R, Chen M, Zhang B, Zhang Y, et al. Polyphenol-rich oolong tea alleviates obesity and modulates gut microbiota in high-fat diet-fed mice. Front Nutr [Internet]. 2022 Jul 28;9. Available from: https://www.frontiersin.org/articles/10.3389/fnut.2022.937279/full
294. Lee ES, Kwon M-H, Kim HM, Woo HB, Ahn CM, Chung CH. Curcumin analog CUR5–8 ameliorates nonalcoholic fatty liver disease in mice with high-fat diet-induced obesity. Metabolism [Internet]. 2020 Feb;103:154015. Available from: https://linkinghub.elsevier.com/retrieve/pii/S0026049519302306
295. Faghfouri AH, Khajebishak Y, Payahoo L, Faghfuri E, Alivand M. PPAR-gamma agonists: Potential modulators of autophagy in obesity. Eur J Pharmacol [Internet]. 2021 Dec;912:174562. Available from: https://linkinghub.elsevier.com/retrieve/pii/S0014299921007184
296. Pan J, Zhou W, Xu R, Xing L, Ji G, Dang Y. Natural PPARs agonists for the treatment of nonalcoholic fatty liver disease. Biomed Pharmacother [Internet]. 2022 Jul;151:113127. Available from: https://linkinghub.elsevier.com/retrieve/pii/S0753332222005169
297. Chopra I, Li HF, Wang H, Webster KA. Phosphorylation of the insulin receptor by AMP-activated protein kinase (AMPK) promotes ligand-independent activation of the insulin signalling pathway in rodent muscle. Diabetologia [Internet]. 2012 Mar 30;55(3):783–94. Available from: http://link.springer.com/10.1007/s00125-011-2407-y
298. Portincasa P, Bonfrate L, Khalil M, Angelis M De, Calabrese FM, D'Amato M, et al. Intestinal Barrier and Permeability in Health, Obesity and NAFLD. Biomedicines [Internet]. 2021 Dec 31;10(1):83. Available from: https://www.mdpi.com/2227-9059/10/1/83
299. Nickel L, Sünderhauf A, Rawish E, Stölting I, Derer S, Thorns C, et al. The AT1 Receptor Blocker Telmisartan Reduces Intestinal Mucus Thickness in Obese Mice. Front Pharmacol [Internet]. 2022 Mar 31;13. Available from: https://www.frontiersin.org/articles/10.3389/fphar.2022.815353/full
300. Rohr MW, Narasimhulu CA, Rudeski-Rohr TA, Parthasarathy S. Negative Effects of a High-Fat Diet on Intestinal Permeability: A Review. Adv Nutr [Internet]. 2020 Jan;11(1):77–91. Available from: https://linkinghub.elsevier.com/retrieve/pii/S216183132200237X

APPENDIX

Supplementary Material: Data from the identification of substances by mass spectrometry

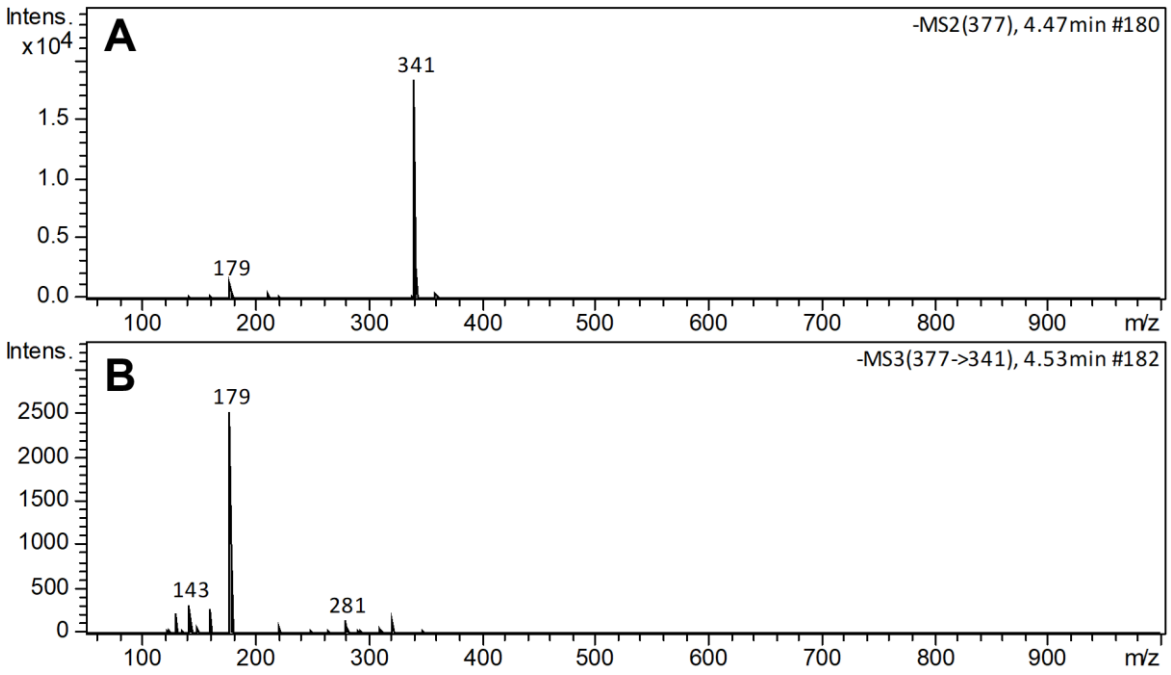

Figure S1. CID-MS^n mass spectra in negative ion mode for compound **1**: (**A**) CID-MS^2 spectrum of the precursor ion at *m/z* 377; (**B**) CID-MS^3 mass spectrum of the product ion at *m/z* 341.

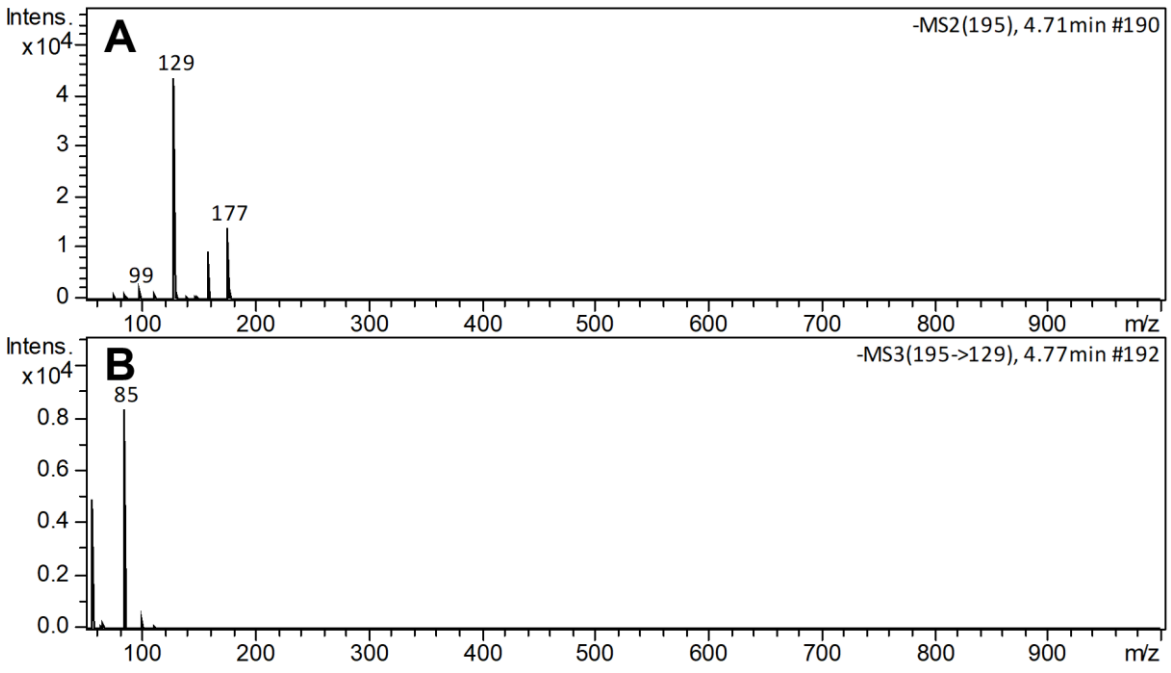

Figure S2. CID-MS^n mass spectra in negative ion mode for compound **2**: (**A**) CID-MS^2 spectrum of the precursor ion at *m/z* 195; (**B**) CID-MS^3 mass spectrum of the product ion at *m/z* 129.

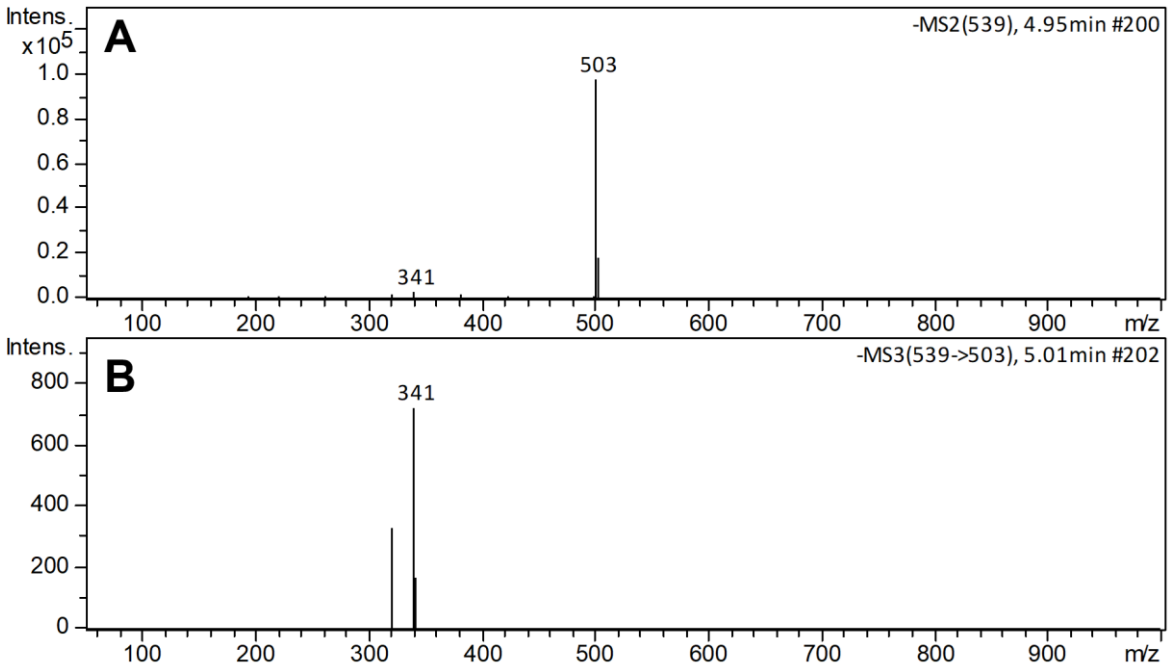

Figure S3. CID-MS^n mass spectra in negative ion mode for compound **3**: (**A**) CID-MS^2 spectrum of the precursor ion at *m/z* 539; (**B**) CID-MS^3 mass spectrum of the product ion at *m/z* 503.

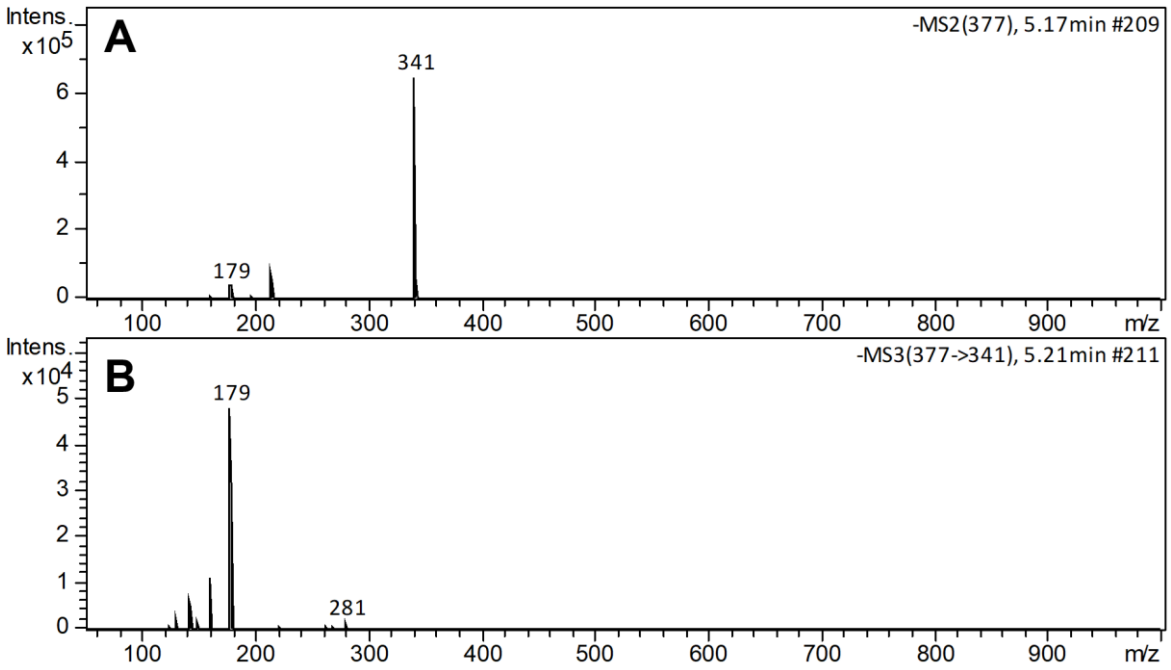

Figure S4. CID-MS^n mass spectra in negative ion mode for compound **4**: (**A**) CID-MS^2 spectrum of the precursor ion at *m/z* 377; (**B**) CID-MS^3 mass spectrum of the product ion at *m/z* 341.

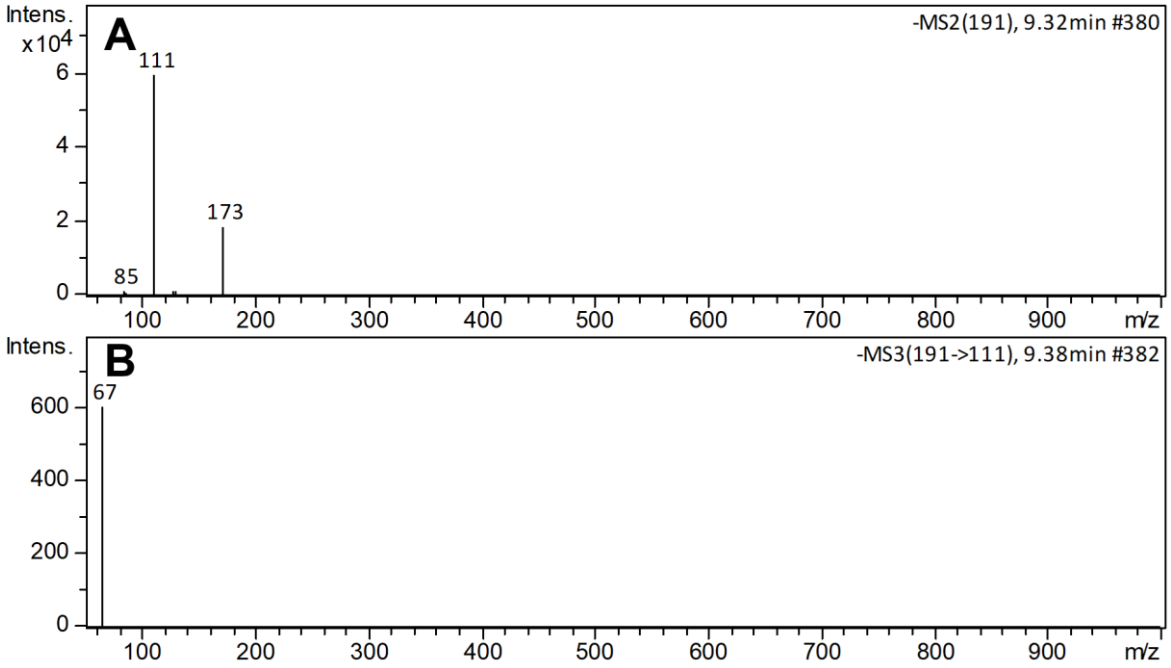

Figure S5. CID-MS^n mass spectra in negative ion mode for compound **5**: (**A**) CID-MS^2 spectrum of the precursor ion at *m/z* 191; (**B**) CID-MS^3 mass spectrum of the product ion at *m/z* 111.

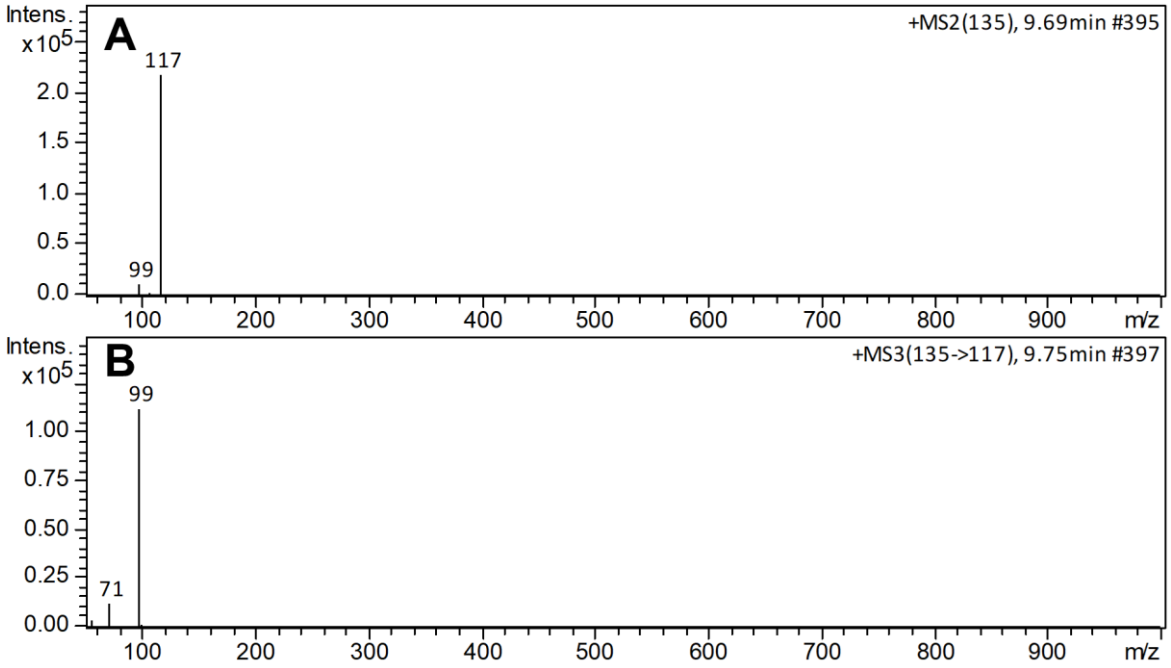

Figure S6. CID-MS^n mass spectra in negative ion mode for compound **6**: (**A**) CID-MS^2 spectrum of the precursor ion at *m/z* 135; (**B**) CID-MS^3 mass spectrum of the product ion at *m/z* 117.

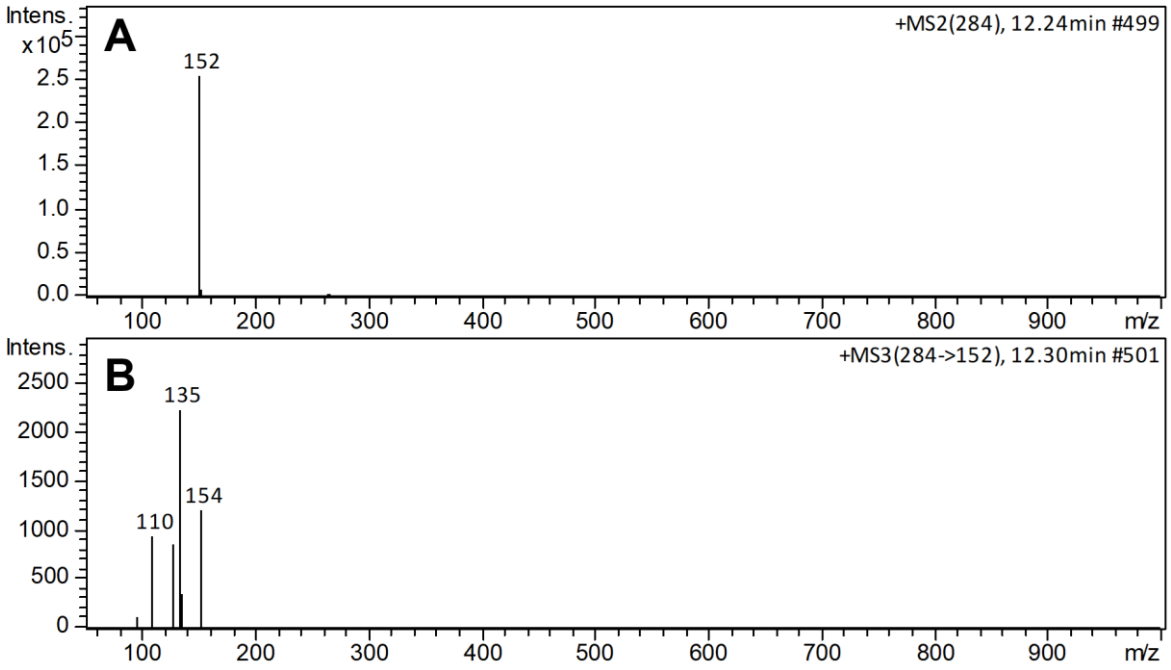

Figure S7. CID-MS^n mass spectra in positive ion mode for compound **7**: (**A**) CID-MS^2 spectrum of the precursor ion at *m/z* 284; (**B**) CID-MS^3 mass spectrum of the product ion at *m/z* 152.

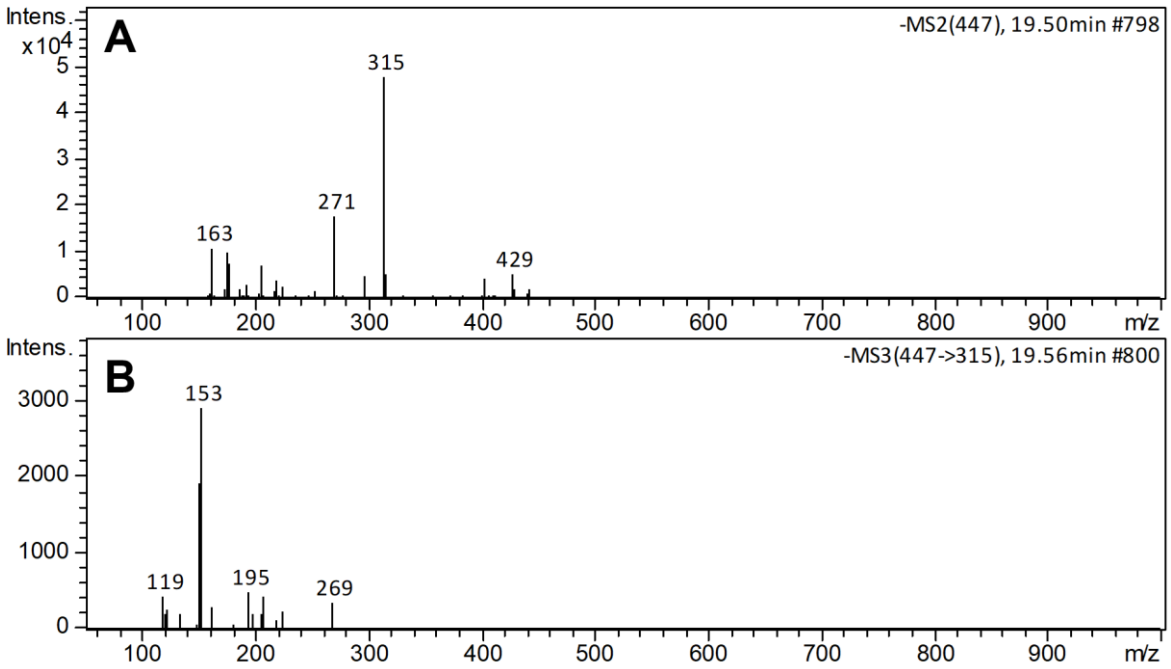

Figure S8. CID-MS^n mass spectra in negative ion mode for compound **8**: (**A**) CID-MS^2 spectrum of the precursor ion at *m/z* 447; (**B**) CID-MS^3 mass spectrum of the product ion at *m/z* 315.

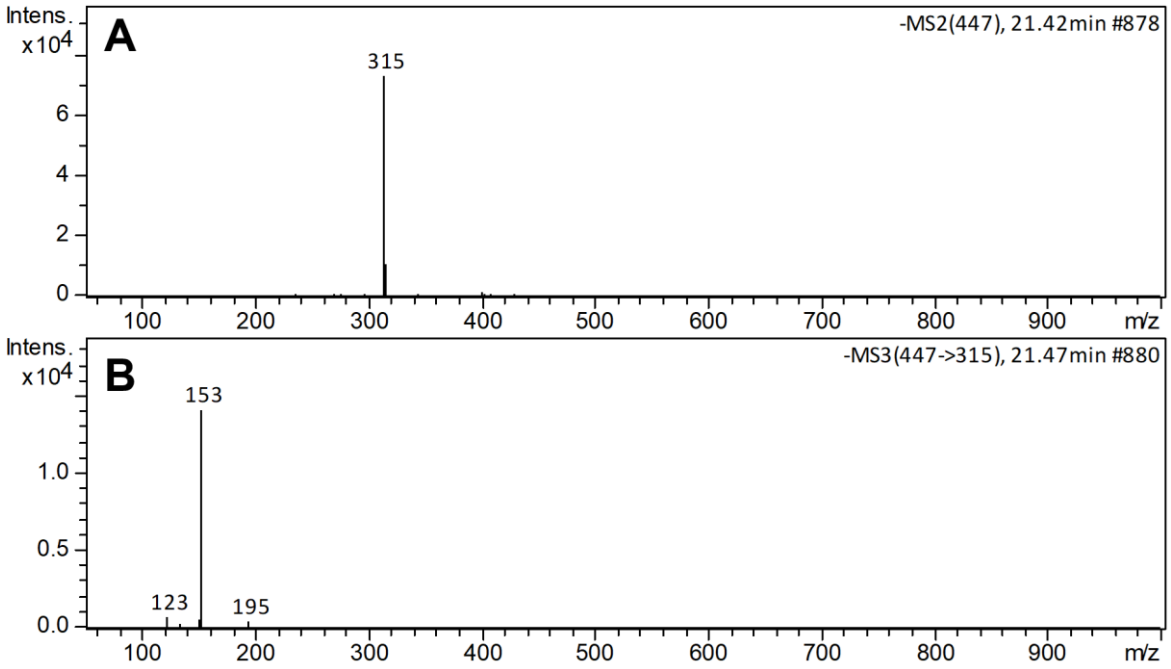

Figure S9. CID-MS^n mass spectra in negative ion mode for compound **9**: (**A**) CID-MS^2 spectrum of the precursor ion at *m/z* 447; (**B**) CID-MS^3 mass spectrum of the product ion at *m/z* 315.

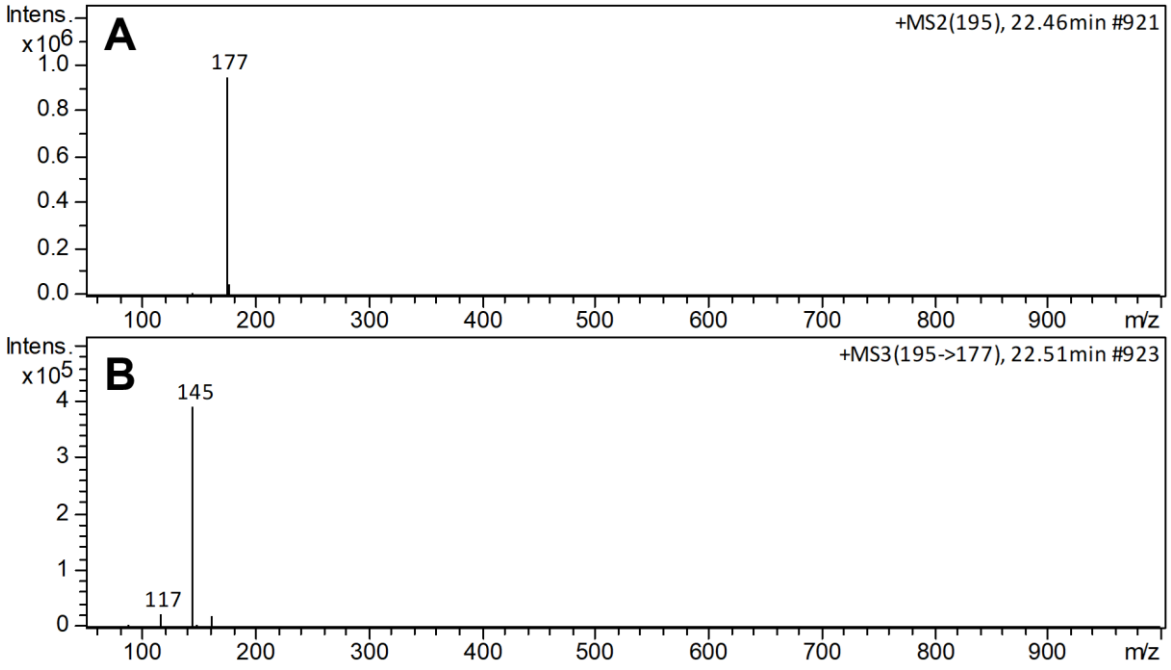

Figure S10. CID-MS^n mass spectra in positive ion mode for compound **10**: (**A**) CID-MS^2 spectrum of the precursor ion at *m/z* 195; (**B**) CID-MS^3 mass spectrum of the product ion at *m/z* 177.

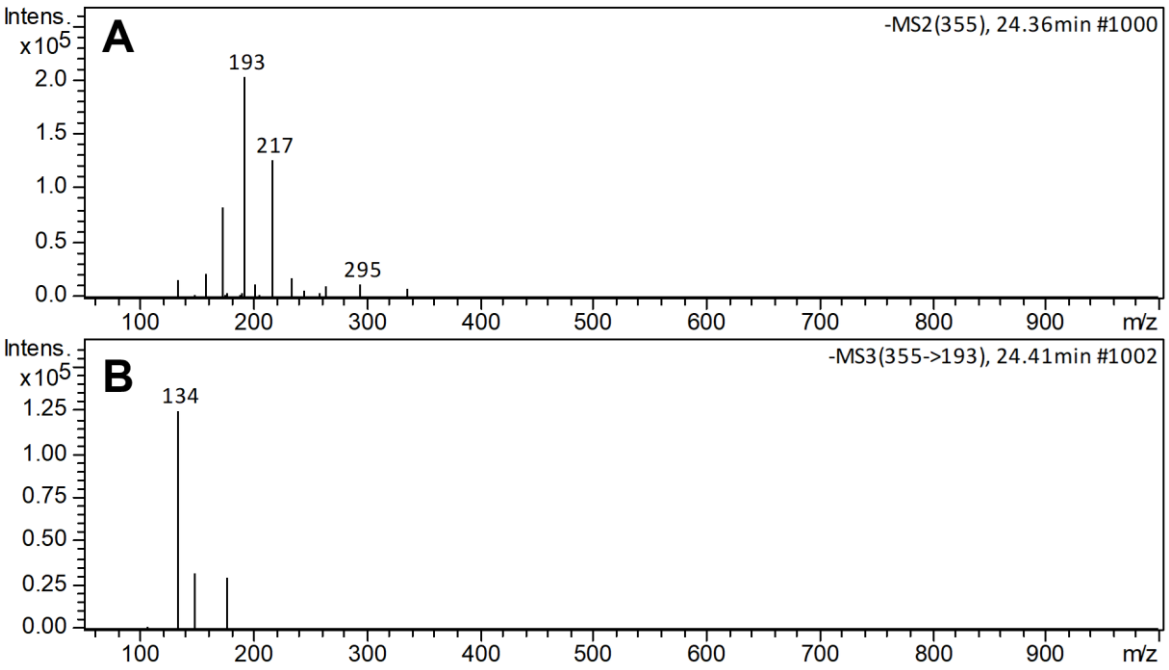

Figure S11. CID-MS^n mass spectra in negative ion mode for compound **11**: (**A**) CID-MS^2 spectrum of the precursor ion at *m/z* 355; (**B**) CID-MS^3 mass spectrum of the product ion at *m/z* 193.

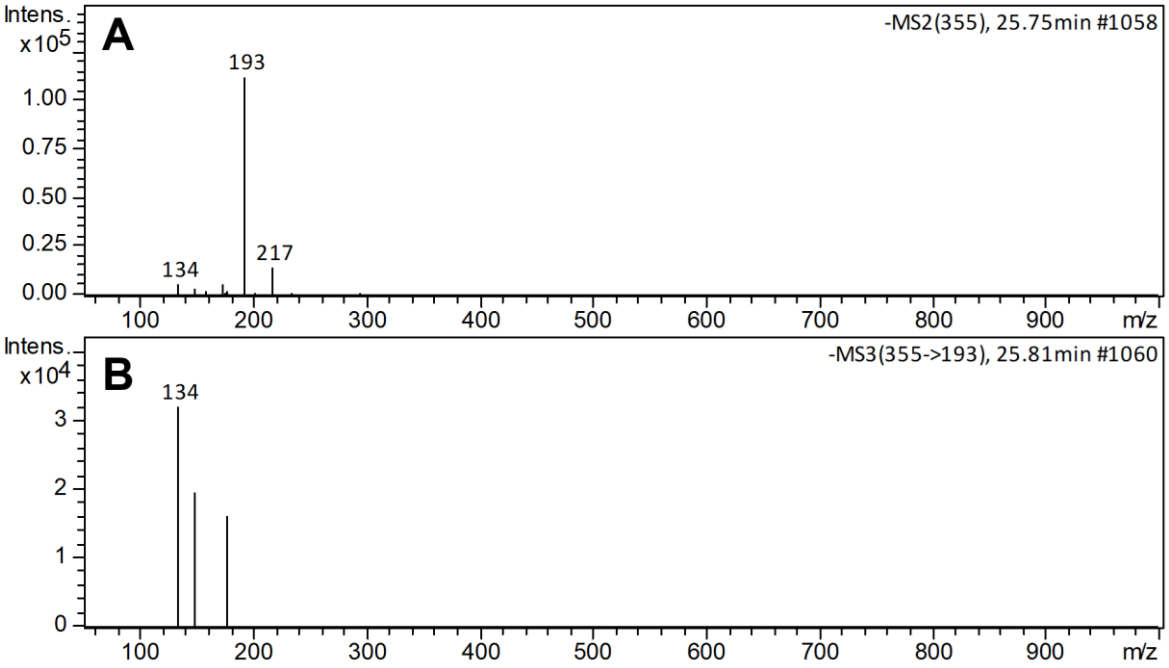

Figure S12. CID-MS^n mass spectra in negative ion mode for compound **12**: (**A**) CID-MS^2 spectrum of the precursor ion at *m/z* 355; (**B**) CID-MS^3 mass spectrum of the product ion at *m/z* 193.

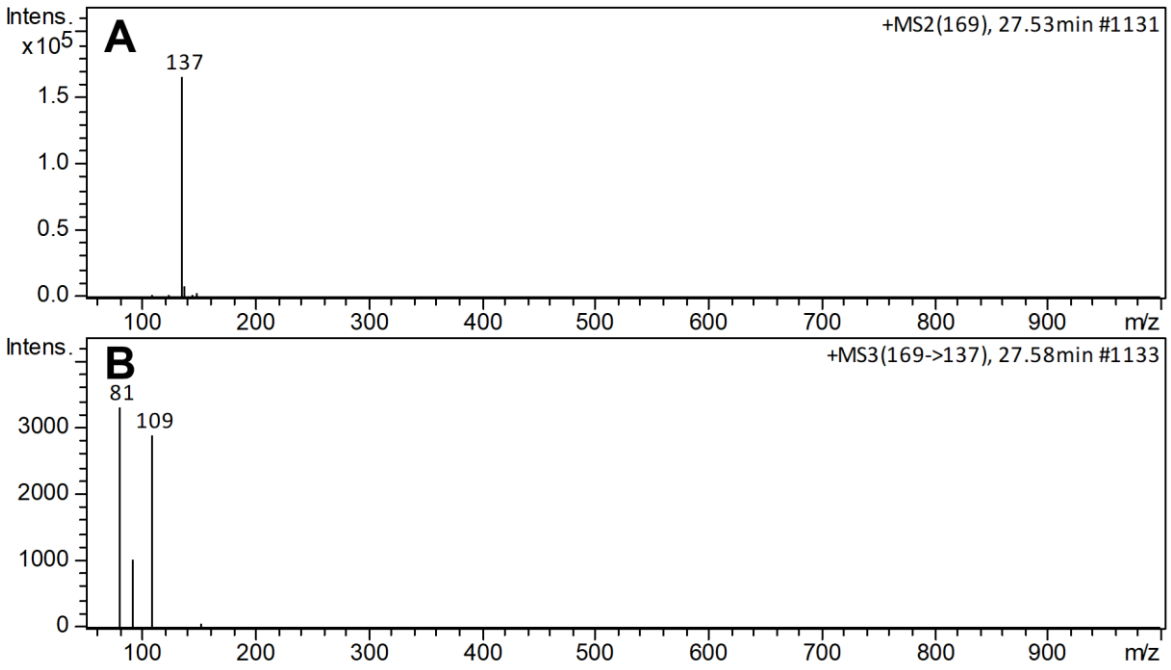

Figure S13. CID-MS^n mass spectra in positive ion mode for compound **13**: (**A**) CID-MS^2 spectrum of the precursor ion at *m/z* 169; (**B**) CID-MS^3 mass spectrum of the product ion at *m/z* 137.

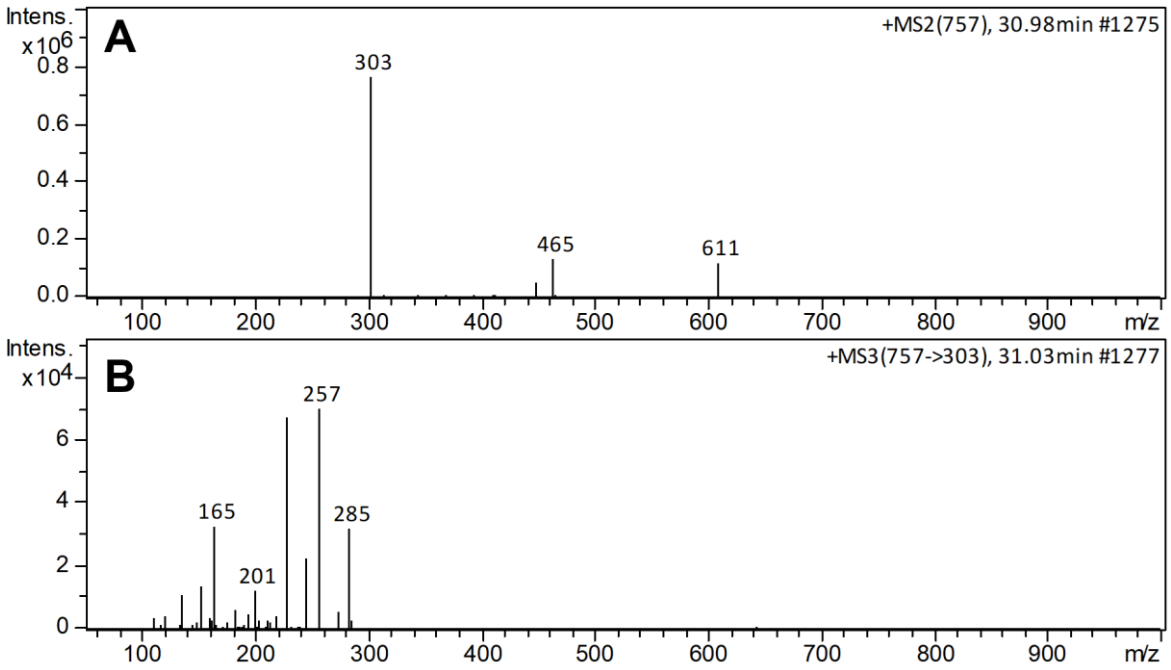

Figure S14. CID-MS^n mass spectra in positive ion mode for compound **14**: (**A**) CID-MS^2 spectrum of the precursor ion at *m/z* 757; (**B**) CID-MS^3 mass spectrum of the product ion at *m/z* 303.

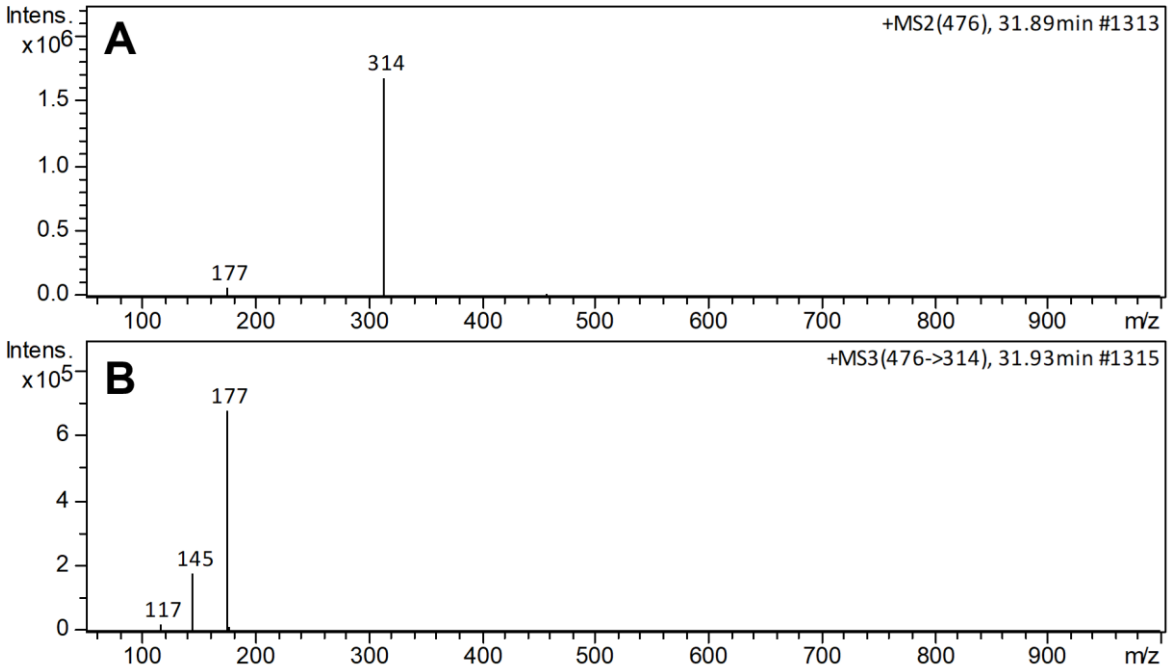

Figure S15. CID-MS^n mass spectra in positive ion mode for compound **15**: (**A**) CID-MS^2 spectrum of the precursor ion at *m/z* 476; (**B**) CID-MS^3 mass spectrum of the product ion at *m/z* 177.

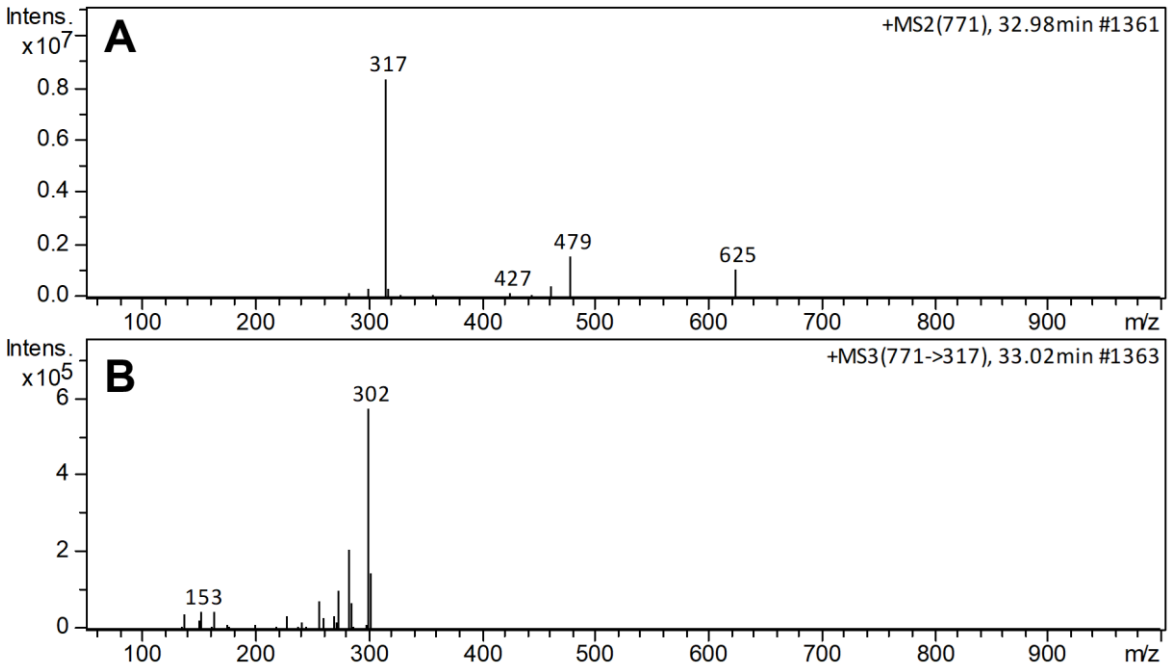

Figure S16. CID-MS^n mass spectra in positive ion mode for compound **16**: (**A**) CID-MS^2 spectrum of the precursor ion at *m/z* 771; (**B**) CID-MS^3 mass spectrum of the product ion at *m/z* 317.

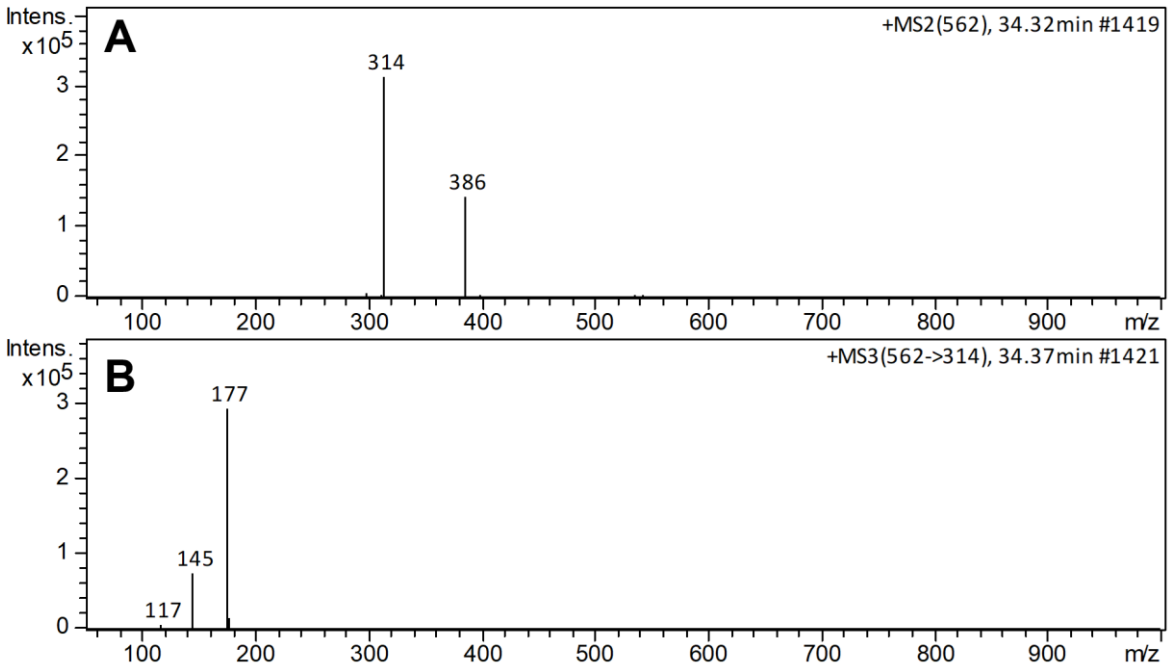

Figure S17. CID-MS^n mass spectra in positive ion mode for compound **17**: (**A**) CID-MS^2 spectrum of the precursor ion at *m/z* 562; (**B**) CID-MS^3 mass spectrum of the product ion at *m/z* 314.

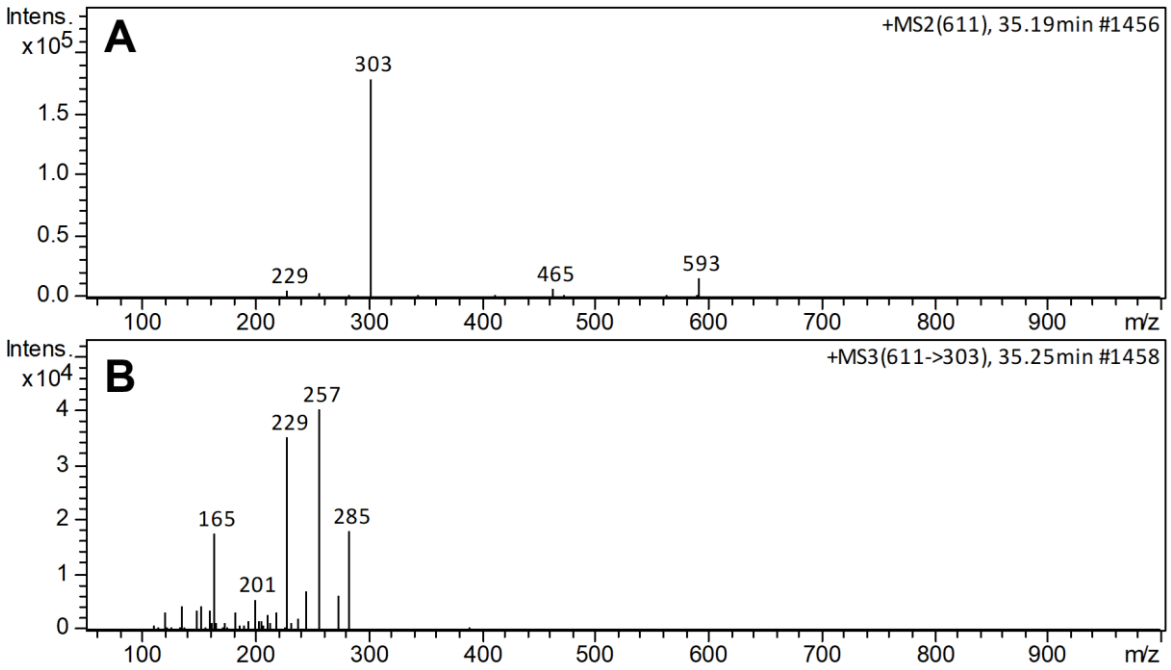

Figure S18. CID-MS^n mass spectra in positive ion mode for compound **18**: (**A**) CID-MS^2 spectrum of the precursor ion at *m/z* 611; (**B**) CID-MS^3 mass spectrum of the product ion at *m/z* 303.

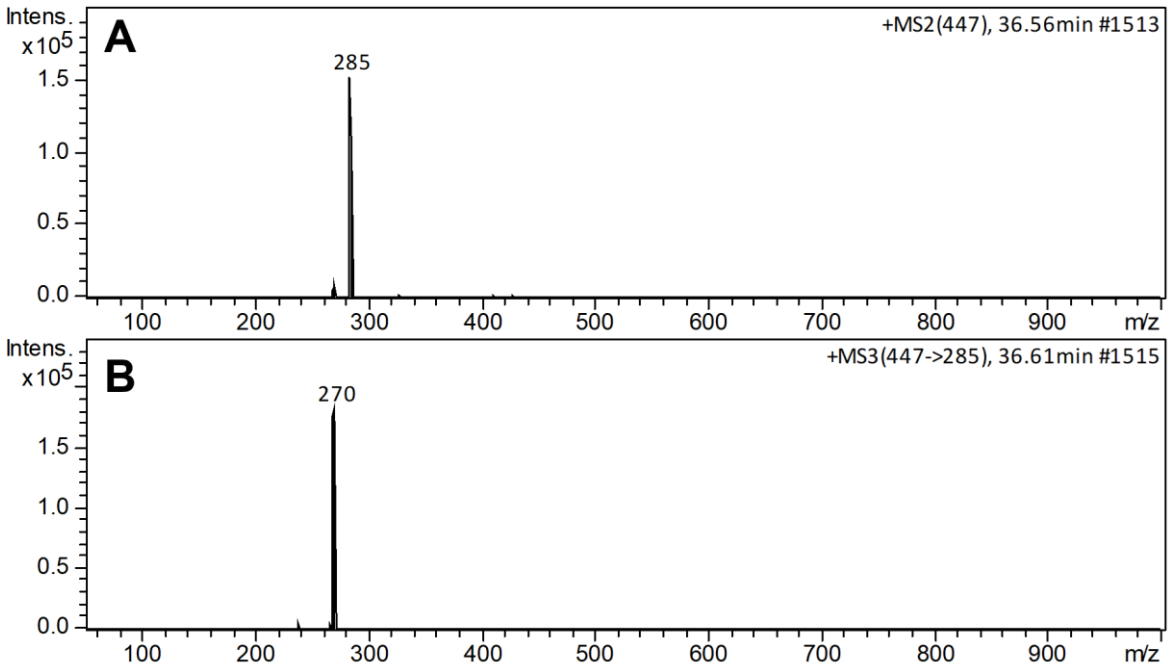

Figure S19. CID-MS^n mass spectra in positive ion mode for compound **19**: (**A**) CID-MS^2 spectrum of the precursor ion at *m/z* 447; (**B**) CID-MS^3 mass spectrum of the product ion at *m/z* 285.

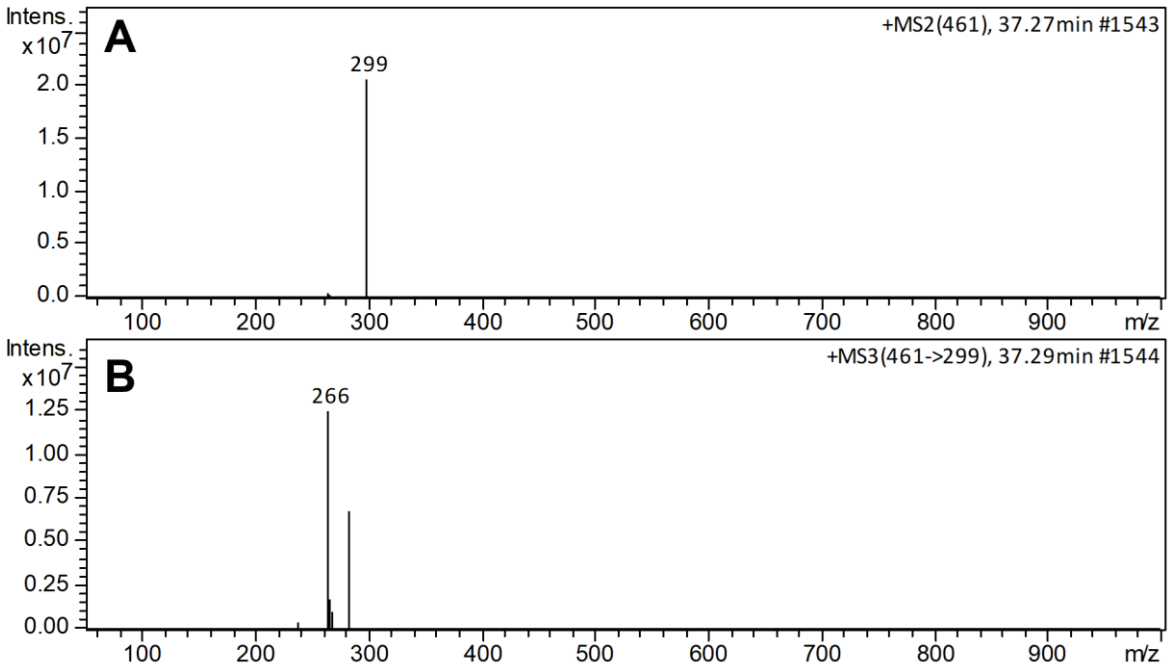

Figure S20. CID-MS^n mass spectra in positive ion mode for compound **20**: (**A**) CID-MS^2 spectrum of the precursor ion at *m/z* 461; (**B**) CID-MS^3 mass spectrum of the product ion at *m/z* 299.

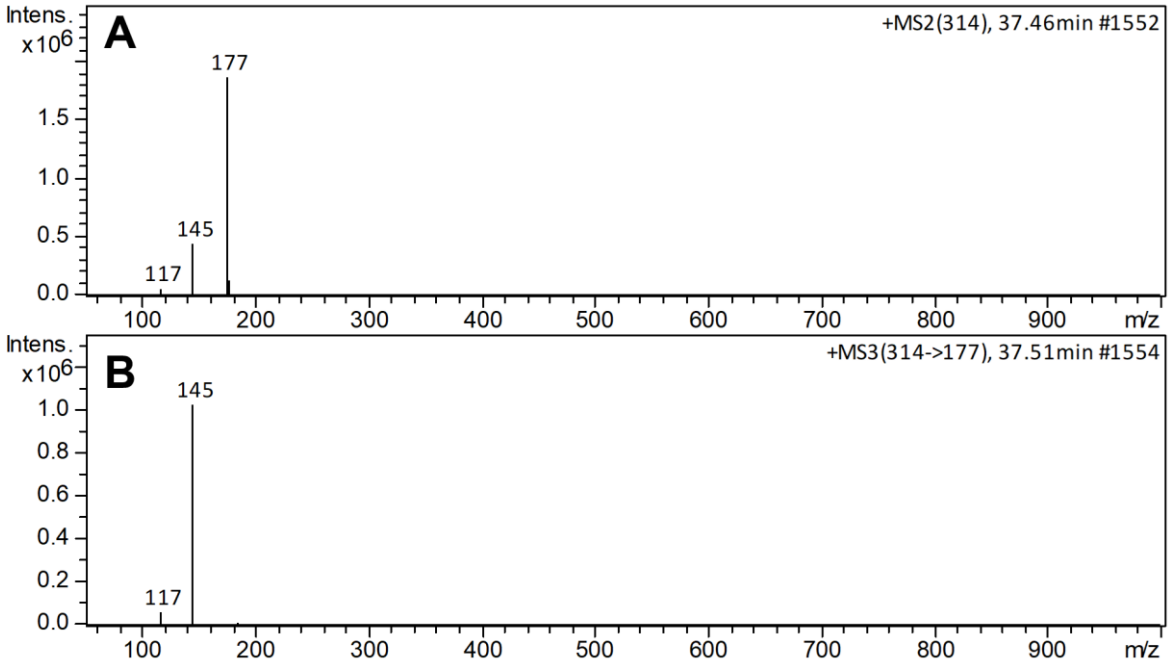

Figure S21. CID-MS^n mass spectra in positive ion mode for compound **21**: (**A**) CID-MS^2 spectrum of the precursor ion at *m/z* 314; (**B**) CID-MS^3 mass spectrum of the product ion at *m/z* 177.

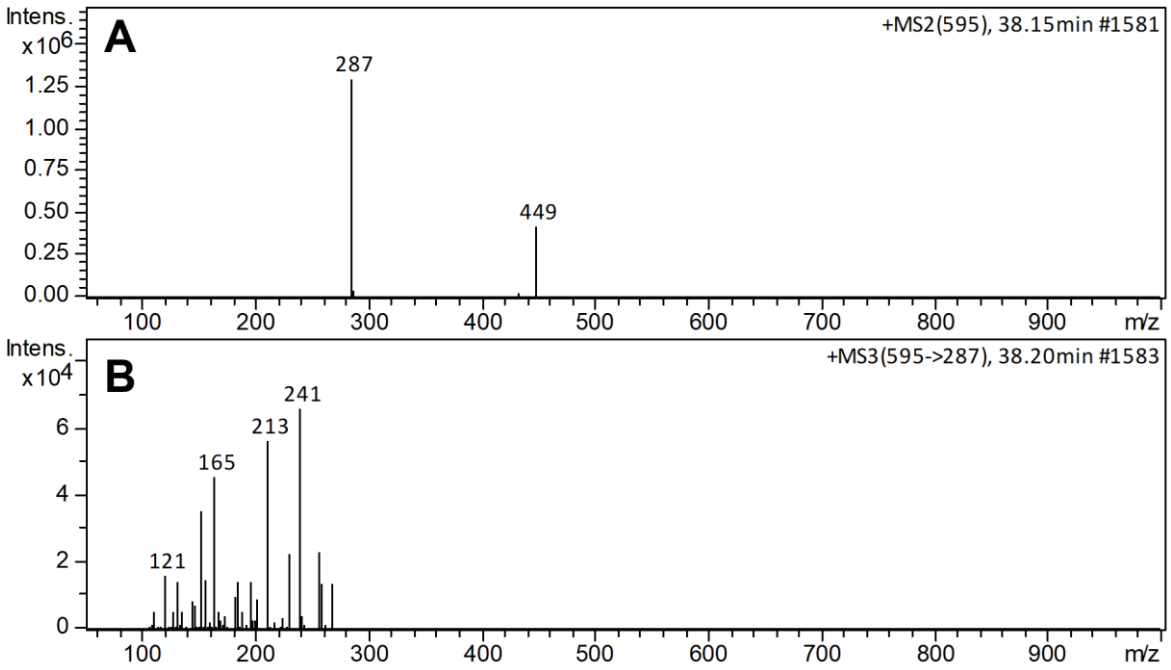

Figure S22. CID-MS^n mass spectra in positive ion mode for compound **22**: (**A**) CID-MS^2 spectrum of the precursor ion at *m/z* 595; (**B**) CID-MS^3 mass spectrum of the product ion at *m/z* 287.

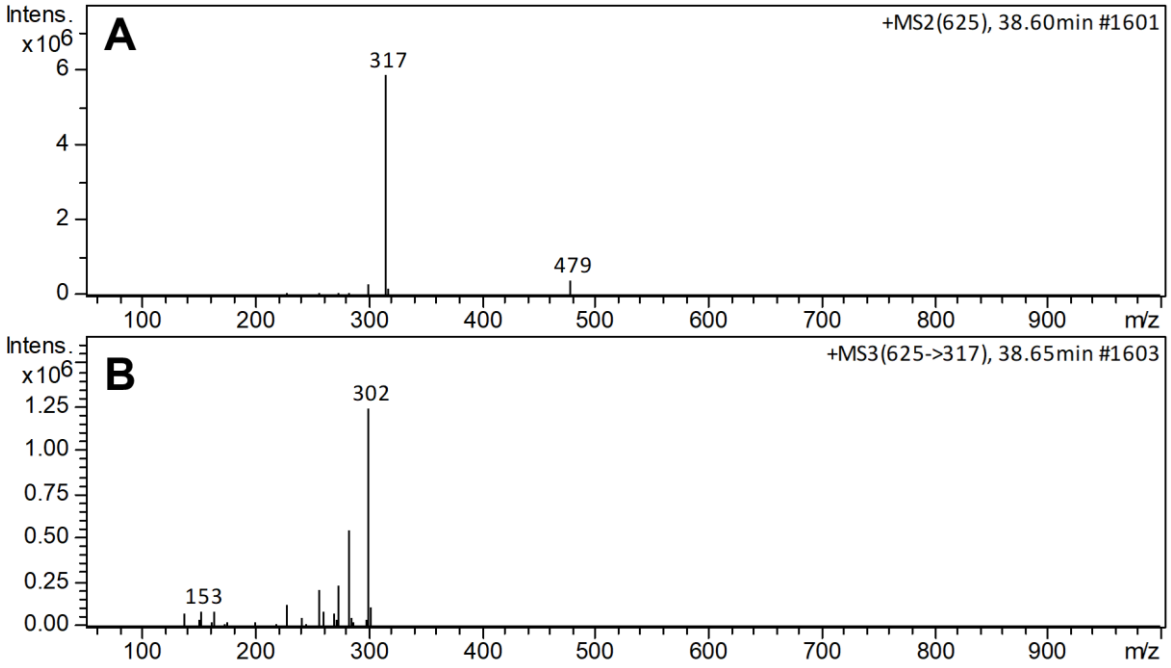

Figure S23. CID-MS^n mass spectra in positive ion mode for compound **23**: (**A**) CID-MS^2 spectrum of the precursor ion at *m/z* 625; (**B**) CID-MS^3 mass spectrum of the product ion at *m/z* 317.

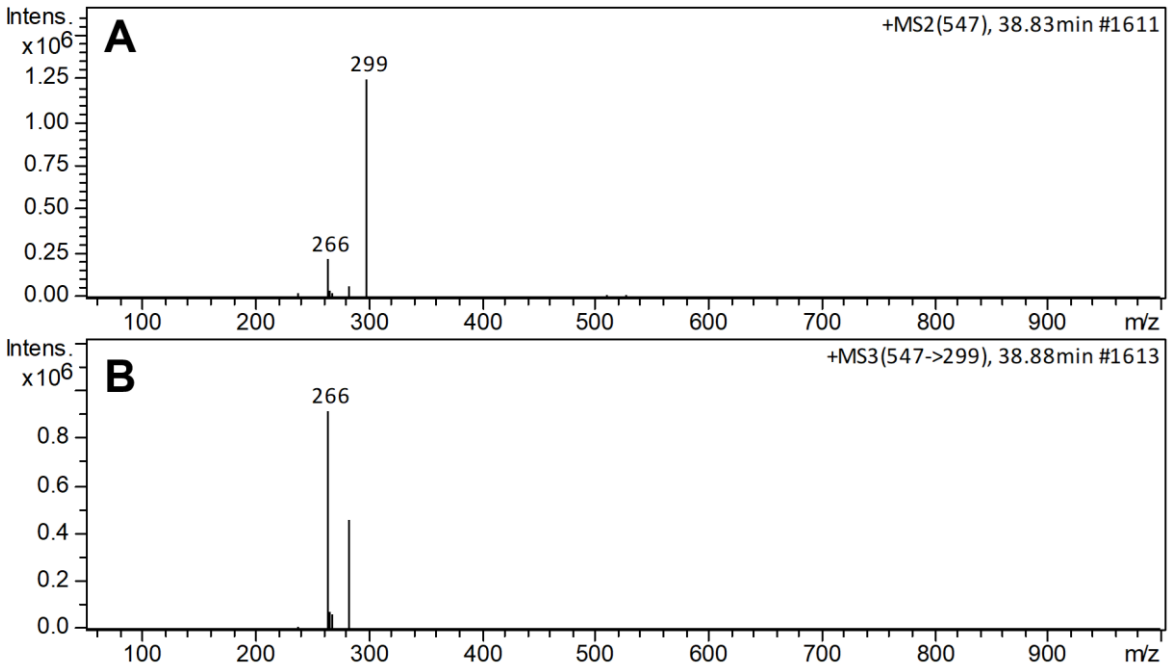

Figure S24. CID-MS^n mass spectra in positive ion mode for compound **24**: (**A**) CID-MS^2 spectrum of the precursor ion at *m/z* 547; (**B**) CID-MS^3 mass spectrum of the product ion at *m/z* 299.

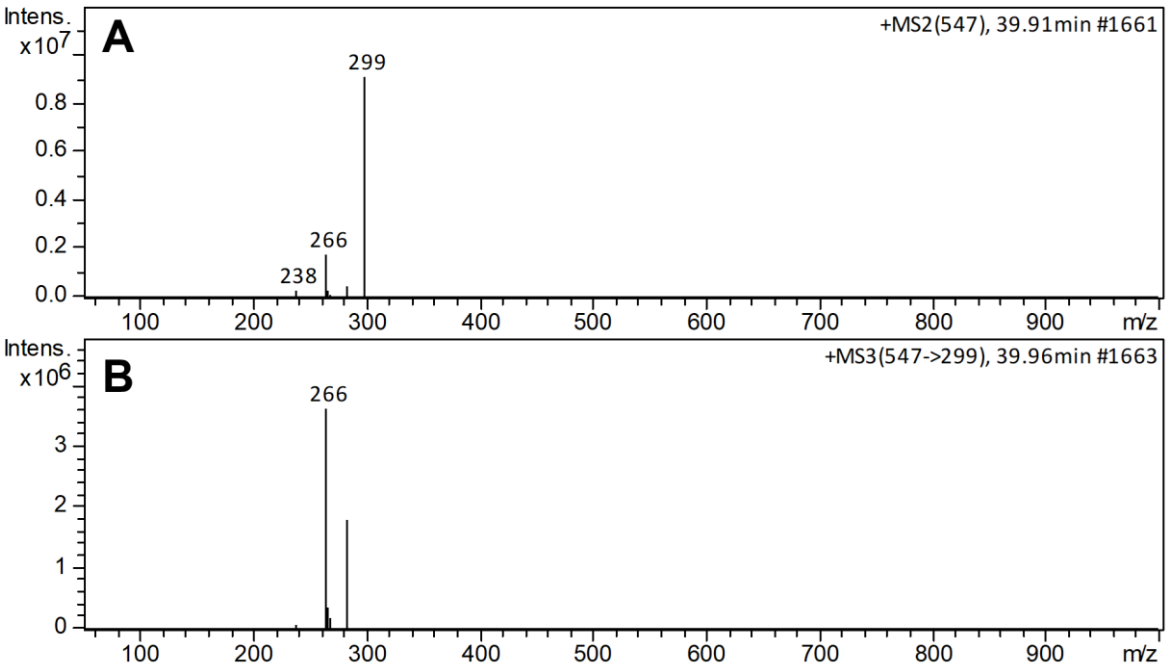

Figure S25. CID-MS^n mass spectra in positive ion mode for compound **25**: (**A**) CID-MS^2 spectrum of the precursor ion at *m/z* 547; (**B**) CID-MS^3 mass spectrum of the product ion at *m/z* 299.

ANNEX I

MINISTÉRIO DA EDUCAÇÃO
UNIVERSIDADE FEDERAL DO RIO GRANDE DO NORTE
COMISSÃO DE ÉTICA NO USO DE ANIMAIS – CEUA
Av. Salgado Filho, S/N – CEP: 59072-970 – Natal / RN
Fone: (84) 99229-6491 / e-mail: ceua@reitoria.ufrn.br

CERTIFICADO

Natal (RN), 09 de agosto de 2019.

Certificamos que a proposta intitulada **"Desenvolvimento de fitoterápico com aplicção de nanotecnologia: estudo fitoquímico e farmacológico de *Nopalea cochenillifera* Salm-Dyck"**, protocolo 027/2019, **CERTIFICADO nº 176.027/2019**, sob a responsabilidade de **Silvana Maria Zucolotto Langassner** - que envolve a produção, manutenção e/ou utilização de animais pertencentes ao filo Chordata, subfilo Vertebrata (exceto o homem), para fins de pesquisa científica (ou ensino) - encontra-se de acordo com os preceitos da Lei n.º 11.794, de 8 de outubro de 2008, do Decreto n.º 6.899, de 15 de julho de 2009, e com as normas editadas pelo Conselho Nacional de Controle da Experimentação Animal (CONCEA), foi aprovada, após adequações, pela COMISSÃO DE ÉTICA NO USO DE ANIMAIS da Universidade Federal do Rio Grande do Norte – CEUA/UFRN.

Vigência do Projeto	**Janeiro 2023**					
RELATÓRIOS	**FEVEREIRO 2023**					
Espécie	**Linhagem**	**Idade**	**Peso aprox.**	**Quantidade**		
				M	**F**	**Total**
Rattus norvegicus albinus	Wistar	8-12 semanas	220±20 g	-	**298**	**298**
Origem	Biotério Central do Centro de Ciências da Saúde – CCS – UFRN					
Manutenção	Biotério Central do Centro de Ciências da Saúde – CCS – UFRN					

Informamos ainda que, segundo o Cap. 2, Art. 13, do Regimento Interno desta CEUA, é função do professor/pesquisador responsável pelo projeto a **elaboração de relatório** de acompanhamento que deverá ser entregue tão logo a pesquisa seja concluída. **O descumprimento desta norma poderá inviabilizar a submissão de projetos futuros.**

Alianda Maira Cornélio da Silva
Vice-Coordenadora da CEUA-UFRN
Gestão 2019-2020

ANNEX II

An official website of the United States government
Here's how you know

FULL TEXT LINKS

Plants (Basel). 2023 Jan 29;12(3):594. doi: 10.3390/plants12030594.

Toxicity and Anti-Inflammatory Activity of Phenolic-Rich Extract from *Nopalea cochenillifera* (Cactaceae): A Preclinical Study on the Prevention of Inflammatory Bowel Diseases

Emanuella de Aragão Tavares [1], Gerlane Coelho Bernardo Guerra [1 2 3], Nadja Maria da Costa Melo [1], Renato Dantas-Medeiros [1], Elaine Cristine Souza da Silva [3], Anderson Wilbur Lopes Andrade [1], Daline Fernandes de Souza Araújo [4], Valéria Costa da Silva [1], Ana Caroline Zanatta [5], Thaís Gomes de Carvalho [6], Aurigena Antunes de Araújo [2 3 6], Raimundo Fernandes de Araújo-Júnior [1 6 7], Silvana Maria Zucolotto [1 3]

Affiliations

PMID: 36771677 PMCID: PMC9921826 DOI: 10.3390/plants12030594
Free PMC article

Abstract

Phenolic compounds have been scientifically recognized as beneficial to intestinal health. The cactus *Nopalea cochenillifera*, used as anti-inflammatory in traditional medicine, is a rich source of these bioactive compounds. The present study aimed to investigate the phytochemical profile of *N. cochenillifera* extract and evaluate its acute toxicity and anti-inflammatory effect on 2,4-dinitrobenzenesulfonic acid (DNBS)-induced colitis in rats. The total phenolic content per gram of dry extract was 67.85 mg. Through HPLC-IES-MS^n, a total of 25 compounds such as saccharides, organic acids, phenolic acids and flavonoids were characterized. The dose of 2000 mg/kg of extract by an oral route showed no signs of toxicity, mortality or significant changes in biochemical and hematological parameters. Regarding intestinal anti-inflammatory effects, animals were treated with three different doses of extract or sulfasalazine. Macroscopic analysis of the colon indicated that the extract decreased the disease activity index. Levels of IL-1β and TNF-α decreased, IL-10 increased and MDA and MPO enzyme levels decreased when compared with the control group. In addition, a down-regulation of MAPK1/ERK2 and NF-κB p65 pathway markers in colon tissue was observed. The epithelial integrity was improved according to histopathological and immunohistological analysis. Thus, the extract provided strong preclinical evidence of being effective in maintaining the remission of colitis.

Keywords: Cactaceae; colitis; flavonoids; functional foods; herbal medicines; inflammatory chronic diseases.

ANNEX III

PRODUÇÃO CIENTÍFICA E ATIVIDADES DESENVOLVIDAS NA VIGÊNCIA DO DOUTORADO

CAPES/PRINT - Estágio doutoral modalidade sanduíche

Estágio doutoral (Doutorado Sanduíche) nos laboratórios do Departamento de Farmacologia do Centro de Investigación Biomédica de la Universidad de Granada – Espanha. Supervisores: Júlio Juan Gálvez Peralta e Maria Elena Rodriguez Cabezas. Período: Setembro de 2021 a setembro de 2022.

Exame de proficiência em Língua Espanhola - DELE - Nível B2 - Intermediário Avançado - 2020

Tese em Cotutela – UFRN – Universidad de Granada (UGR)

Doutoramento em regime de cotutela UFRN – UGR sob supervisão da Profa. Dra. Maria Elena Rodriguez Cabezas.

CAPÍTULO DE LIVRO

ARAÚJO, D.F.D.S; OLIVEIRA, M. E. G.; CARVALHO, P. O. A.; **TAVARES, E. A.**; GUERRA, G. C. B.; LANGASSNER, S. M. Z. et al. Food Plants in the Caatinga. In: Jacob, M.C.M., Albuquerque, U.P. (eds) Local Food Plants of Brazil. Ethnobiology, Springer, Cham. 2021. https://doi.org/10.1007/978-3-030-69139-4_11

ARTIGOS COMPLETOS PUBLICADOS EM PERIÓDICOS

1. **TAVARES, EMANUELLA DE ARAGÃO**; GUERRA, GERLANE COELHO BERNARDO; DA COSTA MELO, NADJA MARIA; DANTAS-MEDEIROS, RENATO; DA SILVA, ELAINE CRISTINE SOUZA; ANDRADE, ANDERSON WILBUR LOPES; DE SOUZA ARAÚJO, DALINE FERNANDES; DA SILVA, VALÉRIA COSTA; ZANATTA, ANA CAROLINE; DE CARVALHO, THAÍS GOMES; DE ARAÚJO, AURIGENA ANTUNES; DE ARAÚJO-JÚNIOR, RAIMUNDO FERNANDES; ZUCOLOTTO, SILVANA MARIA. Toxicity and Anti-Inflammatory Activity of

Phenolic-Rich Extract from Nopalea cochenillifera (*Cactaceae*): A Preclinical Study on the Prevention of Inflammatory Bowel Diseases. PLANTS, v. 12, p. 594, 2023.

2. DA SILVA, ELAINE CRISTINE SOUZA; GUERRA, GERLANE COELHO; DE ARAÚJO, EDILANE RODRIGUES DANTAS; SCHLAMB, JADE; SILVA, VALÉRIA; **TAVARES, EMANUELLA DE ARAGÃO**; DANTAS-MEDEIROS, RENATO; ABREU, LUCAS SILVA; FECHINE-TAVARES, JOSEAN; DE ARAÚJO JÚNIOR, RAIMUNDO FERNANDES; ESPOSITO, DEBORA; MONCADA, MARVIN; ZUCOLOTTO, SILVANA. Phenolic-rich extract from Nopalea cochenillifera attenuates gastric lesion induced in experimental model through inhibiting oxidative stress, modulating inflammatory markers and cytoprotective effect. Food & Function, v. 1, p. 1, 2023.

3. DE ARAÚJO, E. R. D., GUERRA, G. C. B., ANDRADE, A. W. L., FERNANDES, J. M., DA SILVA, V. C., **DE ARAGÃO TAVARES**, E., DE ARAÚJO, A. A., DE ARAÚJO JÚNIOR, R. F., & ZUCOLOTTO, S. M. (2021). Gastric Ulcer Healing Property of *Bryophyllum pinnatum* Leaf Extract in Chronic Model *In Vivo* and Gastroprotective Activity of Its Major Flavonoid. *Frontiers in pharmacology*, *12*, 744192. https://doi.org/10.3389/fphar.2021.744192

4. DE ALMEIDA MAGALHÃES, T. S. S., DE OLIVEIRA MACEDO, P. C., DA COSTA, É. C. P., **DE ARAGÃO TAVARES, E.**, DA SILVA, V. C., GUERRA, G. C. B., PEREIRA, J. R., DE ARAÚJO MOURA LEMOS, T. M., DE NEGREIROS, M. M. F., DE OLIVEIRA ROCHA, H. A., CONVERTI, A., & DE LIMA, Á. A. N. (2021). Increase in the Antioxidant and Anti-Inflammatory Activity of *Euterpe oleracea* Martius Oil Complexed in β-Cyclodextrin and Hydroxypropyl-β-Cyclodextrin. *International journal of molecular sciences*, *22*(21), 11524. https://doi.org/10.3390/ijms222111524

5. MONTEIRO, CIBELE; **TAVARES, EMANUELLA**; CÂMARA, ALICE; NOBRE, JONAS Regulação molecular do ritmo circadiano e transtornos psiquiátricos: uma revisão sistemática. Jornal Brasileiro de Psiquiatria, v. 69, p. 57-72, 2020.

6. **DE ARAGÃO TAVARES, EMANUELLA**; DE MEDEIROS, WENDY MARINA TOSCANO QUEIROZ; DE ASSIS PONTES, TALITA PEREIRA; BARBOSA, MAISIE

MITCHELE; DE ARAÚJO, AURIGENA ANTUNES; DE ARAÚJO, RAIMUNDO FERNANDES; FIGUEIREDO, JOZI GODOY; LEITÃO, RENATA CARVALHO; DA SILVA MARTINS, CONCEIÇÃO; DA SILVA, FRANCISCO ORDELEI NASCIMENTO; DE BRITO PONTES, ANA CRISTINA FACUNDO; DE LIMA PONTES, DANIEL; DE MEDEIROS, CAROLINE ADDISON CARVALHO XAVIER Chitosan Membrane Modified With a New Zinc (II)-Vanillin Complex Improves Skin Wound Healing in Diabetic Rats. Frontiers in Pharmacology, v. 9, p. 1511, 2019.

7. BARBOSA, MAISIE M.; DE ARAÚJO, AURIGENA A.; DE ARAÚJO JÚNIOR, RAIMUNDO F.; GUERRA, GERLANE C. B.; DE CASTRO BRITO, GERLY A.; LEITÃO, RENATA C.; RIBEIRO, SUSANA B.; **DE ARAGÃO TAVARES, EMANUELLA**; VASCONCELOS, ROSEANE C.; GARCIA, VINÍCIUS B.; DE MEDEIROS, CAROLINE A. C. X. Telmisartan Modulates the Oral Mucositis Induced by 5-Fluorouracil in Hamsters. Frontiers in Physiology, v. 9, p. 1204, 2018.

8. PINHEIRO, J. G. O.; **TAVARES, E. A.**; SILVA, S. S.; Silva, J. F.; CARVALHO, Y. M. B. G.; FERREIRA, M. R. A.; ARAUJO, A. A. S.; BARBOSA, E. G.; PEDROSA, M. F. F.; SOARES, L. A. L.; AZEVEDO, E. P.; VEIGA JUNIOR, V. F.; LIMA, A. A. N. Inclusion Complexes of Copaiba (Copaifera multijuga Hayne) Oleoresin and Cyclodextrins: Physicochemical Characterization and Anti-Inflammatory Activity. INTERNATIONAL JOURNAL OF MOLECULAR SCIENCES, v. 18, p. 2388, 2017.

PATENTS

CARTA PATENTE CONCEDIDA

LIMA, A. A. N., PEDROSA, M. F. F., SILVA-JUNIOR, A. S., PINHEIRO, J G. O., **TAVARES, E. A**., SILVA, S. S., SILVA, J. F., VEIGA-JUNIOR, V. V., SOARES, L. A. L. Complexos de inclusão da oleorresina de copaíba (gênero Copaifera) com ciclodextrinas e sua aplicação no tratamento de doenças inflamatórias e tem como autores os cientistas. **PEDIDO:** BR 10 2016 025108 7 B1, **DATA DA CONCESSÃO:** 15/06/2021

DEPÓSITO

LIMA, A. A. N.; TAVARES, E. A.; PEDROSA, M. F. F.; SILVA, N. E.; ALMEIDA, T. S. S. 'DESENVOLVIMENTO DE FILMES POLIMÉRICOS COM ÓLEO DE ... E SUA MICROEMULSÃO PARA APLICAÇÃO ANTIINFLAMATÓRIA, CICATRIZANTE E

ANTIMICROBIANA'. 2016, Brasil. Patente: Privilégio de Inovação. **Número do registro:** BR1020160178541, Instituição de registro: INPI - Instituto Nacional da Propriedade Industrial. **Depósito PCT:** 01/08/2016

PARTICIPAÇÃO EM EVENTOS, CONGRESSOS E CURSOS

(Durante o período doutoral)

1. Estudo fitoquímico e farmacológico do extrato livre de *Nopalea cochenillifera* Salm-Dyck no modelo de colite ulcerativa experimental. VI Fórum PPGDITM (UFRPE-UFPB-UFRN-UFC), Recife, Brasil. Participante. 2019.

2. XXX Congresso de Iniciação Científica e Tecnológica. Avaliador. 2019.

3. XXXI Congresso de Iniciação Científica e Tecnológica da UFRN. Avaliador. 2020.

4. Curso em Capacitação no Uso e Manejo de Animais de Laboratório (60h). Universidade de São Paulo, Brasil. 2020.

5. PARTICIPACIÓN en el II CONGRESO INVESTIGACIÓN PTS. Efecto antiinflamatorio del extracto de *Nopalea cochenillifera* en modelo de colitis inducida por DNBS. Autores: **TAVARES EA**, MELO NMC, ANDRADE AWL, ARAÚJO DFS, SILVA ECS, DANTAS-MEDEIROS R, CARVALHO TG, ARAÚJO-JÚNIOR RF, FECHINE-TAVARES J, RODRÍGUEZ-SOJO MJ, GÁLVEZ J, GUERRA GBC, ZUCOLOTTO-LANGASSNER SM. Universidad de Granada, Espanha. 9 - 11 de Febrero de 2022

6. FB2NP - SECOND WEBINAR OF THE FRANCO-BRAZILIAN NETWORK ON NATURAL PRODUCTS - Phytochemical study and pharmacological evaluation of *Nopalea cochenillifera* extract: a cactus as a source of bioactive compounds for the development of new active ingredient to pharmaceutical or food industries. **DE ARAGÃO TAVARES EA**, SILVA ECS, ARAÚJO-JÚNIOR RF, DA SILVA JUNIOR AA, RODRIGUEZ-CABEZAS ME, GALVEZ JP, GUERRA GBC, ZUCOLOTTO SM. 11-12/07/2022

PROJETOS

ALMEIDA, A.J.A.A; ALVES, J.S.F.; ANDRADE, A.W.L.; BARBOSA, R.R.; CABRAL, B.; DE ARAÚJO, E.R.D.; FERNANDES, J.M.; FERREIRA, M.M.C.; JALES, F.L.M.L.; LACERDA, C.G.S.; LANGASSNER, S.M.Z.; LIMA, S.G.M.; MEDEIROS, R.D.; SILVA, L.M.P.; SILVA, L.V.; SIQUEIRA, E.M.S.; SOUZA, L.H.S.; **TAVARES, E. A. T**. Uso do Instagram @fitoterapia.com.ciencia como ferramenta de cientistas conversarem com a sociedade sobre o uso seguro e racional de produtos naturais e fitoterápico. **Projeto de Extensão**. 2019 – 2020.

PARTICIPAÇÃO EM BANCAS

Membro avaliador convidado(a) na banca de defesa do Trabalho de Conclusão de Curso (TCC) – Curso de Graduação em Farmácia - "MEDICAMENTOS UTILIZADOS PARA O USO ABUSIVO DE OPIÓIDES: UMA REVISÃO BIBLIOGRÁFICA" apresentado pelo o LUCIAN ELAN TEIXEIRA DE BARROS no dia 21/12/2020 na unidade de Capim Macio da Universidade Maurício de Nassau - UNINASSAU/Natal.